

University of Southern Queensland
Faculty of Health, Engineering and Sciences

Improving infiltration modelling for crusting soils

A dissertation submitted by

Cameron Leckie

In fulfilment of the requirements for

ENG4111 and 4112 Research Project

Towards the degree of

Bachelor of Engineering (Honours) (Agricultural)

Submitted October, 2019

Abstract

Infiltration and surface runoff modelling is important in many disciplines including environmental engineering, mine site rehabilitation, ecology and agronomy. Major errors in modelling can occur when the throttling effect of soil surface crusts, which reduce infiltration and subsequently increase surface runoff, are not considered. The aim of this project was to improve the modelling of infiltration on crusting soils by measuring the density of the soil surface crust.

A rainfall simulator was used to create a surface crust on soils (Sodosol and Chromosol) susceptible to surface crusting. The surface crusts resulted in greater than 90 per cent of applied rainfall becoming runoff. Several methods of measuring the crust density were trialled, with X-ray micro Computed Tomography (X-ray CT), when combined with the traditional soil core method, found to be the most accurate and reliable.

The HYDRUS-1D software application was used to model infiltration. Measured soil parameters, including crust density, and applied rainfall rates were used as model inputs. The inclusion of crust density into HYDRUS-1D resulted in insignificant improvements to modelling accuracy. Inverse modelling identified that this was as a result of HYDRUS-1D predicted saturated hydraulic conductivity values being three to four orders of magnitude larger than obtained from the inverse solution. The application of average crust hydraulic parameters, obtained from the set of inverse solutions, was found to provide a close approximation of infiltration rates—once surface runoff had commenced—and cumulative infiltration.

The findings of this project indicate that the use of average surface crust hydraulic parameters could provide major improvements in infiltration modelling accuracy using HYDRUS-1D without the requirement for additional sampling and analysis during field surveys. Further experimentation on a broader range of soils under differing vegetation regimes is required to validate the conclusions of this project.

University of Southern Queensland
Faculty of Health, Engineering and Sciences
ENG4111/ENG4112 Research Project

Limitations of Use

The Council of the University of Southern Queensland, its Faculty of Health, Engineering & Sciences, and the staff of the University of Southern Queensland, do not accept any responsibility for the truth, accuracy or completeness of material contained within or associated with this dissertation.

Persons using all or any part of this material do so at their own risk, and not at the risk of the Council of the University of Southern Queensland, its Faculty of Health, Engineering & Sciences or the staff of the University of Southern Queensland.

This dissertation reports an educational exercise and has no purpose or validity beyond this exercise. The sole purpose of the course pair entitled “Research Project” is to contribute to the overall education within the student’s chosen degree program. This document, the associated hardware, software, drawings, and other material set out in the associated appendices should not be used for any other purpose: if they are so used, it is entirely at the risk of the user.

University of Southern Queensland
Faculty of Health, Engineering and Sciences
ENG4111/ENG4112 Research Project

Certification of Dissertation

I certify that the ideas, designs and experimental work, results, analyses and conclusions set out in this dissertation are entirely my own effort, except where otherwise indicated and acknowledged.

I further certify that the work is original and has not been previously submitted for assessment in any other course or institution, except where specifically stated.

Cameron Leckie

Student Number: [REDACTED]

Acknowledgements

Completing this project could not have been completed without the assistance of many people.

Firstly I would like to thank my supervisor, Professor John McLean Bennett. His encouragement resulted in me joining Soil Science Australia and provided a much needed focus on the direction of my studies. Without that encouragement, and his subsequent support and guidance, this project may never have been initiated let alone completed.

Another pivotal supporter of this project was Dr Rob Loch from Landloch Pty Ltd. It was as a result of a presentation delivered by Dr Loch at a Soil Science Australia meeting that the idea for this project was conceived. Dr Loch was extremely generous in allowing me to use his premises and facilities for the conduct of the rainfall simulator experiments. The support of Landloch staff including Tim, Rikki, Locky and Geoff is also greatly appreciated.

Dr Richard Flavel from the University of New England facilitated access to the X-ray CT apparatus. His generous support, including taking time out of his busy schedule, to provide advice and assistance with X-ray CT and image processing was pivotal. Thank you Richard.

The staff and students at the Centre for Sustainable Agricultural Systems also provided significant practical support throughout the project. Dr Afshin Ghahramani provided a great deal of assistance with the modelling aspects of the project whilst Stirling, David, Aram, Yingcan and Alla provided support and advice related to the various laboratory activities. Thanks team!

Finally I would like to thank my wife Beverley and family for their love and support. I will make soil scientists out of you yet!

Table of Contents

LIST OF FIGURES	11
LIST OF TABLES.....	14
SYMBOLS AND ABBREVIATIONS	16
1. CHAPTER ONE – INTRODUCTION	17
1.1. Project aim	17
1.2. Project objectives	18
1.3. Dissertation overview	18
1.3.1. Literature review	18
1.3.2. Modelling.....	18
1.3.3. Methods and materials	18
1.3.4. Results.....	18
1.3.5. Discussion	18
1.3.6. Conclusion	18
2. CHAPTER TWO – LITERATURE REVIEW	19
2.1. Introduction.....	19
2.2. Section One - Infiltration and Surface Runoff	19
2.2.1. Infiltration Overview.....	19
2.2.2. Surface runoff overview.....	20
2.2.3. Measurement of infiltration - infiltrometers	20
2.2.4. Measurement of infiltration – rainfall simulators	21
2.2.5. Measurement and modelling of surface runoff – catchment scale.....	21
2.3. Section Two - Surface Crusts.....	22
2.3.1. Description.....	22
2.3.2. Types.....	22
2.3.3. Crust formation	23
2.3.4. Crust thickness	23
2.3.5. Soils prone to crusting.....	24
2.3.6. Rainfall characteristics	25
2.3.7. Crusting and Australian Soils	25
2.4. Section Three - Soil Properties	26
2.4.1. Bulk density	26
2.4.2. Bulk density of surface crusts	26
2.4.3. Porosity	28
2.4.4. Measuring ρ_b and ϕ using X-Ray Computed Tomography.....	29
2.4.5. Soil texture and textural class	29

2.5.	Section Four - Soil Hydraulic Properties	30
2.5.1.	Moisture Content.....	30
2.5.2.	Matric Potential.....	31
2.5.3.	Soil Water Characteristic	32
2.5.4.	Hydraulic conductivity.....	33
2.5.5.	Hydraulic Conductivity Function.....	33
2.6.	Section Six - Modelling infiltration	35
2.6.1.	Background	35
2.6.2.	Darcy's law	35
2.6.3.	Richards Equation.....	35
2.6.4.	HYDRUS-1D.....	35
2.7.	Section Seven - Pedotransfer functions and the prediction of soil hydraulic properties.....	36
2.7.1.	Overview of Pedotransfer Functions.....	36
2.7.2.	Bulk density as a predictor of soil hydraulic properties.....	36
2.8.	Section Eight - Conclusions and knowledge gap.....	37
3.	CHAPTER THREE – MODELLING THE IMPACT OF SURFACE SEALS/CRUSTS ON SOIL HYDRAULIC PROPERTIES AND INFILTRATION	39
3.1.	Introduction.....	39
3.2.	Automating modelling activities.....	39
3.3.	Impact of increasing bulk density on infiltration	39
3.3.1.	Simulation One: Pondered Head.....	40
3.3.2.	Simulation Two: Rainfall.....	41
3.3.3.	Simulation Three: Changing matric potential	42
3.3.4.	Simulation Four: Changing time.....	44
3.3.5.	Simulation Five: Non-uniform crusts	45
3.3.6.	Conclusion	46
3.4.	Determining the Soil Water Characteristic from the observed data.....	47
3.5.	Observed soil water retention data.....	47
3.5.1.	RETC modelling without retention data	48
3.5.2.	RETC modelling incorporating retention data.....	49
3.6.	Modelling the Soil Water Characteristic as ρ_b increases	51
3.6.1.	Retention data only	51
3.6.2.	Forward problem and correction factor function	52
3.7.	Soil Water Characteristic Pedotransfer development	55
3.7.1.	Relationship between SWC 'a' and 'b' regression coefficients.....	55
3.8.	Modelling the Hydraulic Conductivity Function	63

3.9.	Modelling infiltration.....	65
3.9.1.	Infiltration on a single layered soil under ponding conditions.....	66
3.9.2.	Infiltration on a two layered soil with a uniform crust under ponding conditions.....	69
3.9.3.	Infiltration on a multilayered layered soil with a non-uniform crust under ponding conditions.....	69
3.9.4.	Results from infiltration modelling on crusted soils.....	70
3.9.5.	Comparing ROSETTA predicted K_s values.....	70
3.9.6.	Modelling infiltration with new K_s values.....	71
3.10.	Summary.....	75
4.	CHAPTER FOUR – METHODS AND MATERIALS.....	77
4.1.	Overview and Experimental Approach.....	77
4.2.	Soils.....	77
4.3.	Soil physical and chemical properties.....	78
4.4.	Rainfall simulation.....	80
4.4.1.	Rainfall Simulator.....	80
4.4.2.	Preparation for rainfall simulator experiments.....	81
4.4.3.	Conduct of rainfall simulator experiments.....	82
4.4.4.	Sampling.....	83
4.5.	Bulk density determination.....	85
4.5.1.	Soil core method.....	85
4.5.2.	Water Retention Method.....	86
4.5.3.	Thin Slice Method.....	87
4.5.4.	Modified intact clod method.....	88
4.5.5.	X-ray Computed Tomography (CT) method.....	89
4.6.	Soil hydraulic properties.....	91
4.6.1.	Application of the modified Standard Compaction Test.....	92
4.6.2.	Determination of saturated hydraulic conductivity.....	92
4.6.3.	Determination of the soil water characteristic.....	93
4.7.	Comparing observed infiltration to HYDRUS-1D predicted infiltration.....	94
5.	CHAPTER FIVE - RESULTS.....	95
5.1.	Soil physical and chemical properties.....	95
5.1.1.	Physical Properties.....	95
5.1.2.	Chemical Properties.....	95
5.2.	Soil hydraulic properties.....	95
5.2.1.	Saturated hydraulic conductivity.....	95
5.2.2.	Soil water characteristic van Genuchten parameters.....	96

5.3.	Rainfall simulation experiments	97
5.3.1.	Initial data	97
5.3.2.	Data cleaning.....	101
5.3.3.	Infiltration and runoff results	101
5.3.4.	Sources of error.....	102
5.4.	Bulk density measurements (less X-Ray CT)	104
5.4.1.	Bulk soil	104
5.4.2.	Water Retention Method.....	104
5.4.3.	Thin Slice Method.....	105
5.4.4.	Modified intact clod method	105
5.5.	Bulk density measurements (X-ray CT)	106
5.5.1.	Introduction.....	106
5.5.2.	Crust porosity	107
5.5.3.	Determination of bulk soil porosity	108
5.5.4.	Identification of changes in soil ρ_b with depth.....	110
5.5.5.	Summary of bulk density results.....	111
5.6.	Modelling observed infiltration using HYDRUS-1D	112
5.6.1.	Introduction.....	112
5.6.2.	Modelling using SSCBD inputs	113
5.6.3.	Modelling using SSCBD and θ_{33} inputs.....	114
5.6.4.	Inverse solution	115
5.6.5.	Modelling using average parameters	118
5.6.6.	Comparing cumulative infiltration.....	120
6.	CHAPTER SIX – DISCUSSION	122
6.1.	Modelling.....	122
6.2.	Infiltration into a crusting soil.....	122
6.3.	Measurement of crust bulk density	123
6.4.	Applications of X-ray CT for soil porosity profiling	123
6.5.	HYDRUS-1D predicted soil hydraulic properties	124
6.6.	HYDRUS-1D modelling of crusted soils.....	124
6.7.	Use of average crust parameters	125
6.8.	Assessing the accuracy of laboratory based compaction	126
6.9.	Recommendations for field survey	127
6.10.	Further work.....	128
7.	CHAPTER SEVEN - CONCLUSIONS	129
	APPENDICES	131

REFERENCES 132

LIST OF FIGURES

Figure 1 Infiltration capacity versus time (Turner et al. 1984)	19
Figure 2 Physical processes involved in runoff generation (Tarboton 2003)	20
Figure 3 Decline of surface crust bulk density with depth (Roth 1997)	27
Figure 4 Soil mass and volume relationships for the solid, water and air phases within a soil. M denotes mass (M) and V denotes volume (L^3). Subscripts a, w, s and p respectively denote air, water, solids and pores respectively (Cresswell & Hamilton 2002).	31
Figure 5 Soil Water Characteristic (Hillel 2003, p. 115). Note that the axes are reversed in many instances.	32
Figure 6 Graphical depiction of example Hydraulic Conductivity Function's for a clay soil and a sandy soil (log – log scale).....	34
Figure 7 Soil profiles used in HYDRUS-1D simulations. Black rectangles at the top of the soil profile represent uniform surface crusts. White rectangles represent underlying soil. The profile on the right represents a non-uniform crust with bulk density decreasing each mm until the underlying soil profile is reached.	40
Figure 8 Simulation One: Cumulative Infiltration Under 10mm Pondered Head Conditions for a Clay Loam. The infiltration rate is plotted on a log – log axis.	41
Figure 9 Simulation Two: Cumulative infiltration under 100 mm/h rainfall for a Clay Loam.	42
Figure 10 Infiltration Rate and Cumulative Infiltration for Medium Clay Soil with 6 mm crust.....	43
Figure 11 Comparison of cumulative infiltration at $h = -100\text{mm}$	43
Figure 12 Comparison of cumulative infiltration at $h = -150,000\text{ mm}$ (PWP)	44
Figure 13 Infiltration rates over 24 h for the Sandy Loam on a log – log scale.....	45
Figure 14 Infiltration and cumulative infiltration rate comparison for medium clay	46
Figure 15 Soil Water Characteristic - Loam Soil Code 2590	48
Figure 16 Comparison of Predicted vs Observed Results - Loam Soil Code 2590	49
Figure 17 Example Retention Parameter Modelling using RETC	50
Figure 18 Clay soil 2620 - Impact of changed ρ_b on SWC	51
Figure 19 Example development of the correction factor function for clay soil code 2620 (logarithmic x scale)	53
Figure 20 Soil Water Characteristic with increasing ρ_b for two clay soils.....	53
Figure 21 Soil Water Characteristic with increasing ρ_b for four loam soils.....	54
Figure 22 Soil Water Characteristic with increasing ρ_b for four loamy sand soils	54
Figure 23 Relationship between 'a' and 'b' coefficients for clay, loam and loamy sand soils	56
Figure 24 Relationship between 'a' and 'b' coefficients by soil textural class.....	57
Figure 25 Relationship between 'a' and 'b' coefficients for all soils.....	58
Figure 26 Relationships between 'b' coefficient and ρ_b	59
Figure 27 SWC comparison by textural class	61
Figure 28 Modelled SWC with Correction Factor.....	63
Figure 29 Plot of Mualem equation against RETC Predicted $\log(K)$ output	64
Figure 30 Example HCF for loam soil (Code 2580).....	65
Figure 31 Infiltration rate comparison using different Soil Hydraulic Properties	66
Figure 32 Impact of increasing ρ_b on infiltration for clay soil (2620)	67
Figure 33 Impact of increasing ρ_b on infiltration for Loam soil (2750).....	68
Figure 34 Impact of increasing ρ_b on infiltration for Loamy Sand soil (4010).....	68
Figure 35 Comparison of infiltration with a soil crust - Clay soil 2620	70

Figure 36 Comparison of ROSETTA PTF predicted K_s values for three soils. (min) is for the lowest modelled ρ_b and (max) is for the highest modelled ρ_b value.....	71
Figure 37 Impact of increasing ρ_b on infiltration rate - Clay 2620.....	72
Figure 38 - Impact of increasing ρ_b on infiltration rate - Loam 2750	72
Figure 39 - Impact of increasing ρ_b on infiltration rate - Loamy Sand 010.....	73
Figure 40 Infiltration under three crusting scenarios - Clay 2620	74
Figure 41 Infiltration under three crust scenarios - Loam 2750.....	74
Figure 42 - Infiltration under three crust scenarios - Loamy Sand 4010	75
Figure 43 Surface seal in close proximity to the Sodosol sampling site at Millmerran Queensland....	78
Figure 44 Landloch Rainfall Simulator with two large trays sitting on the mounting frame at a 20 degree angle.	80
Figure 45 Packed soil Tray	82
Figure 46 Sample tray layout.....	82
Figure 47 Sampling locations and method.....	84
Figure 48 Flyscreen mesh placed over soil core ring to prevent thickening of the soil crust during subsequent rainfall simulations. Small pebbles on top of screen provide an indication of how rainfall can move particles.....	85
Figure 49 Water Replacement Method (Cresswell & Hamilton 2002).....	86
Figure 50 Water Replacement Method Apparatus.....	87
Figure 51 Thin slice method explanation. The left hand diagram shows the soil core once it is removed from the soil. The right hand diagram demonstrates how the soil surface was exposed above the core in preparation for removal using a thin wire.	88
Figure 52 Soil crust examples from a Sodosol prior to thinning	89
Figure 53 Soil core on mount in X-ray CT scanner.....	90
Figure 54 Hydraulic Conductivity experimental set up	93
Figure 55 Comparison of HYDRUS-1D predicted and observed saturated hydraulic conductivity. Error bars represent +/- one standard deviation	96
Figure 56 Infiltration curves for Sodosol #1	98
Figure 57 Infiltration curves for Sodosol #2.....	98
Figure 58 Infiltration curves for Sodosol #3.....	99
Figure 59 Infiltration curves for Chromosol	99
Figure 60 Infiltration curves for Ferrosol	100
Figure 61 Infiltration curves for Hydrosol.....	100
Figure 62 Close up of example Sodosol crust. Visual examination suggests a crust of 1 - 3 mm. Pencil lead is 2 mm thick.	105
Figure 63 Example soil core profile from core number 2 (Sodosol). The black within the soil mass represents voids (or organic matter as annotated). The grey represents the soil particles.	107
Figure 64 ImageJ derived average ρ_b (not adjusted) with depth below soil surface.	110
Figure 65 Determining the thickness of the surface crust (Sodosol #3)	111
Figure 66 Comparison of bulk density results by different methods	112
Figure 67 Comparison of approximate observed infiltration against modelled infiltration with and without a surface crust for the Chromosol	113
Figure 68 HYDRUS-1D modelling including incorporation of θ_{33} (value of 0.47) compared to observed infiltration	115
Figure 69 HYDRUS-1D modelling including incorporation of θ_{33} (value of 0.85) compared to observed infiltration	115
Figure 70 Comparison of observed infiltration with modelled infiltration and inverse solution – Chromosol.....	116

Figure 71 Comparison of K_s between inverse and direct HYDRUS-1D simulations using a log scale. Sodosol is abbreviated to ‘Sod’ and Chromosol to ‘Chr’. (I) indicates inverse method and (D) direct method.	117
Figure 72 Check of inverse derived soil hydraulic properties – Sodosol #3.....	118
Figure 73 Comparison of inverse solution, direct solution using average parameters and the observed infiltration for Sodosol #1	119
Figure 74 Results of sensitivity analysis when K_s is changed by plus or minus the standard deviation of inverse solution K_s values for Sodosol #3	120
Figure 75 Cumulative infiltration comparison – Sodosol 3.....	121
Figure 76 Soil Water Characteristic using inverse solution derived average hydraulic parameters with comparison where $n = 1.01$	126

LIST OF TABLES

Table 1 Abbreviations.....	16
Table 2 Typical saturated hydraulic conductivity (K_s) values (Hillel 2003).....	33
Table 3 Input Parameters for ROSETTA PTF Models.....	37
Table 4 Soil properties used in HYDRUS-1D to predict parameters for soil hydraulic modelling.....	40
Table 5 Cumulative infiltration results from ponded head scenario	41
Table 6 Cumulative infiltration results from 100 mm/h rainfall intensity simulation	41
Table 7 Impact of small changes in ψ on final infiltration rate and cumulative infiltration for Sandy Loam with a 6 mm crust under ponded head conditions	44
Table 8 Summary of results for final infiltration rates and cumulative infiltration rates after 24 h simulation under ponded head conditions.....	45
Table 9 Comparison of cumulative infiltration for no crust, 2mm crust, 6 mm crust and variable crust simulations	46
Table 10 Observed Soil Data Summary.....	47
Table 11 'a' and 'b' parameters for Soil Water Characteristic	51
Table 12 RETC generated and model predicted values for 'a' and 'b' coefficients	60
Table 13 Correction factor coefficients	62
Table 14 Average 'a' and 'b' coefficient values	62
Table 15 Reduction in steady infiltration rate from initial ρ_b value.....	69
Table 16 Soil profile set up for non-uniform crust	70
Table 17 Comparison of cumulative infiltration differences for three soils	73
Table 18 Project Soil Overview.....	77
Table 19 Soil Physical and Chemical Data Requirements and Standard Methods.....	79
Table 20 X-Ray CT Scan Settings	90
Table 21 Optimum moisture content range for different soil types (Arjun 2019)	92
Table 22 Models used to obtain VG equation parameters for use in HYDRUS-1 simulations.	94
Table 23 Soil texture and textural classes using both the Australian and US particle sizes/classes. HYDRUS-1D uses the US particle size system.....	95
Table 24 Soil Chemical Properties.....	95
Table 25 Densities of soil cores used in K_s experiments.....	96
Table 26 HYPROP derived VG equation parameters.....	97
Table 27 Summary of rainfall simulation experiments.....	97
Table 28 Regression equations and r^2 values for observed infiltration where $I(t)$ is the infiltration rate at time (t) and t is time in seconds	101
Table 29 Cumulative infiltration calculations from rainfall simulation experiments	102
Table 30 Average rainfall (mm/h) collected in rain gauges.....	102
Table 31 Average bulk densities and standard deviation for underlying soil based on a sample of four	104
Table 32 Summary of water retention method crust bulk densities.....	104
Table 33 Results from modified intact clod method for bulk density determination	105
Table 34 Average ρ_b results for the modified clod immersion method sensitivity analysis. Units are in g/cm^3 . Average range results between the 10 mL and 100 mL measuring cylinder are also provided.	106
Table 35 Bulk density results from surface crust method.....	106
Table 36 Comparison of porosity and bulk density results for 18 and 36 vertical slices per core.....	107
Table 37 ImageJ calculated crust porosity and ρ_b	107

Table 38 ImageJ calculated bulk soil porosity and ρ_b	108
Table 39 Comparison of adjusted crust ρ_b to measured bulk soil ρ_b	109
Table 40 Crust thickness determination.....	111
Table 41 Summary of bulk density crust results.....	112
Table 42 SSCBD parameter values for HYDRUS-1D modelling comparison to observed infiltration	113
Table 43 Objective function values	114
Table 44 Values obtained from optimisation activity.....	114
Table 45 Nash-Sutcliffe criterion for inverse solution modelled versus observed infiltration data....	116
Table 46 Inverse solution soil hydraulic parameters.....	117
Table 47 Comparison of average soil hydraulic parameters obtained from inverse and direct HYDRUS-1D simulations	118
Table 48 Nash-Sutcliffe Criterion values for average parameter simulations	119
Table 49 Summary of cumulative infiltration results and percentage difference from observed rainfall simulation infiltration.....	121
Table 50 Average crust parameters.....	125

SYMBOLS AND ABBREVIATIONS

Table 1 details the symbols and abbreviations that have been used in this project.

Table 1 Abbreviations

Abbreviation	Description
ρ_b	Bulk Density
ψ	Matric potential
θ	Moisture content
K_s	Saturated hydraulic conductivity
ϕ	Porosity
CT	Computed Tomography
HCF	Hydraulic Conductivity Function
MC	Measuring Cylinder
PTF	Pedotransfer Function
SWC	Soil Water Characteristic
VG	Van Genuchten

1. CHAPTER ONE – INTRODUCTION

*I love a sunburnt country,
A land of sweeping plains,
Of ragged mountain ranges,
Of droughts and flooding rains.*

Dorothea Mackellar, My Country Mackellar (2016)

All models are wrong, but some are useful.

George Box (Box & Draper 2007)

Managing the flow and storage of water, whether for flood mitigation, irrigation or provision of drinking water, has been of great importance since at least Sumerian times (Sprague De Camp 1963). Both ancient and contemporary civilisations have invested significant effort in managing their water resources. For Australia, a land of weather extremes, as famously noted by Dorothea Mackellar, managing water resources remains of particular importance. Modelling is one of the primary tools that support the management of water resources.

Until the mid-nineteenth century experientially based rules of thumb and large factors of safety were used to guide water management requirements (Linsley et al. 1992). These approaches have been replaced over the last 150 years by scientific/engineering processes. The prediction of infiltration and surface runoff, critical in water engineering, mine-site rehabilitation, agricultural and environmental disciplines, has become increasingly sophisticated. A range of empirical and physically based models have been developed to assist in the prediction of infiltration and runoff. Some of many models include Darcy's law (Darcy 1856), the Green and Ampt equation (Rawls et al. 1990), Horton's equation (Horton 1941) and the Philip equation (Philip 1954). The 21st century has seen further advances through the application of advanced computing, Geographic Information Systems (GIS) and remote sensing to improve watershed modelling (Migliaccio & Srivastava 2007).

Despite the significant advances in modelling infiltration and surface runoff, the spatial and temporal variability of precipitation and soil still result in model error, confirming George Box's observation that 'all models are wrong.' One of the soil based sources of modelling error is the impact of surface crusts. Surface crusts are thin compacted layers of soil that have higher bulk density and reduced porosity compared to the underlying soil. Surface crusts act as a throttle to infiltration and thus increase surface runoff. When predictive models fail to consider the impact of the surface crust on infiltration this reduces the accuracy of model predictions.

This project seeks to improve the accuracy of infiltration modelling, and subsequently the prediction of surface runoff, by incorporating the density of the surface crust into the commonly used infiltration modelling application, HYDRUS-1D.

1.1. Project aim

The aim of this project is to improve the modelling capability for infiltration and surface runoff on soils that form a surface crust.

1.2. Project objectives

The objectives required to achieve the aim are as follows:

1. Review the literature on modelling infiltration and surface runoff on crusting soils.
2. Use previous experimental data to determine the potential contribution of surface crust density to model error.
3. Identify and/or develop a reliable method of collecting surface crust/seal samples for the purposes of accurately calculating crust bulk density and/or porosity.
4. Optimise an infiltration and/or surface runoff model that incorporates surface crust parameters such as bulk density and porosity.
5. Validate whether incorporation of soil crust parameters into the infiltration/surface runoff models improves model accuracy.
6. Make recommendations on changes to current soil survey processes to improve infiltration and surface runoff predictions.

The project specification can be found in Appendix A.

1.3. Dissertation overview

1.3.1. Literature review

This chapter presents the background literature relevant to this project including sections on infiltration, surface crusts, related soil properties, infiltration modelling and pedotransfer functions (PTF). The chapter concludes by identifying the knowledge gap.

1.3.2. Modelling

This chapter details the modelling completed as part of the project. The modelling includes investigating the impact of various parameters and soil crust profiles on infiltration modelling using HYDRUS-1D using arbitrarily selected input data. Subsequent sections include the modelling of the Soil Water Characteristic (SWC) as ρ_b increases using externally sourced observed water retention data and the RETC and HYDRUS-1D software applications to develop a PTF. The chapter concludes by modelling infiltration as soil ρ_b increases.

1.3.3. Methods and materials

This chapter explains the experimental methodology applied to address the projects aims and objectives.

1.3.4. Results

This chapter details the results from the various experimental activities completed during the project including. This includes both the results from the physical experiments required as input data for subsequent modelling and the results of the modelling using HYDRUS-1D.

1.3.5. Discussion

This chapter draws together the key observations and findings from the initial modelling activity and the experimental phase of the project. Conclusions are drawn on whether measuring the ρ_b of the surface crust improves the accuracy of infiltration modelling.

1.3.6. Conclusion

This chapter summarises the major findings of the project and a final evaluation of the results against the project aim.

2. CHAPTER TWO – LITERATURE REVIEW

2.1. Introduction

The aim of this chapter is to review the literature related to infiltration/surface runoff and surface seals/crusts. The literature review consists of eight sections. The first section provides a general overview of infiltration and surface runoff. Section two defines surface seals/crusts and associated characteristics. Section three describes soil physical and chemical properties that influence, or are influenced by, surface sealing/crusting. Relevant soil hydraulic properties are defined in section four. Section five reviews some of the commonly used approaches to model infiltration on soils affected by surface seals/crusts. The sixth section describes modelling approaches to infiltration relevant to this project. Section seven introduces Pedotransfer functions (PTFs) whilst the final section defines the knowledge gap and draws conclusions relevant to this project.

2.2. Section One - Infiltration and Surface Runoff

2.2.1. Infiltration Overview

Infiltration is defined as the movement of water through the soil surface and into soil (Linsley et al. 1992). Infiltration capacity is the ‘maximum rate at which a given soil when in a given condition can absorb rain as it falls’ (Horton 1933, p. 399). For a soil’s infiltration capacity to be reached requires water to be ponded on the soil surface otherwise water will not always be available at all times for infiltration. The infiltration capacity starts with a high rate and decays to a steady level which in many soils approximates the saturated hydraulic conductivity (K_s) of the soil as shown in Figure 1. The shape of this curve will vary depending upon factors including the soil porosity, colloidal properties and the antecedent moisture content (Turner et al. 1984).

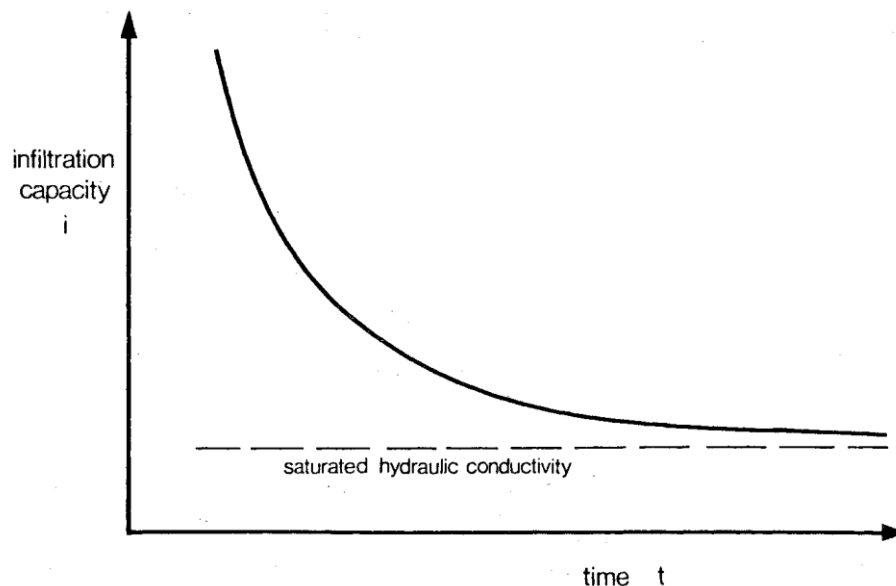


Figure 4.9 Infiltration capacity-time curve.

Figure 1 Infiltration capacity versus time (Turner et al. 1984)

The infiltration rate is the actual rate or flux of water passing through the soil surface at a point in time. The maximum possible infiltration rate at a specified time is equal to the infiltration capacity at that time. Often, under light rainfall for example, the infiltration rate will be less than the infiltration capacity. Both infiltration rate and infiltration capacity use the dimension of length per unit time (LT^{-1}).

The hydraulic properties of the soil surface control the portioning of precipitation between infiltration and surface runoff (Badorreck et al. 2013, p. 1) which will now be described.

2.2.2. Surface runoff overview

Water falling as precipitation follows several paths (Linsley et al. 1992). Some of this water is intercepted by vegetation (interception) and does not reach the ground. Some of the water is retained in depressions (depression storage) on the soil surface forming puddles. Much of the water is infiltrated into the soil as previously identified. Evapotranspiration results in some water returning to the atmosphere as water vapour. Surface runoff (or overland flow) results when the intensity of the precipitation is greater than the infiltration capacity of the soil or the soil surface is saturated. A summary of the physical processes involved in runoff generation is detailed in Figure 2.

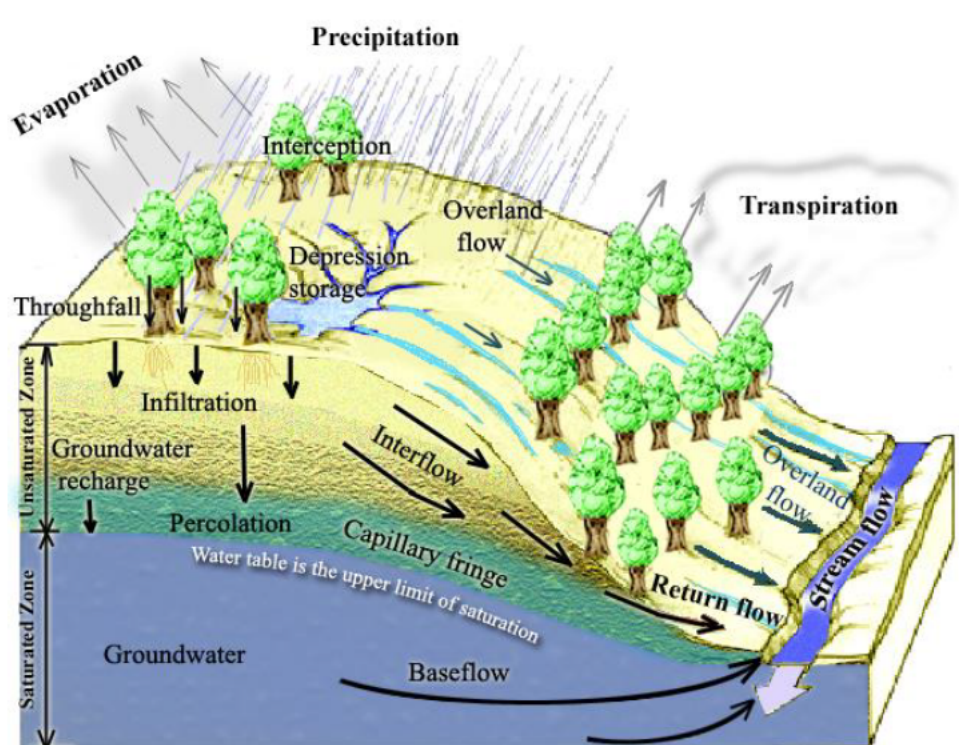


Figure 2 Physical processes involved in runoff generation (Tarboton 2003)

The measurement of surface runoff and infiltration is required in many fields including hydrology, ecology, agriculture and civil engineering. Common methods of measuring infiltration and surface runoff will now be reviewed.

2.2.3. Measurement of infiltration - infiltrometers

Physically based models of infiltration and runoff processes require the ability to obtain accurate estimates of soil hydraulic properties, such as sorptivity (S) and hydraulic conductivity (K) (Latorre et al. 2013, p. 581). Infiltrometers are devices that can be used to directly estimate soil hydraulic properties.

There are multiple types of infiltrometers such as single ring, double ring and tension (also known as disc permeameters) infiltrometers. Soil hydraulic conductivity is often determined in situ using double-ring infiltrometers (Lai & Ren 2007). These consist of two concentric metal rings that are inserted into the soil surface. Both the inner and outer rings are filled with water with the water level being measured from which the infiltration rate and saturated hydraulic conductivity can be

determined. Tension infiltrometers consist of a disc base in contact with the underlying soil connected to a graduated water-supply reservoir and a bubble tower. The soil hydraulic properties are calculated from the cumulative infiltration curves which are measured from the drop in the reservoir level (Latorre et al. 2013).

Despite intensive research over time, a large variability in results, particularly for K_s , is a common occurrence. As an example, Lai and Ren (2007) report that K_s can change by an order of magnitude or more within a short distance. Factors leading to this variability include spatial variability and heterogeneity of soils, measurement errors (Lai & Ren 2007) and the calculation method used (Verbist et al. 2010).

2.2.4. Measurement of infiltration – rainfall simulators

Rainfall simulators have been used successfully for over 90 years to conduct research on infiltration, surface runoff, soil erosion (Humphry et al. 2002) and soil crusting (Abudi et al. 2012). An advantage of rainfall simulators is their ability to create controlled and repeatable artificial rainfall. This allows for expeditious data collection, particularly when compared to natural rainfall, and comparisons between different soil types and soil management approaches (Humphry et al. 2002). Rainfall simulators consist of a method of delivering simulated rainfall (either via a nozzle or drop forming tubes (Ogden et al. 1997)) onto a plot of specified dimensions and a mechanism to collect and measure the runoff from the plot (Bertrand 1965). Rainfall simulators also have the ability to specify rainfall characteristics including drop–size distribution, raindrop velocity and kinetic energy, rainfall intensity and uniformity and whether rainfall is continuous or not (Humphry et al. 2002). Infiltration is determined by calculating the difference between the known application rate and runoff using a water balance approach.

Rainfall simulators, like infiltrometers have disadvantages. For example many rainfall simulators have difficulty in applying an energy flux to the soil similar to that of natural rainfall which is a major disadvantage for runoff studies (Abudi et al. 2012).

2.2.5. Measurement and modelling of surface runoff – catchment scale

Rainfall simulators and infiltrometers provide measurement of hydraulic variables at a point/small plot scale. Due to the heterogeneity of soils and surface conditions (Blöschl & Sivapalan 1995), both because of the nature of the soil itself (e.g. mineral composition, texture and structure) and macrostructures (such as root systems, root perforations, sun-checks, earthworm perforations and other biologic structures) (Horton 1941) point values maybe inaccurate by orders of magnitude if applied at field and/or catchment level. In most cases the ability to collect a statistically valid number of point measurements is unachievable. The use of sub-catchment/catchment level hydrologic rainfall-runoff models offers a method to address the deficiency of point measurements for hydrologic studies.

There are currently hundreds of hydrologic models based on catchment water balance methods in use (Boughton 2005). The Conservation of Mass principle is adopted in these models (accounting for all water entering, leaving and stored in a catchment) which limits the potential for error (Boughton 2005). Infiltration and other water losses (e.g. vegetation and depression storage) are treated in a simplified manner using conceptual loss models such as Initial Loss – Continuing Loss (Hill et al. 1998). Whilst these models may not be theoretically correct, for catchment level hydrologic modelling purposes they are sufficiently accurate. One study compared the use of a point infiltration equation (Green & Ampt) against simplified catchment level conceptual loss models. The results indicated that on average the results using the simplified loss models to the point infiltration equation were superior (Hill et al. 1998).

2.3. Section Two - Surface Crusts

2.3.1. Description

Under some conditions soils form a seal (seals develop in wet soil) or crust (crusts develop as the soil dries) at the soil surface. There is much debate and sometimes contradictory/interchangeable use of these terms in the literature however it is generally agreed that a seal relates to the wet soil state and a crust the dry soil state (Nciizah & Wakindiki 2015). This terminology will be used throughout this project.

A soil crust is a layer of increased ρ_b of the top few millimetres of soil (Singer & Munns 2006). The International Society of Soil Science defines a soil crust as thin surface layer which is much more compact, hard and brittle when dry than the material immediately underneath the crust with a thickness of up to three centimetres (Nciizah & Wakindiki 2015). Additionally crusts exhibit reduced porosity and changes to pore size distribution (Bajracharya & Lal 1999).

Surface crusts significantly reduce the infiltration rate and cumulative infiltration (acting as a throttle on infiltration), decrease water storage in the underlying soil, increase runoff volumes (and thus soil erosion) whilst reducing or preventing seedling emergence (Valentin & Bresson 1992). Loch (1989) describes the behaviour of the surface seal under rainfall as a rigid, impenetrable surface.

The significance of the negative impact of surface seals is demonstrated by Moore and Eigel (1981) whose research found that both the infiltration rate and cumulative infiltration can be reduced by up to 80 percent. Other studies show results of similar magnitude. Whilst the impacts of soil crusts in agricultural settings are primarily deleterious, crusts also play an important ecological role including stabilising soils, regulating the balance between infiltration and runoff as well as fixation of carbon and nitrogen (Read et al. 2008).

It should be noted that the scientific study of the uppermost surface layer of the soil is much younger than the study of soil science; as a result general agreement on terminology, definitions and classification systems is still a work in progress (Patrick 2002).

2.3.2. Types

Patrick (2002) classifies three major crust types being physical, chemical and biological. Physical crusts, which Patrick (2002) argues should be described as physico-chemical crusts due to the interaction of soil and water physical and chemical properties, are formed when the soil surface is reorganised due to the kinetic energy imparted by raindrops. Chemical crusts, generally found in hot arid areas, are formed by the precipitation of salts. Biological crusts are formed by a variety of organisms including cyanobacteria, green algae, mosses, bryophytes, lichens and fungi and are prominent in arid and semi-arid ecosystems globally (Read et al. 2008). This project focuses on physical crusts, as such biological and chemical crusts will not be considered any further.

Valentin and Bresson (1992) classified three classes of physical crust (each with sub-classes) being structural, erosion and depositional. Structural crusts are formed by the in situ rearrangement of soil particles; depositional crusts are formed by the micro-bedding (sorting, packing and orientation) of both coarse and fine particles; erosion crusts consist of a thin single, rigid and smooth surface layer of fine particles. Moss (1991) describes two physically distinct crust types. The first comprises of a thin 'skin seal' overlying a 'washed in layer' that form where ponding occurs under turbid water conditions. The second, which aligns with Valentin and Bresson's structural crust, comprises of a surface soil layer that has been compacted with little to no addition of surface solids. Above this layer, in patches, can form thin densely packed layers of silt. Moss describes this type as a 'rain-impact soil crust.' The rain-impact soil crust is the focus of this project.

2.3.3. Crust formation

The formation of a surface crust/seal is a complex process. Three different descriptions of seal/crust formation are provided, each of which assists in developing an understanding of crust formation.

Bajracharya and Lal (1999) identified five overlapping and simultaneous sub processes that occur during soil crust formation. These are (1) aggregate disruption and slaking, (2) void filling and illuviation, (3) compaction and particle rearrangement, (4) smoothing and lowering of the surface and (5) drying and consolidation.

Loch (1989) describes the visually observable formation of surface seal formation, for an initially dry soil, as having three stages, being:

1. Penetration of raindrops into the soil forming large craters. The soil surface is wetted and aggregate breakdown commences
2. The soil surface flattens, rather than being cratered, with free water becoming visible on the surface
3. The soil surface becomes distinctly flat. Surface ponding occurs as the infiltration rate is reduced.

Moss (1991) identified three temporal stages in the formation of a surface seal. During Stage One (which only occurs on dry soil) raindrops and lateral outflow from raindrop impact enter the soil immediately by hydraulic penetration with little soil disturbance. Stage Two sees less water entering the soil directly, rates of lateral outflow increasing and surface water taking longer to enter the soil. Craters are formed penetrating up to 5 mm below the soil surface. Air splashing of soil particles becomes intense and aggregate breakdown rapid. During Stage Three the craters become shallower and eventually the surface develops a planar geometry.

Seal formation can occur quickly and with little rain. On a pre-wetted soil, Moss (1991) using rainfall of 40 mm/h intensity, found that the transition from Stage Two to Three had commenced after one minute of rain (0.67 mm of rainfall applied) with a fully developed rain-impact soil crust becoming fully developed between eight (5.3 mm rain) and 16 minutes (10.7 mm rain) of rainfall commencement. A more recent study (Armenise et al. 2018) found that less than nine minutes of rain was required to develop a seal greater than 2.5 mm in thickness in three different soils seeing infiltration being reduced by 60 per cent.

Whilst the physical processes leading to surface seal formation are not directly important in this project, the time required to form a seal and the associated rainfall intensity are important for informing experimental design.

2.3.4. Crust thickness

A wide range of crust thicknesses are reported in the literature. Bajracharya and Lal (1999) describe a crust from being a few millimetres to a few centimetres thick whilst Valentin and Bresson (1992) identified erosion crusts that were well less than a millimetre thick.

Crust thickness is of importance in many hydraulic models. For example Loch (1989) provides a version of the Darcy equation relevant to a surface crust (Equation 1) where, K is the hydraulic conductivity (LT^{-1}), i is the infiltration rate (LT^{-1}), H_c is the pressure head at the bottom of the seal (L), and L_c is the thickness of the seal (L). The denominator is the crust depth implying that relatively small inaccuracies can result in significantly different values for hydraulic conductivity.

$$K = i \frac{H_c}{L_c} \quad \text{Equation 1}$$

Until relatively recently visual observation methods using tools such as Vernier callipers or microphotographs have been used to measure crust thickness (Armenise et al. 2018). These methods can be imprecise and thus error prone. X-ray techniques (Valentin & Bresson 1992; Bresson et al. 2004) have been used to characterise crust ρ_b (from which crust thickness can be determined). X-ray Computed Tomography (CT) has also been used to enable a non-subjective assessment of seal formation and depth (Armenise et al. 2018).

There are a number of difficulties in determining the thickness of the surface crust. The first difficulty is that whilst some transitions from the crust to the underlying soil are abrupt (providing a clearly defined surface crust), some crusts are gradual, increasing the difficulty of determining the actual depth of the crust (see for example Roth (1997)). A second difficulty is that the surface crust can be spatially variable even over small distances (Loch 1989). This has led some researchers to generalise the depths of surface crusts.

2.3.5. Soils prone to crusting

Soil surface seal/crust formation is influenced by many factors. These include soil texture, aggregate stability, organic matter, tillage practices, cropping history, cultivation methods, rainfall intensity and duration (Moore 1981; Moore & Eigel 1981). Cultivated soils are often particularly susceptible to crusting. This is due to cultivated soils not having any protection from the impact of rainfall which vegetation and surface covers provide and often having reduced levels of soil organic matter that aids in aggregate stability.

Each of the three previous soil crust formation descriptions identify soil aggregate breakdown as being a key factor in crust formation. A soil aggregate is defined as ‘a group of primary soil particles that cohere to each other more strongly than to other surrounding particles’ (Nimmo & Perkins 2002). Aggregate stability influences the physical behaviour of the soil and is thus related to infiltration and erosion. Soils with low aggregate stability are susceptible to crusting and erosion (Le Bissonnais 2016).

Le Bissonnais (2016) describes four major mechanisms that cause aggregate breakdown being (1) the slaking of aggregates pressure of compressed air due to wetting being greater than the aggregates mechanical strength, (2) differential swelling of clay particles, (3) raindrop impact mechanically breaking down aggregates and (4) dispersion by osmotic stress.

These mechanisms vary in multiple ways including the forces involved, soil properties that control the mechanism, the resulting fragments and the intensity of the disaggregation (Le Bissonnais 2016). Whilst many soil properties influence aggregate stability, three properties play a major role. These are the Exchangeable Sodium Percentage (ESP), iron and aluminium oxides and oxyhydroxides (sesquioxides) and organic matter (Le Bissonnais 2016). Sodic soils, soils with an ESP greater than 6 (Isbell 2016) tend to be dispersive and susceptible to crust formation. Sesquioxides cement soil particles together whilst organic matter protects the soil surface from the impact of rain drops and improves infiltration. Knowledge of these properties is required to assist in selecting appropriate soils for this project.

2.3.6. Rainfall characteristics

Rainfall characteristics play a major role in the formation of surface crusts. These characteristics include the kinetic energy of falling raindrops, cumulative rainfall depth, rainfall intensity and raindrop size (Nciizah & Wakindiki 2015).

The kinetic energy of a raindrop is calculated using Equation 2 where KE is the kinetic energy (Joules), m is the mass (M) and v is the velocity (LT^{-1}). Clearly velocity plays a major role in the kinetic energy of a raindrop. When a raindrop impacts the soil surface the absorption of the raindrops kinetic energy can break down soil aggregates into smaller aggregates or singular grains (Nciizah & Wakindiki 2015). Surface cover (e.g. plants and plant residue) can significantly reduce the velocity of raindrops and hence the kinetic energy impacting the soil surface resulting in much slower rates of surface sealing (Geeves 1997). Raindrop size (which influences raindrop mass) also impacts seal formation with larger drops forming deeper and denser crusts (Moss 1991). Rainfall kinetic energy flux tends towards constant values in the range of 25 to 29 $J\ m^{-2}\ mm^{-1}$ at rainfall intensities of 40 $mm\ h^{-1}$.

$$KE = \frac{1}{2} \times m \times v^2 \quad \text{Equation 2}$$

Rainfall intensity influences the rate of soil wetting and thus aggregate breakdown due to slaking caused by rapid wetting (Geeves 1997). As previously identified seal formation under high intensity rain can occur rapidly. Cumulative rainfall positively influences crust thickness meaning that the longer the applied rainfall the thicker the surface crust (Armenise et al. 2018). To artificially create a surface crust thus requires high intensity rainfall for a period of time which can be achieved through the use of a rainfall simulator.

2.3.7. Crusting and Australian Soils

Large areas of Australia are affected by soil crusting, including both physical and biological crusts. Biological crusts are common in arid and semi-arid areas (Eldridge et al. 2000). The soils most commonly affected by surface sealing/crusting are Chromosols, Sodosols and Kandosols, particularly where the soil surface is degraded, as well as Vertosols with sodic surface conditions (Murphy 2015).

Sodic soils readily disperse and are prone to surface crusting. Approximately 28 per cent of the Australian continent is assessed as having sodic soils (Rengasamy & Olsson 1991). Raine and Loch (2003) report that in Queensland 25% of soils are strongly sodic and 20% are variably sodic. Sodicity occurs when there are a high proportion of sodium cations in comparison to other cations. Raine and Loch (2003) argue that the term dispersive soils is a more appropriate term to use than sodic due to the fact that higher clay soils, soils with no mulch/vegetation and cultivated soils can all tend to disperse even if the Exchangeable Sodium Percentage (ESP) results do not classify the soil as sodic. Dispersive soils can develop surface crusts under a number of conditions (Raine & Loch 2003).

The wide scale susceptibility of Australian soils to surface crusting has potentially large impacts on hydrologic/agronomic modelling and subsequently the prediction of infiltration, runoff and crop growth highlighting the importance of being able to accurately model the impacts of surface crusting crusts.

2.4. Section Three - Soil Properties

A number of soil properties are relevant to the study soil crusts and this project. These include bulk density, porosity and soil texture. Soil hydraulic properties will be considered in the next section.

2.4.1. Bulk density

Bulk density (ρ_b) is a measure of the level of compaction within a soil. It is defined as the ratio of the oven dried soil mass to its bulk volume and is defined by Equation 3 (Singer & Munns 2006) where ρ_b is the bulk density (ML^{-3}), M_s is the mass of the sample (M) and V_t is the bulk volume (L^3) of the sample.

$$\rho_b = \frac{M_s}{V_t} \quad \text{Equation 3}$$

Typical ρ_b values in coarse textured soils typically range from 1.2 to 1.8 g/cm^3 and in finer textured soils range from 1.0 to 1.6 g/cm^3 (Tan 1996). Low bulk densities from 1 – 1.5 g/cm^3 indicate favourable conditions for plant root growth whilst high bulk densities from 1.8 – 2 g/cm^3 indicate compacted soils with few pore spaces that are unfavourable for plant root growth (Tan 1996). In compacted soils plant root growth is restricted due to the difficulty of plant roots penetrating the soil, thus limiting water and nutrient uptake (Stirzaker et al. 1996).

Two main approaches to measuring bulk density have been developed; direct and indirect methods. Direct methods include the core, clod and excavation methods. The core method involves removal of a soil core of known volume from the soil mass using a soil core sampler. The soil core is dried at 105°C until the soil reach a constant weight at which point Equation 3 is applied to calculate the bulk density (Blake 1965). The clod method involves covering an air dry clod or soil ped in a resin to provide a waterproof covering and weighing the clod whilst in the air and in the water from which the volume can be determined (Blake 1965). The water replacement (also known as compliant cavity) method involves using a water filled plastic liner to measure the volume of soil excavated (Cresswell & Hamilton 2002).

Indirect methods use radiation to determine ρ_b . Gamma radiation determination is based on empirical relationships between radiation and the ρ_b of soil (Yin Chan 2002). High resolution X-radiography has also been to determine the bulk density of soil crusts (Bresson et al. 2004) and will be discussed later.

Direct methods of determining ρ_b are typically used for land resource survey activities as they are relatively fast and use simple equipment that is portable whilst being accurate (Cresswell & Hamilton 2002). The soil core method is recommended for laboratory determination of ρ_b whilst the excavation method is recommended for field determination (Cresswell & Hamilton 2002).

2.4.2. Bulk density of surface crusts

The methods previously described all have limitations when it comes to determining the ρ_b of a soil crust. Soil core sampling devices produce a soil core sample of much greater depth than the thickness of a soil crust. For example a commonly used 100 cc soil sample ring with an internal diameter of 50 mm has a depth of 51 mm, many times the depth of a surface crust. Use of the soil core method will therefore underestimate crust ρ_b .

The primary disadvantage of the soil clod method for crust ρ_b determination relates to sample size and obtaining samples. Larger samples (fist sized according to Grossman and Reinsch (2002) and greater

than 100 g oven dry weight according to (Cresswell & Hamilton 2002) are recommended as they provide a more representative representation of ρ_b than smaller samples. For thin surface crusts this is not practical and/or difficult to obtain due to the thinness/fragility of the crust and the ability to separate it from the underlying soil.

The water replacement method also has limitations for measuring crust ρ_b . Grossman and Reinsch (2002) indicate that the sample thickness should exceed 2 cm whilst (Cresswell & Hamilton 2002) state that accurate measurements occur when the excavation is deep in proportion to the excavation diameter. Both of these requirements are problematic for determining surface crust ρ_b . Recent research by Hardie and Almajmaie (2019) however recommends the use of the water replacement method as an in situ method of obtaining crust porosity/ ρ_b .

Researchers have also used a number of other methods to determine surface crust ρ_b . For example, Fohrer et al. (1999) collected micro soil cores, used an oil immersion method and X-ray Computer-assisted Tomograph (CT) to determine crust ρ_b . The micro soil cores provided an average ρ_b value for the 0 – 10 mm depth layer (Fohrer et al. 1999) and whilst likely to be more accurate than traditional soil cores will underestimate crust ρ_b where crust depth is less than 10 mm. Roth (1997) used an oil immersion method (similar in concept to the clod method) without raising concerns on sample size.

Determination of surface crust ρ_b is further complicated by the changing ρ_b of the crust with depth. Until relatively recently, soil seals/crusts were considered to be discrete layers (Roth 1997). Recent studies have however identified that the ρ_b of surface crusts demonstrate a gradual decrease with depth (Roth 1997), as highlighted in Figure 3, and should be considered in terms of non-uniform layers (Bresson et al. 2004). Further complications are the lateral heterogeneity of surface crusts and the process by which a crust is formed also influences ρ_b (Bresson et al. 2004).

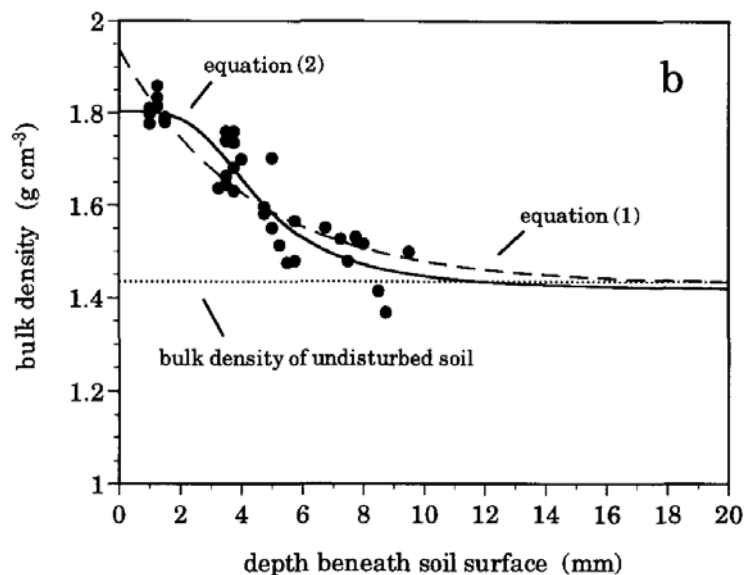


Figure 3 Decline of surface crust bulk density with depth (Roth 1997)

X-ray CT has been used to measure, with high resolution, several soil crust properties including ρ_b (Fohrer et al. 1999) and depth (Armenise et al. 2018). Whilst producing accurate data, X-ray CT scanners are very expensive and might not be easily accessible (Bresson et al. 2004), indicating that they are not suitable for routine determination of soil crust ρ_b .

X-ray CT has however been used to validate ρ_b depth functions that can be used to determine the ρ_b of a crust at various depths (Bresson et al. 2004). An example of a bulk density depth function for structural crusts is shown in Equation 4 (from (Roth 1997)) where ρ_c is the surface crust bulk density (ML^{-3}), ρ is the bulk density of the undisturbed soil (ML^{-3}), $\Delta\rho_o$ is the maximum change in the bulk density at the soil surface (ML^{-3}), γ is a shape factor describing soil-rain interaction (dimensionless) and z is the depth from soil surface (L).

$$\rho_c = \rho + \Delta\rho_o \times e^{(-\gamma.z)} \quad \text{Equation 4}$$

Some modelling applications can include different values of ρ_b throughout the soil profile. The use of X-ray CT is assessed as the only practical method of obtaining this data.

The determination of surface crust ρ_b using commonly practiced methods remains problematic. Sophisticated techniques such as X-ray CT can provide accurate data but are unlikely to be available for routine use. This highlights the need to:

- Develop a new method, or adapt a current method, for the determination of soil crust ρ_b , and
- Determine to what level of accuracy is the ρ_b of the surface crust required for the purposes of modelling infiltration and runoff.

2.4.3. Porosity

Soil is a three phase system consisting of solids, liquids and gases. The spaces in between the solid phase of the soil matrix are known as pores and are occupied by either liquids or gases. Approximately 50 per cent of the volume of an uncompacted volume of soil consists of pores (Singer & Munns 2006).

Mathematically the porosity (φ) of the soil is defined as the ratio of the pore volume to the total volume as detailed in Equation 5 (from Singer and Munns (2006)) where φ is the soil porosity (dimensionless), V_p is the pore volume (L^3) and V_t is the total volume (L^3) of the soil.

$$\varphi = \frac{V_p}{V_t} \quad \text{Equation 5}$$

The porosity of the soil can be used to calculate the soil bulk density and vice versa as detailed in Equation 6 where ρ_s is the particle density (ML^{-3}) and the other terms have been previously defined.

Laboratory (Flint and Flint (2002)) and X-Ray Computed Tomography (CT) methods (Armenise et al. 2018) can be used to calculate particle density however 2.65 g/cm^3 is generally used as the particle density for most mineral soils (Cresswell & Hamilton 2002).

$$\varphi = 1 - \frac{\rho_b}{\rho_s} \quad \text{Equation 6}$$

One of the characteristics of soil crusts is a low porosity (Nciizah & Wakindiki 2015) leaving less pore space available for plant root growth and water movement/storage.

2.4.4. Measuring ρ_b and ϕ using X-Ray Computed Tomography

Over the last few decades advanced techniques have been developed to quantitatively measure soil properties at the micro scale. One of these is X-Ray Computed Tomography (CT). X-ray CT is a non-destructive method of visualising the interior of objects including their three dimensional properties by measuring the attenuation of X-ray radiation (Ketcham 2017). This is achieved by taking images of a thin slice of an object. Whilst normal digital images are composed of pixels, or picture elements, an X-ray CT image is composed of a three dimensional volume element known as a voxel (Ketcham 2017).

X-ray CT has been used to support research across a range of soil science topics including: mineral grains and constituents, soil physical properties (ρ_b and ϕ), solute transport and soil biota (Taina et al. 2008). Of relevance to this project, X-ray CT has recently been used to accurately measure the thickness of surface seals. This was achieved by selecting a reference porosity at a depth beneath the soil surface not affected by the surface crust. Porosity was determined from this depth to the soil surface. The thickness of the crust was equal to the depth where the porosity equalled the reference porosity (Armenise et al. 2018). This approach of determining seal thickness appears to be far more accurate than traditional methods of measurement by visual observation and the uses of calipers/rulers. X-ray CT has also been used to measure the change in ρ_b with depth below the soil surface (Bresson et al. 2004).

The use of CT can provide an extremely accurate quantification of key soil seal/crust physical properties such as ϕ and ρ_b , particularly when compared to more traditional methods. Whilst CT is unlikely to be available for routine quantification of soil crusts properties, it does provide the opportunity in this project to compare the accuracy of different surface crust soil ρ_b sampling techniques and investigate the impact, in conjunction with ρ_b depth functions, of inaccuracies in measuring surface crust ρ_b on infiltration modelling.

2.4.5. Soil texture and textural class

Soil texture is an important parameter as it influences a broad range of soil properties including fertility, bearing strength, erosivity and hydraulic conductivity (Bowman & Hutka 2002).

The mineralogical parts of the soils solid phase consists of three types of particle differentiated by size; being sand, silt and clay. In Australia clay particles are defined as being smaller than 0.002 mm in diameter, silt particles between 0.02 and 0.02 mm and clay particles are between 0.02 mm and 2 mm (National Committee on Soil and Terrain 2009). Other classification systems exist that define particle sizes differently. Each soil sample can be classified into a soil textural class based upon the percentage of sand, silt and clay. Commonly a soil textural triangle is used to assign a soil sample to a textural class.

Field and laboratory evaluation of textural class can vary (National Committee on Soil and Terrain 2009) as a result of factors other than percentages of sand, silt and clay influencing determination of texture in the field. This indicates the requirement for laboratory determination of soil texture as many pedotransfer functions (PTF) use soil textural percentages for prediction of other soil properties (Nemes & Rawls 2004). A number of laboratory techniques are available for accurate particle size analysis (Gee & Or) including sieving, pipette and hydrometer methods. Particle Size Analysis laboratory procedures recommended for Australia are detailed in Bowman and Hutka (2002).

2.5. Section Four - Soil Hydraulic Properties

The prediction of water movement through soil is of critical importance to modelling infiltration and surface runoff. Two key soil moisture parameters (moisture content and matric potential) will be described followed by the Soil Water Characteristic (SWC) (or Water Retention Curve). Hydraulic conductivity will then be defined followed by the Hydraulic Conductivity Function (HCF). The SWC describes the ability of the soil to store water and the HCF describes the soils ability to transmit water (Bristow et al. 1995). These two functions allow the complete description of soil hydraulic behaviour.

2.5.1. Moisture Content

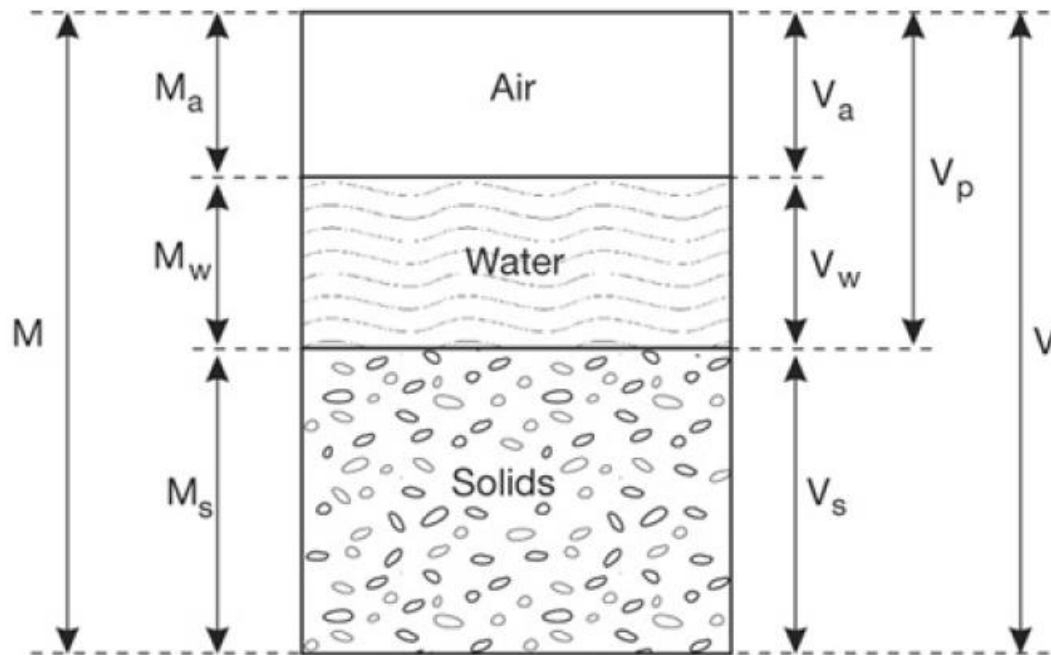
Soil is a three phase system consisting of solids, water and gases (Figure 4). The moisture content (θ) of a soil is required for many purposes in soil physics. The θ of a soil can be defined gravimetrically (θ_g) (Equation 7) or volumetrically (θ_v) (Equation 8). θ_v and θ_g are related by Equation 9. M_w , M_s , V_w , V_s and ρ_w refer to the mass of water, mass of soil, volume of water, volume of soil and density of water respectively.

$$\theta_g = \frac{M_w}{M_s} \quad \text{Equation 7}$$

$$\theta_v = \frac{V_w}{V_s} \quad \text{Equation 8}$$

$$\theta_v = \theta_g \times \frac{\rho_b}{\rho_w} \quad \text{Equation 9}$$

Mass relations



Volume relations

Figure 4 Soil mass and volume relationships for the solid, water and air phases within a soil. M denotes mass (M) and V denotes volume (L^3). Subscripts a, w, s and p respectively denote air, water, solids and pores respectively (Cresswell & Hamilton 2002).

There are a number of landmark values for θ that are of importance in soil physics. These are (Singer & Munns 2006):

- Saturation (θ_s) where all soil pores are filled by water.
- Field Capacity (θ_{FC}) where gravity has emptied the largest soil pores.
- Permanent Wilting Point (θ_{PWP}) where plants can no longer draw moisture from the soil pores.
- Oven Dry (θ_{OD}) where almost all soil pores have been emptied/evaporated after drying in an oven for 24 hours at 105 °C.

2.5.2. Matric Potential

The adhesive and cohesive properties of water and capillary forces give rise to a negative pressure (or potential) within the soil matrix. This is known as the matric potential (ψ_m). The matric potential is measured in a number of different units including kPa, Bar or metres head of water. As ψ_m is a negative quantity, small negative values represent a small suction and large negative values represent a large suction.

When suction (negative pressure) is applied to a saturated soil, water begins to empty from the soil pores. The largest pores will empty first with progressively smaller pores emptying as the suction increases. At very high suctions (large values of ψ_m) only the smallest of pores will retain water, held tightly to soil particles via adsorption. Thus as suction increases water content decreases (Hillel 2003).

The landmark values of θ described above are related to ψ_m values. For example Permanent Wilting Point (PWP) corresponds to the soil water content (θ_{PWP}) at $\psi_m = -153.30$ m and Field Capacity

corresponds to soil water content (θ_{FC}) at $\psi_m = -1$ m for sandy soils, -3.5 m for medium textured soils and -5.0 m for clayey soils (Radcliffe & Simunek 2010). Plant Available Water is the difference between these two values multiplied by the depth of soil.

The relationship between θ and ψ_m is described by the Soil Water Characteristic curve.

2.5.3. Soil Water Characteristic

The Soil Water Characteristic (SWC) is extremely important in modelling the storage of water in soils. By measuring θ at varying values of ψ_m a curve can be developed that is known as the Soil Water Characteristic (SWC) (Tuller & Or 2004). An example SWC for a clay soil and a sandy soil is shown in Figure 5.

The difference between the two soils can be explained via soil texture and structure. At low suction (between saturation and around $\psi_m = -10$ kPa), water content is related primarily to capillarity and pore size distribution both of which are linked to soil structure (Cresswell et al. 1992). At high suctions water content is mainly due to the adsorption of water to soil particles which is linked to soil texture (Hillel 2003, p. 114). Sandy soils tend to have larger and more regular pore sizes thus at even relatively low suctions will have a lower water content than a clay soil. The negative charge on clay particles adsorbs water which when combined with a range of pore sizes means that the slope of the curve is less steep than that of a sandy soil.

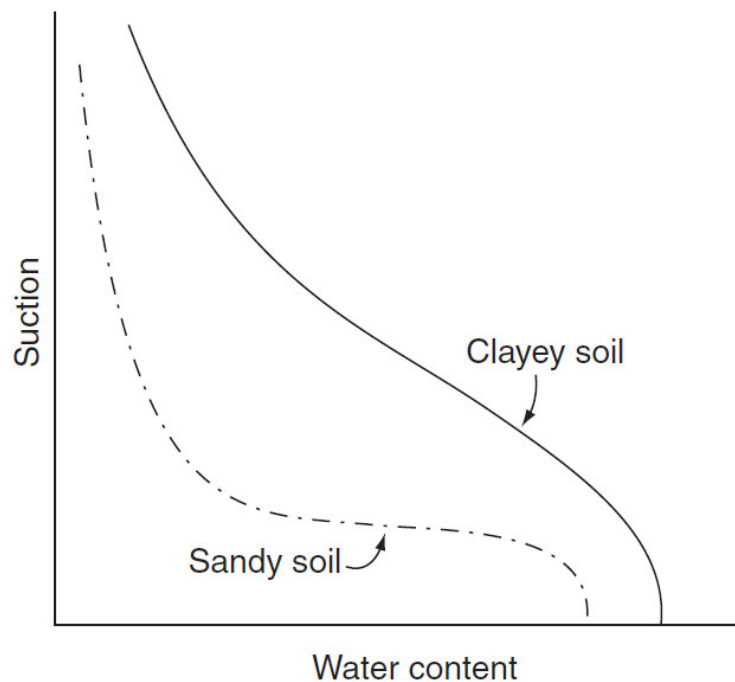


Figure 5 Soil Water Characteristic (Hillel 2003, p. 115). Note that the axes are reversed in many instances.

Many equations have been developed to describe the relationship between θ and ψ_m . A commonly used model is the van Genuchten (VG) retention curve model (Equation 10) (Tuller & Or 2004) where θ , θ_s and θ_r are the water content, water content at saturation and residual water content respectively and ψ_m is the matric potential. Parameters α , m and n are parameters related to the shape of the soil water characteristic.

$$\text{Effective saturation } (S_e) = \frac{\theta - \theta_r}{\theta_s - \theta_r} = \left[\frac{1}{1 + (\alpha\psi_m)^n} \right]^m \quad \text{Equation 10}$$

Software applications have been developed that use equations such as Equation 8 to determine soil hydraulic parameters. The RETC (Retention Curve) software application (van Genuchten et al. 1991) is an example that can derive both the SWC and HCF.

2.5.4. Hydraulic conductivity

Saturated hydraulic conductivity (K_s) is a measure of the soil's ability to transmit water under saturated conditions (Jabro 1992). K_s is a function of a soil's particle size distribution, pore size distribution, pore configuration and bulk density (Jabro 1992). K_s is a key soil hydraulic variable that controls the partition of rainfall between infiltration and runoff as well as being a primary variable in all models related to the hydrological cycle (Sobieraj et al. 2001). K_s is one of the most sensitive input parameters used in hydrological models (Zhao et al. 2016).

Estimating K_s values directly, either in the field or laboratory is time consuming and labour intensive (Rawls et al. 1998). There are numerous methods of directly determining saturated hydraulic conductivity including; the Guelph permeameter, constant-head well permeameter, double tube method, Amoozemeter, small detached cores using falling head or constant head, large attached columns, instantaneous profile, cylindrical infiltrometers, dripper method, piezometer and detached core heat-shrinkable plastic (Rawls et al. 1998). (Rawls et al. 1998) found that over 80% of the measurements were obtained using the falling head or constant head on small detached cores or instantaneous profile methods. Typical values of K_s are detailed in Table 2.

Table 2 Typical saturated hydraulic conductivity (K_s) values (Hillel 2003)

Soil texture	K_s (m/sec)
Clay	$10^{-10} - 10^{-8}$
Silt	$10^{-8} - 10^{-6}$
Sand	$10^{-5} - 10^{-3}$
Gravel	$10^{-2} - 10^{-1}$

The importance of saturated hydraulic conductivity and the difficulties of calculating it directly have led to the development of indirect methods via pore-size distribution, inverse methods or Pedo-Transfer Functions (PTF) (Sobieraj et al. 2001).

Despite the importance of K_s , in the majority of cases the soil is not saturated. Water still flows in unsaturated soil. The driving force of water movement in unsaturated soils is differences in soil matric potential. This creates a gradient causing water to flow from where the suction is higher (large ψ_m) to where it is lower (small ψ_m) (Hillel 2003). Hydraulic conductivity drops steeply in the transition from saturated to unsaturated conditions as the largest pores which conduct the most water are emptied first (Hillel 2003). The relationship between K and ψ_m , or θ , is described by the Hydraulic Conductivity Function (HCF).

2.5.5. Hydraulic Conductivity Function

Figure 6 depicts examples of the HCF for a sandy soil and a clayey soil. The HCF is normally displayed on log – log scales as the values for both K and ψ_m can vary by orders of magnitude. Under saturated conditions, the sandy soil conducts more water due to the distribution of larger pore sizes within the soil. However as the suction is increased, these pores are rapidly emptied of water resulting

in a rapid decline in K . For the clay soil, which has a much higher proportion of small pores, the rate of decline in K is much less.

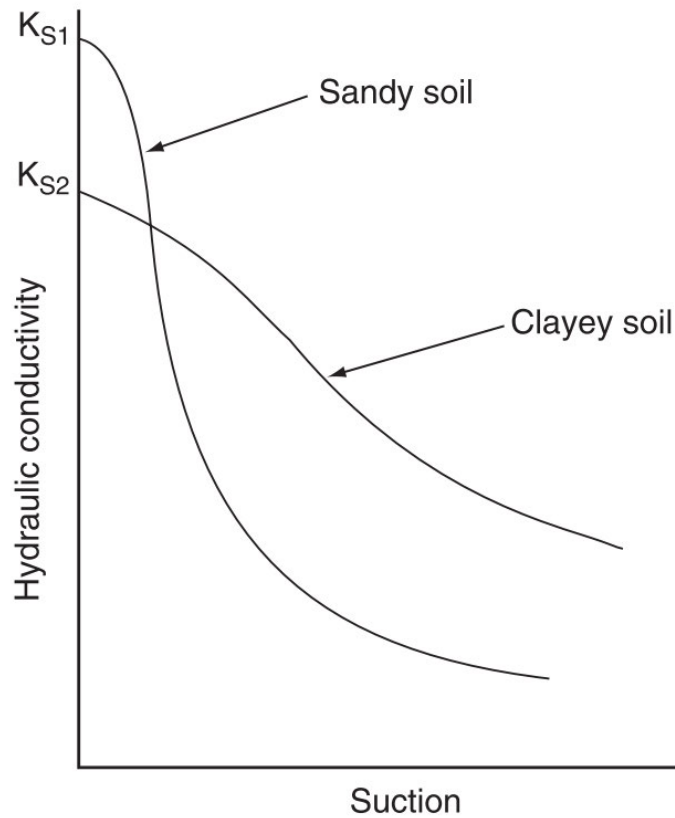


Figure 6 Graphical depiction of example Hydraulic Conductivity Function's for a clay soil and a sandy soil (log – log scale)

Multiple empirical equations have been proposed to relate K to ψ_m or θ (Hillel 2003). These equations are often depicted as $K(\psi)$ or $K(\theta)$. Mualem's hydraulic conductivity model is most commonly coupled with the previously described VG retention curve model (Equation 10) (Radcliffe & Simunek 2010). Mualem's model in terms of both effective saturation (S_e) and ψ_m are detailed in Equation 11 (Radcliffe & Simunek 2010) and Equation 12 (van Genuchten et al. 1991) where all terms have been previously defined.

$$K(S_e) = K_s \times S_e^l \times \left[1 - \left(1 - S_e^{\frac{1}{m}} \right)^m \right]^2 \quad \text{Equation 11}$$

$$K(\psi) = \frac{K_s \times \{ (1 - (\alpha\psi)^{mn}) \times [1 + (\alpha\psi)^n]^{-m} \}^2}{[1 + (\alpha\psi)^n]^{ml}} \quad \text{Equation 12}$$

The RETC software application can derive the parameters for the Mualem HCF (van Genuchten et al. 1991).

2.6. Section Six - Modelling infiltration

2.6.1. Background

The measurement and understanding of the factors controlling the infiltration process has proven exceedingly difficult over a long period of time (Betson 1964). This may explain the large number of models that have been developed, tested and modified to predict infiltration. These models vary in complexity from simple empirical equations, such as the modified Kostiakov equation, to physically based models such as the Green and Ampt equation, through to computationally intensive numerical solutions to the Richards' equation (Souchere et al. 2001). The commonly used HYDRUS-1D software application solves the Richards equation to model infiltration.

2.6.2. Darcy's law

The one dimensional flow of water through a porous medium, such as soil can be mathematically defined by the commonly used Darcy's law. Equation 13 details Darcy's law where Q is the flow of water per unit time (L^3T^{-1}) through an area A (L^2), K is the hydraulic conductivity and $d\psi/dx$ is the water potential gradient (L/L) (Singer & Munns 2006).

$$Q = A \times K \times \frac{d\psi}{dx} \quad \text{Equation 13}$$

Darcy's law is used within the Richards equation. Saturated hydraulic conductivity can be calculated by rearranging Darcy's law to solve for K once the Q has reached a constant value.

2.6.3. Richards Equation

The Richards' equation can be described as a combination of the unsaturated Darcy's law combined with the equation of continuity that results in a second-order non-linear partial differential equation for unsaturated flow in porous media (Moore & Eigel 1981).

Equation 14 details the Richards' equation where h is the pressure head (L), θ is the volumetric water content (L^3L^{-3}), t is time (T), x is a spatial coordinate (L), S is a sink term ($L^3L^{-3}T^{-1}$), α denotes the flow direction relative to the vertical axis and K is the HCF (LT^{-1}) (Šimůnek et al. 2009).

$$\frac{\delta\theta}{\delta t} = \frac{\delta}{x} \left[K \left(\frac{\delta h}{\delta x} + \cos \alpha \right) \right] - S \quad \text{Equation 14}$$

In most circumstances the Richard's equation can only be solved by numerical methods and is much more computationally intensive than other methods such as the Green and Ampt model. As a result it is best applied using a software application such as HYDRUS-1D.

2.6.4. HYDRUS-1D

A software package known as HYDRUS-1D has been developed to model one dimensional flow in a variably saturated porous medium using the Richards' equation (Šimůnek et al. 2009). HYDRUS-1D is freely available and widely used for simulating infiltration, heat and solute movement in soils.

HYDRUS-1D has a graphical interface which simplifies the setup and execution of simulations. Inbuilt within HYDRUS-1D is the ROSETTA database (see Section 2.7.2 for more information on ROSETTA) which is a hierarchical PTF that enables the prediction of soil hydraulic properties based on user inputted data (Schaap et al. 2001). The advantage of this approach is that readily available soil properties such as texture and ρ_b can then be used as inputs for the determination of the parameters required to solve the Richards equation.

HYDRUS-1D is used for the modelling of infiltration throughout this project.

2.7. Section Seven - Pedotransfer functions and the prediction of soil hydraulic properties

2.7.1. Overview of Pedotransfer Functions

There is a requirement in many soil related disciplines for data on soil hydraulic properties to quantify plant available water and to model the movement of water and solutes through the soil (Contreras & Bonilla 2018). In many instances, due to time and cost, there will be limits on how many measurements of soil hydraulic properties are made (McKenzie & Cresswell 2002). To address this deficiency a significant research effort has been made over time to establish relationships between soil hydraulic properties and other more readily measurable soil properties. These relationships are known as Pedotransfer Functions (PTF).

There are multiple different types of PTF from simple look up tables to regression equations and neural network analysis (Radcliffe & Simunek 2010). PTFs are used in different ways. Some PTFs predict soil hydraulic properties directly (such as the moisture content at a specified matric potential) or as input parameters into analytical models that estimate soil hydraulic properties (Radcliffe & Simunek 2010).

Soil physical properties that are commonly used as inputs into PTFs include soil texture/particle size distribution, organic matter content and ρ_b (Contreras & Bonilla 2018). Some of the numerous examples of PTF that have been developed include Jabro (1992) who identified that an empirical relationship existed between K_s , soil texture and ρ_b , and (Rawls et al. 1998) who included ρ_b values as a discriminator in developing mean values for K_s .

PTF are not necessarily a panacea for a lack of soil hydraulic data. Sobieraj et al. (2001) reviewed nine PTFs that used various soil properties to predict K_s . Their conclusion after applying PTFs to predict soil hydraulic parameters and hydrological outputs found that they were inadequate. Another paper studied six PTFs and found they are an inaccurate method of predicting K_s due to the inherent variability of K_s whilst noting that including ρ_b as a parameter can improve error ratios (Tietje & Hennings 1996). Selle et al. (2011) concluded that water transmission properties using PTFs were poorly correlated with basic soils data, including ρ_b , in the Shepparton irrigation region.

Not all studies have had negative results however. Multiple studies have shown that systematic variation in K_s can be explained by soil texture, porosity and ρ_b (Zhao et al. 2016). Zhao et al. (2016) also identified that PTFs are not easily transferrable between bioclimatic zones and require optimisation using local data if they are to be reliable. Paydar and Ringrose-Voase (2003) and Minasny and McBratney (2000) reported similar findings identifying that local calibration is required as well as ensuring that standardised sample volumes and measurement techniques are considered.

2.7.2. Bulk density as a predictor of soil hydraulic properties

Bulk density is a commonly used input parameter in PTFs. For example Patil and Singh (2016) found that ρ_b was used as a parameter in 15 of 19 PTFs they reviewed that were used to estimate saturated hydraulic conductivity. A recent review by Zhang and Schaap (2019) also identified that ρ_b is used in many PTFs.

The ROSETTA application, included in HYDRUS-1D and RETC, provides five hierarchical PTF to predict water retention parameters and saturated hydraulic conductivity based on available input data as detailed in Table 3 (Schaap et al. 2001). The models that use more input parameters perform better

than those that use less (Schaap et al. 2001). The three PTF at the top end of the hierarchy include ρ_b as a parameter. Zhang and Schaap (2019) reported an increase in r^2 values between estimated and measured K_s values from 0.45 to 0.55 when ρ_b was included as a predictor.

Table 3 Input Parameters for ROSETTA PTF Models

Model	Input Parameters	Comment
H1	Textural class	USDA textural classes
H2	Sand, Silt, Clay (SSC)	Percentages
H3	SSC, Bulk Density (BD)	
H4	SSCBD, water content at 3.3 m suction ($\theta_{3.3}$)	
H5	SSCBD, $\theta_{3.3}$, water content at 150 m suction (θ_{150})	

Few studies have however discussed the impact of the increased ρ_b of surface crusts when using PTFs. Paydar and Ringrose-Voase (2003) found that a Kozeny-Carman model based PTF had poor predictive capability and failed to predict K_s values for soils that hard set, had surface crusts or high levels of organic matter. Jarvis et al. (2002) identified that one source of error in measuring hydraulic conductivity could be attributed to different approaches in dealing with surface seals. The increased ρ_b of the seal is a likely contributor to this error. As the first few millimetres of the soil surface under sealing conditions control infiltration (Di Prima et al. 2018), these errors could be propagated via PTFs and affect their accuracy and reliability.

Bulk density is commonly used as an input into PTF used to predict saturated hydraulic conductivity and subsequently infiltration. There are mixed reviews on the effectiveness of PTF, including the inclusion of ρ_b as a predictive variable. The literature on the impact of surface seals when using PTFs is sparse. The ρ_b of the soil surface is generally determined from samples with a depth that is many times greater than the depth of a surface seal/crust. This suggests that values of ρ_b being used in PTFs to predict K_s will be systematically lower, potentially by a significant margin, than the ρ_b of the surface crust. This is a potential, and perhaps major, source of error in predicting soil hydraulic properties on soils susceptible to crusting. The development of a PTF that predicts the hydraulic behaviour of a surface crust thus offers an opportunity to improve infiltration modelling.

2.8. Section Eight - Conclusions and knowledge gap

Accurate values of soil hydraulic properties are required in a broad range of disciplines including water engineering, mine-site rehabilitation, ecology and agronomy, for the purposes of predicting infiltration, drainage, plant available water, modelling the impact of management actions, and watershed modelling (Timlin et al. 2004). Despite intensive efforts over a prolonged period of time; developing models of infiltration and surface runoff that are both accurate and widely applicable remains a challenge. This is largely due to the spatial heterogeneity of soil characteristics as well as surface seals/crusts which significantly reduce infiltration whilst increasing runoff. Combined these characteristics have resulted in no particular model of infiltration or runoff being generally accepted (Nciizah & Wakindiki 2015).

The literature review has identified that whilst ρ_b , and other basic soil properties such as texture, have been used to varying degrees of success to predict soil hydraulic parameters such as K_s ; very limited research has been conducted on incorporating the impact of surface crust properties such as ρ_b upon infiltration modelling. This is evidenced by the use of ρ_b values throughout the literature measured from surface horizons of a depth that are many times the depth of a surface crust. The resultant underestimation of ρ_b values is a source of error in infiltration modelling. Noting that surface crusts

can reduce infiltration by 80 per cent (Moore & Eigel 1981) the resulting errors can be large with potential consequential impacts.

The literature indicates that traditional methods of ρ_b determination are not suited or practical for surface crusts. X-ray CT has been identified as a method that can be used to accurately measure surface crust porosity and/or ρ_b . These values can subsequently be incorporated into an infiltration model such as HYDRUS-1D to determine whether measuring the ρ_b of the surface crust improves model accuracy.

Rainfall simulators have been identified as a reliable method of applying rainfall to a soil surface that will result in a surface crust being formed. Rainfall simulators also enable the collection of surface runoff/infiltration observed data that can be compared to model outputs. Combined, the use of a rainfall simulator, the ability to accurately measure crust ρ_b and the use of a modelling application such as HYDRUS-1D enable an experiment to be designed and implemented that will determine whether measuring surface crust ρ_b will improve the accuracy of infiltration modelling.

There is an increasing demand for accurate data on soil hydraulic properties that are required for use in hydrological models that inform policy making at both the catchment and regional scale (Paydar & Ringrose-Voase 2003) and crop simulation models. When combined with the large land area in Queensland and Australia susceptible to soil crusting, this indicates the requirement to determine whether incorporating the impact of surface crusts in infiltration modelling improves model accuracy. The literature review has identified a gap in the research related to the impact of surface crusts upon infiltration as well as methods that can be applied to fill this knowledge gap.

3. CHAPTER THREE – MODELLING THE IMPACT OF SURFACE SEALS/CRUSTS ON SOIL HYDRAULIC PROPERTIES AND INFILTRATION

3.1. Introduction

Due to the difficulty, time and resource requirements required to accurately measure soil hydraulic properties, infiltration and surface runoff; modelling plays a critical role in most hydrologic investigations. The aim of this chapter is thus to investigate the impact of increasing ρ_b on soil hydraulic properties and infiltration with commonly used modelling applications (RETC and HYDRUS-1D).

The modelling approach is summarised below:

1. Initial modelling using HYDRUS-1D to determine whether increasing the soil ρ_b , representing a soil crust, has an impact on infiltration.
2. Obtain observed water retention and hydraulic data for a number of soils across a range of soil textures.
3. Determine the Soil Water Characteristic (SWC) and Hydraulic Conductivity Function (HCF) using the observed water retention and hydraulic conductivity data for the selected soils using RETC.
4. Increase the ρ_b of the soils (representing a seal/crust) and determine predicted SWC and HCF using RETC.
5. Use the observed and predicted soil hydraulic properties to model infiltration using HYDRUS-1D under different scenarios.
6. Develop PTF/s for modelling impact of increased ρ_b on soil hydraulic properties.

3.2. Automating modelling activities

To reduce the time taken to complete modelling activities using RETC and HYDRUS-1D, MATLAB scripts and functions were developed to automate a number of repetitive tasks. These tasks included:

- Changing parameter values in HYDRUS-1D input files
- Executing HYDRUS-1D simulations
- Importing HYDRUS-1D (and RETC) output files for analysis and charting.

Selected MATLAB code developed for this project is detailed in Appendix B.

3.3. Impact of increasing bulk density on infiltration

To confirm the importance of considering surface crust ρ_b as a parameter in modelling infiltration (and subsequently runoff) a number of simulations were conducted to calculate the infiltration rate and cumulative infiltration under different crust conditions using HYDRUS-1D.

A 100 mm deep soil profile was used for the simulations allowing for 1 mm depth segmentation within HYDRUS-1D. Four crust conditions were modelled, being: no crust, 2 mm, 6 mm and 10 mm crusts with the crust being a constant ρ_b throughout its depth (Figure 7). A constant crust ρ_b was selected for the initial simulations for simplicity although this does not align with the findings of Roth (1997), Bresson et al. (2004) and others, which indicate that surface crust ρ_b should be considered in terms of non-uniform layers. A uniform matric potential was applied to the soil profile.

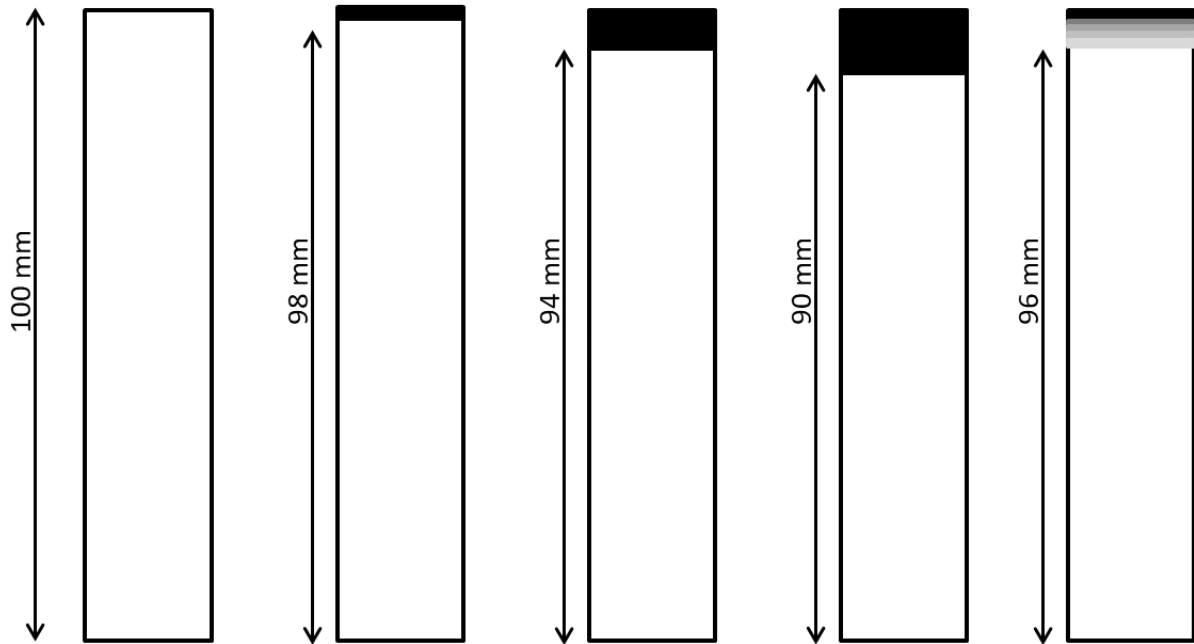


Figure 7 Soil profiles used in HYDRUS-1D simulations. Black rectangles at the top of the soil profile represent uniform surface crusts. White rectangles represent underlying soil. The profile on the right represents a non-uniform crust with bulk density decreasing each mm until the underlying soil profile is reached.

The underlying soil was assigned a constant but lower ρ_b than the crust. ρ_b figures were arbitrarily selected based on ranges discussed by (Tan 1996). A coarse (Sandy Loam), medium (Clay Loam) and fine (Medium Clay) texture class were selected as representative soils. The simulations were run for 10 minutes. A summary of the soil properties is detailed in Table 4. Water retention data was not used to derive soil hydraulic parameters from the ROSETTA database within HYDRUS-1D.

Table 4 Soil properties used in HYDRUS-1D to predict parameters for soil hydraulic modelling

Texture	% Sand	% Silt	% Clay	Soil ρ_b	Crust ρ_b
Sandy Loam	60	30	10	1.4	1.8
Clay Loam	35	35	30	1.4	1.8
Medium Clay	25	25	50	1.4	1.8

3.3.1. Simulation One: Ponded Head

The first simulation involved a ponded head of 10 mm being applied to each soil type (matric potential at the surface was changed to 10 mm) with the underlying soil having a constant head value of -1000 mm (Field Capacity). The results are detailed in Table 5, which highlights major reductions in cumulative infiltration under all crusts with the reduction increasing with crust thickness. Figure 8 provides a graphical representation of infiltration rate and cumulative infiltration under the different crust scenario's for the Clay Loam, which was representative of all three soils. The infiltration rate is higher at all times for the un-crusted soil than the crusted soils, with the initial and final infiltration rates declining as crust thickness increases.

Table 5 Cumulative infiltration results from ponded head scenario

Crust thickness	Medium Clay		Clay Loam		Sandy Loam	
	Cumulative Infiltration (mm)	Percentage reduction	Cumulative Infiltration (mm)	Percentage reduction	Cumulative Infiltration (mm)	Percentage reduction
No Crust	3.42		6.51		9.89	
2 mm crust	2.67	22%	3.59	45%	8.85	11%
6 mm crust	1.11	67%	1.27	80%	4.77	52%
10 mm crust	0.78	77%	0.78	88%	3.28	67%

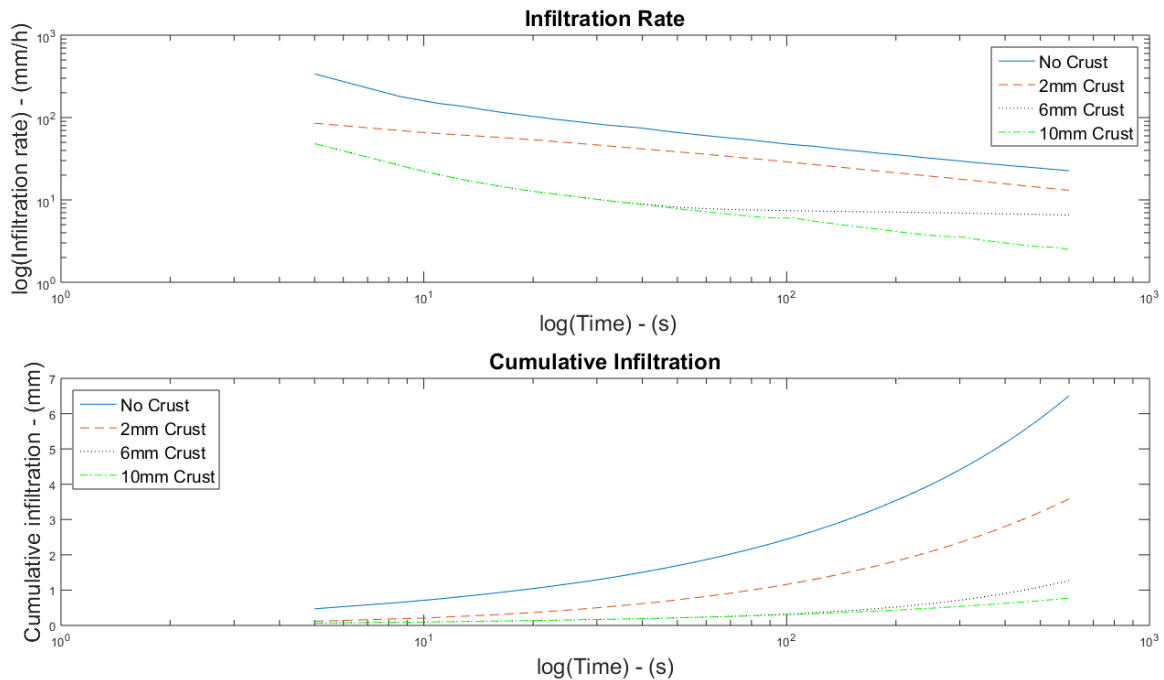


Figure 8 Simulation One: Cumulative Infiltration Under 10mm Ponded Head Conditions for a Clay Loam. The infiltration rate is plotted on a log – log axis.

3.3.2.Simulation Two: Rainfall

A second simulation, using the same depth, texture and crust parameters, was modelled that involved rainfall. A rainfall intensity of 100 mm/h was selected (0.02778 mm/s). The cumulative infiltration results are detailed in Table 6 and follow a similar pattern to that identified in Simulation Two.

Table 6 Cumulative infiltration results from 100 mm/h rainfall intensity simulation

Crust thickness	Medium Clay		Clay Loam		Sandy Loam	
	Cumulative Infiltration (mm)	Percentage reduction	Cumulative Infiltration (mm)	Percentage reduction	Cumulative Infiltration (mm)	Percentage reduction
No Crust	3.11		4.10		11.41	
2 mm crust	2.57	17%	3.53	14%	10.87	5%
6 mm crust	0.90	71%	1.18	71%	8.64	24%
10 mm crust	0.64	79%	0.81	80%	6.59	42%

Figure 9 provides a graphical representation of cumulative infiltration and infiltration rate for the Clay Loam soil. The differences in the infiltration rate profile, compared to the smooth curves for the

ponded head scenario, are assessed as being a result of the additional time required for saturation of the soil surface under rainfall before the infiltration rates decline.

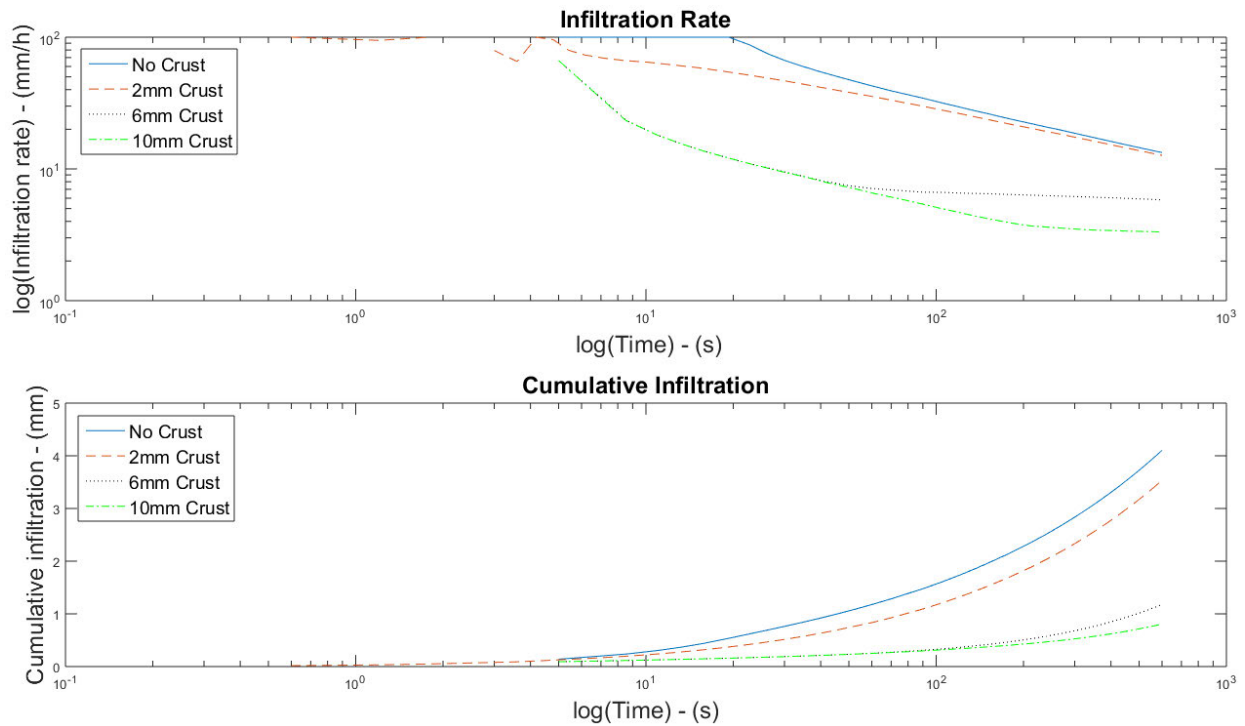


Figure 9 Simulation Two: Cumulative infiltration under 100 mm/h rainfall for a Clay Loam.

3.3.3. Simulation Three: Changing matric potential

The matric potential of the soil profile was changed to investigate the impact that this parameter, reflecting varying degrees of soil wetness, had on infiltration. Four values of matric potential were simulated being: -100 mm (default value in HYDRUS-1D), -1000 mm (Field Capacity), -10,000 mm (an intermediate value between Field Capacity and Permanent Wilting Point) and -150,000 mm (Permanent Wilting Point). A 10 mm ponded head condition was used for all simulations.

Figure 10 provides an example of infiltration rates and cumulative infiltration under changing values of matric potential for the Medium Clay profile with a 6 mm crust. All simulations provided similar infiltration and cumulative infiltration profiles. It is clear from Figure 10 that the drier the soil the greater the infiltration rate and cumulative infiltration.

Figure 11 and Figure 12 provide comparisons across the texture classes of cumulative infiltration at matric potential values of -100 mm and -150000 mm respectively. These Figures highlight that the impact of matric potential upon infiltration and cumulative infiltration extend across the texture classes.

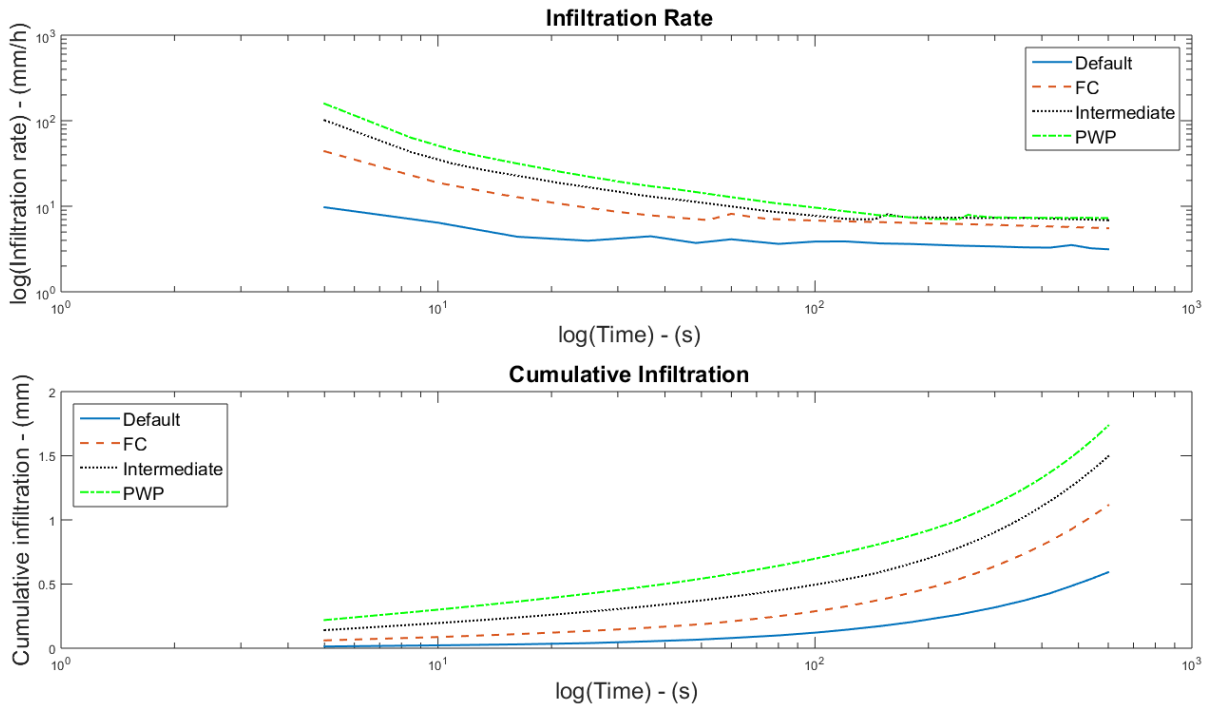


Figure 10 Infiltration Rate and Cumulative Infiltration for Medium Clay Soil with 6 mm crust

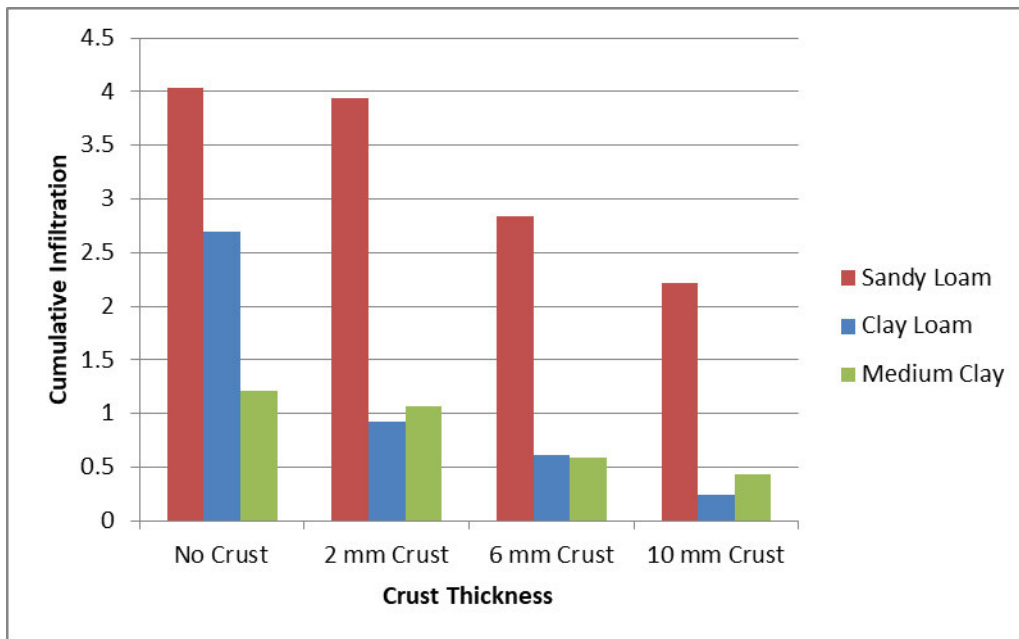


Figure 11 Comparison of cumulative infiltration at h = -100mm

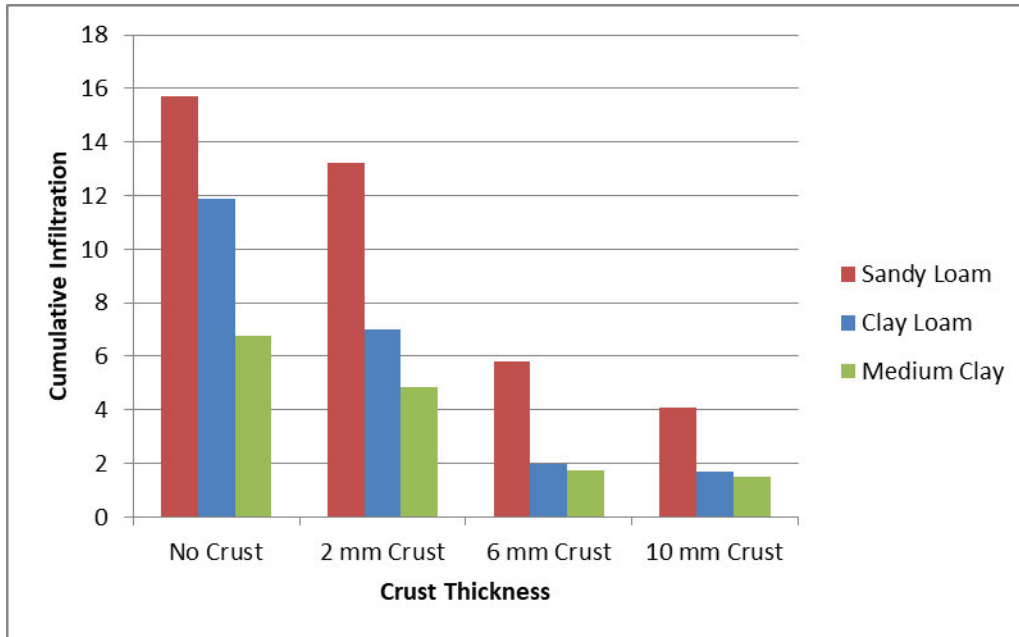


Figure 12 Comparison of cumulative infiltration at $h = -150,000$ mm (PWP)

Matric potential of the soil profile is a required input parameter for HYDRUS-1D simulations. Whilst it is clear that large changes in ψ have a substantial impact on infiltration, quantifying the impact of smaller scale changes is important to identify how accurately the input values for ψ must be. To address this, a simulation was conducted using ψ values of -2000 mm, -3000 mm, -4000 mm and -5000 mm. The results are detailed in Table 7 and identify that small changes in ψ have an insignificant impact upon the final infiltration rate and cumulative infiltration, over the short time period of the simulation. Similar results were obtained for simulations using other textures and crust thicknesses.

Table 7 Impact of small changes in ψ on final infiltration rate and cumulative infiltration for Sandy Loam with a 6 mm crust under ponded head conditions

Ψ (mm)	Final infiltration rate (mm/h)	Cumulative infiltration (mm)
-2000	26.3	5.1
-3000	26.8	5.3
-4000	27.2	5.3
-5000	27.5	5.4

The finding that small changes in ψ result in insignificant changes in infiltration will be important in the modelling of infiltration during the experimental phase of this project.

3.3.4. Simulation Four: Changing time

Simulations to this point have been run for a short period of time. To investigate the impact of time on infiltration the parameters used in Simulation One were retained however the time was extended to 24 h (86400 s).

Table 8 details the results for both final infiltration rates and cumulative infiltration. For two of the three textures the final infiltration rates for the no crust and 2 mm crust reach the same value with cumulative infiltration rates also reaching a similar value. For the 6 mm and 10 mm crusts there is a marked reduction in final infiltration rates and cumulative infiltration compared to the un-crust soil.

Table 8 Summary of results for final infiltration rates and cumulative infiltration rates after 24 h simulation under ponded head conditions

Final infiltration rate (mm/h)				
Soil	No crust	2 mm crust	6 mm crust	10 mm crust
Sandy Loam	20.52	20.52	14.4	11.52
Clay Loam	13.68	4.32	2.88	0.72
Medium Clay	5.4	5.4	2.88	2.16
Cumulative infiltration (mm)				
Soil	No crust	2 mm crust	6 mm crust	10 mm crust
Sandy Loam	489.97	498.08	364.51	281.39
Clay Loam	330.7	105.37	70.963	17.663
Medium Clay	129.85	128.75	68.234	50.877

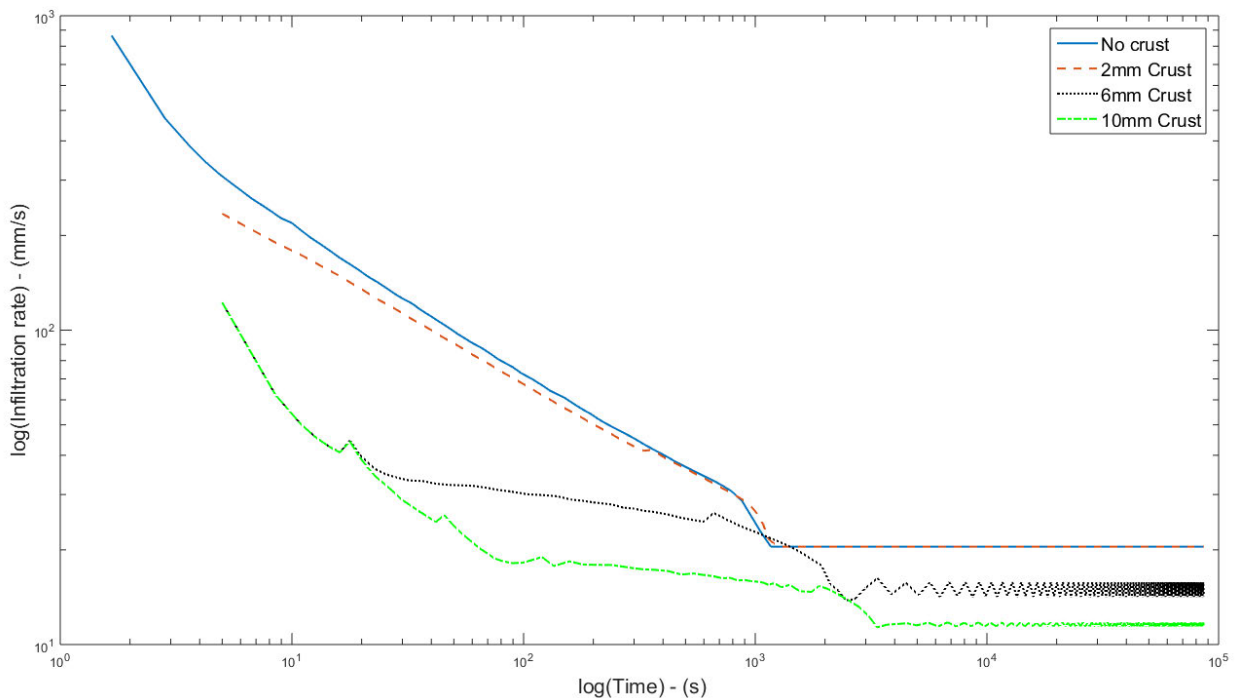


Figure 13 Infiltration rates over 24 h for the Sandy Loam on a log – log scale

Figure 13 is an example of the infiltration rates over a 24 h period for the Sandy Loam soil. The other soils had a similar profile. All soils reached a steady infiltration rate within the 24 h time period of the simulation. The time taken to reach the steady infiltration rate was roughly similar for the no crust and 2 mm crust simulations and progressively longer for the 6 mm and 10 mm crust across all simulations.

3.3.5. Simulation Five: Non-uniform crusts

The impact of non-uniform crusts was simulated by changing the soil profile to have five soil layers. The top four layers (with a thickness of 1 mm) had densities descending from 1.8 g/cm^3 in 0.1 g/cm^3 increments until the underlying soil ρ_b was reached (the right hand most profile in Figure 7 provides a visual representation of the profile). The ponded head scenario was selected as it ensures that the infiltration capacity of the soil was exceeded throughout the simulation with a simulation time of 600 s. All other parameters remained the same as detailed in Simulation One.

Table 9 Comparison of cumulative infiltration for no crust, 2mm crust, 6 mm crust and variable crust simulations

Cumulative Infiltration (mm)				
Soil	No crust	2 mm Crust	6 mm Crust	Variable Crust
Sandy Loam	9.8928	8.8522	4.7709	8.6848
Clay Loam	6.5078	3.5861	1.2744	3.5168
Medium Clay	3.4166	2.6691	1.1146	2.3978

Table 9 details the cumulative infiltration values for the no crust, 2 mm crust, 6 mm crust and variable crust simulations. Cumulative infiltration under the variable crust simulation approximates cumulative infiltration with a 2 mm crust for all three soils. Figure 14 provides a comparison of infiltration rates and cumulative infiltration for the Medium Clay soil. Similar profiles were obtained for the other two textures. Infiltration rates in all cases under the variable crust condition were similar to the 2 mm crust.

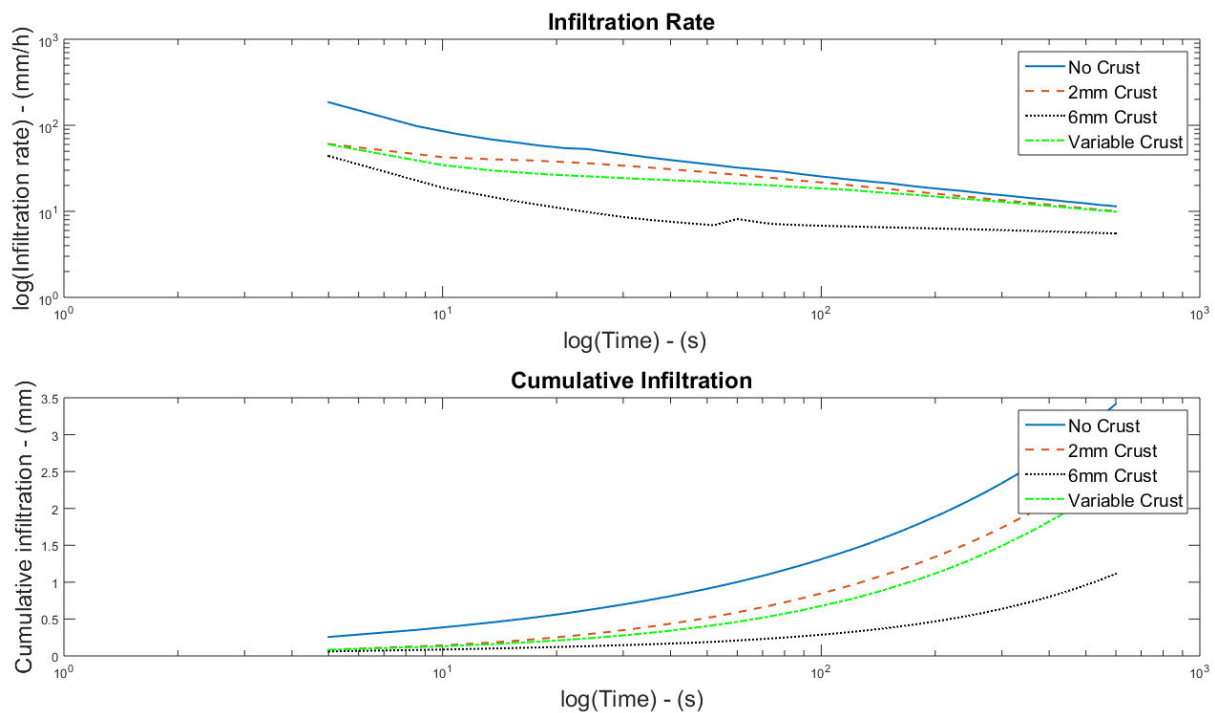


Figure 14 Infiltration and cumulative infiltration rate comparison for medium clay

3.3.6. Conclusion

A number of simulations testing different parameters have been completed to assess the effectiveness of HYDRUS-1D in modelling infiltration on crusted soils.

The simulations indicate that a surface seal/crust of higher ρ_b than the underlying soil results in substantially less cumulative infiltration than an un-crust soil. These results align with what has been identified in the literature and confirm the importance of considering surface crust ρ_b for hydrologic modelling. One potential issue was identified in the results, under the ponded head simulation, where there was very little difference in cumulative infiltration between the no crust and 2 mm crust. This result does not align with the literature which indicates that even thin crusts can result in a large reduction in infiltration. The results from the non-uniform crust simulation suggest that

there is little advantage in modelling a crust as a non-uniform layer, which suggests a limitation in the model parameters given the literature observations of naturally occurring crusts.

Having identified/confirmed that increasing the ρ_b has an impact on infiltration, more realistic modelling of soil hydraulic properties and infiltration based on observed data will now be examined.

3.4. Determining the Soil Water Characteristic from the observed data

The parameters for the SWC were obtained by using the RETC software application (van Genuchten et al. 1991). RETC can be used to derive the input parameters required by a number of models that generate a SWC and HCF. These models include the Brooks and Corey and VG equations for soil water retention and Burdine and Mualem pore-size distribution models (van Genuchten et al. 1991).

3.5. Observed soil water retention data

Modelling in the previous section used arbitrarily selected ρ_b values to identify the impact of a surface crust upon infiltration. The modelling conducted in the remainder of this chapter makes use of measured soil properties as input data. The data has been obtained from the US Department of Agriculture's (USDA) UNSaturated SOil hydraulic DATabase (UNSODA) database (Nemes et al. 2015). UNSODA is a database of soil hydraulic properties from nearly 800 soil samples across the world (Nemes et al. 2015). Data included in UNSODA includes:

- Site details
- Profile information
- Lab and field data for hydraulic conductivity, water retention and other soil hydraulic properties
- Soil texture and bulk density data.

Data from soils representing fine, medium and coarse grained textures were selected that met the following characteristics:

- Data was for the surface horizon.
- A minimum of eight soil water characteristic data points measured for drying of the soil (very few samples had soil water characteristic data for wetting).
- Where possible, soil water retention data was available to a suction of 153 m (Permanent Wilting Point). For a couple of soils the retention data was not available at or near the 153 m suction.

The aim was to select four soils per texture class however there were only two clay textured soils that met these requirements. A summary of the selected soils is shown in Table 10.

Table 10 Observed Soil Data Summary

Soil code	Texture	Location	Sand	Silt	Clay	ρ_b
2620	clay	Rotenbach, Schwarzsee, Switzerland	17%	36%	48%	1.07
4120	clay	Kalloo (Antwerp), Belgium	14%	35%	51%	1.24
2580	loam	Burgdorf, Switzerland	36%	50%	14%	1.08
2590	loam	Marthalen, Switzerland	34%	48%	18%	1.07
2650	loam	Marthalen, Switzerland	49%	33%	19%	1.22
2750	loam	Zugerberg, Switzerland	52%	30%	19%	1.01
1090	loamy sand	Lillington, NC, USA	81%	10%	9%	1.13

2570	loamy sand	Rheinau, Switzerland	87%	10%	3%	1.5
3130	loamy sand	Dickey Co., ND, USA	76%	19%	6%	1.44
4010	loamy sand	Booischoot (Mechelen), Belgium	79%	17%	5%	1.59

3.5.1.RETC modelling without retention data

Initially the RETC 'Direct' (or forward fitting) option was selected to determine the SWC. The VG Retention Curve Model (with $m = 1 - 1/n$) and Mualem Conductivity Model were selected, see Equation 10 and Equation 11. The Mualem Conductivity Model is most commonly paired with the VG Retention Curve Model (Radcliffe & Simunek 2010). Soil hydraulic parameters were calculated by entering the Sand, Silt, Clay and ρ_b (SSCBD) data into the ROSETTA PTF which is inbuilt into RETC (and HYDRUS-1D).

The predicted (RETC) and observed (UNSODA) data were plotted against each other for each of the selected soils. The Direct fitting option in RETC does not calculate the parameters required to apply the VG equation, therefore linear regression in Microsoft Excel using the LINEST function was used to develop a function to relate the water content to the matric potential. In all instances a logarithmic function was found to be the best fit.

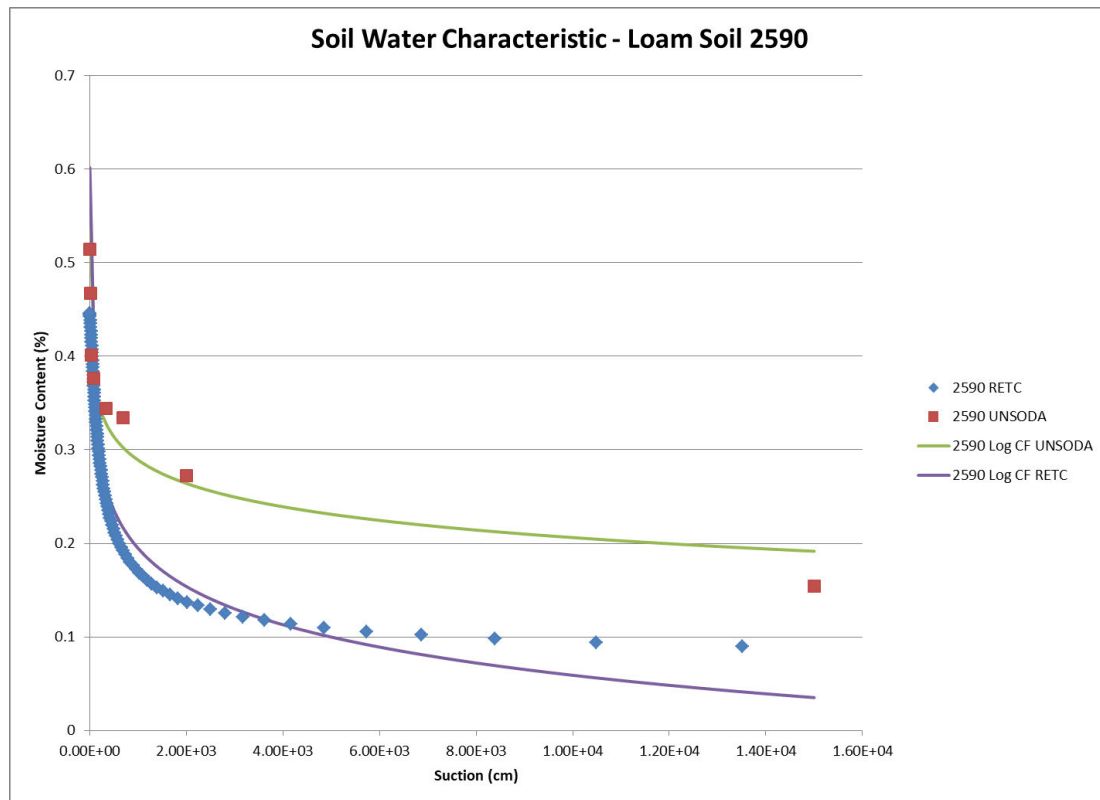


Figure 15 Soil Water Characteristic - Loam Soil Code 2590

Figure 15 is an example of the predicted versus observed soil water characteristic. The points represent the predicted or observed data points from RETC and UNSODA respectively whilst the lines represent the curve generated from the LINEST function ($r^2 = 0.94$ for the RETC data curve fit and $r^2 = 0.96$ for the UNSODA data curve fit).

Figure 16 compares the predicted versus observed results and the 1:1 line. If the predicted (P) and observed (O) data closely aligned the 1:1 and P-O lines would be very close to one another. In this instance it can be seen that there is not good alignment between the 1:1 and P-O lines indicating that the predicted data does not align closely to the observed data. This result was seen to a greater or lesser with all of the soils examined. This is an indication that the selected fitting model (Direct fitting) within RETC does not provide the required level of accuracy.

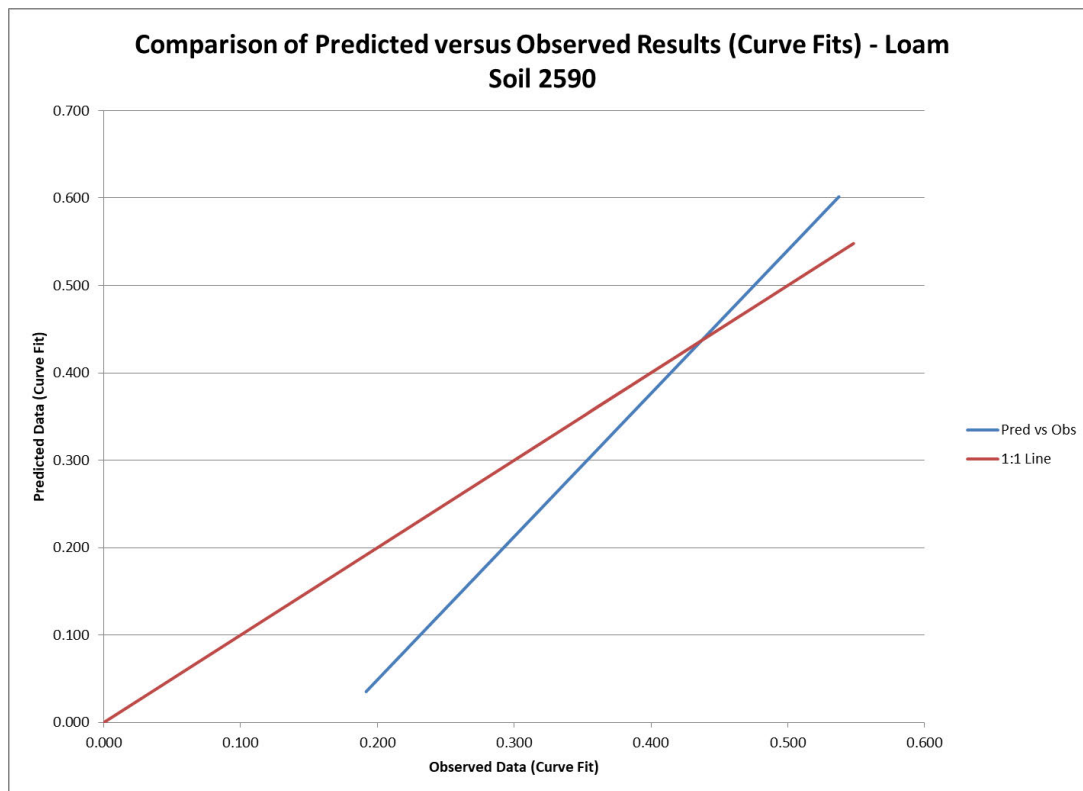


Figure 16 Comparison of Predicted vs Observed Results - Loam Soil Code 2590

3.5.2.RETC modelling incorporating retention data

The next modelling activity used the 'Retention data only' fitting type within RETC. All other inputs remained the same with the exception of using the observed hydraulic retention data parameters from the UNSODA database.

Figure 17 provides examples of the Soil Water Characteristic (Figure 17a, c & e) and Predicted versus Observed results (Figure 17b, d & f) respectively for three of the soils. The results are substantially better than those achieved from the 'Direct' fitting type within RETC. The close alignment of the results indicates that the logarithmic curve fitted equation from the RETC modelling can be used as a proxy for the SWC. These equations will be used in the next modelling step where the ρ_b will be increased to investigate the impact on the SWC.

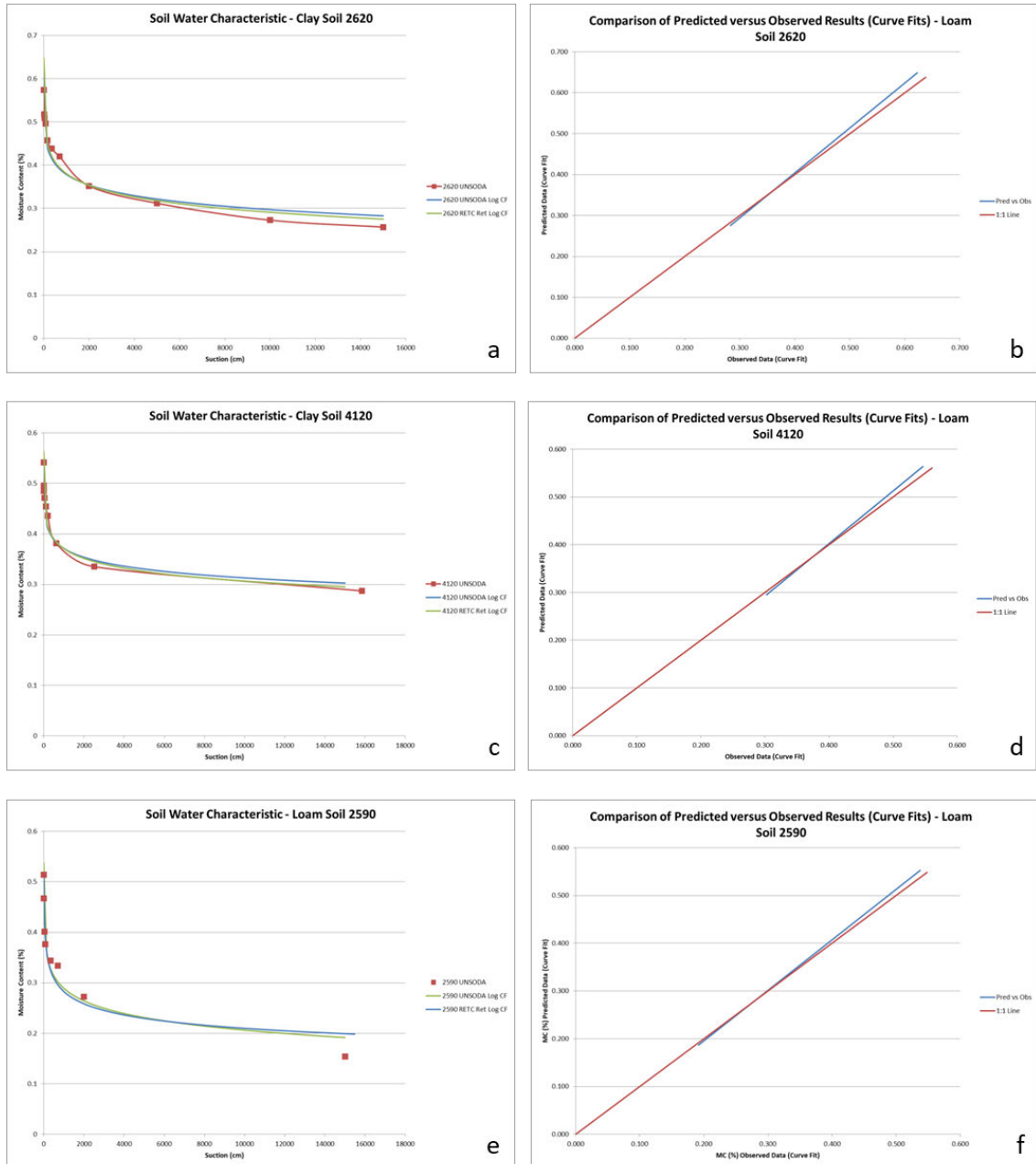


Figure 17 Example Retention Parameter Modelling using RETC

The relationship between these logarithmic curve fitting functions is defined by Equation 15 where θ (%) is the moisture content and ψ is the matric potential or suction (cm). 'a' and 'b' are fitted parameters determined from the LINEST function within Microsoft Excel.

$$\theta = a \times \log_{10} \psi + b \quad \text{Equation 15}$$

The parameters 'a' and 'b' and associated r^2 value for each of the soils are detailed in Table 11. The parameters for soils code 4010 has not been provided due to spurious results in RETC/the LINEST function, which has not been resolved. The minimum r^2 value is 0.843 (Loamy Sand 3130) with all other values being greater than 0.9 indicating that the developed functions are a good fit to the data.

Table 11 'a' and 'b' parameters for Soil Water Characteristic

Soil code	Texture	a	b	r ²
2620	clay	-0.0893	0.6223	0.964
4120	clay	-0.0643	0.5637	0.969
2580	loam	-0.0785	0.6443	0.994
2590	loam	-0.0875	0.5523	0.939
2650	loam	-0.1131	0.5808	0.988
2750	loam	-0.1047	0.6518	0.992
1090	loamy sand	-0.1144	0.4312	0.933
2570	loamy sand	-0.1742	0.6322	0.904
3130	loamy sand	-0.2289	0.7039	0.843

3.6. Modelling the Soil Water Characteristic as ρ_b increases

3.6.1. Retention data only

The first attempt at modelling the changes in the SWC resulting from increased ρ_b used the 'Retention data only' fit option in RETC. The soil hydraulic properties were recalculated using the inbuilt ROSETTA PTF with the ρ_b of the soil samples being increased by 0.1 g/cm³ per iteration. Soil texture and the observed water retention data points remained the same.

The Clay soil code 2620 was modelled with four bulk densities (1.07 (initial value), 1.17, 1.27 and 1.37 g/cm³). The results of the RETC predicted soil water characteristic are detailed in Figure 18. The results from each scenario are the same.

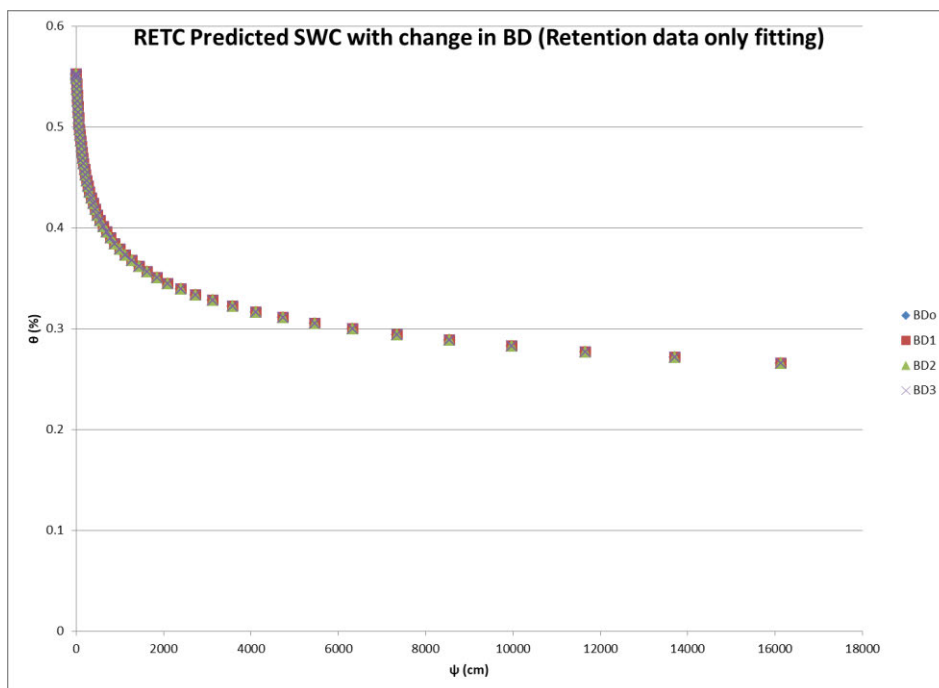


Figure 18 Clay soil 2620 - Impact of changed ρ_b on SWC

Initially this result caused some confusion. The RETC output file (RETC.OUT) for each scenario was compared. The initial hydraulic properties were different for each scenario. However the iterative approach used by RETC to develop the soil water characteristic when combined with the selected curve fitting option (using observed retention data) resulted in the output for each scenario converging

to the same result. In hindsight this became clear and indicated that the ‘Retention data only’ fit option was inappropriate for this modelling.

3.6.2. Forward problem and correction factor function

The second attempt used the ‘Forward problem’ fitting option (i.e. no retention data was used in predicting the soil water characteristic). The substantial difference between the RETC predicted results using the ‘Forward problem’ and the observed retention points, as visually demonstrated in Figure 15, was identified as a problem. To overcome this, a correction factor function was determined by:

- Determining the difference between the RETC predicted forward problem and UNSODA observed functions for 100 equally spaced water potential data points (ψ range 1 cm to 15,000 cm).
- Use the LINEST function to complete a curve fit of the difference and derive the ‘a’ and ‘b’ parameters to develop a correction factor function.
- The correction factor function was added to the curve fit function derived from the RETC forward problem solution.

An example of the correction factor function is detailed in Figure 19. The blue line represents the curve fitted function of the observed water retention data from the UNSODA data base. The red line is the RETC predicted SWC function using the forward problem fit type. The difference between the observed and predicted functions is the purple line. The green points are the total of the RETC predicted SWC and correction factor functions, which provides a very good approximation of the original UNSODA observed function. Equation 3 represents the SWC for the clay soil code 2620 with the original ρ_b .

$$\theta = (-0.136 \times \log_{10} \psi) + 0.703 + (0.055 \times \log_{10} \psi) - 0.081 \quad \text{Equation 16}$$

The results demonstrated in Figure 19 validate the correction factor approach to using the RETC forward problem fitting option. This approach was taken for all of the soils with similar results.

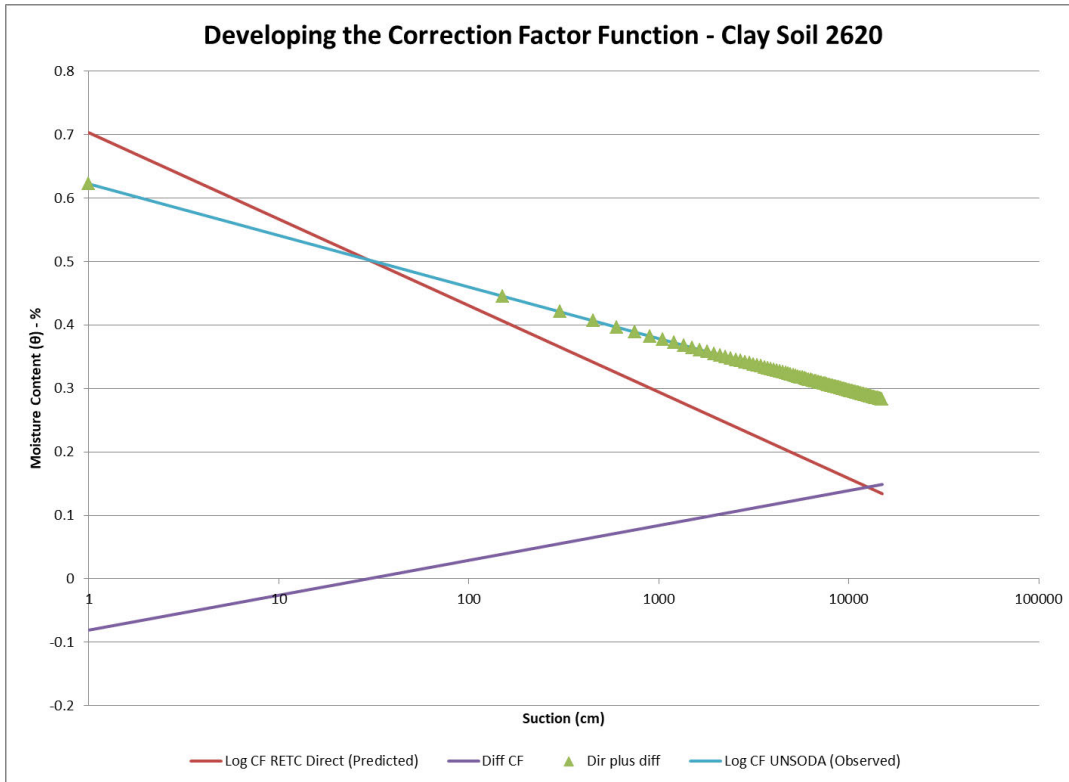


Figure 19 Example development of the correction factor function for clay soil code 2620 (logarithmic x scale)

With this approach validated, five bulk densities were simulated for each soil sample being the original ρ_b value and subsequent increments of 0.1 g/cm^3 . For example, the following ρ_b values were used for clay soil code 2620: 1.07, 1.17, 1.27, 1.37 and 1.47 g/cm^3 .

The results for the clay, loam and loamy sand soils are detailed in Figure 20, Figure 21 and Figure 22 respectively with a logarithmic x-axis. For all soils the change in ρ_b results in a change to the SWC. As ρ_b increases, θ decreases for a given ψ . This is particularly the case for smaller ψ values. As ψ increases θ , particularly for the clay and loam textured soils either converge or come close to converging. This is not the case for the loamy sand soils where the results appear less reliable with the SWC intersecting and in some instances negative θ values being predicted.

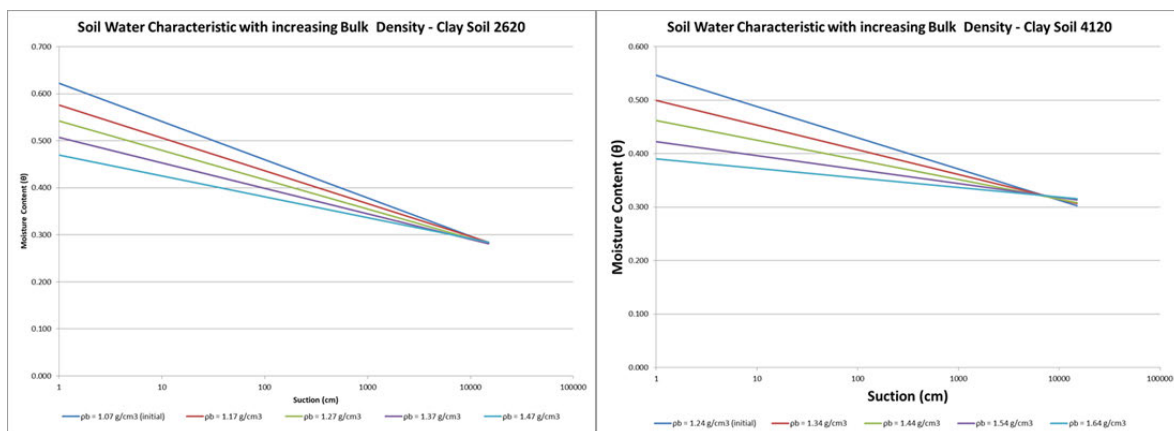


Figure 20 Soil Water Characteristic with increasing ρ_b for two clay soils

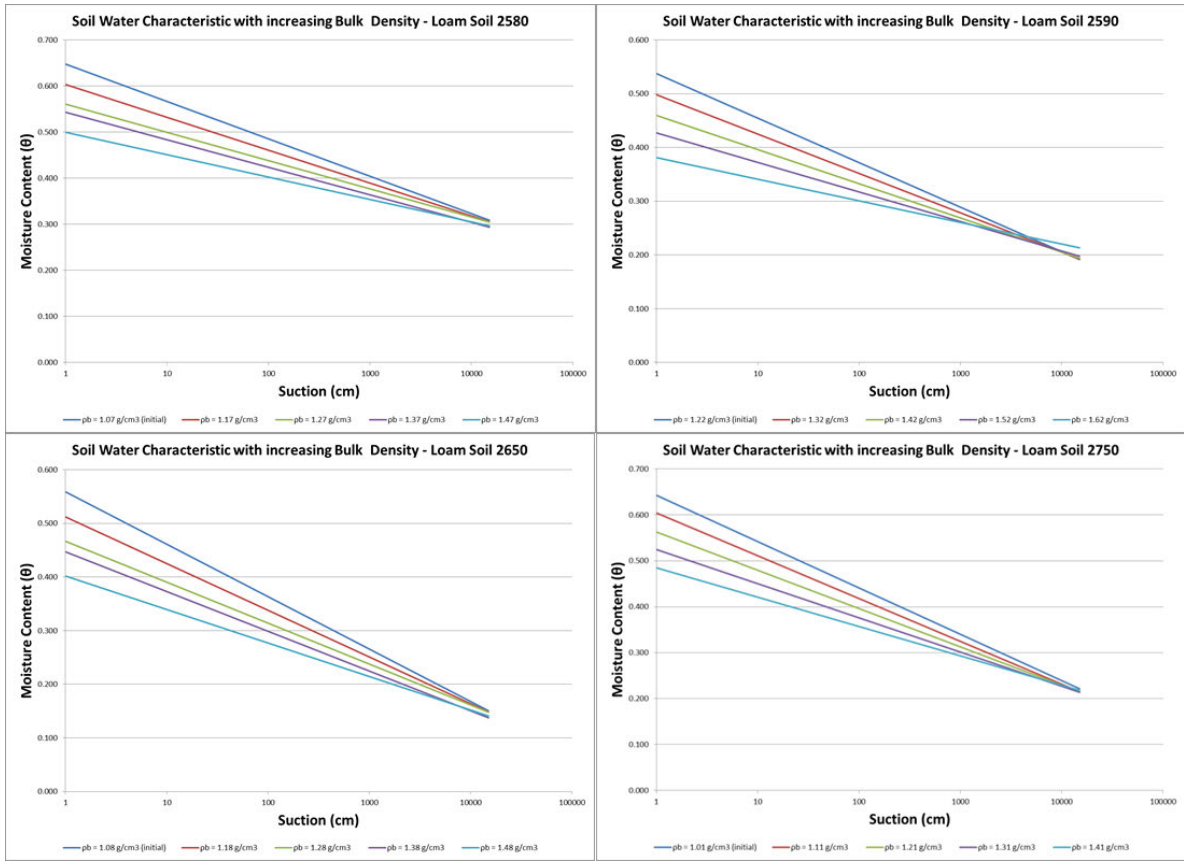


Figure 21 Soil Water Characteristic with increasing ρ_b for four loam soils

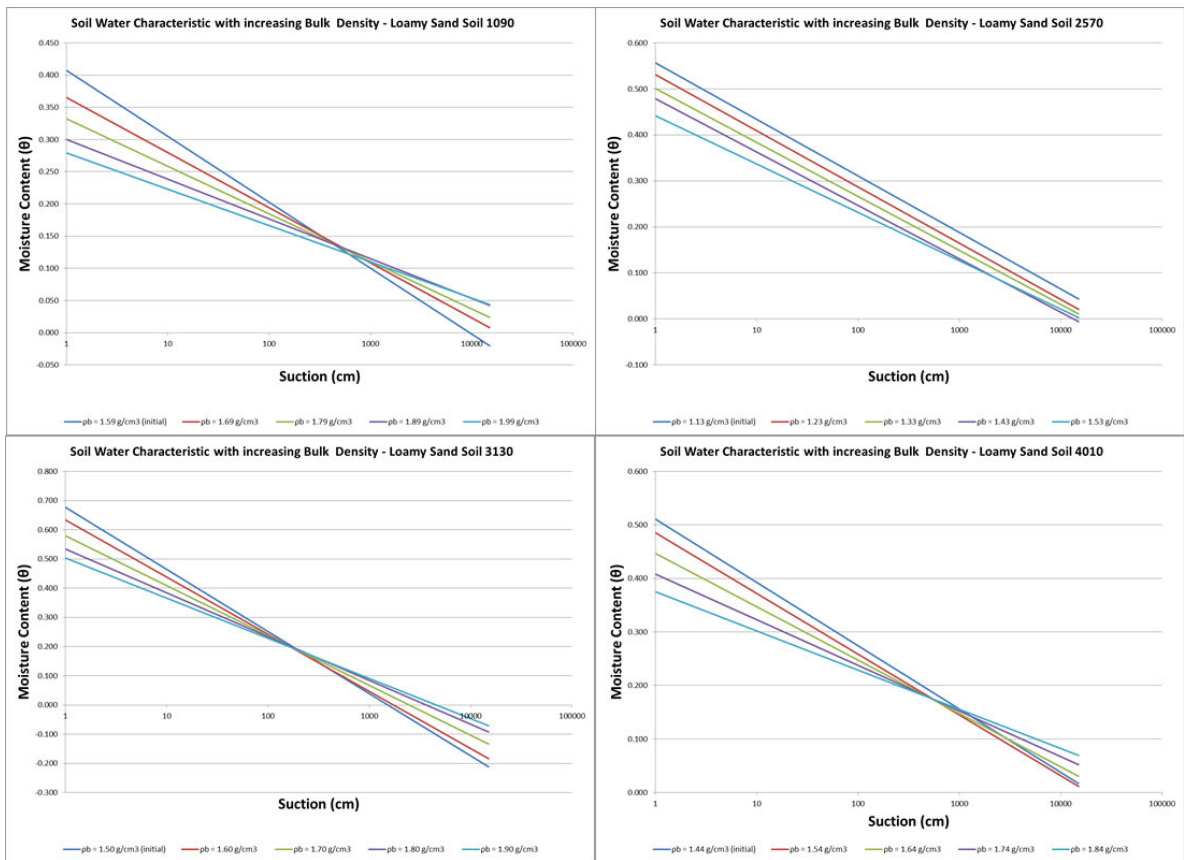


Figure 22 Soil Water Characteristic with increasing ρ_b for four loamy sand soils

3.7. Soil Water Characteristic Pedotransfer development

PTF enable the prediction of soil hydraulic properties without requiring extensive measurement of these properties. This section, based on the modelling completed to date aims to determine whether a PTF can be developed to predict the SWC of a soil as the ρ_b increases. A reliable PTF that achieves this aim could have significant benefits across a number of agronomic and hydrologic applications relating to soil water.

3.7.1. Relationship between SWC 'a' and 'b' regression coefficients

The correction factor approach taken in modelling the SWC as ρ_b increases results in two regression coefficients for 'a' and 'b.' The SWC regression coefficients have been determined for all soils and all ρ_b values.

Relationships between these coefficients were analysed to determine their predictive value for an individual soil, for soils of a single texture class and for all soils. This was achieved by obtaining the regression equation from a scatter plot of the 'b' versus the 'a' coefficients.

Figure 23 details the scatter plots for each of the soils grouped by textural class and highlights that for all soils there is a linear relationship between the coefficients. Figure 24 includes a line of best fit and regression equation for the 'a' and 'b' coefficients grouped by textural class. There is a strong relationship between these coefficients for clay ($r^2 = 0.93$) and loam ($r^2 = 0.99$) soils and a moderate relationship for the loamy sand textured soils ($r^2 = 0.76$).

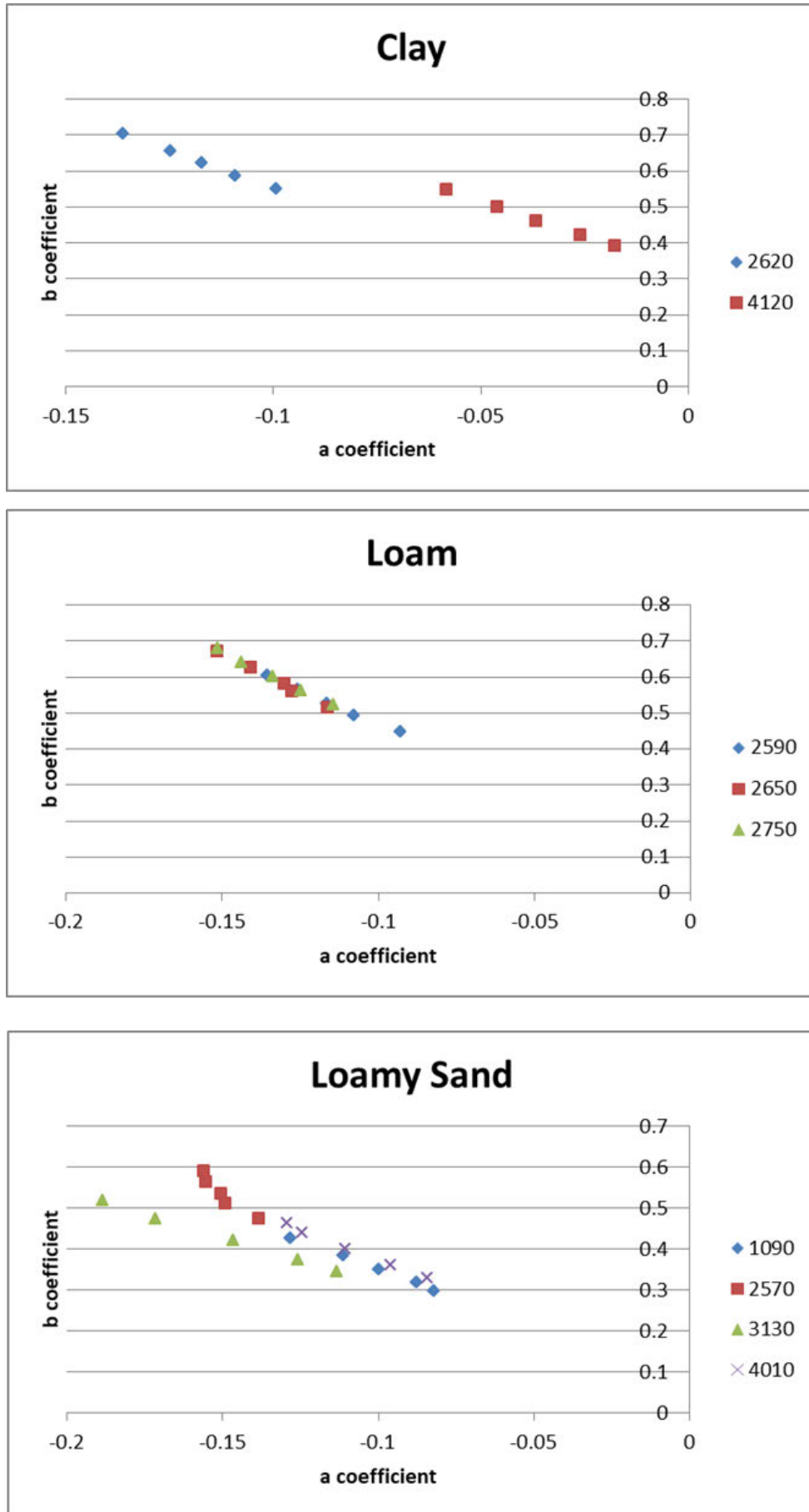


Figure 23 Relationship between 'a' and 'b' coefficients for clay, loam and loamy sand soils

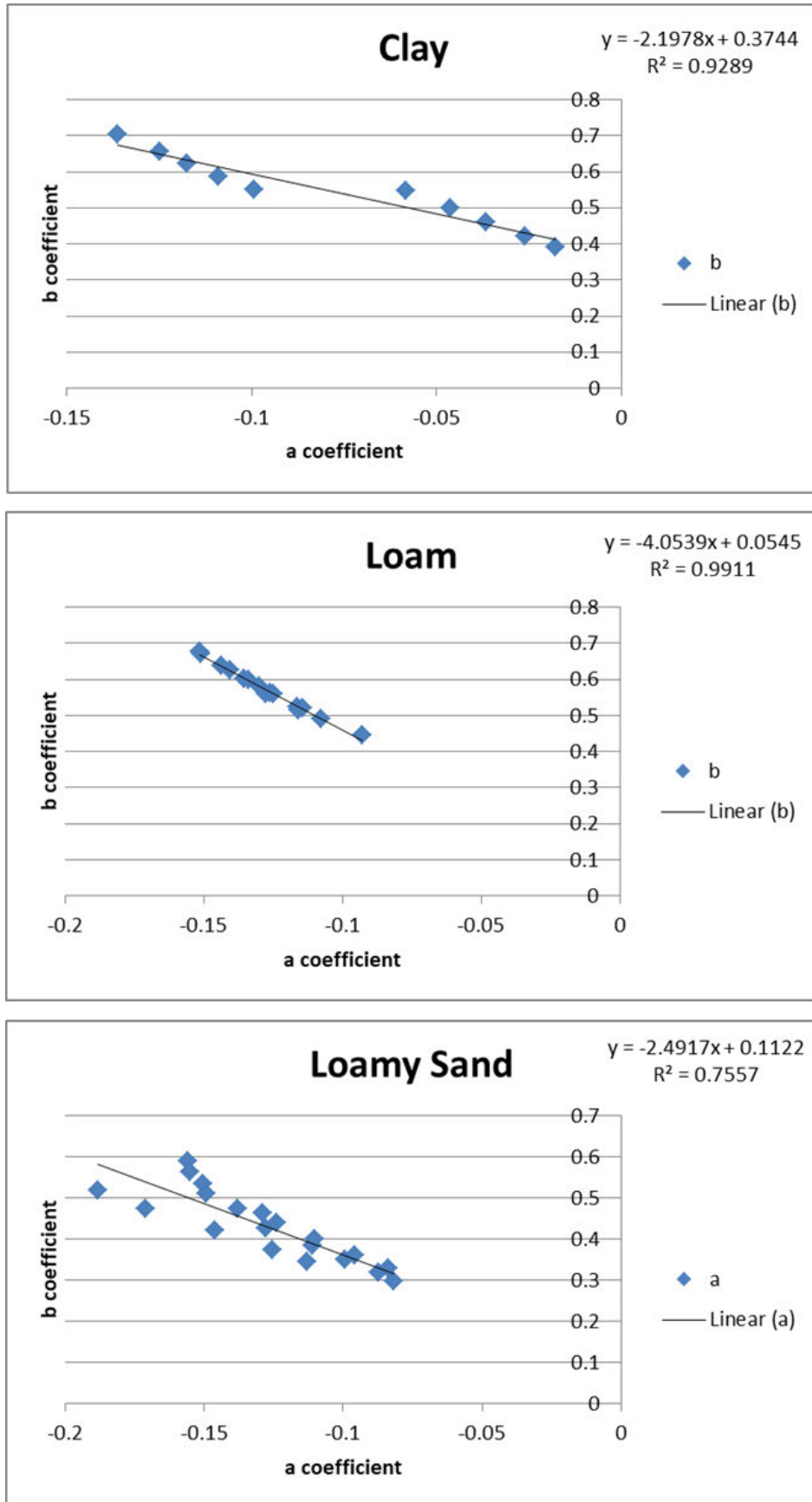


Figure 24 Relationship between 'a' and 'b' coefficients by soil textural class

Figure 25 demonstrates that the global relationship for all soils is weak ($r^2 = 0.20$) indicating that the relationship between the coefficients is potentially useful at the soil textural class level but not for all soils.

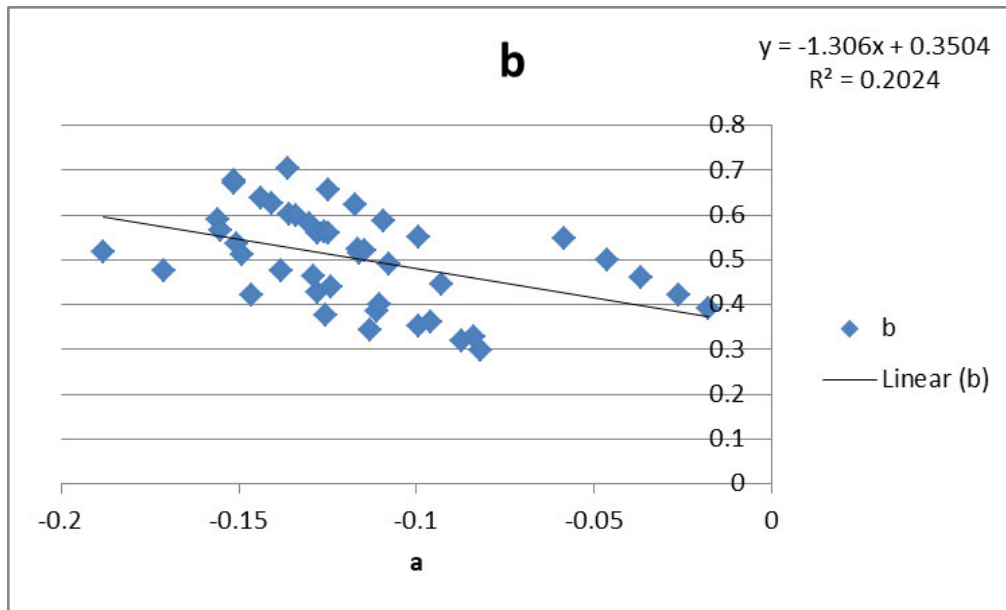


Figure 25 Relationship between 'a' and 'b' coefficients for all soils

For the relationship between the coefficients to be practically useful requires a relationship to be established between the coefficients and a measurable soil property such as ρ_b . Figure 26 details the relationships between the 'b' coefficient and ρ_b . Moderate relationships exist between the coefficients with r^2 values of 0.55, 0.75 and 0.58 for the clay, loam and loamy sand textural classes respectively.

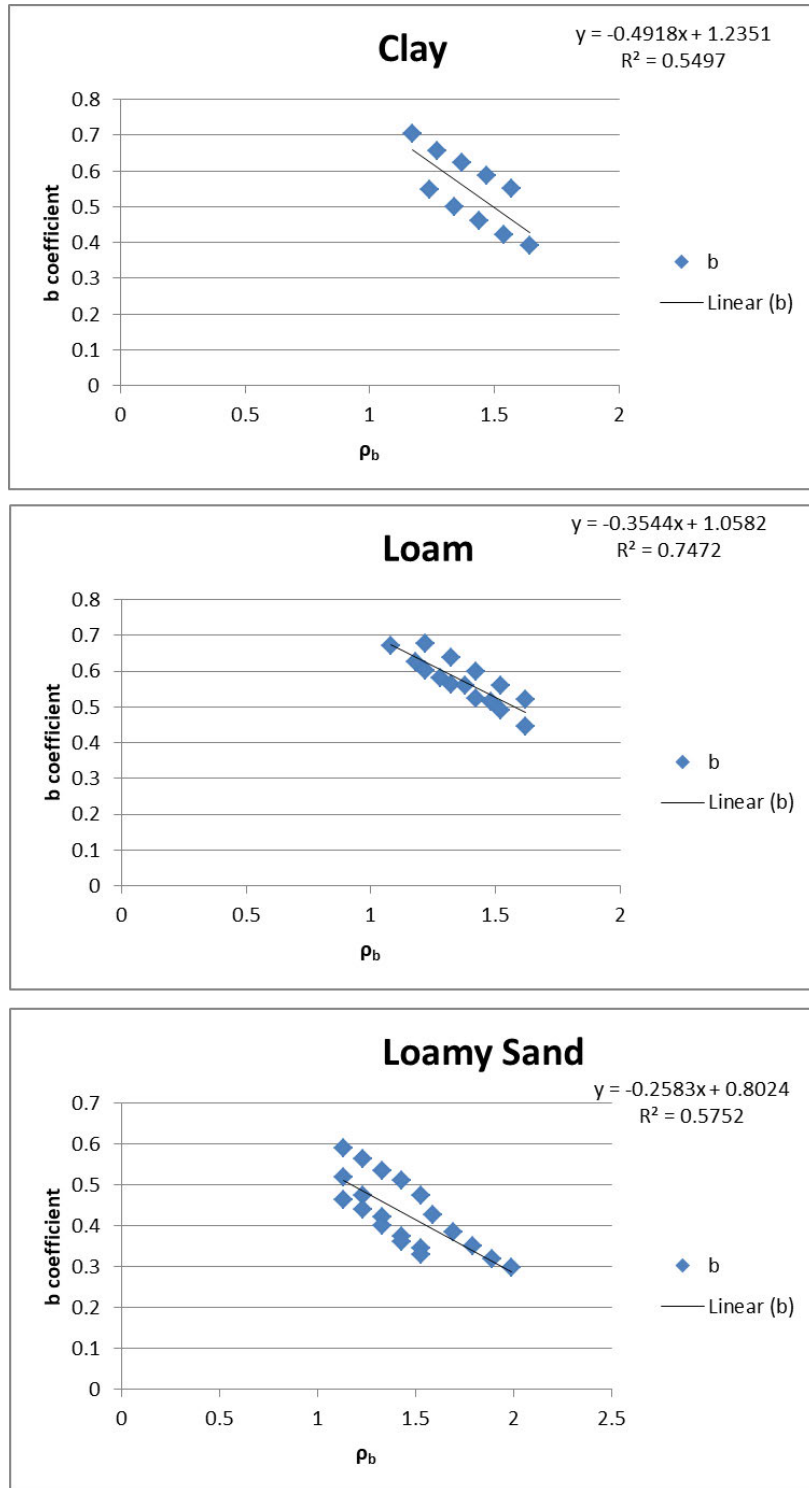


Figure 26 Relationships between 'b' coefficient and ρ_b

To determine whether the 'a' and 'b' coefficients are useful at the soil textural class level the regression equations relating the 'b' coefficient to the initial ρ_b value and subsequently the 'a' coefficient to the 'b' coefficient were applied. The resulting coefficients along with the coefficients obtained from the RETC Forward (Direct) data fitting option are detailed in Table 12. The average difference between the modelled and RETC 'a' and 'b' coefficients are -3.9% and -4.1% respectively. Soil 3130 (loamy sand) can be considered as an outlier because the highest observed ψ data point is 834 cm compared to the other soils with the highest ψ data point being at or around 15,000 cm. If the

coefficient for soil 3130 is thus ignored the average difference between the modelled and RETC 'a' and 'b' coefficients reduces to 1.3% and -1.2% respectively.

Table 12 RETC generated and model predicted values for 'a' and 'b' coefficients

Texture	Code	ρ_b	Modelled 'a'	RETC 'a'	% diff Δ 'a'	Modelled 'b'	RETC 'b'	% diff Δ 'b'
Clay	2620	1.07	-0.1468	- 0.1362	7.8%	0.7089	0.7031	0.8%
Clay	4120	1.24	-0.1115	- 0.1205	-7.4%	0.6253	0.6458	-3.2%
Loam	2650	1.08	-0.1529	- 0.1514	1.0%	0.6754	0.6726	0.4%
Loam	2580	1.07	-0.1538	- 0.1514	1.6%	0.6790	0.6836	-0.7%
Loam	2590	1.22	-0.1408	- 0.1356	3.8%	0.6258	0.6016	4.0%
Loam	2750	1.01	-0.1590	- 0.1514	5.0%	0.7003	0.6774	3.4%
Loamy Sand	2570	1.13	-0.1518	- 0.1560	-2.7%	0.5105	0.5900	-13.5%
Loamy Sand	3130	1.5	-0.1229	- 0.1883	-34.8%	0.4150	0.5183	-19.9%
Loamy Sand	1090	1.59	-0.1158	- 0.1279	-9.4%	0.3917	0.4264	-8.1%

These coefficients were used to generate a SWC for each soil using Equation 1. The results for a representative soil from each texture class are detailed in Figure 27 and compared with the SWC curve fitted function developed from the RETC Direct fit data output (i.e. using the RETC coefficients detailed in Table 12) as well as the observed data from the UNSODA database. The results across all soils (less the outlier soil code 3130) were similar and indicate that the approach of obtaining coefficients at the textural class level and then applying the coefficients to the ρ_b of an individual soil result in a SWC that matches closely with the SWC predicted from RETC using the Direct fitting option. The predicted SWC does differ considerably from the observed values however the addition of a correction factor function (as was applied to the direct fitting option) could enable a close match to the observed data.

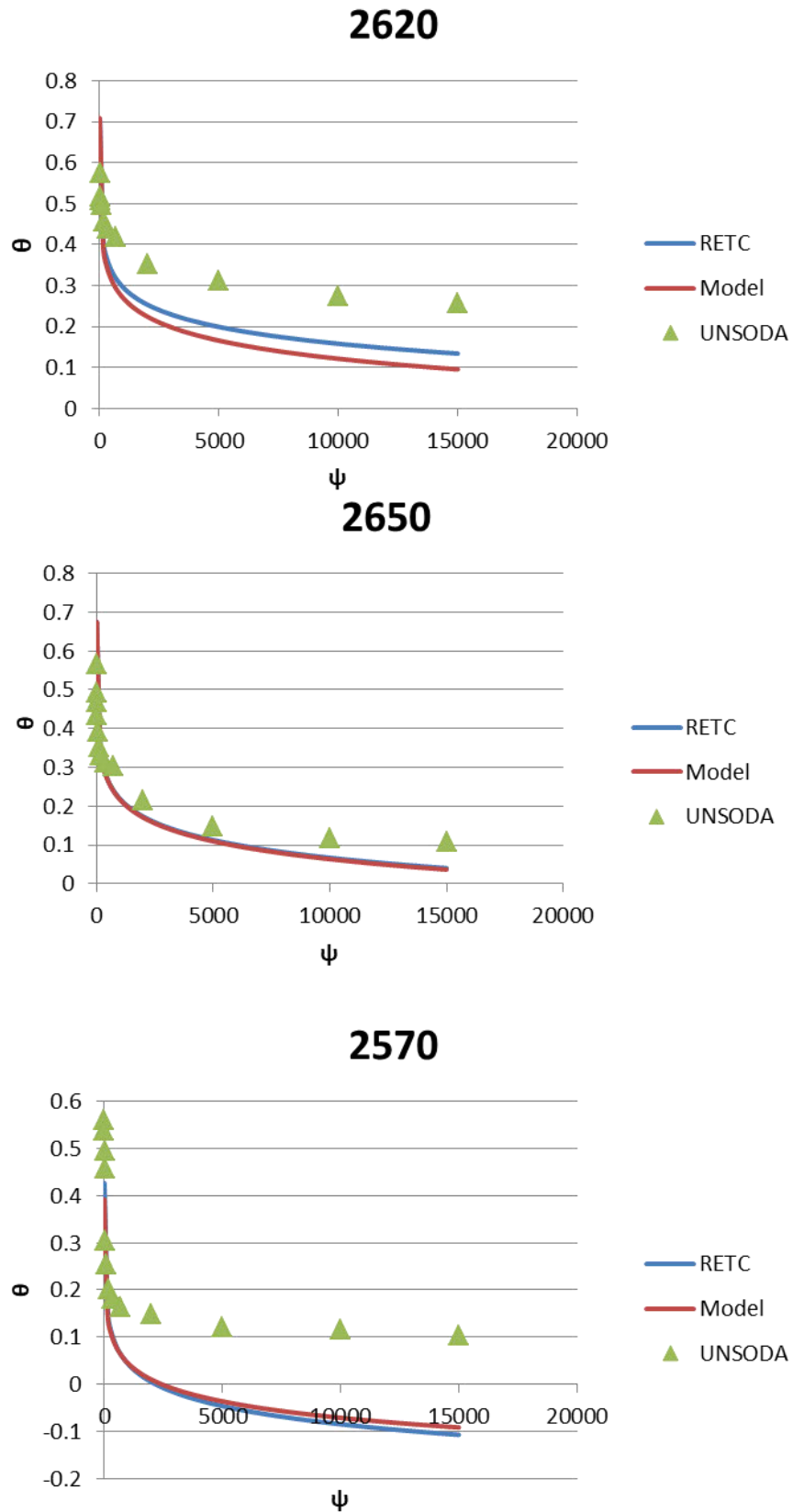


Figure 27 SWC comparison by textural class

To achieve this, regression coefficients of the correction factor function coefficients (Table 13) for each soil were averaged by textural class (Table 14).

Table 13 Correction factor coefficients

Soil code	Texture	'a' coefficient	'b' coefficient
2620	clay	0.054967	-0.080731
4120	clay	0.062084	-0.099439
2580	loam	0.070317	-0.036020
2590	loam	0.052848	-0.064232
2650	loam	0.053620	-0.113744
2750	loam	0.050584	-0.034962
1090	loamy sand	0.025544	-0.019199
2570	loamy sand	0.033149	-0.033427
3130	loamy sand	-0.024440	0.158535
4010	loamy sand	0.010645	0.046412

Table 14 Average 'a' and 'b' coefficient values

Texture	'a' Average	'a' STDEV	'b' average	'b' STDEV
Clay	0.0585256	0.003558	-0.090085	0.009354
Loam	0.056842	0.03197	-0.062239	0.03197
Loamy sand	0.0112242	0.075784	0.0380802	0.075784

The correction factor function was then added to the predicted SWC and plotted. The results for six soils are detailed in Figure 28. For most of the soils this approach produced a SWC that was similar to the observed water retention data points however was not as consistently accurate as the SWC developed from the individual soils modelling.

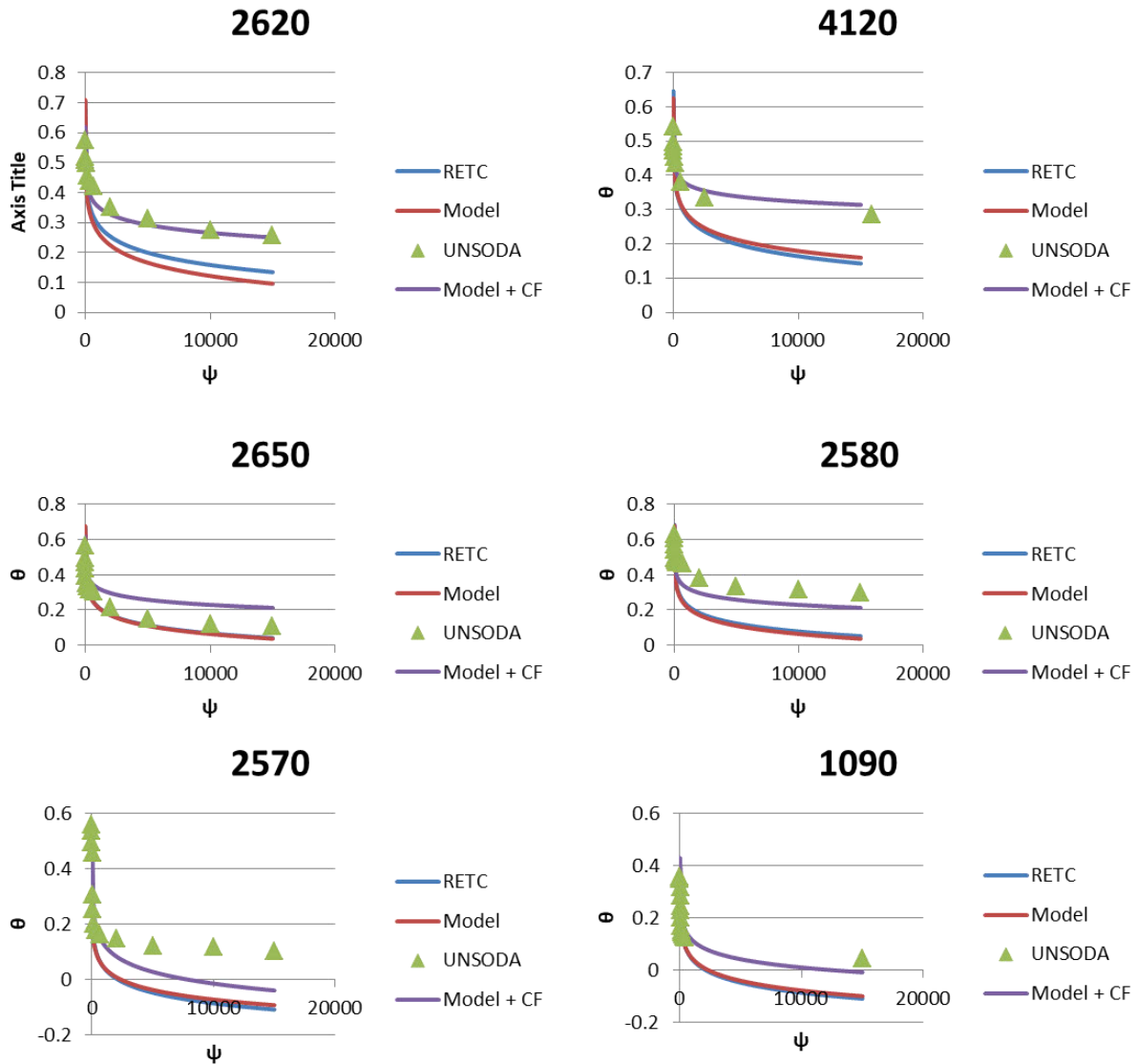


Figure 28 Modelled SWC with Correction Factor

This modelling indicates that a PTF can be developed that enables the SWC to be predicted reasonably accurately as ρ_b increases. Further modelling using a larger sample size and more soil types should be completed to refine the PTF and test its usefulness. More sophisticated analysis techniques, such as regression trees, could also be applied to identify whether other soil parameters, such as clay content, could be incorporated to improve the reliability/applicability in predicting the SWC.

3.8. Modelling the Hydraulic Conductivity Function

The Hydraulic Conductivity Function (HCF) is the second function required to fully describe soil hydraulic behaviour. Mualem's hydraulic conductivity model is most commonly coupled with the VG retention equation (Radcliffe & Simunek 2010). The HCF can be expressed in terms of ψ or θ . Mualem's model in terms of both effective saturation (S_e) and ψ are detailed in Equation 11 (Radcliffe & Simunek 2010) and Equation 12 (van Genuchten et al. 1991) where the effective saturation (S_e) = $(\theta - \theta_r)/(\theta_s - \theta_r)$ and $m = 1 - 1/n$.

The parameters required to model these functions are provided when the Retention data fit option is used in RETC. Figure 29 details a plot the HCF for loam soil 2580 from the log(K) values in the

RETc output file and $\log(K)$ values calculated using Equation 12. As would be expected the results align exactly.

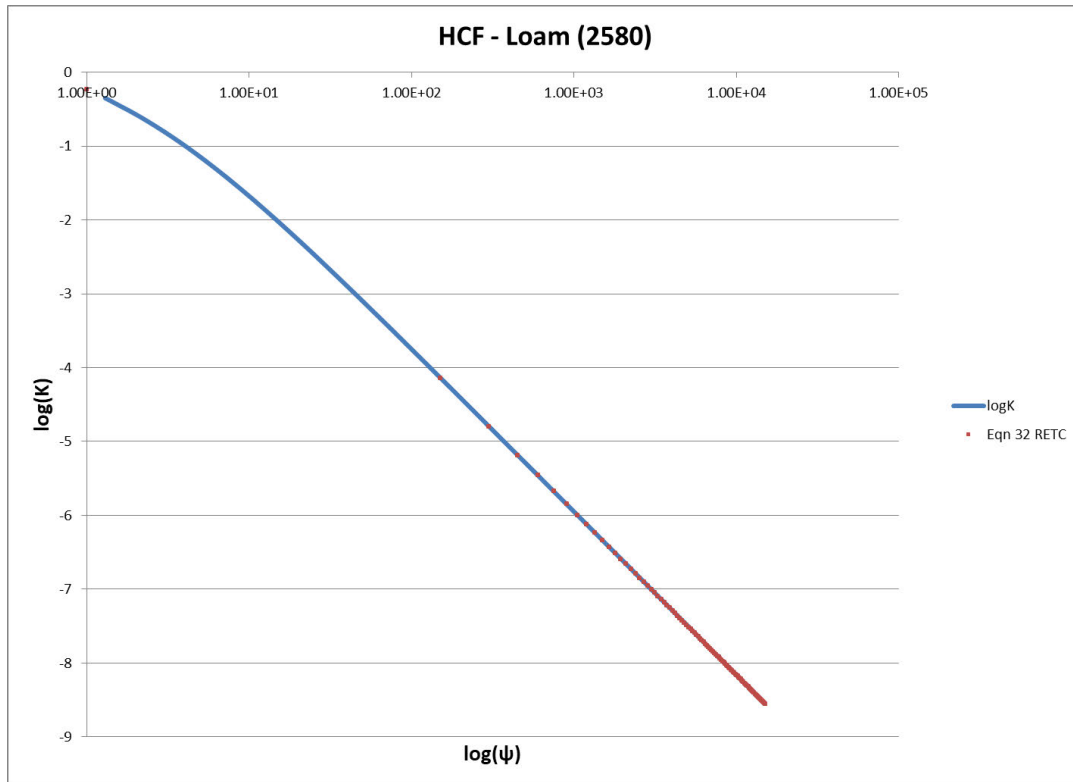


Figure 29 Plot of Mualem equation against RETc Predicted $\log(K)$ output

The RETc predicted values for HCF for each value of ρ_b were plotted. An example is provided in Figure 30 (plotted on a log – log scale). In a corollary to the SWC, as the ρ_b of the soil increases the hydraulic conductivity reduces for a given matric potential. The results were similar for all soils across the texture classes.

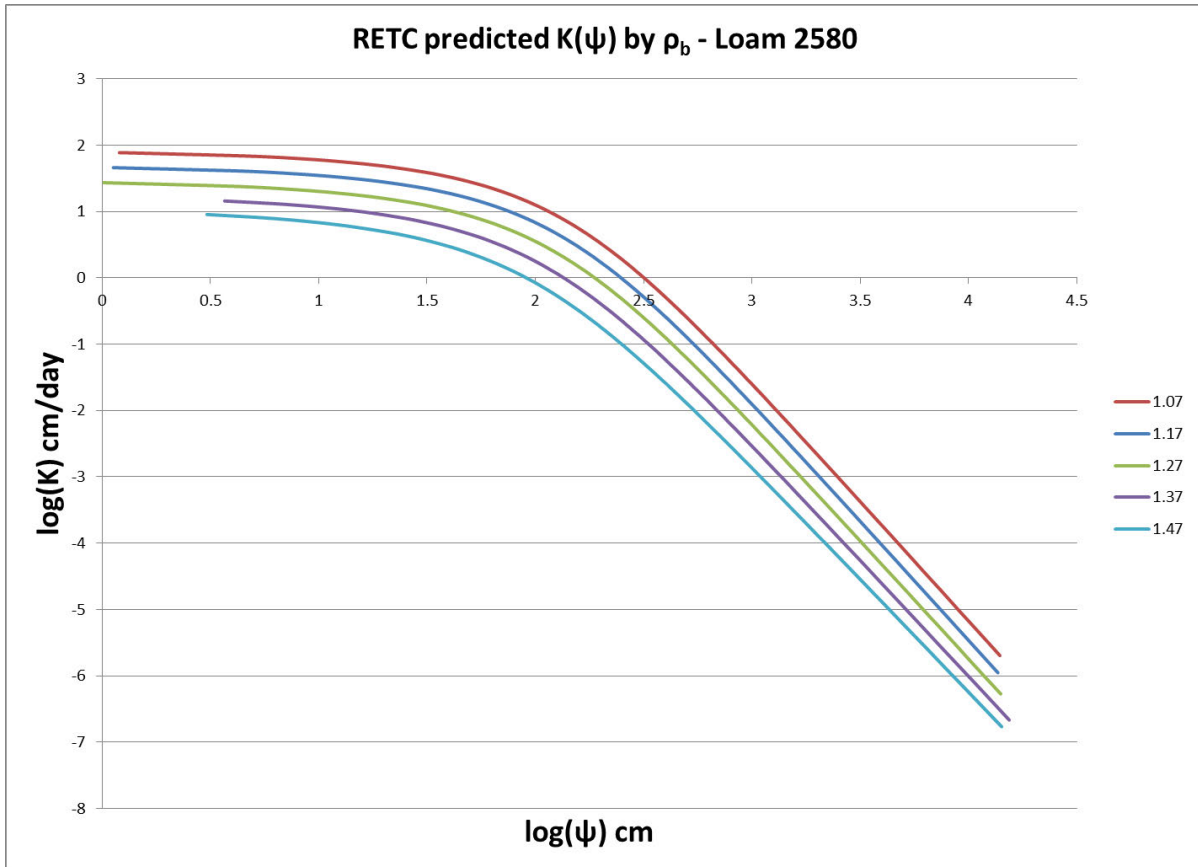


Figure 30 Example HCF for loam soil (Code 2580)

The similar shape of the curves suggests that there is a relationship between the hydraulic conductivity functions. Regression equations for each of the HCFs were developed. Polynomials of degree six were found to be the best fit with the r^2 value approaching 1 in all instances.

Whilst developing a relationship between increasing ρ_b and the HCF is important, further modelling was not required to meet the objectives of the project. As such this aspect of the modelling was not progressed any further but would be a useful extension of the project.

3.9. Modelling infiltration

The modelling completed using RETC from both the observed and predicted soil hydraulic properties provide the soil hydraulic parameters required in HYDRUS-1D. Whilst these parameters can be predicted within HYDRUS-1D using the ROSETTA PTF, the accuracy of the results are poor compared to those obtained from the Retention fitting option in RETC which is calculated from observed data. Five independent soil hydraulic parameters (θ_r , θ_s , α , n , l and K_s) are required by HYDRUS-1D. The first four parameters have been obtained from RETC. 'l' has been assumed to be a constant value of 0.5 which is common practice (Šimůnek et al. 2009) and K_s has been derived from the ROSETTA PTF.

A number of scenarios were modelled to investigate the impact of increased ρ_b on infiltration. The scenarios were:

- Infiltration as ρ_b increases on a single layered soil under ponding conditions
- Infiltration on a two layered soil (with the top layer representing a surface crust as a uniform layer) under ponding conditions

- Infiltration on a multi layered soil (with the top layers representing a surface crust of non-uniform ρ_b) under ponding conditions.

For all scenario's a soil profile segment of 100 mm depth was selected which allows 1 mm segmentation within HYDRUS-1D. Additionally the weighting of the segments was changed to 0.1 to allow much greater fidelity in modelling infiltration through the surface crust. The ψ value was kept at constant value of 100 mm throughout the soil profile segment (the default value in HYDRUS-1D) except for the top of the soil surface which was assigned a value of 0 to represent ponding conditions.

3.9.1. Infiltration on a single layered soil under ponding conditions

The initial modelling of infiltration into a single layered soil under ponding conditions was modelled in HYDRUS-1D for two scenarios. The first scenario used the soil hydraulic parameters obtained from the ROSETTA PTF using the SSCBD data only (i.e. the Direct fit option in RETC). The second scenario used the soil hydraulic parameters obtained by using the SSCBD, water retention and hydraulic conductivity (where available) data (i.e. the Retention or Retention and Conductivity fit options in RETC).

Figure 31 details the results for the clay soil 2620 highlighting that the infiltration predicted using the Direct fit derived soil hydraulic properties is significantly higher at all times, including the steady infiltration rate. The steady infiltration rate is 157% higher in the Direct Fit modelled infiltration.

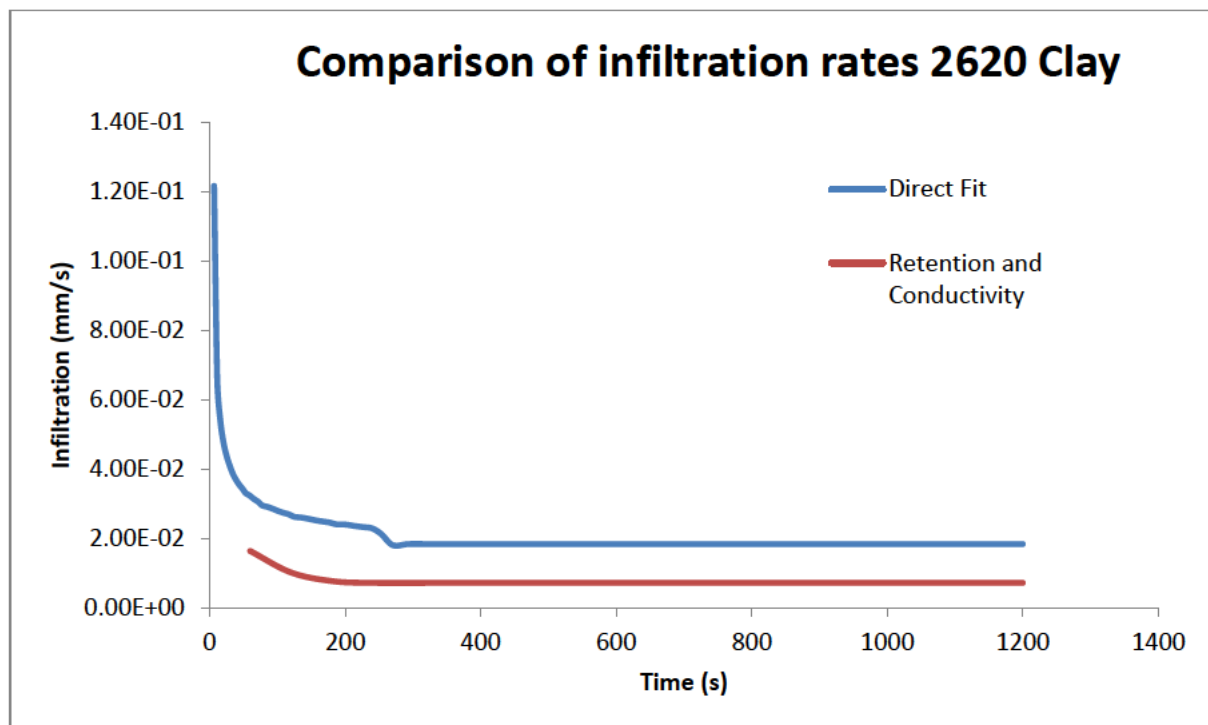


Figure 31 Infiltration rate comparison using different Soil Hydraulic Properties

To model the impact of increasing ρ_b on infiltration the 'correction factor' SWC obtained for each of the values of ρ_b was used to provide water retention data. This data was then used as an input into RETC from which the VG parameters could subsequently be obtained. Only the θ_s , θ_r , α and n parameters were fitted using the 'Retention data only' fitting option in RETC. The l parameter was left as the default value of 0.5 and the K_s value was that predicted by the ROSETTA PTF using the SSCBD data. Retention Curve data was added for 10 values of ψ ($\psi = 1, 151, 601, 1201, 2401, 5101, 6601, 8250, 10050$ and 15000 cm). The RETC determined VG parameters were subsequently used as

the soil hydraulic parameters in a 20 minute infiltration simulation on HYDRUS-1D. All other parameters remained constant except the soil hydraulic parameters between the simulations. The results for three soils (Clay 2620, Loam 2750 and Loamy Sand 4010) are detailed in Figure 32, Figure 33 and Figure 34.

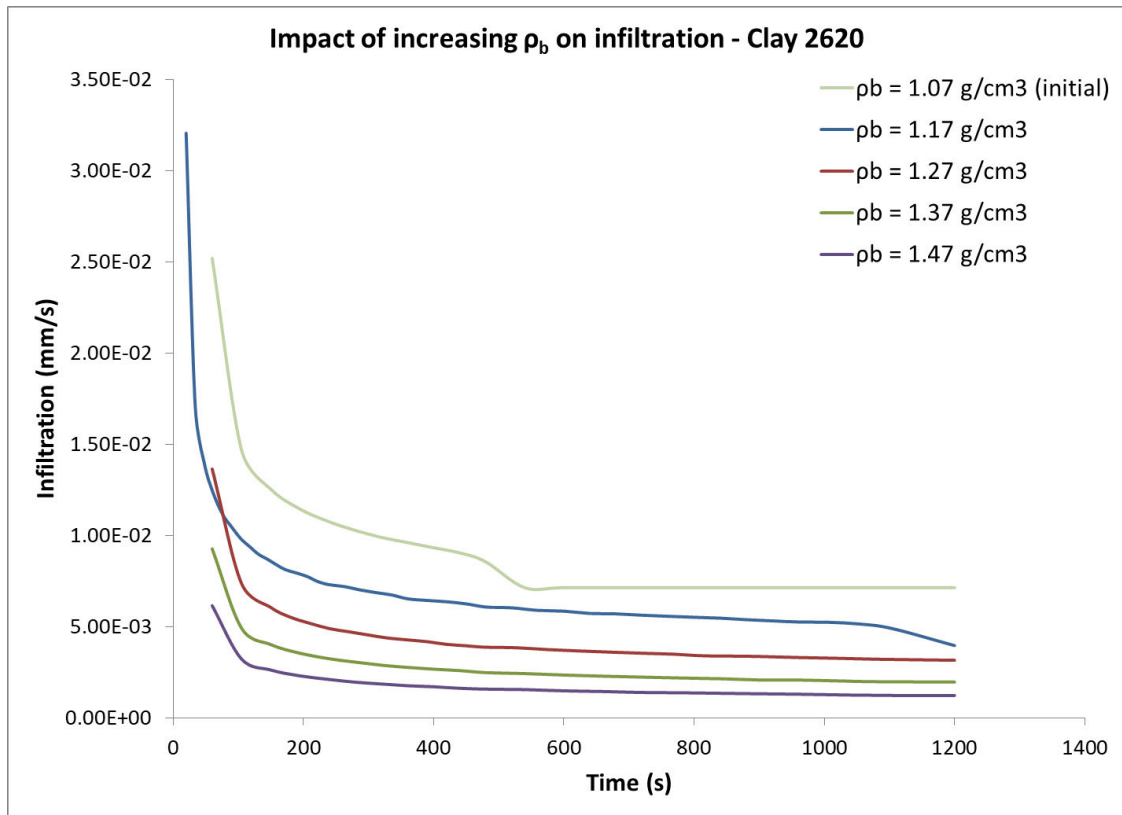


Figure 32 Impact of increasing ρ_b on infiltration for clay soil (2620)

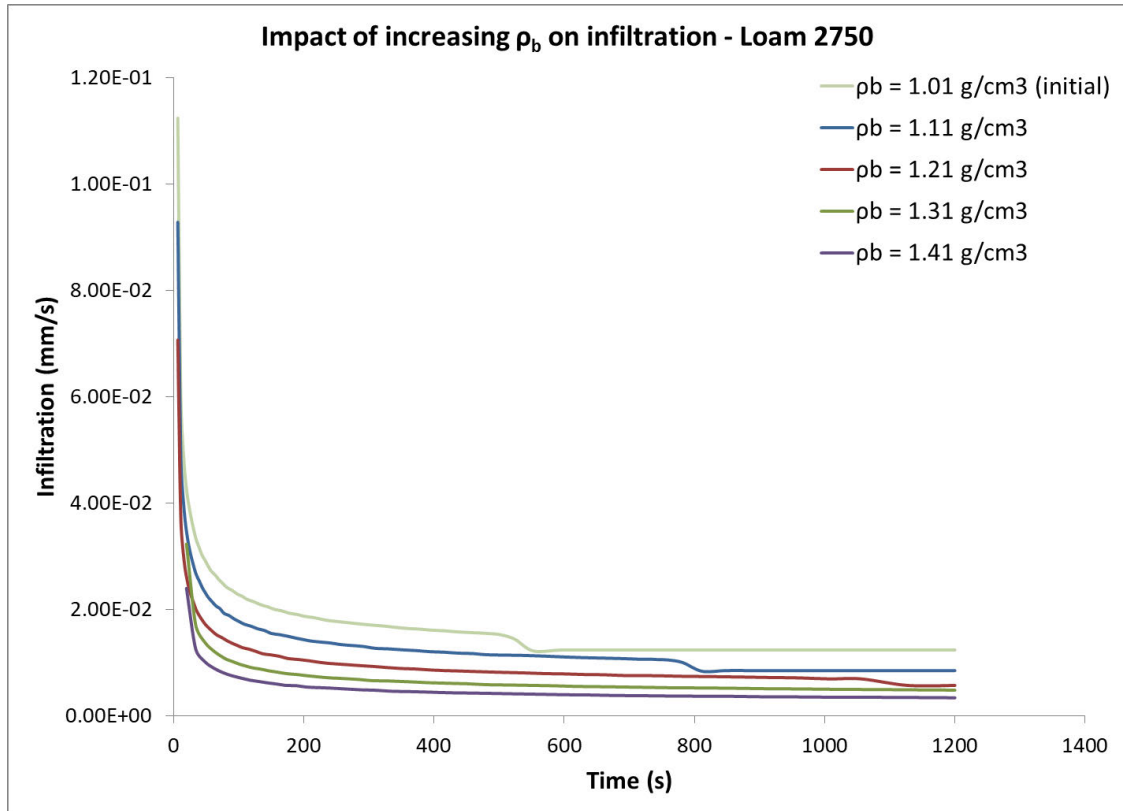


Figure 33 Impact of increasing ρ_b on infiltration for Loam soil (2750)

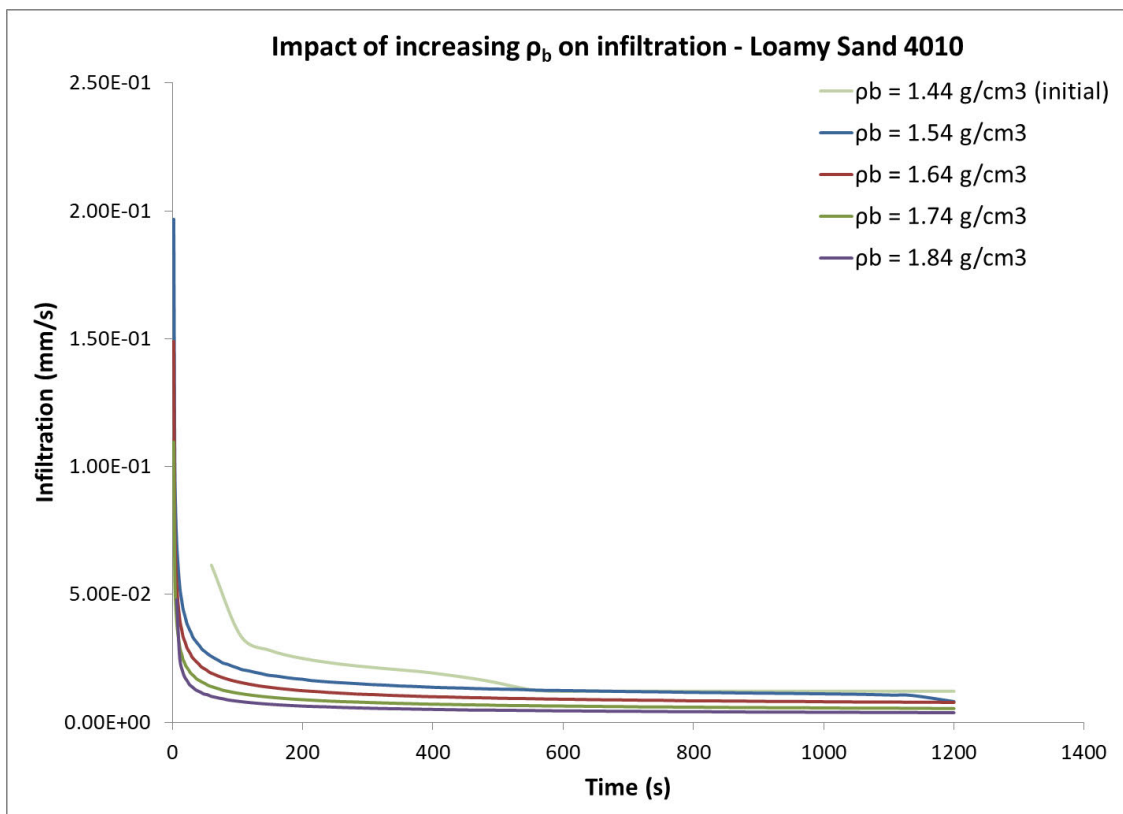


Figure 34 Impact of increasing ρ_b on infiltration for Loamy Sand soil (4010)

The results highlight that as ρ_b increases both the initial infiltration rate and steady infiltration rate reduce. The water retention data used in determining the soil hydraulic properties for the initial ρ_b was observed data whereas for the other simulations the predicted data from the derived SWC. This explains why the infiltration curve is not as smooth for the initial value of ρ_b when compared to the predicted values. The reduction in infiltration rates is substantial in all instances, as shown in Table 15 and highlights the impact of increasing ρ_b on infiltration.

Table 15 Reduction in steady infiltration rate from initial ρ_b value

Clay - 2620		Loam - 2750		Loamy Sand - 4010	
Density	Reduction in final infiltration rate	Density	Reduction in final infiltration rate	Density	Reduction in final infiltration rate
$\rho_b = 1.07 \text{ g/cm}^3$		$\rho_b = 1.01 \text{ g/cm}^3$		$\rho_b = 1.44 \text{ g/cm}^3$	
$\rho_b = 1.17 \text{ g/cm}^3$	44%	$\rho_b = 1.11 \text{ g/cm}^3$	50%	$\rho_b = 1.54 \text{ g/cm}^3$	33%
$\rho_b = 1.27 \text{ g/cm}^3$	56%	$\rho_b = 1.21 \text{ g/cm}^3$	56%	$\rho_b = 1.64 \text{ g/cm}^3$	36%
$\rho_b = 1.37 \text{ g/cm}^3$	72%	$\rho_b = 1.31 \text{ g/cm}^3$	71%	$\rho_b = 1.74 \text{ g/cm}^3$	56%
$\rho_b = 1.47 \text{ g/cm}^3$	83%	$\rho_b = 1.41 \text{ g/cm}^3$	81%	$\rho_b = 1.84 \text{ g/cm}^3$	69%

The reduction in infiltration as ρ_b increases predicted in the modelling aligns with the findings in the literature.

3.9.2. Infiltration on a two layered soil with a uniform crust under ponding conditions

The first crusted soil infiltration simulation considered the crust as being uniform, that is the ρ_b of the crust was uniform throughout the depth of the crust. A two layer profile was set up in HYDRUS-1D with the first layer (representing the crust) ending 5.339 mm below the soil surface and the second layer ending 100 mm below the surface. A crust depth of 5 mm was assumed, being in the middle range of crust depths reported in the literature. HYDRUS-1D allows the distribution of nodes to be increased near the surface compared to the bottom of the soil profile. This option was selected which resulted in the surface layer being changed to a depth of 5.339 mm.

The crust layer was assigned the VG parameters obtained for the highest value of ρ_b that had been modelled (i.e. the initial ρ_b plus 0.4 g/cm^3). The VG parameters developed from the initial ρ_b was applied to the underlying soil layer. The value for K_s was obtained for both layers using the ROSETTA PTF.

A 20 minute infiltration simulation was run under ponding conditions represented by a pressure head of zero at the soil surface. The initial pressure head throughout the remainder of the soil profile was kept at the default value of -100 cm.

3.9.3. Infiltration on a multilayered layered soil with a non-uniform crust under ponding conditions

The literature (Roth 1997) indicates that surface crusts are not of uniform density and should be considered as non-uniform layers with a ρ_b that gradually reduces until the ρ_b of the underlying soil is reached. A non-uniform crust was modelled by splitting the surface crust into four layers each with a lower ρ_b than the ρ_b of the layer above it as detailed in Table 16. The VG parameters developed from the correction factor function in RETC was applied to the crust layers. The K_s values calculated by the ROSETTA PTF were used. All other conditions were kept the same.

Table 16 Soil profile set up for non-uniform crust

Layer	ρ_b	Depth below surface (mm)	Comment
1 (top of profile)	Initial $\rho_b + 0.4 \text{ g/cm}^3$	0.0 – 0.826	Crust
2	Initial $\rho_b + 0.3 \text{ g/cm}^3$	0.826 - 1.917	Crust
3	Initial $\rho_b + 0.2 \text{ g/cm}^3$	1.917 - 3.273	Crust
4	Initial $\rho_b + 0.1 \text{ g/cm}^3$	3.273 - 5.339	Crust
5 (bottom of profile)	Initial ρ_b	5.339 – 100.0	Underlying soil

3.9.4. Results from infiltration modelling on crusted soils

Simulations for the uniform and non-uniform crusts were modelled for one soil from each of the three texture classes (Clay 2620, Loam 2750 and Loamy Sand 4010). Example results for infiltration into the Clay soil 2620 are detailed in Figure 35.

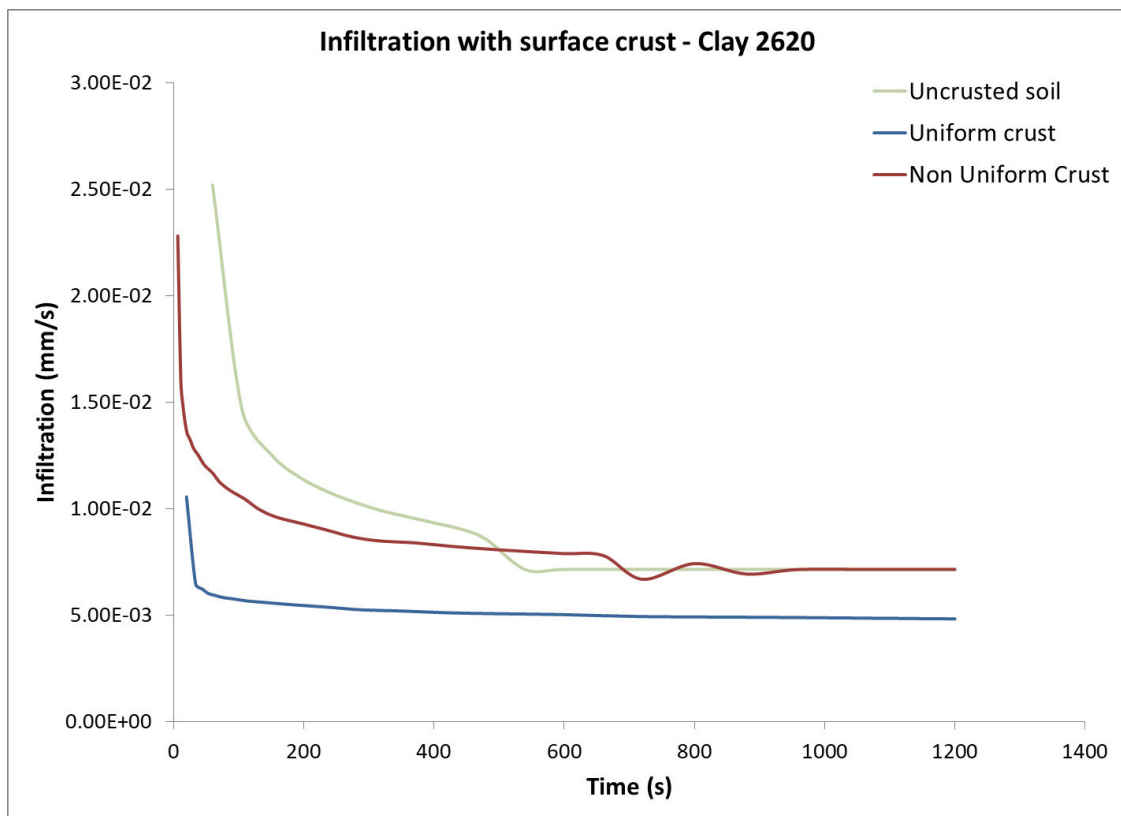


Figure 35 Comparison of infiltration with a soil crust - Clay soil 2620

The difference in infiltration rates and cumulative infiltration rates are not as great as could be expected. The reason for this was considered to be that the K_s predicted by ROSETTA were greater than has been observed elsewhere in surface seals. For example the K_s value predicted by ROSETTA for the Loam soil was 0.980 cm/h. This compares with a measured hydraulic conductivity value for a seal on a loam soil of 0.062 cm/h (Moore 1981). The potential for a substantial overestimation of infiltration using the ROSETTA PTF derived K_s value is thus possible.

3.9.5. Comparing ROSETTA predicted K_s values

To investigate whether ROSETTA predicted K_s values are appropriate for application to a surface crust the K_s values for the same three soils were predicted using all five options within the ROSETTA PTF (textural class, Sand, Silt and Clay percentages (SSC), SSC plus ρ_b , (SSCBD), SSCBD plus θ at 33 kPa and the same plus θ at 1500 kPa). The θ values were obtained from the SWC curve fit (including the correction factor function) of the modelled data.

ROSETTA uses a hierarchical model to determine parameters such that the more input data that is provided the more accurate the prediction of soil hydraulic properties including K_s (Schaap et al. 2001).

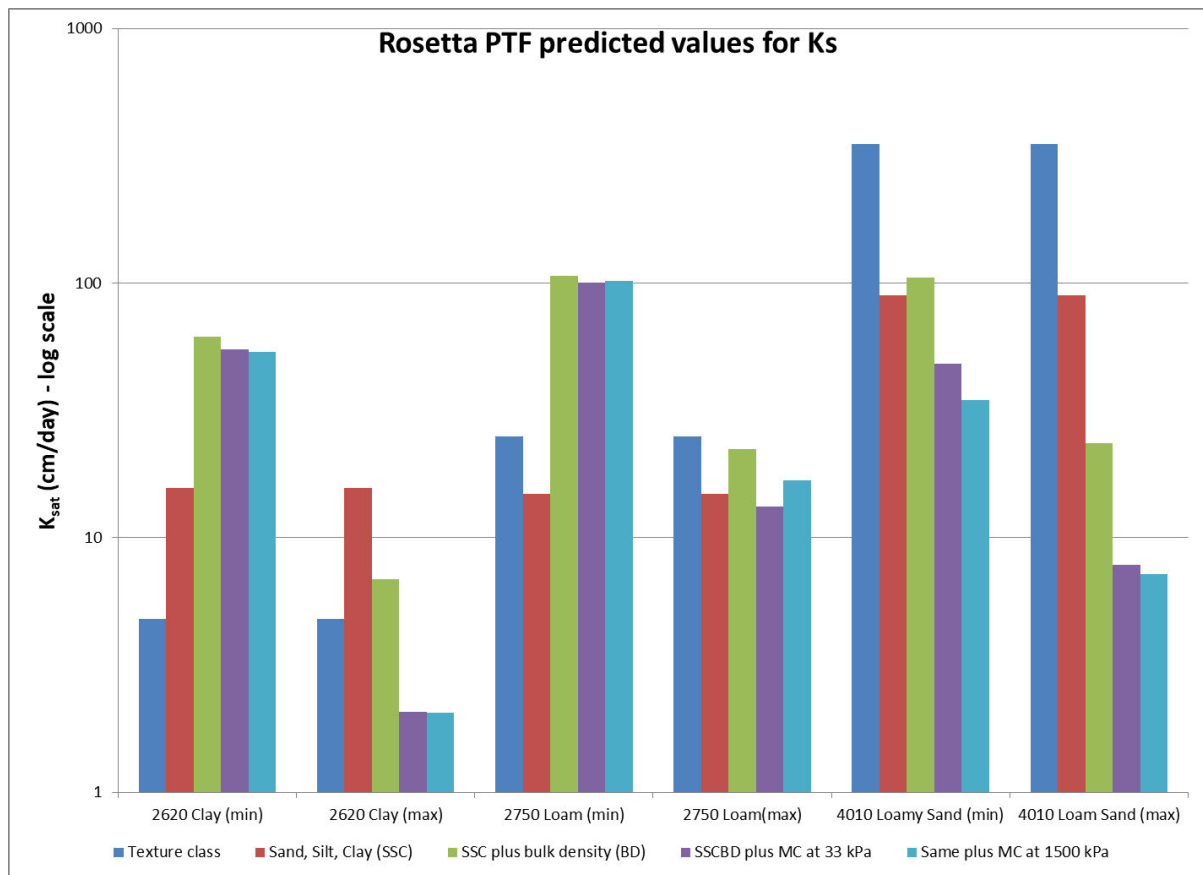


Figure 36 Comparison of ROSETTA PTF predicted K_s values for three soils. (min) is for the lowest modelled ρ_b and (max) is for the highest modelled ρ_b value.

The results are detailed in Figure 36. The texture class and SSC values are the same for both the minimum and maximum ρ_b values for each soil as they rely upon the same data. It is clear that there are major differences in predicted K_s values depending upon what data is inputted into ROSETTA. Some K_s values change by one to two orders of magnitude when ρ_b and water retention data is included. Based on the design of the ROSETTA PTF, the K_s values predicted using ρ_b and water retention data should be more accurate than the values determined using the SSCBD data only (Schaap et al. 2001) thus providing more accurate predictions of infiltration.

3.9.6. Modelling infiltration with new K_s values

Based on the difference in K_s values identified in Figure 36 the infiltration simulations were repeated with K_s values obtained from ROSETTA using all of the available data (SSCBD and ϑ at 33 and 1500 kPa).

The impact upon infiltration rate for a homogenous soil profile as ρ_b increases are detailed in Figure 37 (Clay 2620), Figure 38 (Loam 2750) and Figure 39 (Loamy Sand). The results indicate that there is a substantial difference in infiltration rates as ρ_b increases. Similar results were obtained for cumulative infiltration.

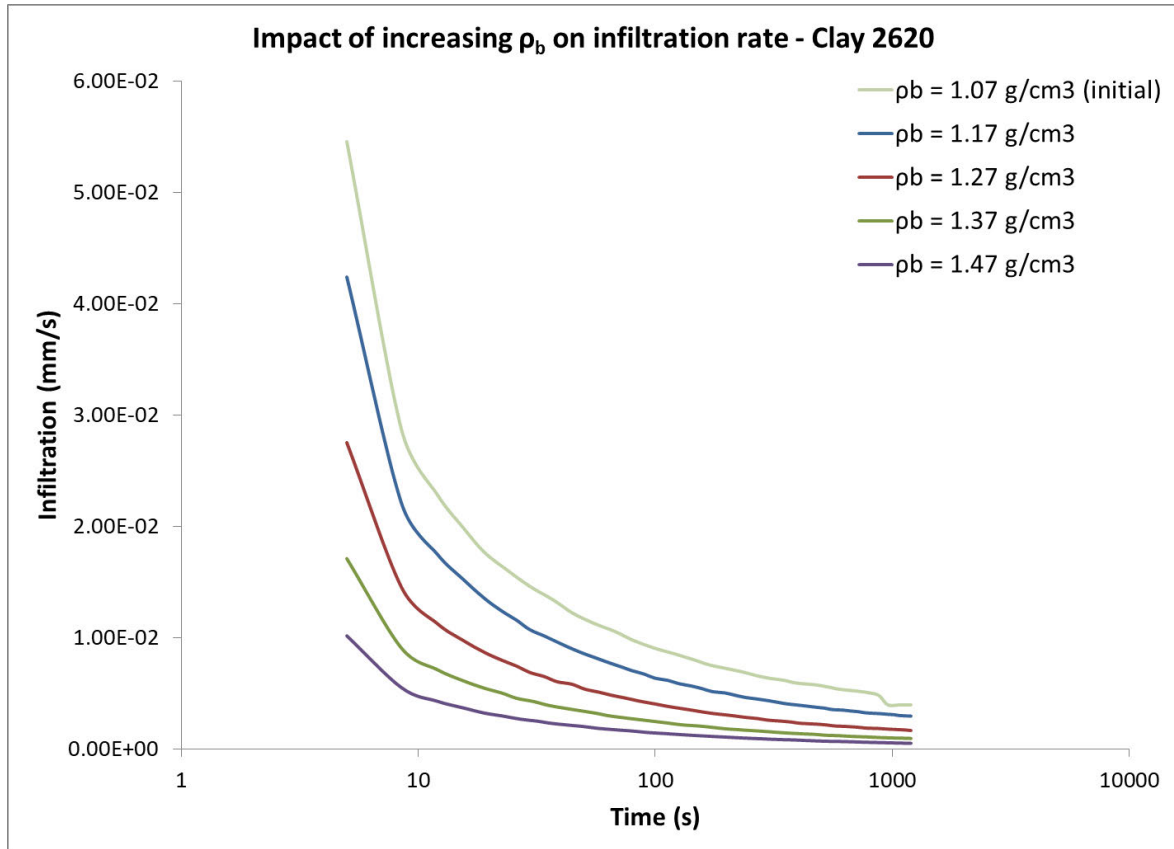


Figure 37 Impact of increasing ρ_b on infiltration rate - Clay 2620

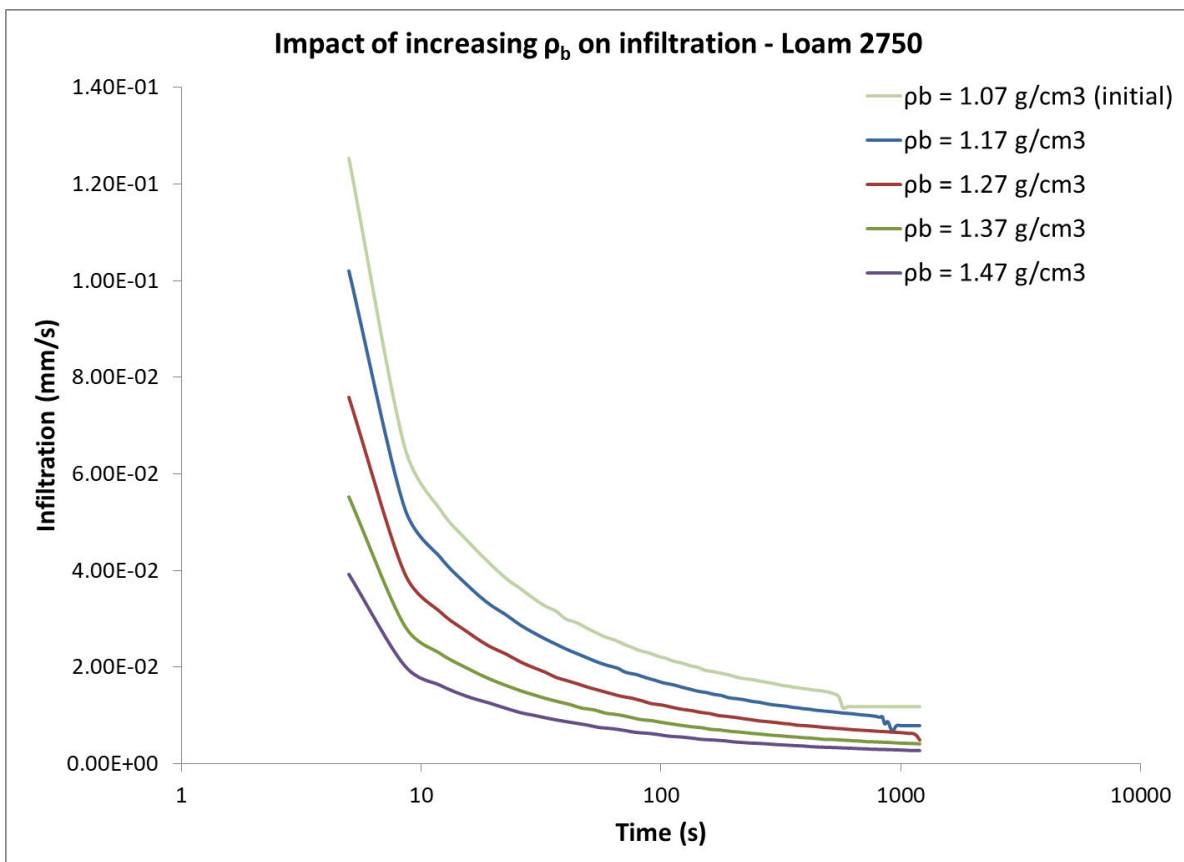


Figure 38 - Impact of increasing ρ_b on infiltration rate - Loam 2750

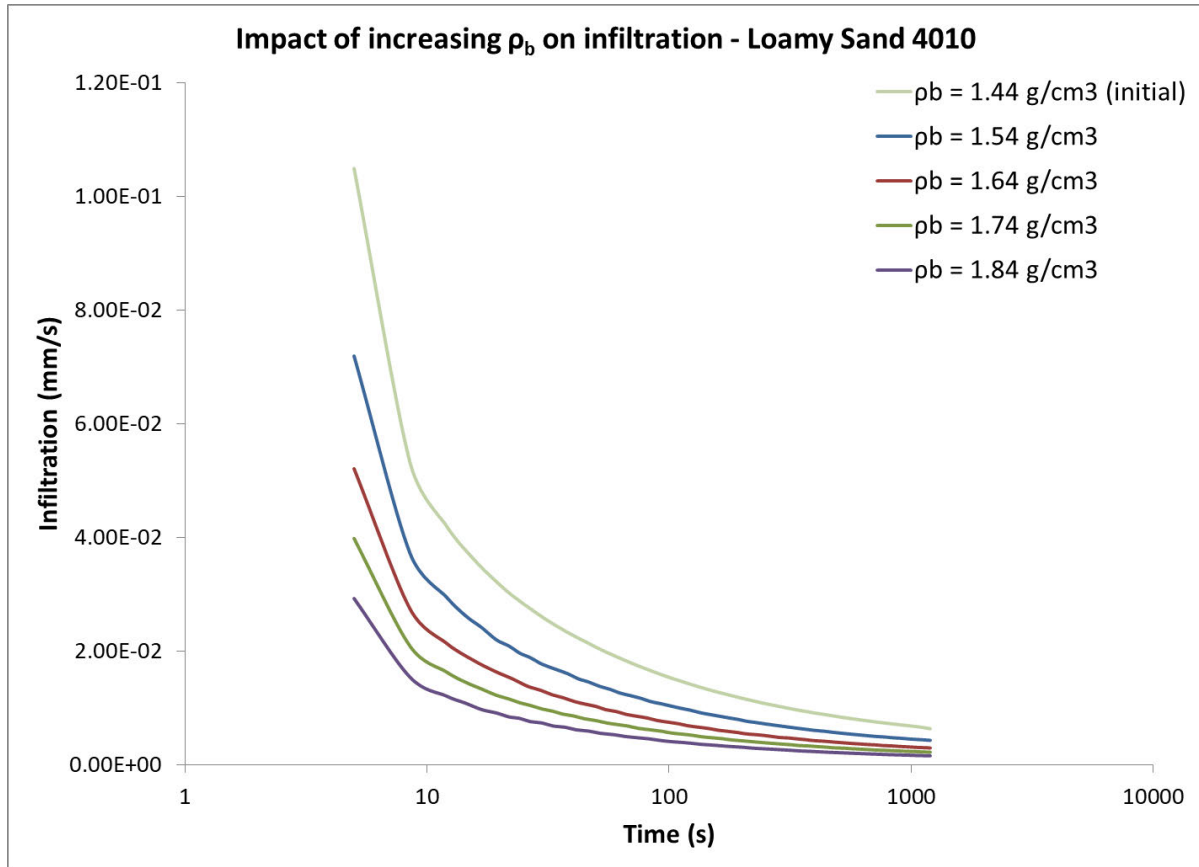


Figure 39 - Impact of increasing ρ_b on infiltration rate - Loamy Sand 010

Infiltration simulations for an un-crusted, uniform crust and non-uniform crust were repeated. The results are detailed in Figure 40 (Clay 2620), Figure 41 (Loam 2750) and Figure 42 (Loamy Sand 4010).

Table 17 details the differences in cumulative infiltration compared to the un-crusted soil. The results highlight a substantial difference in infiltration rates between the different crust scenarios for the Clay and Loam soils. The Loamy Sand soil appears as an anomaly with infiltration increasing under the un-crusted soil scenario. All input data has been checked for this simulation and the results remain the same. The result for the Clay and Loam soils are a more accurate reflection of the expected impact of surface crusts upon infiltration based upon the findings from the literature review than the modelling results using the less accurate SSCBD derived ρ_b values. Experimental data will be compared with these results to determine the validity of this modelling approach.

Table 17 Comparison of cumulative infiltration differences for three soils

	2620 Clay		2750 Loam		4010 Loamy Sand	
	Infiltration (mm)	% difference from uncrusted	Infiltration (mm)	% difference from uncrusted	Infiltration (mm)	% difference from uncrusted
Uncrusted	7.3		18.7		11.8	
Uniform Crust	2.2	-70%	12.9	-31%	19.6	66%
Non Uniform Crust	6.0	-18%	17.1	-9%	10.3	-13%

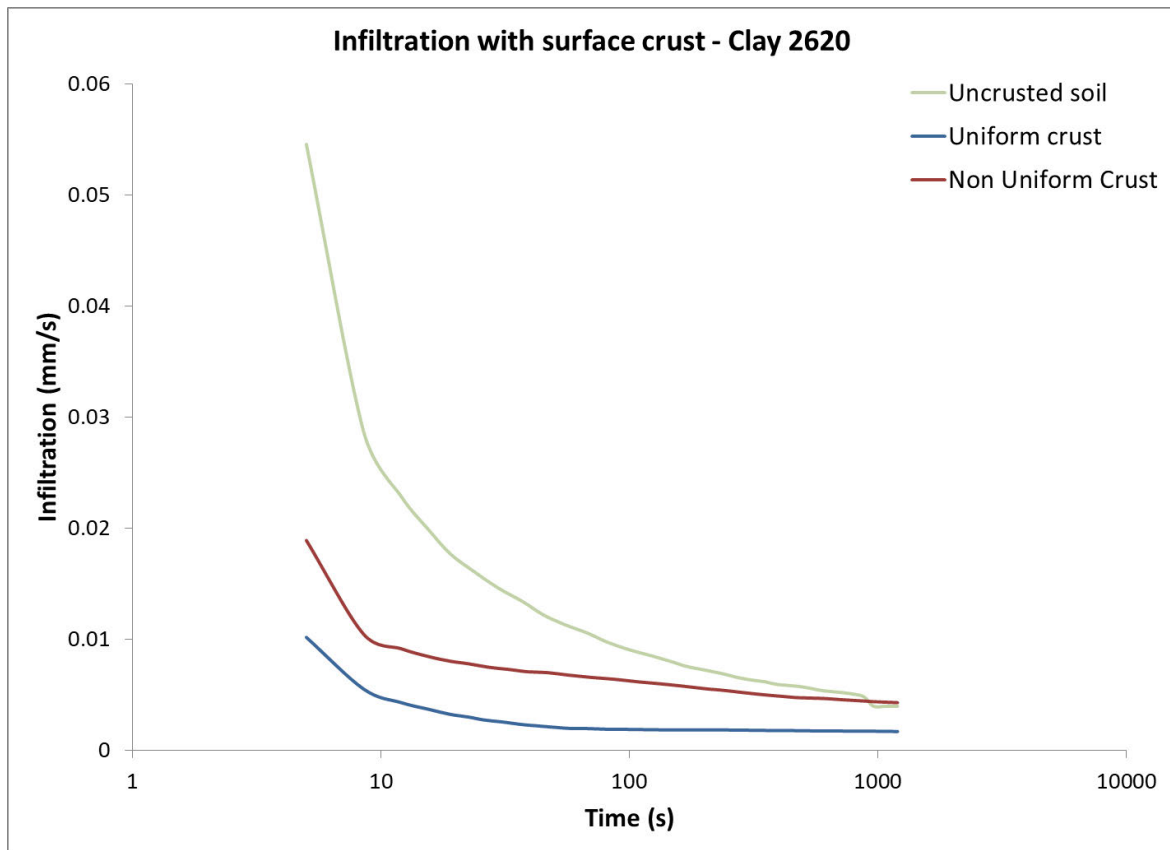


Figure 40 Infiltration under three crusting scenarios - Clay 2620

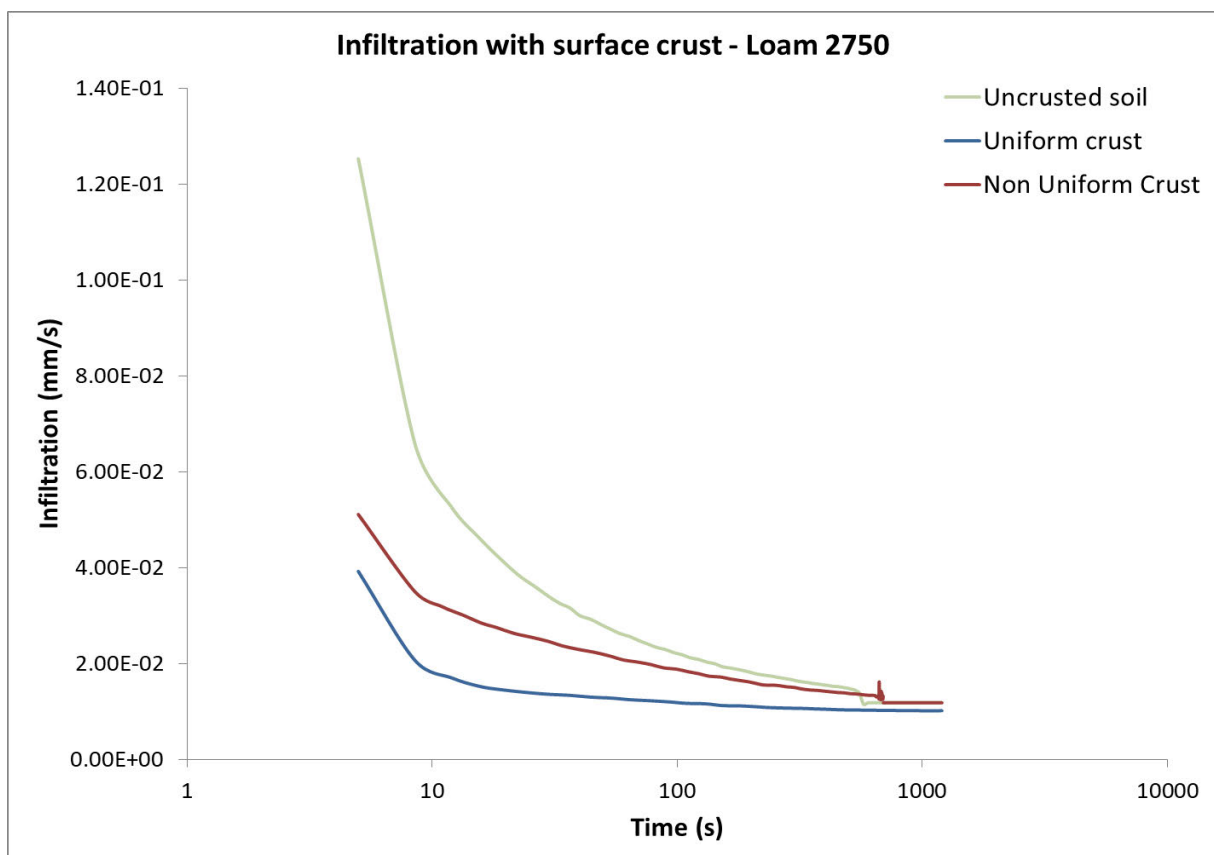


Figure 41 Infiltration under three crust scenarios - Loam 2750

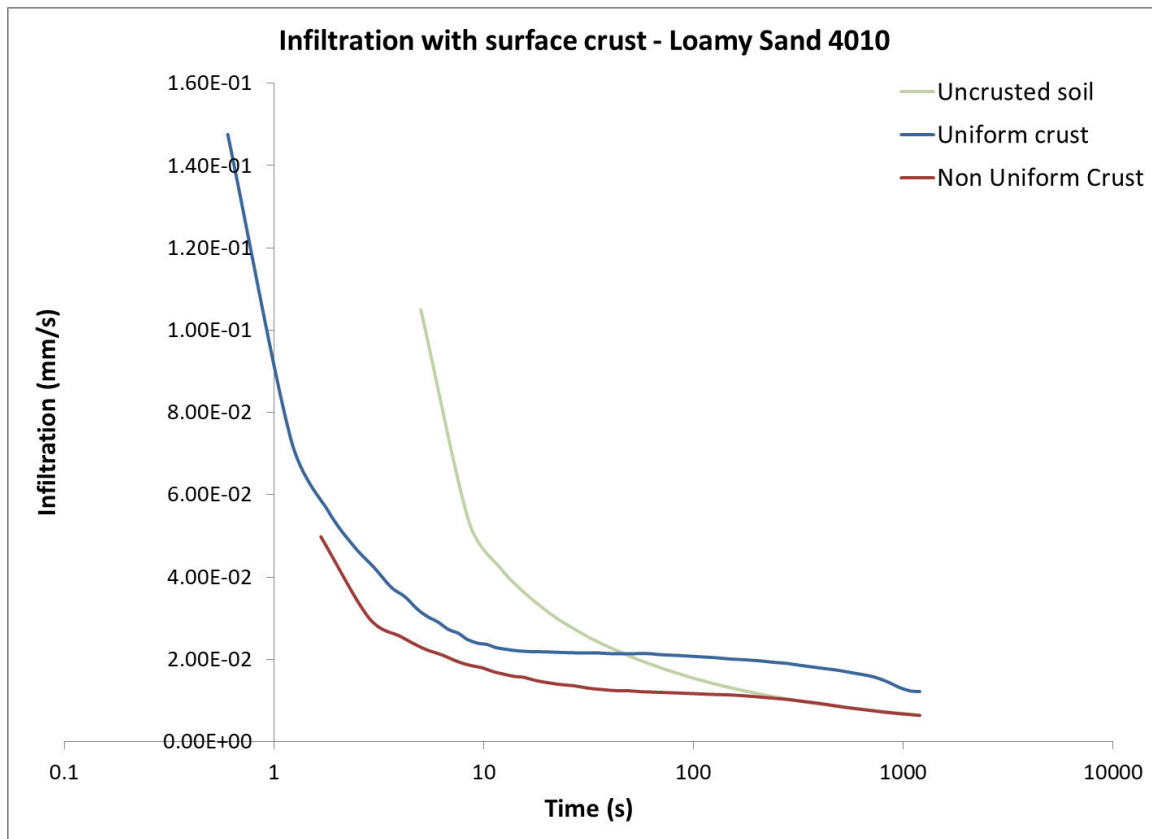


Figure 42 - Infiltration under three crust scenarios - Loamy Sand 4010

3.10. Summary

A number of conclusions can be drawn from the modelling that has been completed.

Firstly the accuracy of the RETC predicted SWC improved considerably when both observed water retention data and SSCBD data was used. The fitted SWC function using Equation 1 resulted in mean r^2 values of 0.967, 0.978 and 0.894 for the clay, loam and loamy sand textural classes, respectively. This indicates that the developed SWC functions provide an accurate representation of the observed data. As a result the developed SWC functions were used as a baseline against which the impact of increased ρ_b was compared.

The observed soil water retention data could not be used to model the SWC as ρ_b increased. This required the use of the substantially less accurate forward fitting option in RETC where only SSCBD data was used to predict the hydraulic properties. To improve the accuracy of the direct fit SWC a correction factor was applied which resulted in a very good alignment with the observed data.

An assumption was made that the correction factor could be applied to the SWC functions as ρ_b was iteratively increased. Whether this assumption is valid needs to be tested experimentally. The modelled SWC for each soil changed as the ρ_b was increased with, in the main, θ being less for a given value of ψ as the ρ_b increased until θ values converged/nearly converged at large matric potentials. This behaviour was expected.

The SWC function (Equation 1) required two fitted coefficients ('a' and 'b') which were obtained through linear regression. There was a strong linear relationship between these coefficients for each soil, a moderate relationship at the textural class level and a weak relationship when all soils were considered. A moderate relationship also existed between the ρ_b and the coefficients. To determine whether these relationships were of practical use values for the coefficients were developed using the

regression equations developed for each textural class. These coefficients were then applied to all soils and compared with the SWC functions developed using the RETC Retention Data fit option. In all instances the SWC obtained through the regression equations compared very poorly with the RETC developed SWC. This indicates, based on the small dataset and limited textural classes considered that this global approach does not assist in developing an accurate SWC functions. The approach did however develop reasonable predictions of the SWC at the textural class level.

Textural class has been identified as having an impact upon the modelling results. The coarse grained textural class (loamy sand) had consistently less reliable results than the fine and medium class soils examined. This indicates that the modelling approach taken here may vary in accuracy/applicability dependent upon the textural class.

Further modelling is required to extend the work already completed on the development of the SWC to the Hydraulic Conductivity Function ($K(\psi)$) which will enable a complete description of the impact of increasing ρ_b on soil water. Expanding the modelling to cover different soil textural classes would also be of use, particularly to examine the relative reliability of the modelling approach for the coarse grained classes.

Validating the identified impact of increased ρ_b on the SWC as identified during the modelling requires experimentation. Experimentation will require obtaining water retention data (θ and ψ) for soils at several ρ_b values. This will enable a comparison of the predicted versus observed SWC and subsequently validation of the modelling that has been completed. This experimentation could be extended to investigate whether a compacted soil behaves the same when it includes a surface crust.

Infiltration modelling demonstrated that as the ρ_b increased the infiltration rate decreased, supporting what has been identified in the literature. The initial infiltration results into a crusted soil profile, particularly a non-uniform crust, were somewhat surprising. Whilst the uniform crust results in a lower infiltration rate than the other two scenarios the final infiltration rate of the non-uniform crust is approximately the non-crusted soil.

These results led to a comparison of predicted K_s values using the various options in the ROSETTA PTF. This identified that there are differences, some substantial, in the K_s values between the different data input options. The ROSETTA PTF is designed such that the more data provided, the more accurate the predicted K_s value. As such for all modelling requiring K_s the SSCBD and two water retention point option predicted K_s values was applied to one soil from each texture class.

The infiltration modelling was repeated using the new K_s values. For the clay and loam soils the results were as was expected with substantial differences as ρ_b increased and in the three crusting scenarios. The results from the loamy sand however indicated an increase in the infiltration rate under a uniform crust compared to an un-crusted soil. Whether this is anomaly for that particular soil or representative of modelling limitations on coarser grained soils is yet to be determined.

4. CHAPTER FOUR – METHODS AND MATERIALS

4.1. Overview and Experimental Approach

The aim of the experimental component of this project was to collect experimental data that could be analysed to determine whether measuring the ρ_b of the surface crust would lead to improved modelling predictions of infiltration and/or runoff. This experimental design was based around the conclusions drawn from the literature review.

To achieve this aim the following experimental work was planned:

- Source soils for use in rainfall simulation experiments and soil hydraulic property determination.
- Measure the relevant soil physical and chemical properties.
- Conduct rainfall simulation experiments that would provide two outputs: 1) runoff and infiltration data, and 2) a soil crust.
- Measure the ρ_b of the surface crust using multiple methods.
- Determine the hydraulic properties of soil samples of varying ρ_b to provide θ data required for HYDRUS-1D modelling and validate predicted soil hydraulic properties.
- Use measured soil properties to model infiltration using HYDRUS-1D and compare against observed infiltration from the rainfall simulation experiments.

It was assessed that this experimental approach would enable the aim of the project to be met.

4.2. Soils

Four soils were used during the project (summarised in Table 18). The A horizon from a Sodosol sourced from near Millmerran, Queensland, was the primary soil used, with approximately 0.6 m³ of the A horizon (0–20 cm depth) being collected. This was sufficient soil to fill three large rainfall simulator trays (see Rainfall simulation section) for the rainfall simulation experiments. The Sodosol was selected based on their tendency to form surface seals/crusts (Murphy 2015). Surface sealing was in evidence throughout the area surrounding the sampling site (Figure 43). Smaller quantities of three other soils were also collected to enable a comparison to be made against the Sodosol as well as providing different soil textures for soil hydraulic property modelling. It was expected that the Chromosol and Ferrosol samples would form a crust during the rainfall simulation experiments based on observations of crusting in the vicinity of the sampling sites.

Table 18 Project Soil Overview

Soil	Australian Soil Classification	Sourced from
1	Sodosol	Millmerran QLD Lat: 27.85553 Long: 151.23521
2	Chromosol	Riverhills QLD Lat: -27.563494 Long: 152.919188
3	Ferrosol	Sumner QLD Lat: -27.564151 Long: 152.930637
4	Hydrosol	Riverhills QLD Lat: -27.561364 Long: 152.898057



Figure 43 Surface seal in close proximity to the Sodosol sampling site at Millmerran Queensland

The soils were air dried, screened to remove large pieces of organic matter, stones and break up large aggregates. Manual mixing was used to homogenise the soil. Approximately 1 kg of soil of each sample was obtained from the homogenised soils for physical and chemical analysis. These samples were dried in an oven at 40 °C for three days and ground to pass a 2 mm sieve.

4.3. Soil physical and chemical properties

Soil chemical and physical data was required primarily as input data for HYDRUS-1D modelling and assistance with soil classification. The soil physical and chemical data requirements and the applicable methods are detailed in Table 19.

Table 19 Soil Physical and Chemical Data Requirements and Standard Methods

Serial	Characteristic	Method /Reference	Comments/Reason
Physical			
1	Particle Size Analysis	Hydrometer method (Burt 2014). This method was selected as it would enable determination of both Australian and US particle sizes. HYDRUS-1D uses US particles sizes for sand, silt and clay.	Define soil texture Input for HYDRUS modelling
2	Moisture Content	Weighing of wet soil and oven dried soil	Input for calculation of ρ_b
3	Bulk density (bulk soil)	503.01 Intact Core Method (Cresswell & Hamilton)	Input for HYDRUS modelling
4	Aggregate Stability	Aggregate Stability in Water (ASWAT), (Field et al. 1997)	Results analysis/discussion (aggregate stability)
Chemical			
5	pH	4A1 pH of 1:5 soil/water suspension (Rayment & Lyons 2011)	Soil classification
6	Electrical Conductivity (EC)	3A1 EC of 1:5 Soil/water extract Soil Chemical Methods Australasia (Rayment & Lyons 2011, pp. 20 - 2).	Results analysis/discussion Determine EC of solution for saturated hydraulic conductivity experiments

4.4. Rainfall simulation

Rainfall simulation was used for two primary purposes:

- Development of a soil seal/crust that could be sampled to determine crust ρ_b and associated soil parameters.
- To provide infiltration and runoff data to compare modelled infiltration results against.

The rainfall simulation activities generally followed the guidance provided in Connolly et al. (2002) adapted as required based on the particulars of the Landloch rainfall simulator used for experimental work and the requirements of this project.

4.4.1. Rainfall Simulator

A laboratory rainfall simulator (see Figure 44) from the environmental consultancy Landloch was used in this project. Landloch primarily uses this simulator for runoff and erosional studies. The simulator consisted of:

- An A-frame supporting three horizontally rotating Veejet nozzles.
- A control system enabling control of simulated rainfall application.
- A water supply system including rainwater tanks, a pump and associated plumbing.
- A mounting frame to hold two soil sample trays at a selected angle. The trays can be set at three different angles from the horizontal (0, 20 and 30 degrees) to simulate different slope angles. Two tray sizes were available. The dimensions of the large tray are 750 mm x 750 mm x 220 mm or 0.124 m³. The dimensions of the small tray are 400 mm x 400 mm x 115 mm or 0.0184 m³.



Figure 44 Landloch Rainfall Simulator with two large trays sitting on the mounting frame at a 20 degree angle.

The following settings were used for the rainfall simulator:

- **Water supply pressure.** 60 kPa +/- 1 kPa. Advice provided by *Landloch* staff indicated that this was the pressure required to provide simulated rainfall that is similar to natural rainfall in drop size and energy.
- **Dwell time.** When the simulator is operating the nozzles emit water continuously. At either extreme of the nozzles rotation the water is captured in baffles and returned to the water

supply system. The length of time that the nozzles remain at these extremes is known as the dwell time. Increased dwell time results in lower rainfall being applied to the soil samples.

- **Sweep speed.** Sweep speed is the time taken for the nozzles to rotate from one extreme to the opposite extreme of its axis. This is the time when the simulated rainfall is applied to the soil samples. Increasing the sweep speed increases the rainfall applied to the soil samples.
- **Rainfall intensity.** Varying the dwell time and sweep speed changes the rainfall intensity (mm/h). Simulator settings aimed to produce a rainfall intensity of 100 mm/h. After reviewing the literature (Armenise et al. 2018), (Hyväluoma et al. 2012) and (Moss 1991) a high intensity was selected as it was assessed that this would provide a high certainty of a surface seal developing. Each soil tray had rain gauges on each side, front and rear (four gauges total). The applied rainfall was determined by averaging the depth of rainfall in the gauges.
- **Tray angle.** Trays were mounted at a 20 degree angle to the horizontal based on the advice of Landloch staff.

4.4.2. Preparation for rainfall simulator experiments

The rainfall simulator experiments included three parts being preparation, conduct and sampling.

Soil samples were prepared to ensure that they approximated the soil in a field condition (e.g. ρ_b and surface condition) and that there were no macro-pores or anomalies that would result in misleading results. Sample preparation consisted of the following steps:

- A layer of air dried soil was placed into the sampling tray.
- The layer was compacted manually using a ram (block of timber with a handle).
- The tray was filled with soil and compacted again.
- The soil surface was smoothed to align to the top of the tray.
- Additionally soil fines were added to the front lip of the tray and each corner until the soil was level with the lip on the tray. This step is critical otherwise runoff ponds on the soil surface and cannot be measured as runoff.
- The soil surface was gently wetted with a fine mist and allowed to air dry. This cycle was repeated several times.

An image of a packed soil tray is detailed in Figure 45.



Figure 45 Packed soil Tray

The layout of the tray (top view) is presented in Figure 46 Sample tray layout. A sampling exclusion zone of 100 mm around the edge of the sample was applied to minimise any edge effects.

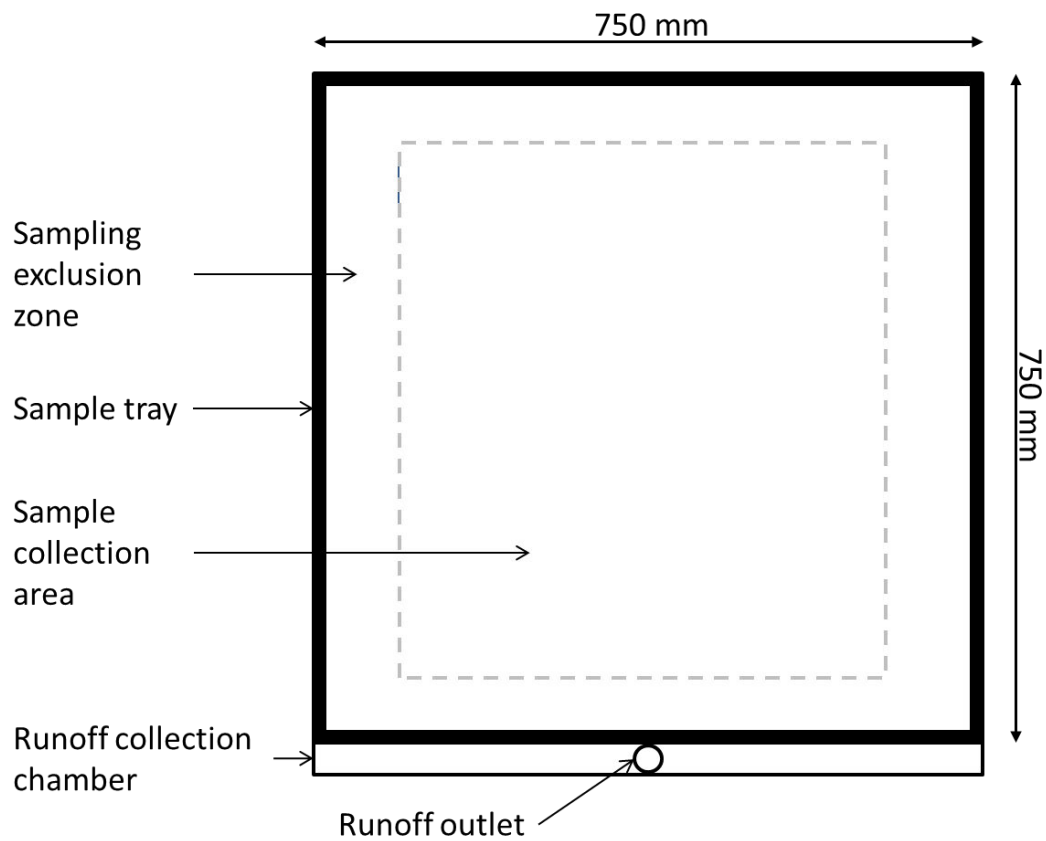


Figure 46 Sample tray layout

4.4.3. Conduct of rainfall simulator experiments

Experimental conduct consisted of the following steps:

- A sample of the pre-simulation soil surface was obtained by scraping approximately 50 g of soil from the surface from multiple points across the sample surface. The surface was then gently smoothed by hand.
- Photographs were taken of the soil surface prior to rainfall application.
- The rainfall simulator was powered on and tested to ensure that the nozzles rotated freely.
- The pump to the rainfall simulator was turned on and the main valve adjusted until the correct pressure was obtained.
- A final check was made to ensure that all requirements had been completed prior to commencing the simulation.
- The rainfall simulator was activated and timing, using a stop watch, commenced.
- The outlet from the soil tray was observed to identify runoff commencement. Some water comes through the outlet almost immediately (some water enters the runoff collection chamber on each sweep of the simulator). This is not considered runoff. Runoff was determined once there was evidence of water ponding at the front of the soil tray and a continuous flow of water was flowing through the runoff outlet. This time was recorded.
- Approximately one minute after runoff commencement was determined the first sample was taken. This involved placing a 500 mL jar under the runoff outlet for approximately 15 seconds (exact time was recorded). Measurements were taken at one minute intervals, two minute intervals and five minutes intervals with the interval increasing as time progressed from runoff commencement.
- Rainfall simulation experiments were run for 25 minutes (for soils when runoff commenced within a couple of minutes of rainfall commencement) to 30 minutes (for soils that required longer time periods for runoff to commence. This gave a minimum of 20 minutes of runoff data.
- At the completion of the simulation all sample jars were weighed. Flocculent was added to jars containing greater than 50 mL of water and subsequently excess water drained. All samples were then placed into an oven set a 105 °C for 24 hours. The dry weights were then measured. This allowed calculation of runoff and sediment from each sampling.

4.4.4. Sampling

- Upon completion of each rainfall simulation experiment the soil within the trays was sampled. The sampling locations and method are detailed in Figure 47 [Sampling locations and method](#)
- Bulk density measurements were taken using the soil core method and the water retention method (Cresswell & Hamilton 2002). Three samples from each tray were taken for each method in the exclusion zone on the sides and rear of the tray. Samples were not taken from the front of the tray in case this impacted upon subsequent runoff results. Apart from small amounts of soil required to determine θ , the remainder of the soil was replaced in the trays and tamped until the soil surface was smooth.

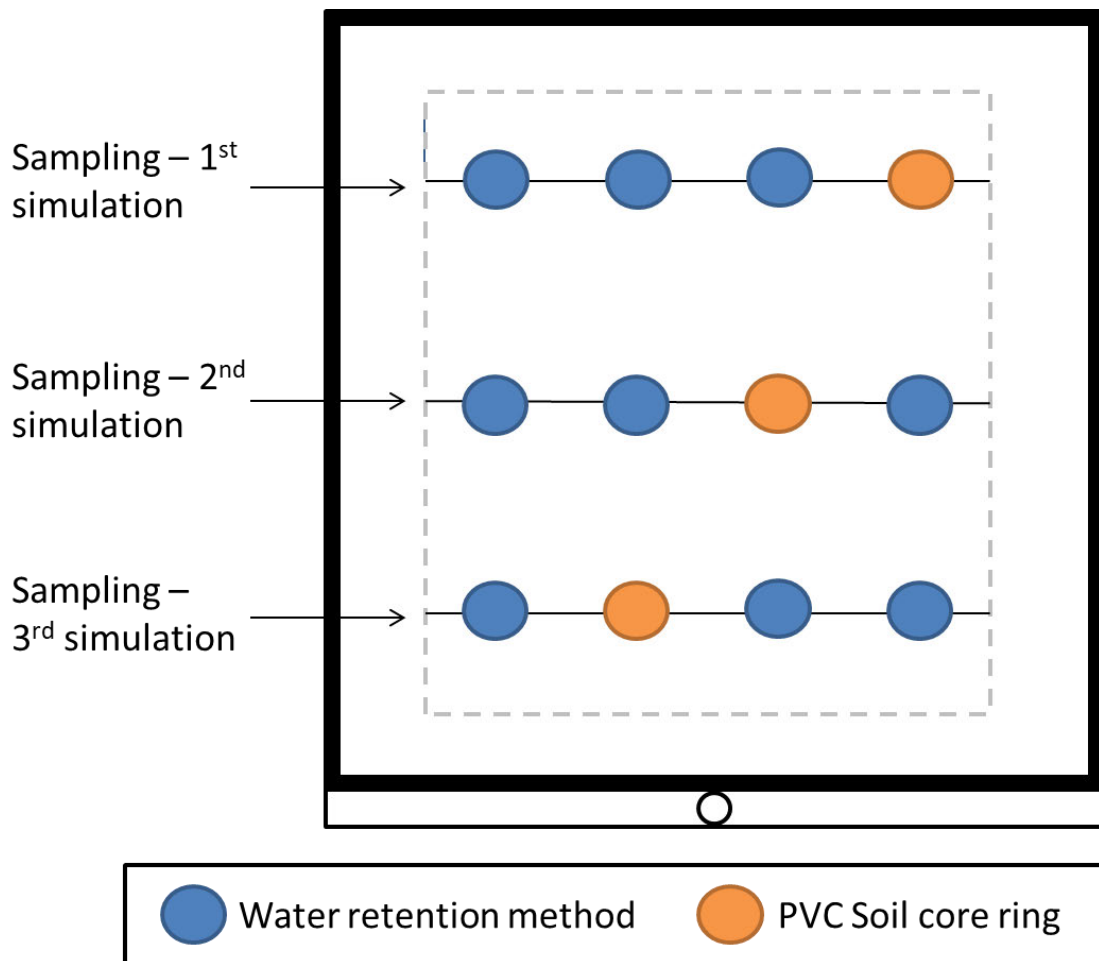


Figure 47 Sampling locations and method

Sampling was conducted as follows:

- A PVC soil core ring (with a 30° bevel at one end) was gently inserted into the soil using a mallet and cork block until the soil surface aligned to the top of the ring. The PVC rings were left in place until all three rainfall simulation experiments were complete. To prevent further development of a surface seal a flywire mesh cover was gently inserted over the soil core ring (Figure 48). The fly-wire mesh was used to reduce the kinetic energy of incoming raindrops to a level that was less than what is required to create a seal. Upon completion of the rainfall simulation experiments the soil around the rings was gently excavated. The rings were removed, bottoms trimmed and weighed to allow ρ_b determination of the entire sample. The cores were then wrapped in plastic cling wrap and placed into a refrigerator/esky for storage.
- Three surface seal ρ_b samples were taken using the water retention method.
- Once the seal sample had been taken, a further sample to the depth of the wetting front was also taken to allow determination of θ .



Figure 48 Flyscreen mesh placed over soil core ring to prevent thickening of the soil crust during subsequent rainfall simulations. Small pebbles on top of screen provide an indication of how rainfall can move particles.

4.5. Bulk density determination

The literature review identified that:

- Current soil survey methods do not determine bulk density of surface crusts.
- Most commonly used methods of determining ρ_b are not suitable for determining the bulk density of thin surface seals/crusts.
- Bulk density can be calculated indirectly via relationship between porosity and bulk density using an assumed (2.65 g/cm^3) or measured value of particle density.
- There are advanced methods available to determine crust ρ_b such as X-Ray CT however they are not practical for routine use.

Five methods were used to obtain ρ_b being:

- The soil core method for the bulk soil underlying the surface crust
- The water retention method
- The thin slice method
- Modified intact clod method
- X-ray Computed Tomography.

These methods are explained in detail below.

4.5.1. Soil core method

A similar procedure as described in (Cresswell & Hamilton 2002) was used for determining the underlying soil ρ_b . Four ρ_b samples from the underlying soil were taken using a 50mm PVC soil core ring. The cores were inserted into the soil approximately 50 mm below the soil surface. The surrounding soil was excavated from around the core before it was removed. The top and bottom of the core were gently trimmed with a blade to ensure that they were flat. The cores were weighed and then a sample placed in an oven for 24 h at 105°C to determine the moisture content. The dry weight of the sample (minus the mass of the core ring) was calculated using Equation 17 where ρ is the density of the moist sample and θ is the gravimetric moisture content of the sample as a percentage.

$$\rho_b = \frac{\rho}{1 + \theta} \quad \text{Equation 17}$$

4.5.2. Water Retention Method

The water replacement method is described in (Cresswell & Hamilton 2002). A schematic of a device to determine ρ_b using this approach is displayed in Figure 49.

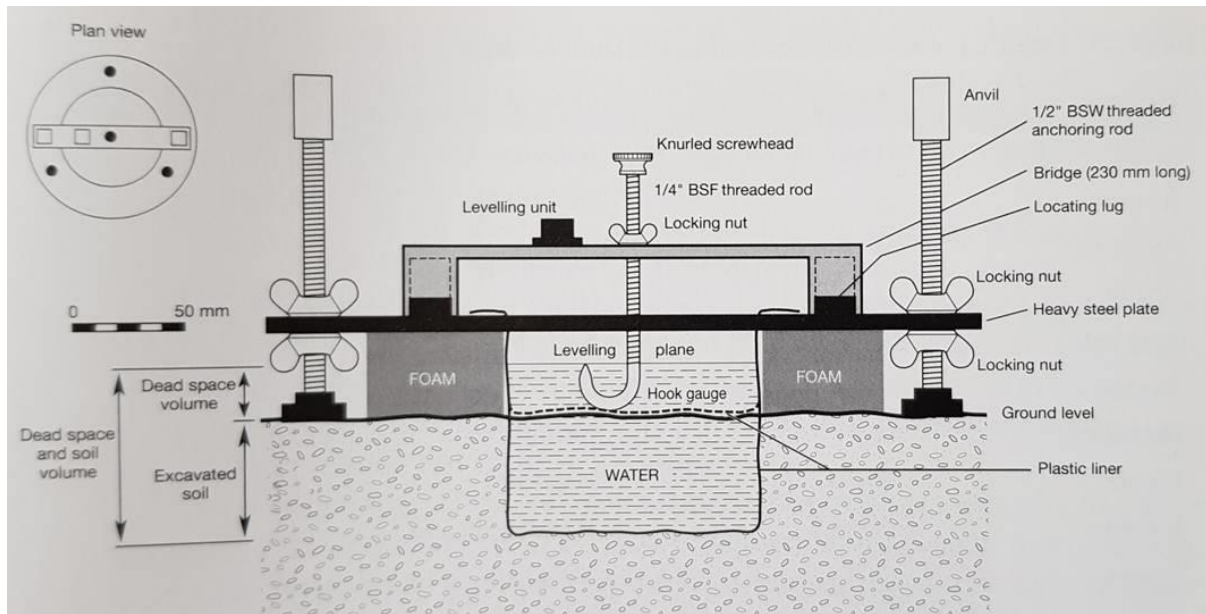


Figure 49 Water Replacement Method (Cresswell & Hamilton 2002)

An apparatus similar to that shown in Figure 49 was constructed and is shown in Figure 50. The internal diameter of the annulus was 110 mm.



Figure 50 Water Replacement Method Apparatus

The following procedure was used to determine ρ_b using this apparatus:

- The apparatus was placed on the soil surface such that the three metal rods were inserted for stability and the underlying foam was flush with the soil surface.
- A thin plastic bag was inserted into the annulus and filled with water until the water level just touched the screw (forming a meniscus with the tip of the screw, a syringe was used to assist with this). This was the control volume.
- The plastic bag with the control volume was carefully removed and weighed.
- A sharp knife was used to cut around the circumference of the annulus to a shallow depth. A criss-cross pattern was then cut across the top of the seal. A bent teaspoon was used to carefully excavate the surface seal with the aim of achieving a relatively level excavation of the surface seal.
- The removed soil was weighed, placed in an oven at 105 °C for 24 hours and reweighed to obtain the dry mass of soil.
- A plastic bag was re-inserted into the annulus and water added until the water just touched the screw tip. The plastic bag was removed and weighed.
- The volume of the crust was calculated by subtracting the control volume from final volume enabling ρ_b to be calculated with the measured oven dry soil mass.

4.5.3. Thin Slice Method

Surface seals/crusts are generally only millimetres in thickness. The aim of the thin slice method was to remove the surface crust from the underlying soil mass. This was to be achieved by inserting the 50 mm PVC soil core into the soil such that the surface crust was kept within the core. Once removed from the soil mass the core was placed on a timber spacer and the soil core forced downward until the

soil surface was just exposed above the soil core (see Figure 51). The crust was removed by slicing using a thin wire (a guitar string).

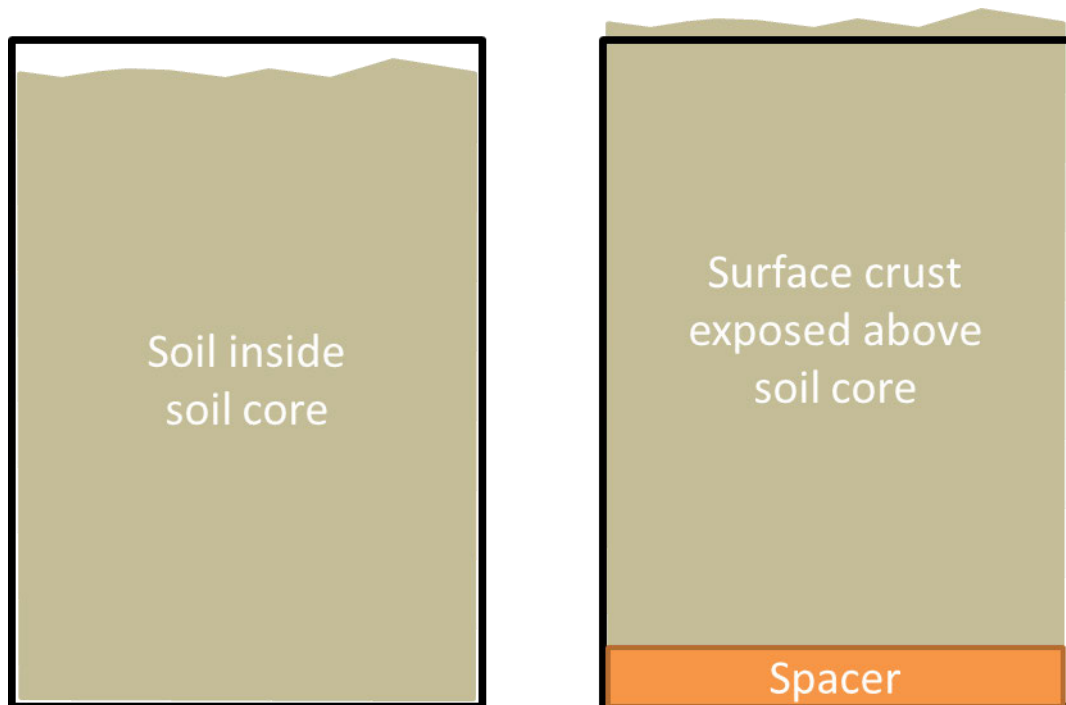


Figure 51 Thin slice method explanation. The left hand diagram shows the soil core once it is removed from the soil. The right hand diagram demonstrates how the soil surface was exposed above the core in preparation for removal using a thin wire.

Prior to removal of the surface crust from the soil, the height above the core was measured using callipers from which the volume of the soil can be calculated. The oven dry weight was then determined to allow calculation of surface crust ρ_b .

4.5.4. Modified intact clod method

The thin slice method described in the section above, as is described in the next Chapter, was unsuccessful. As a result a modified version of the standard immersion method (Cresswell & Hamilton 2002) was used. The method was modified due to the small size and fragility of the soil crust fragments.

Samples of the Sodosols and Chromosol were taken at the completion of the rainfall simulation experiment (Figure 52). After air drying for a week, sandpaper was gently applied to the bottom of the crusts to achieve the thinnest crust section possible. These crust fragments were then oven dried.



Figure 52 Soil crust examples from a Sodosol prior to thinning

Crust ρ_b was determined, using both 10 mL and 100 mL measuring cylinders, as follows:

- The dry measuring cylinder was weighed using laboratory scales.
- Water was added to the measuring cylinder. The cylinder was weighed again.
- The crust fragment was weighed.
- The crust fragment was gently lowered into the measuring cylinder.
- The new volume was measured immediately after the crust was placed inside the cylinder by reading of the scale. The immediate measurement was required to minimise crust volume changes caused by rapid wetting/crust disintegration.
- The initial volume of water was calculated by determined by subtracting the cylinder mass from the recorded value. The difference between the initial and final volume is the volume of the sample.
- The crust fragment ρ_b was calculated.

4.5.5. X-ray Computed Tomography (CT) method

The University of New England X-ray CT apparatus (GE Sensing & Inspection Technologies GmbH, Model v|tome|x s 240/180) was used to determine the porosity of soil core samples from which the crust and subsoil ρ_b were calculated. 50mm PVC soil core rings containing the soil core samples were placed on the sample mount within the CT apparatus (Figure 53).



Figure 53 Soil core on mount in X-ray CT scanner

The CT apparatus was calibrated prior to each scan. Scan settings are detailed in Table 20. The CT apparatus rotates the sample 360 degrees taking a total of 3200 images. Once the images have been completed a Beam Hardening Correction factor of two was applied before the three dimensional volume was reconstructed using the GE Sensing & Inspection Technologies GmbH phoenix datos|x 2 reconstruction software application (Version 2.2.1 RTM). The reconstructed scans were reviewed with the Volume Graphics VGStudio MAX 2.0.5 64 bit software application to check that the scan had been successful.

Table 20 X-Ray CT Scan Settings

Setting	Value	Comment
Voltage	160 kV	Based on standard settings used by UNE.
Current	120 μ A	
Power	19.2 W	
Resolution	30.121 μ m	
Image Capture Timing	200 mS	
Number of images per 360 degree scan	3200	
Mode of operation	Continuous	
Scan length	21 min 20 sec	

Reconstructed volumes were prepared for analysis using the ImageJ software as follows:

- Each scan was imported into ImageJ.
- A circle with a diameter approximately 2.7 mm smaller than the internal diameter of the soil core ring was centred over an image slice (a top view of the scanned data). This was to filter out edge affects which were apparent in most scans. A check was made to ensure that this circle remained central over all image slices. The slice representing the top of the soil profile was identified (this varied from approximately the 100th slice to the 300th horizontal slice of the profile. A total of 1000 horizontal slices were scanned). The 900th slice was selected as the bottom of the profile to remove artefacts present in the bottom slices.
- This selection of data was saved as a 'stack' in .tif format for analysis using ImageJ.

Three outputs were required from the image analysis of the soil core stacks. These were:

- Determination of soil crust porosity (from which ρ_b can be calculated)
- Determination of bulk soil porosity (from which ρ_b can be calculated)
- Determination of soil crust thickness.

ImageJ scripts were developed to semi automate each of these tasks and are included in Appendix D.

The general approach to determining soil porosity for both the crust and bulk soil using ImageJ was as follows:

- Generate a vertical slice of the soil core image stack using the ‘Reslice’ function
- Forming a solid soil surface using Gaussian blurring
- Create a mask of the blurred image
- Create a Euclidean Distance Map (EDM) that enabled the quantification of the distance of a pixel from the soil surface.
- Application of the EDM and Mask to a binary (black and white) image of the soil slice.
- Calculation of the proportion of black pixels within the selected Region of Interest (ROI) using the ‘Measure’ function. This value was assumed to be porosity of the selected ROI. The bulk soil ROI was manually selected for each soil as a rectangular area from the bottom the image stack to a visually determined level below the soil crust. The ROI for the soil crust was selected as being between 10 and 40 pixels below the soil surface (0.3 and 1.2 mm). These settings were selected after testing multiple iterations with the aim of minimising the impact of unconsolidated soil material being incorporated into the ROI whilst maximising the crust thickness for all soil cores.

Porosity values were subsequently converted to ρ_b using Equation 6. The value for ρ_s was assumed to be 2.65 g/cm³.

Research by (Roth 1997) and others has identified that soil crusts should be considered as non-uniform layers where ρ_b changes with depth. To determine whether this conclusion is valid for these soils as well as determining crust thickness, the ImageJ script for determining the soil crust porosity was modified to measure porosity over thin sections parallel to the soil surface. Forty measurements were taken using 10 pixel depth increments (0.3 mm) commencing at one pixel below the soil surface. Values were calculated for two perpendicular vertical image slices per soil core and the results averaged.

This method is not as sophisticated as that used by Bresson et al. (2004), where horizontal sections were smoothed with increasing depth, however was assessed as being sufficient for the purposes of this project.

4.6. Soil hydraulic properties

Measurement of the soil hydraulic properties was required for the following purposes:

- Determination of saturated hydraulic conductivity (K_s) of soil cores of known ρ_b to compare with those predicted by HYDRUS-1D.
- Determination of the Soil Water Characteristic of soil cores of known ρ_b in order to obtain values of θ at ψ values of 33 kPa and 1500 kPa. These values of ψ are required for subsequent HYDRUS-1D modelling.

- Provision of data to compare the Soil Water Characteristic (SWC) and Hydraulic Conductivity Function modelling completed during the modelling phase of the project with measured soil hydraulic property data.

4.6.1. Application of the modified Standard Compaction Test

HYDRUS-1D enables segmentation of a soil profile into layers. Each layer can be assigned a different ρ_b value. As it is very difficult to create thin crusts with a specified density, it was assessed that soil cores could be compacted to provide an analogue of the soil crust for the purposes of determining crust hydraulic properties.

A modified version of the Standard Compaction test (Vickers 1987) was used to create soil core samples of increasing ρ_b . The Standard Compaction Test is used to determine the optimum moisture content and corresponding soil density required for compaction during civil engineering works. The outcome required for this project was the creation of samples of increasing ρ_b such that soil hydraulic properties could be determined for each sample.

The following modifications were made to the Standard Compaction Test as follows:

- The air dried soil was sieved using a sieve with a 2 mm aperture to ensure that only the fine earth fraction was included in the sample.
- Water was added to the air dried sample to reach the approximate optimum moisture content required for maximum compaction as detailed in Table 21 Optimum moisture content range for different soil types . The soil was then manually mixed until the moisture content was consistent.

Table 21 Optimum moisture content range for different soil types (Arjun 2019)

Sand	Sand silt or silty sand	Silt	Clay
6 to 10%	8 to 12%	12 to 16%	14 to 20%

- The number of blows with the 2.5 kg hammer per layer of soil was changed to result in differing ρ_b . The number of applied blows is described in the Results chapter.

4.6.2. Determination of saturated hydraulic conductivity

The aim of the saturated hydraulic conductivity experiments was to allow comparison of HYDRUS-1D predicted K_s values to observed data under different treatments. Saturated hydraulic conductivity of prepared soil cores was obtained using the constant head method (Das & Sobhan 2014). The experimental set up is shown in Figure 54 **Hydraulic Conductivity experimental set up**. The soil cores were placed in a Buchner funnel. The upturned plastic bottles had a polyethylene pipe segment with a sprinkler head attached inserted into the neck which enabled a constant head to be maintained when upturned. Plastic catch cups underneath the funnels were used to collect outflow which was weighed periodically. Two pore volumes were allowed to infiltrate through the soil core and measurements continued until five similar readings were obtained. The infiltration rate was calculated using a re-arranged form of Darcy's law (Equation 13).



Figure 54 Hydraulic Conductivity experimental set up

A 2 dS/m Calcium Chloride solution was used for the infiltration experiments (including overnight soaking) based upon the EC measurement of the soil. This was to ensure that the calculated results were not impacted by the chemical composition of the soils (e.g. to prevent dispersion).

Experiments were completed on the following soil core treatments for both the Chromosol and the Sodosol with three replicates per soil:

- a. A loosely hand tamped soil core (low ρ_b). To achieve consistency the mass of soil in the first core was measured and the same mass of soil placed into the other cores. The soil was then gently compacted until the depth of soil was the same as the first core.
- b. Cores compacted using the modified standard compaction test (high ρ_b). Once the core was removed from the Proctor Device and the ends trimmed, a spacer was placed underneath the core and the soil core ring gently moved downward to expose approximately 2 cm of the soil core. This was removed using a sharp blade. The core was then inverted leaving 2 cm above the soil within the soil core ring where water for the constant head method could be ponded.
- c. Compacted cores with a surface crust (high ρ_b). After drying for several weeks, the compacted cores from the previous step (b) were removed from the PVC soil core ring. The cores were subjected to artificial rain from a 9L garden watering can from a height of approximately 2 m with the aim of forming a surface crust. The core ring was replaced and the cores were allowed to dry for several days in the sun prior to the hydraulic conductivity tests. Petroleum gel was applied around the perimeter of the core, both top and bottom, to prevent preferential flow which could have occurred due to core shrinkage and damage from the artificial rainfall.

4.6.3. Determination of the soil water characteristic

The SWC was obtained using the HYPROP apparatus (UMS GmbH nd). HYPROP uses an evaporation method to determine the SWC (UMS GmbH nd). 100 cc soil cores were extracted from larger soil cores prepared using the modified Standard Compaction test to produce samples with differing values of ρ_b . A sample of the soil from the larger core was oven dried to enable θ determination and subsequently core ρ_b calculation. The samples were soaked until saturated in distilled water before being placed into the HYPROP sensor unit for determination of the SWC. Four

samples were run simultaneously with each measurement run being around five days in length. The SWC and VG parameters were obtained from each sample using the HYPROP-FIT software (Meter Group nd).

As 1500 kPa is outside of the tensiometer range of the HYPROP apparatus, it was planned to use a 1500 kPa pressure plate apparatus to obtain θ_{1500} . This data point could then be incorporated into the HYPROP-FIT derived SWC. Due to issues with the results obtained from the HYPROP measurements (discussed in the Results Chapter) these measurements were not required.

4.7. Comparing observed infiltration to HYDRUS-1D predicted infiltration

The culmination of the experimental work is to compare observed infiltration rates from the rainfall simulator experiments with HYDRUS-1D predicted infiltration based on the measured soil parameters and in particular the ρ_b of the surface crust. This comparison enables an assessment to be made on whether measuring crust ρ_b improves the accuracy of infiltration modelling.

The following steps were required to enable this comparison:

- Observed infiltration data and parameters are prepared from the second and third rainfall simulation experiments for each soil type. The first simulation is not used as the soil crust had not developed and HYDRUS-1D does not support dynamic changes to the soil profile (e.g. changing crust ρ_b with time) within a simulation. An infiltration rate–time regression equation was calculated for each soil.
- HYDRUS-1D simulations were completed using measured and derived parameters for the selected soils. Simulations were completed using the H3 and H4 models within ROSETTA (Schaap et al. 2001), as detailed in Table 22, to derive the VG soil hydraulic parameters.

Table 22 Models used to obtain VG equation parameters for use in HYDRUS-1 simulations.

Model	Input parameters	Comments
H1	Soil textural class	
H2	Sand, Silt, Clay (SSC)	USDA soil particle dimensions used
H3	SSC, Bulk Density (BD)	
H4	SSC, BD, water content at 3.3 m suction ($\theta_{3.3}$)	
H5	SSCBD, $\theta_{3.3}$, water content at 150 m suction (θ_{150})	

- Modelled infiltration data from each simulation is compared with the observed infiltration regression equation. Statistical comparisons of observed and modelled infiltration rates are made using the Nash-Sutcliffe Criterion objective function. This objective function provides a numerical indication of the goodness of fit around the 1:1 line in predicted versus observed data comparisons (Hall 2001). Comparisons of cumulative infiltration between the observed and modelled data are also made.

After completion of these steps for each soil an assessment could be made as to whether measuring the crust ρ_b has improved the accuracy of infiltration modelling and which parameters are the most important in modelling infiltration on a crusted soil.

In the event that the modelling did not produce results similar to observed infiltration the inverse modelling capability (Radcliffe & Simunek 2010) within HYDRUS-1D could be used to obtain surface crust hydraulic properties.

5. CHAPTER FIVE - RESULTS

5.1. Soil physical and chemical properties

5.1.1. Physical Properties

Soil texture and textural class details (using both the Australian and US particle sizes) are detailed in Table 23.

Table 23 Soil texture and textural classes using both the Australian and US particle sizes/classes. HYDRUS-1D uses the US particle size system.

Soil	Australian dimensions				US dimensions			
	Sand	Silt	Clay	Textural Class	Sand	Silt	Clay	Textural Class
	20 - 2000 μm	2 - 20 μm	<2 μm		50 - 2000 μm	2 - 50 μm	<2 μm	
Sodosol A horizon	78%	8%	15%	Sandy Loam	72%	12.9%	15.5%	Sandy Loam
Sodosol B horizon	58%	4%	39%	Clay	56%	5.9%	38.1%	Sandy Clay
Chromosol	65%	8%	28%	Clay Loam	63%	14.7%	22.1%	Sandy Clay Loam
Hydrosol	43%	28%	30%	Silty Clay Loam	35%	40.6%	24.2%	Loam
Ferrosol	38%	13%	50%	Clay	33%	24.3%	43.1%	Clay

5.1.2. Chemical Properties

Soil chemical properties are detailed in Table 24. EC_e , salinity classification and aggregate dispersibility classifications have been obtained from Hazelton and Murphy (2016, pp. 189-91).

Table 24 Soil Chemical Properties

Soil	pH	EC (dS/m)	EC_e (dS/m)	Salinity classification	ASWAT score	Aggregate dispersibility
Sodosol A horizon	5.7	0.08	1.12	Non Saline	0	Negligible/aggregated
Sodosol B horizon	5.7	0.14	1.05	Non Saline	13	Very high
Chromosol	5.8	0.08	0.69	Non Saline	0	Negligible/aggregated
Hydrosol	7.4	1.34	11.5	Highly Saline	9	High to moderate
Ferrosol	6.4	0.19	1.43	Non Saline	0	Negligible/aggregated

5.2. Soil hydraulic properties

5.2.1. Saturated hydraulic conductivity

Observed K_s values as well as a comparison with the ROSETTA predicted values (using the H3 model within ROSETTA (soil texture and ρ_b data only)) are provided in Figure 55 with the corresponding ρ_b of the soil cores detailed in Table 25.

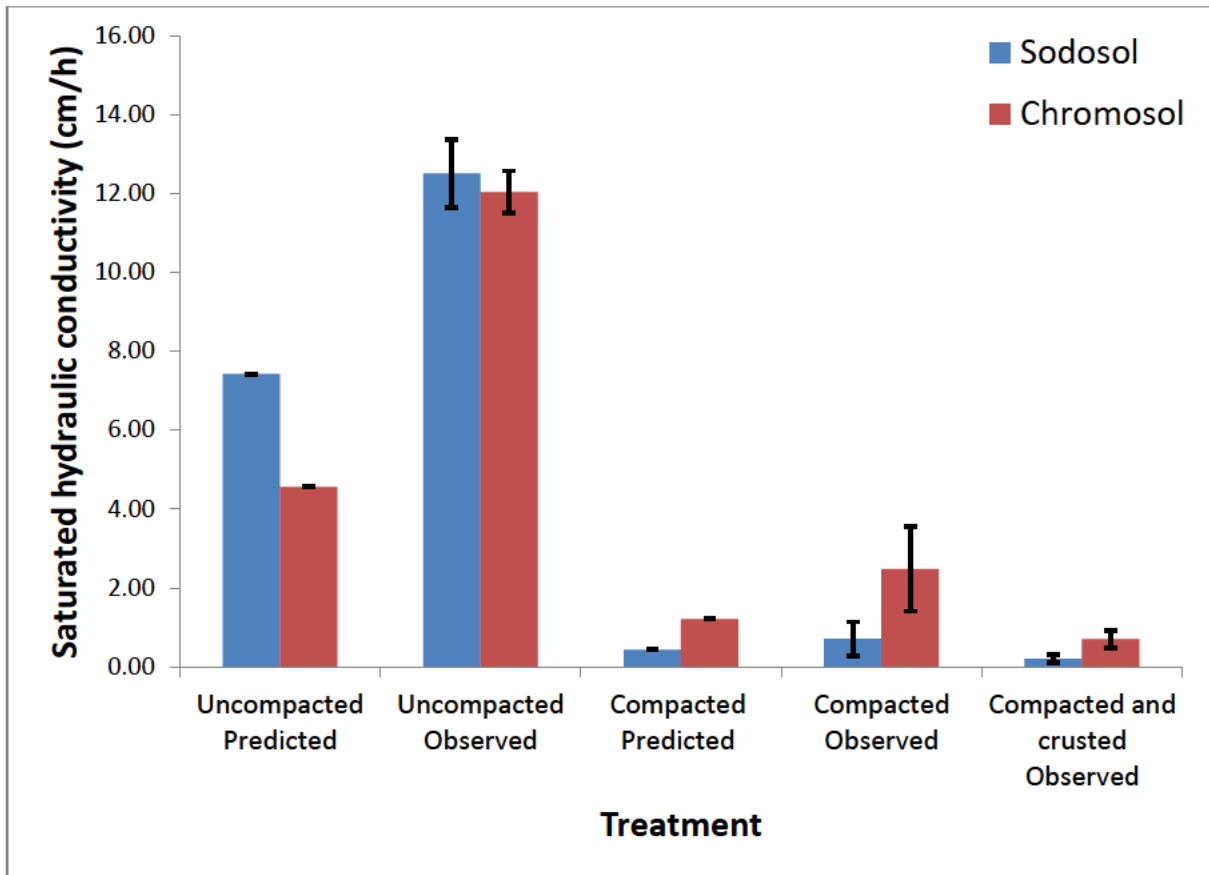


Figure 55 Comparison of HYDRUS-1D predicted and observed saturated hydraulic conductivity. Error bars represent +/- one standard deviation

Table 25 Densities of soil cores used in K_s experiments

Soil	Uncompacted ρ_b (g/cm ³)	Compacted ρ_b (g/cm ³)
Chromosol	1.05	1.46
Sodosol	1.03	1.82

The results detailed in Figure 55 highlight major differences in the observed and HYDRUS-1D predicted K_s values. Whilst the results are of the same magnitude the experimentally determined K_s values were on average double the HYDRUS-1D predicted values. The creation of a rainfall impact crust on the compacted soil cores resulted in a 72 % reduction in K_s for both soils highlighting the impact of surface crusts upon infiltration, as identified in the literature (Moore 1981).

HYDRUS-1D modelling was attempted using the soil texture, core ρ_b , HYDRUS-1D predicted and experimental K_s values to allow a comparison to be made. The numerical solution did not converge however for the compacted and crusted treatment (a problem that was found during subsequent modelling, see Section 5.6.2) so a comparison could not be made.

5.2.2. Soil water characteristic van Genuchten parameters

Results from HYPROP soil water retention measurements are detailed in Table 26. The right hand most column details the content at 33 kPa calculated using Equation 10 and the HYPROP derived soil hydraulic parameters. This value was required for use in HYDRUS-1D to obtain soil hydraulic parameters from the ROSETTA H4 model.

Table 26 HYPROP derived VG equation parameters

Soil	ρ_b	α	n	θ_r	θ_s	K_s	θ_{33kPa}
Chromosol	1.33	0.000131	1.439	0.4	0.889	1.62037E-05	0.85
Chromosol	1.41	0.0045	1.399	0.4	0.598	1.15741E-06	0.47
Chromosol	1.42	0.00368	1.655	0.325	0.560	7.07176E-05	0.37
Chromosol	1.48	0.00337	1.153	0.300	0.657	0.001469907	0.54
Chromosol	1.61	0.00117	1.952	0.198	0.305	2.43056E-05	0.23
Sodosol	1.63	0.01346	1.116	0	0.286	0.004085648	0.18
Sodosol	1.77	0.00769	1.126	0.250	0.483	0.000383102	0.40
Sodosol	1.78	0.00273	1.508	0.394	0.489	2.32639E-06	0.42
Sodosol	1.79	0.0027	1.644	0.034	0.223	0.00012963	0.08
Sodosol	1.79	0.0015	1.141	0.4	0.717	3.40278E-05	0.65
Sodosol	1.87	0.00381	1.108	0	0.350	0.000572917	0.26

The soil hydraulic properties detailed in Table 26 show a great degree of variability even where the ρ_b values are the same or similar. This indicates that the results may not be reliable. The θ_{33} data point was incorporated into several HYDRUS-1D simulations to determine whether this value had a significant impact upon predicted infiltration (see Section 5.6). There was little improvement when this water retention point was incorporated. As a result it was decided not to obtain the θ_{1500} water retention values due to the difficulty in creating ρ_b samples of the same density, the time to obtain this data and the assessment that this data would make little difference in predicted infiltration results.

5.3. Rainfall simulation experiments

Rainfall simulations were conducted on three consecutive days using the Landloch rainfall simulator. A summary of the rainfall simulations is detailed in Table 27.

Table 27 Summary of rainfall simulation experiments

Soil description	Tray size	Number of simulations
Sodosol #1 A horizon	Large	3
Sodosol #2 A horizon	Large	3
Sodosol #3 A horizon	Large	3
Chromosol A horizon	Small	2
Ferrosol A horizon	Small	2
Hydrosol A horizon	Small	3

5.3.1. Initial data

A spreadsheet was developed to record all data associated with the rainfall simulation (including soil details, timings for the simulation and sampling, applied rainfall, runoff as well as sampled wet and dry weights). The spreadsheet was also used to calculate the instantaneous runoff and infiltration rates. Infiltration curves were plotted from the infiltration rate data points. The original data from the rainfall simulation experiments is detailed in Appendix C.

The infiltration curves are detailed in Figure 56 through to Figure 61.

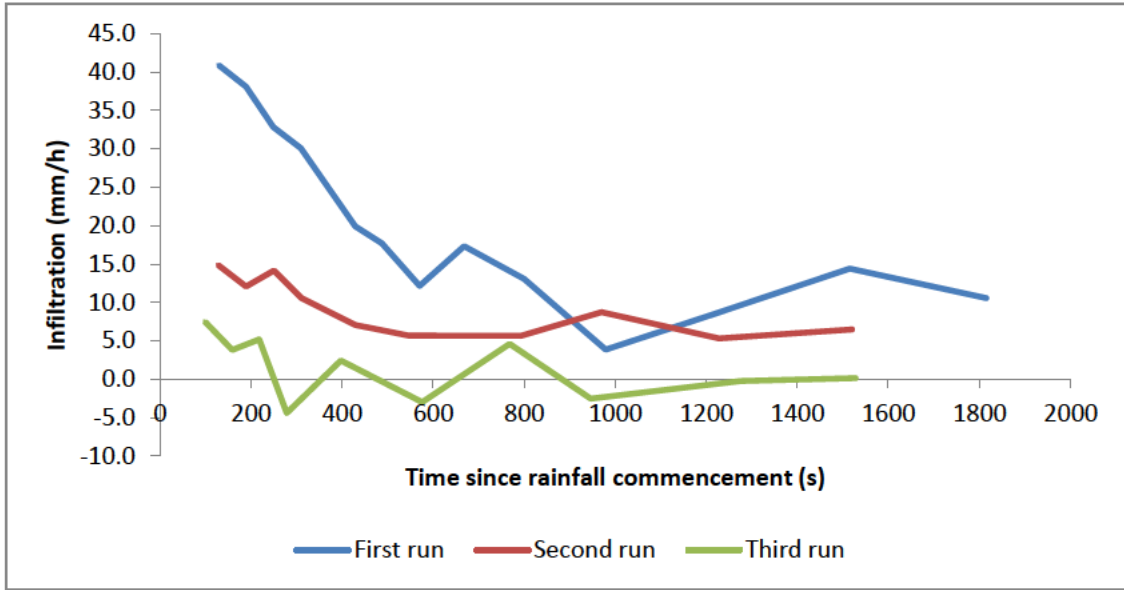


Figure 56 Infiltration curves for Sodosol #1

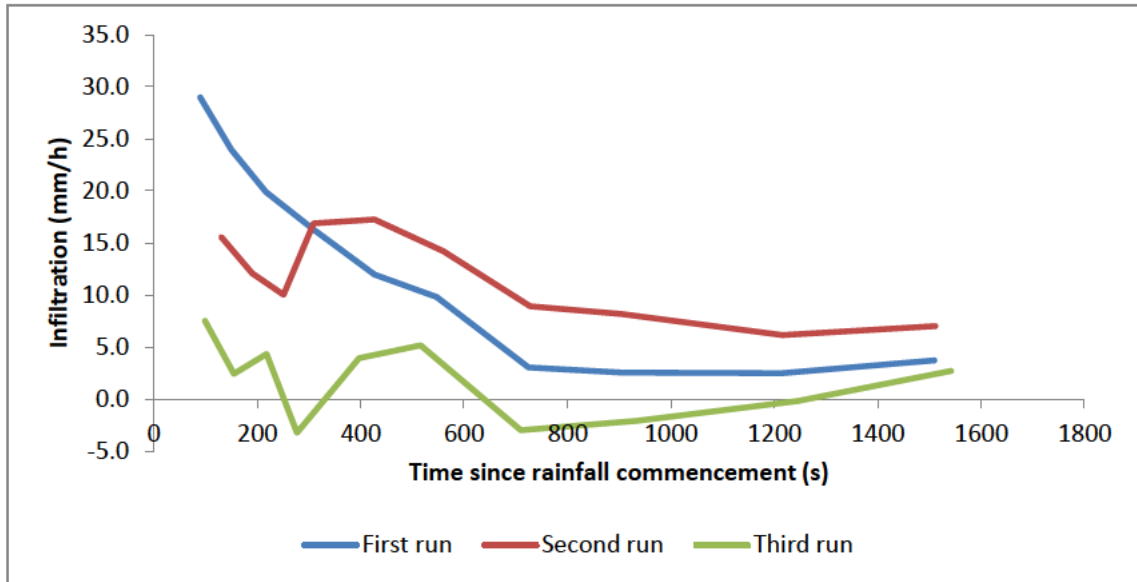


Figure 57 Infiltration curves for Sodosol #2

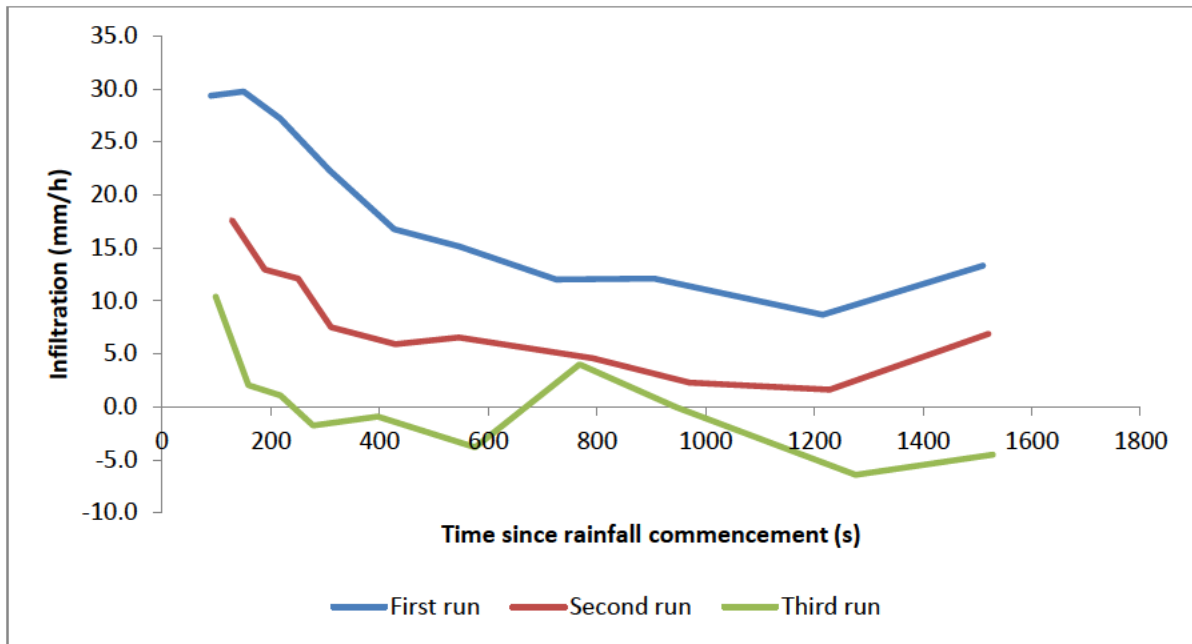


Figure 58 Infiltration curves for Sodosol #3

The Sodosol's demonstrated a general trend of infiltration rates declining with each cycle. When the soil was sampled at the end of the rainfall experiments the bulk soil felt dry (average measured θ was 13%) indicating that most water had runoff and a crust had formed.

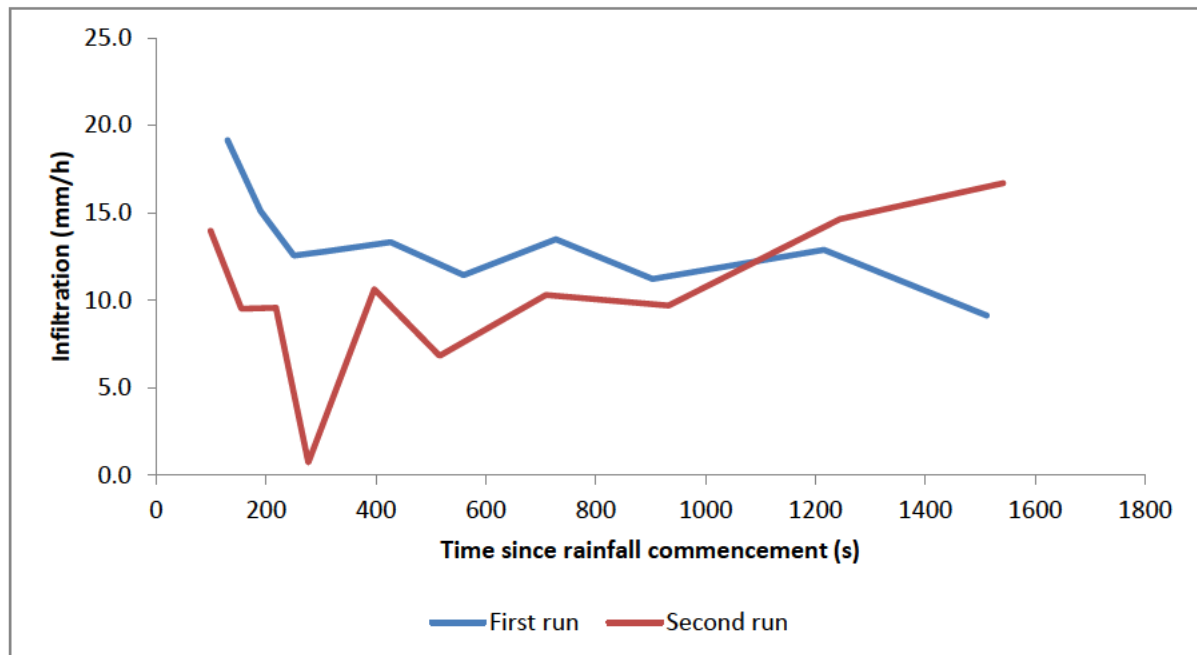


Figure 59 Infiltration curves for Chromosol

The infiltration rate on the second run of the Chromosol was initially less than the first run, as would be expected, however increased towards the end of the simulation. This may have been as a result of a preferential flow path being formed in the tray. The bulk soil of the Chromosol felt drier than the Sodosol's with an average measured θ of 11.7%. This indicated that most of the water had runoff as a result of a crust forming.

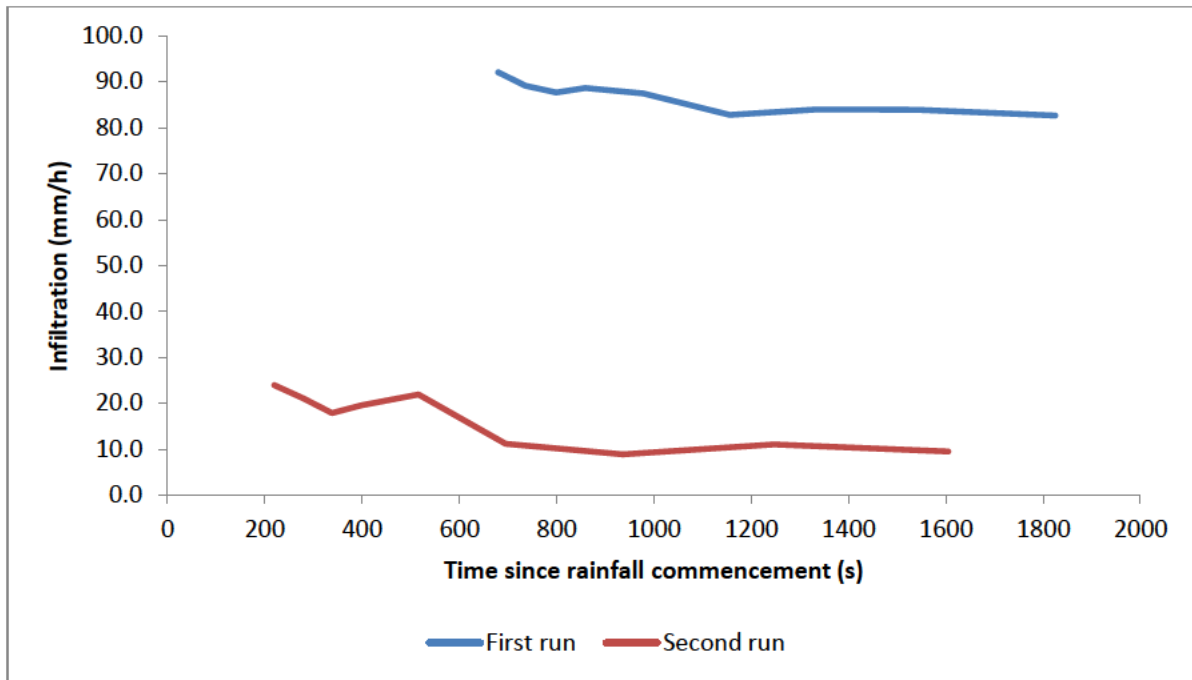


Figure 60 Infiltration curves for Ferrosol

The extremely high infiltration rate on the first run of the Ferrosol is as at least partially a result of insufficient packing of the front lip of the tray resulting in water pooling near the front edge but not running off. The θ of the Ferrosol was not measured after the experiments due to an oversight however the soil felt saturated. There was no evidence of crust formation.

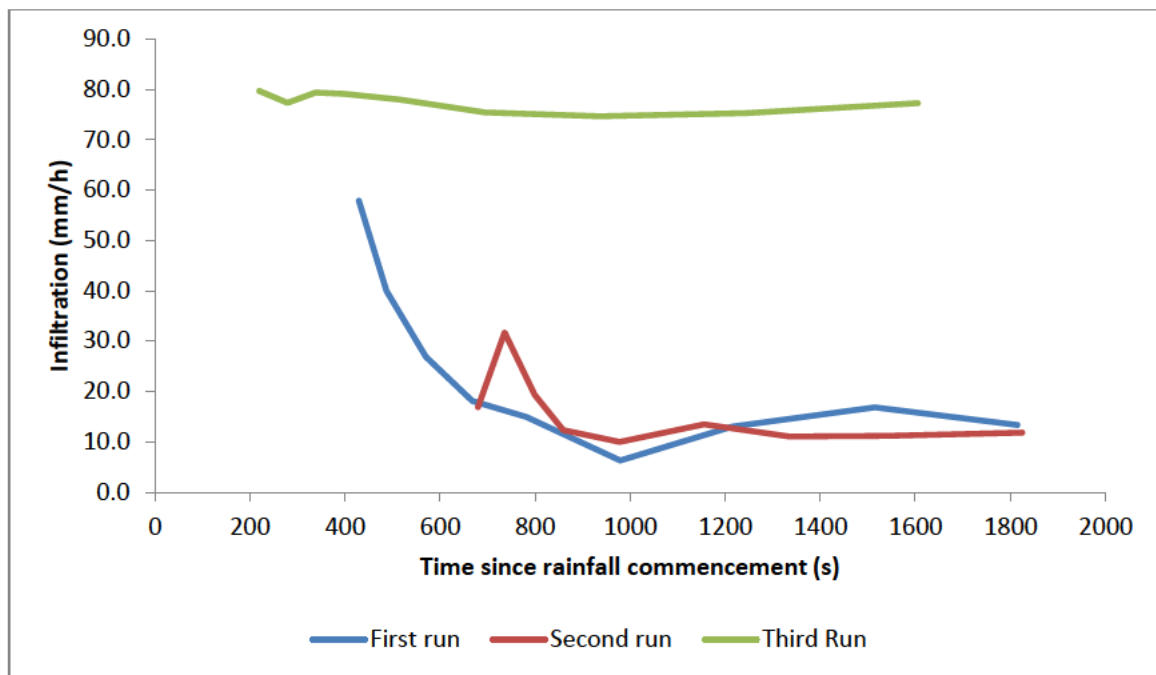


Figure 61 Infiltration curves for Hydrosol

The Hydrosol sample felt saturated after the rainfall simulation experiments with an average measured θ of 54.5%. There was no evidence of crust formation.

Whilst samples demonstrated a general trend of infiltration rates declining overtime there was a substantial ‘noise’ within the data. Landloch staff indicated that this is normal from rainfall simulation experiments. As a result the data was cleaned before further analysis was completed.

5.3.2. Data cleaning

The rainfall simulation data was cleaned by removing unwanted outliers. The process applied was as follows:

- A data entry check was completed to ensure that hand written records from the rainfall simulation had been accurately transcribed into the spreadsheet.
- A zero value was applied to negative infiltration rates on the basis that a negative infiltration rates is physically impossible. It is assessed that negative infiltration rates occurred as a result of temporary ponding on the soil surface caused by rainfall impact reorganising the soil surface.
- Major increases in infiltration rate towards the end of the simulation were removed. This decision was made as it was assessed that the increases are likely to have resulted from preferential flow around the edges of the plot rather than infiltration into the soil mass. There was some evidence of this identified when emptying the trays were it was obvious in some of the trays that the moisture content on the sides of the plot was greater than in the middle of the plot.

5.3.3. Infiltration and runoff results

Infiltration curves were replotted using the final data set for each simulation. A regression equation was derived using Microsoft Excel with the equation type (e.g. linear, polynomial or logarithmic) having the highest r^2 value being selected. These equations are subsequently used to compare the observed infiltration rates to the HYDRUS-1D modelled infiltration rates. In general the r^2 values for the first run were close to 1 and declined substantially on subsequent runs.

Table 28 Regression equations and r^2 values for observed infiltration where $I(t)$ is the infiltration rate at time (t) and t is time in seconds

Soil	Run	Regression equation	R^2
Sodosol #1	1	$I(t) = 1E-08t^2 - 2E-05t + 0.0142$	0.9455
Sodosol #1	2	$I(t) = 3E-09t^2 - 6E-06t + 0.0046$	0.7562
Sodosol #1	3	$I(t) = -6E-04\ln(t) + 0.0043$	0.5203
Sodosol #2	1	$I(t) = 7E-09t^2 - 2E-05t + 0.0089$	0.9852
Sodosol #2	2	$I(t) = 3E-09t^2 - 9E-06t + 0.0075$	0.94
Sodosol #2	3	$I(t) = -5E-04\ln(t) + 0.0036$	0.3426
Sodosol #3	1	$I(t) = 6E-09t^2 - 1E-05t + 0.0096$	0.9694
Sodosol #3	2	$I(t) = 3E-09t^2 - 6E-06t + 0.0046$	0.7562
Sodosol #3	3	$I(t) = -8E-04\ln(t) + 0.0051$	0.2851
Chromosol	1	$I(t) = -7E-04\ln(t) + 0.008$	0.6226
Chromosol	2	$I(t) = 4E-09t^2 - 5E-06t + 0.0038$	0.3947
Ferrosol	1	$I(t) = 3E-09t^2 - 8E-06t + 0.0297$	0.8823
Ferrosol	2	$I(t) = 3E-09t^2 - 9E-06t + 0.0082$	0.8267
Hydrosol	1	$I(t) = 2E-08t^2 - 4E-05t + 0.0266$	0.774
Hydrosol	2	$I(t) = -0.006\ln(t) + 0.0445$	0.7129
Hydrosol	3	$I(t) = -2E-09t^2 + 4E-06t + 0.0059$	0.7624

Cumulative infiltration was determined as follows:

- It was assumed that all rainfall applied prior to runoff commencement infiltrated into the soil. This was calculated by multiplying the average applied rainfall rate (mm/s) by the time until runoff commencement.
- Integrating the regression equation over the time period from runoff commencement until simulation end.
- Adding the two results together.

The cumulative infiltration results are displayed in Table 29. A trend across all soils is that total infiltration is the highest in the first run and declines in subsequent runs.

Table 29 Cumulative infiltration calculations from rainfall simulation experiments

Soil	Run	Rainfall intensity (mm/s)	Time to runoff (s)	Time to last measurement (s)	Pre runoff infiltration (mm) [Col C x Col D]	First integration term	Second integration term	Post runoff infiltration (mm) [Col G - Col H]	Total infiltration (mm) [Col F + Col I]
Sodosol #1	1	0.0317	50	1815	1.58	12.761	0.685	12.08	13.66
Sodosol #1	2	0.0336	40	1520	1.34	3.573	0.179	3.39	4.74
Sodosol #1	3	0.0294	45	1528	1.32	0.765	0.118	0.65	1.97
Sodosol #2	1	0.0289	39	1510	1.13	-1.328	0.332	-1.66	-0.53
Sodosol #2	2	0.0321	309	1512	9.92	4.509	1.917	2.59	12.51
Sodosol #2	3	0.0292	40	1542	1.17	0.662	0.090	0.57	1.74
Sodosol #3	1	0.0308	39	1215	1.20	7.870	0.367	7.50	8.70
Sodosol #3	2	0.0310	40	1520	1.24	3.573	0.179	3.39	4.63
Sodosol #3	3	0.0281	45	768	1.27	0.449	0.128	0.32	1.59
Chromosol	1	0.0282	78	1512	2.20	3.110	0.272	2.84	5.04
Chromosol	2	0.0272	76	933	2.06	2.452	0.275	2.18	4.24
Ferrosol	1	0.0293	669	1825	19.63	46.958	18.378	28.58	48.21
Ferrosol	2	0.0260	344	1605	8.95	5.703	2.329	3.37	12.33
Hydrosol	1	0.0285	400	1815	11.42	22.255	7.867	14.39	25.81
Hydrosol	2	0.0275	440	1825	12.08	9.941	0.410	9.53	21.62
Hydrosol	3	0.0288	344	1605	9.90	11.865	2.239	9.63	19.53

5.3.4. Sources of error

As demonstrated in Figure 56 **Infiltration curves for Sodosol #1** through to Figure 61 there is significant variance in the recorded runoff data. This variance can be attributed to a number of factors, including the rainfall simulator, measurement of runoff and the soil/soil trays.

Potential sources of error from the rainfall simulator include:

- An average rainfall value based on the runoff collected from four rain gauges surrounding the runoff plot is used as the value for applied rainfall. There is substantial variance in the spatial distribution of the applied rainfall as highlighted in Table 30 which details the average rainfall in mm/h collected from each of the four gauges from each plot.

Table 30 Average rainfall (mm/h) collected in rain gauges

		Back				Back			
		114.74				108.30			
Left	115.32	Plot 1	108.53	Right	Left	105.17	Plot 2	100.17	Right
		102.36					92.17		
		Front					Front		

- The rain gauges located at the front and back of the trays were mounted by a magnet to the tray such that the top of the rain gauge was at the same angle to the horizontal as the soil tray (20 per cent gradient). The result is that the effective aperture of the rain gauge, particularly for the gauge located at the front of the tray is substantially reduced resulting in fewer rain drops entering the gauge. This effect can be noticed by the smaller values of recorded rainfall in the front gauge compared to the other gauges. The net effect is that the averaged applied rainfall per plot used in the calculations is less than the actual rainfall applied to the plot. This is estimated to be a difference in the applied rainfall rate of 2.5 – 3 mm/h based on the difference in rainfall from the four gauge rainfall average to a three gauge annual rainfall using the side and back gauges.
- The rainfall simulator is located outside in a semi-protected area but is still exposed to weather conditions, particularly wind. There were no noticeable breezes present during the simulations however, as wind was not measured, there is the potential that wind had a temporal and/or spatial impact upon the applied rainfall but this cannot be quantified.

The major potential source of error from the measurement of runoff is the manual nature of the recording method. Measuring the runoff sample requires two jars to be simultaneously placed under the runoff outlet for each of the plots. Errors can result from one of the jars being placed under the outlet at slightly different times and/or the jar not being centrally placed under the outlet in the first instance resulting in some runoff not being captured. There is also the potential for error in the timing by the recorder. One data point was selected and the sampling time changed by +/- 0.2 s. This resulted in a change to the instantaneous infiltration rate (mm/h) from the original value of 7.5 mm/h to 6.2 mm/h (-0.2 s) or 8.7 mm/h (+0.2 s).

There are several sources of potential error relating to the soils/soil trays. These are:

- Inconsistent packing of the trays. The trays were packed manually with special attention placed on ensuring that the edges and corners of the trays were well packed to minimise any preferential flow that would reduce runoff. However the manual nature of this process implies that inconsistencies could result.
- Insufficient packing of the front lip of the tray. When this occurs water that would be runoff pools at the lip, reducing the runoff and increasing the apparent infiltration. It is possible that this occurred on the Ferrosol run number one where ponding water was visible along the front lip. Additional soil was packed into this tray prior to the second run and the resultant infiltration rate was substantially lower. How much of this change was due to insufficient packing cannot be determined.
- All of the soil was screened prior to being placed into the trays and large stones and pieces of organic matter were removed. This resulted in a reasonably homogenous soil material. It is assessed that the state of the soils used in the simulation contributed little to the potential errors from the rainfall simulation experiments.
- The nature of the soil surface changed over time as a result of crust formation and raindrop impact. The changes impacted upon surface ponding/detention and thus measured runoff at various stages throughout the rainfall simulation. Whilst these changes could be visually observed during the simulations there was no practical measurement. It is assessed that these changes contributed to the noise within the runoff data.

A number of sources of error have been identified that have impacted upon the results from the rainfall simulation experiments. An exact quantification of the error is not possible with the data that

is available however an assessment is that the infiltration rate through time could vary by values of +/- 5 mm/h. This needs to be considered when comparing the results of the rainfall simulation experiments with the HYDRUS-1D modelled results.

5.4. Bulk density measurements (less X-Ray CT)

5.4.1. Bulk soil

The average ρ_b and associated standard deviation for each of the soils are detailed in Table 31. The standard deviation values indicate that the soil was packed relatively evenly in the trays.

Table 31 Average bulk densities and standard deviation for underlying soil based on a sample of four

Soil	ρ_b (g/cm ³)	Standard deviation
Sodosol #1	1.24	0.055
Sodosol #2	1.30	0.051
Sodosol #3	1.36	0.058
Chromosol	1.13	0.053
Ferrosol	0.98	0.014
Hydrosol	0.85	0.015

5.4.2. Water Retention Method

A summary of the results from the Water Retention Method for determining crust ρ_b are detailed in Table 32.

Table 32 Summary of water retention method crust bulk densities

Soil	Mean ρ_b (g/cm ³)	Standard Deviation
Sodosol #1	1.32	0.10
Sodosol #2	1.33	0.47
Sodosol #3	1.56	0.20
Chromosol	0.93	0.20
Ferrosol	0.87	0.06
Hydrosol	0.78	0.20

The obtained values for the Sodosol's were relatively consistent with the exception of two values from Tray #2 which appeared to be outliers. Removing these changed the average density for this sample to 1.21 g/cm³ from 1.33 g/cm³. The Chromosol formed a distinct crust so the crust density is lower than would be expected for a surface crust. The Ferrosol did not appear to form a crust and the low value for density is perhaps an indication that the tray was insufficiently compacted. The low density of the Hydrosol could be related to high levels of organic matter in that sample.

The Water Retention Method was finicky and time consuming (approximately 10 minutes required per sample). It proved very difficult to remove the crust without removing some of the underlying un-crust soil. Based on an effective area of excavation of 100mm and the average volume of soil removed (38.8 mL) an approximate average depth of excavation using this method was 5 mm. Visual analysis of images of the surface crusts suggests that thicknesses of 1 – 3 mm (Figure 62) whilst micro X-ray CT indicated crusts approximately 2 mm thick (see Section 5.5). This indicates that the water retention method sampled to a depth several times thicker than the thickness of the surface crust leading to an underestimation of the crust ρ_b .



Figure 62 Close up of example Sodosol crust. Visual examination suggests a crust of 1 - 3 mm. Pencil lead is 2 mm thick.

5.4.3. Thin Slice Method

This method proved ineffective at removing the crust for two reasons. The first was that in virtually all instances the soil surface was uneven making it difficult to calculate an accurate sample volume. The second reason was that whilst the wire could remove a sample from the top of the core quite effectively, it tended to do so along a plane of weakness within the core that was much thicker than the surface crust. As a result of the uneven segments of crust that were removed it proved impossible to obtain a sample that was shaped sufficiently even to obtain an accurate density measurement. As a result the modified intact clod method was used.

5.4.4. Modified intact clod method

The summarised results of the modified intact clod method are detailed in Table 33.

Table 33 Results from modified intact clod method for bulk density determination

Summary	10 mL		100 mL		Percentage difference
	Mean density	Standard Deviation	Mean density	Standard Deviation	
Sodosol #1	1.99	0.19	1.75	0.28	14%
Sodosol #2	1.94	0.28	1.16	0.06	68%
Sodosol #3	1.99	0.22	1.46	0.26	36%
Sodosol Average	1.97		1.46		35%
Chromosol	1.62	0.19	1.15	0.18	40%

Substantial differences in crust ρ_b are evident based on the size of measuring cylinder (MC) used to determine displaced volume with the 10 mL MC producing higher density values (but more consistent) for all soils. The standard deviations are broadly comparable between the sizes but more consistent for the 10 mL MC. As the soil oven dry mass and initial volume were measured using laboratory scales; it appears that the final volume reading obtained by reading the scale on the MC is a likely source of error, particularly given the small size of the crust fragments used to obtain ρ_b . The average mass of the crust fragments used in the 10 mL and 100mL MC were 0.7 g and 2.4 g respectively. Another potential source of error was air bubbles that formed when the crust fragments were placed into the cylinder. The larger bubbles were popped using a pencil before a reading was

obtained but smaller bubbles may have remained that would result in a larger final volume and hence lower calculated density.

To determine how sensitive the calculated densities were to the final volume measurement a sensitivity analysis was conducted. The gradations were 0.25 mL and 1 mL apart on the 10 and 100 mL MC respectively. A conservative estimate of the largest possible measurement error was half the difference between the gradations (i.e. 0.125 mL and 0.5 mL for the 10 mL and 100 mL measuring cylinders respectively). It was further assumed that this error could be either higher or lower than the actual reading resulting in assumed accuracies of +/- 0.0625 mL and +/- 0.25 for the 10 mL and 100 mL MC respectively. Densities were re-calculated using the Negative Maximum Error (NME, subtracting the maximum volume error) and Positive Maximum Error (PME, adding the maximum volume error) and the range between the NME and PME calculated. The results are detailed in Table 34.

Table 34 Average ρ_b results for the modified clod immersion method sensitivity analysis. Units are in g/cm^3 . Average range results between the 10 mL and 100 mL measuring cylinder are also provided.

Soil	10 mL			100 mL		
	NME	PME	Range	NME	PME	Range
Sodosol #1	2.53	1.26	1.26	2.10	1.20	0.91
Sodosol #2	2.57	1.32	1.25	1.35	1.16	0.19
Sodosol #3	2.41	1.21	1.20	1.76	1.20	0.56
Chromosol	1.88	1.16	0.72	1.32	1.15	0.17
		Average	1.11		Average	0.46

Some of the individual NME results for the 10 mL MC exceeded a ρ_b of 2.65 g/cm^3 which is physically impossible. The average range of the 10 mL MC results is more than twice that of the 100 mL MC results indicating that the accuracy of ρ_b calculated from the 100 mL MC is likely to be better than results from the 10 mL MC. It was decided to use the 100 mL MC calculated ρ_b values for comparison to other methods of ρ_b determination due to its assessed increased accuracy. Additional measurements were made with the average results detailed in Table 35 **Bulk density results from surface crust method**

Table 35 Bulk density results from surface crust method

Soil	Mean ρ_b (g/cm^3)	Standard Deviation
Sodosol #1	1.49	0.26
Sodosol #2	1.27	0.13
Sodosol #3	1.33	0.30
Chromosol	1.25	0.29

5.5. Bulk density measurements (X-ray CT)

5.5.1. Introduction

Imagery produced from the micro X-Ray CT of soil cores was analysed using ImageJ (Schneider et al. 2012) image analysis software. The first step of the analysis process was to obtain a vertical slice of a soil core, an example of which is detailed in Figure 63.

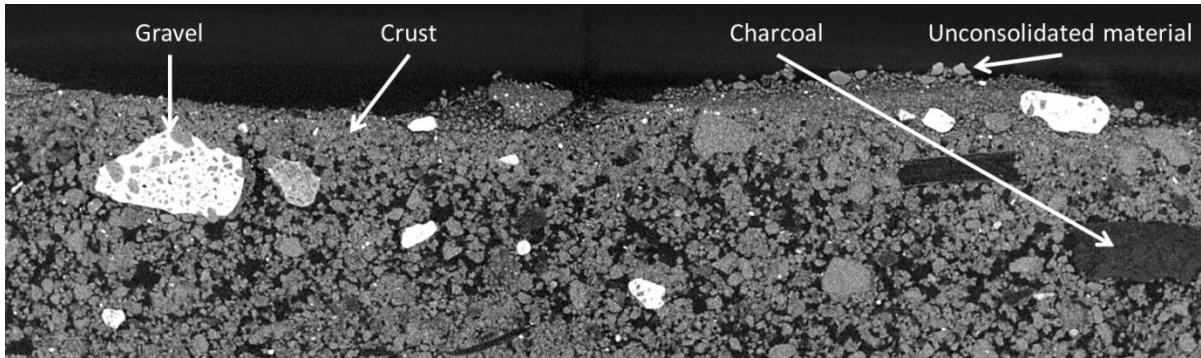


Figure 63 Example soil core profile from core number 2 (Sodosol). The black within the soil mass represents voids (or organic matter as annotated). The grey represents the soil particles.

A visual analysis of Figure 63 highlights the following:

- At the top of the soil surface there are sections of unconsolidated material, likely resulting from the detachment and subsequent deposition of soil particles from raindrop impact.
- Below the unconsolidated material is a thin layer of compacted material with relatively few visible pores of small size. This is the surface crust.
- The bulk soil underneath the soil crust has both a greater number of pores and pores of larger size.

A crust, similar to that identified in Figure 63, was visually identifiable on all of the soil cores.

5.5.2. Crust porosity

For each image stack, the ‘Radial Reslice’ function in ImageJ was executed over a 180 degree arc with 10 degrees rotation between each slice. This resulted in 18 vertical slices per soil core. To determine if there was a loss in accuracy by only using 18 images the ‘Radial Reslice’ function was applied using 5 degrees rotation between each slice (i.e. 36 vertical slices per soil core). A comparison of the two settings (Table 36) indicates that the difference is negligible. This comparison was made to minimise the image processing time with an acceptable level of accuracy.

Table 36 Comparison of porosity and bulk density results for 18 and 36 vertical slices per core

	Calculated porosity	Calculated bulk density
18 slices	0.876931667	2.323868917
36 slices	0.870652778	2.307229861

The initial ImageJ script was amended to enable automatic porosity calculation for each of the 18 slices. The resulting ImageJ determined porosity and resultant ρ_b values are detailed in Table 37.

Table 37 ImageJ calculated crust porosity and ρ_b

Soil	Core	Crust	
		Porosity	ρ_b (g/cm ³)
Chromosol	16	0.09	2.42
Chromosol	11	0.13	2.30
Chromosol	12	0.13	2.32
Sodosol #1	2	0.12	2.32
Sodosol #1	3	0.1	2.39
Sodosol #1	4	0.09	2.42

Soil	Core	Crust	
Sodosol #1	13	0.23	2.03
Sodosol #2	7	0.15	2.25
Sodosol #2	8	0.22	2.06
Sodosol #2	9	0.17	2.21
Sodosol #2	14	0.17	2.20
Sodosol #3	5	0.09	2.40
Sodosol #3	6	0.18	2.16
Sodosol #3	10	0.14	2.28
Sodosol #3	15	0.14	2.28

The results indicate a porosity that is substantially lower than normally observed (and as a result ρ_b is higher). Some of the crust density values are approaching the maximum possible density of soil (assumed to be 2.65 g/cm³). This will be explored further in the next section.

5.5.3. Determination of bulk soil porosity

The bulk soil porosity results for the average of 18 vertical slices per core are detailed in Table 38.

Table 38 ImageJ calculated bulk soil porosity and ρ_b

Soil	Core	Bulk soil	
		Porosity	ρ_b (g/cm ³)
Chromosol	16	0.2	2.13
Chromosol	11	0.27	1.94
Chromosol	12	0.32	1.80
Sodosol #1	2	0.27	1.93
Sodosol #1	3	0.28	1.92
Sodosol #1	4	0.35	1.72
Sodosol #1	13	0.28	1.91
Sodosol #2	7	0.31	1.83
Sodosol #2	8	0.24	2.00
Sodosol #2	9	0.24	2.02
Sodosol #2	14	0.24	2.02
Sodosol #3	5	0.2	2.11
Sodosol #3	6	0.28	1.90
Sodosol #3	10	0.26	1.97
Sodosol #3	15	0.31	1.83

The porosity and ρ_b values calculated by image analysis for both the crust and sub-soil are substantially lower than those reported in the literature. This suggests that the ImageJ calculated values are different than the actual values. There are a number of reasons why this could occur:

- Resolution. The resolution of the imagery is 30 μm . As a result pores of smaller size than this can not be identified and are treated as soil solids. This reduces the apparent porosity.
- Thresholding. The ‘Make Binary’ function in ImageJ was used to threshold the images. There may be a bias in this algorithm that reduces the apparent porosity.

- Soil carbon. Pieces of charcoal were present in many of the soil cores. As demonstrated by Figure 63 soil carbon appears black. When thresholding is applied to the image, pieces of soil carbon can appear as a pore. This would have the effect of increasing the apparent porosity.

The ImageJ derived ρ_b values were considered to be positively biased when compared to the actual values. To correct this bias the average bulk soil measured value for ρ_b using the soil core method (Cresswell & Hamilton 2002) was assumed to be the correct value. The adjusted values for crust ρ_b were then calculated using Equation 18 and are detailed in Table 39.

$$\text{Crust } \rho_b = \frac{\text{ImageJ crust } \rho_b}{\text{ImageJ bulk soil } \rho_b} \times \text{Measured subsoil } \rho_b \quad \text{Equation 18}$$

Table 39 details the adjusted crust ρ_b values and compares them to the measured bulk soil ρ_b values. This indicates that in all instances ρ_b of the crust was greater than the underlying soil as is to be expected if a crust was formed. There is however a large range of differences in densities with the minimum increase being 3 % (Core 8) and the maximum increase being 41 % (Core 4).

Table 39 Comparison of adjusted crust ρ_b to measured bulk soil ρ_b

Soil	Core	Adjusted crust ρ_b (g/cm ³)	Average measured bulk soil ρ_b (g/cm ³)	Absolute difference between crust and subsoil density (g/cm ³)	Percentage difference (%)
Chromosol	16	1.28	1.13	0.15	14%
Chromosol	11	1.34		0.21	19%
Chromosol	12	1.45		0.32	28%
Sodosol #1	2	1.49	1.24	0.25	20%
Sodosol #1	3	1.55		0.31	25%
Sodosol #1	4	1.74		0.50	41%
Sodosol #1	13	1.32		0.08	6%
Sodosol #2	7	1.59	1.30	0.29	22%
Sodosol #2	8	1.34		0.04	3%
Sodosol #2	9	1.42		0.12	9%
Sodosol #2	14	1.41		0.11	9%
Sodosol #3	5	1.55	1.36	0.19	14%
Sodosol #3	6	1.55		0.19	14%
Sodosol #3	10	1.57		0.21	16%
Sodosol #3	15	1.69		0.33	24%

The purpose of deriving density values was for use as an input into HYDRUS-1D modelling for both the surface crust layer and the underlying soil. The average of the adjusted crust ρ_b value for each soil was used for the surface crust ρ_b and the average measured ρ_b using the soil core ring method used for the soil underlying the crust.

5.5.4. Identification of changes in soil ρ_b with depth

The average ρ_b with increasing depth for each of the soils is shown in Figure 64. The impact of unconsolidated material at the top of the soil surface is shown by a lower density than the crust immediately below the soil surface for all soils. The increased density below the soil surface is a result of the surface crust. The density declines with increasing depth below the surface however there is substantial variation of ρ_b with depth for all soils.

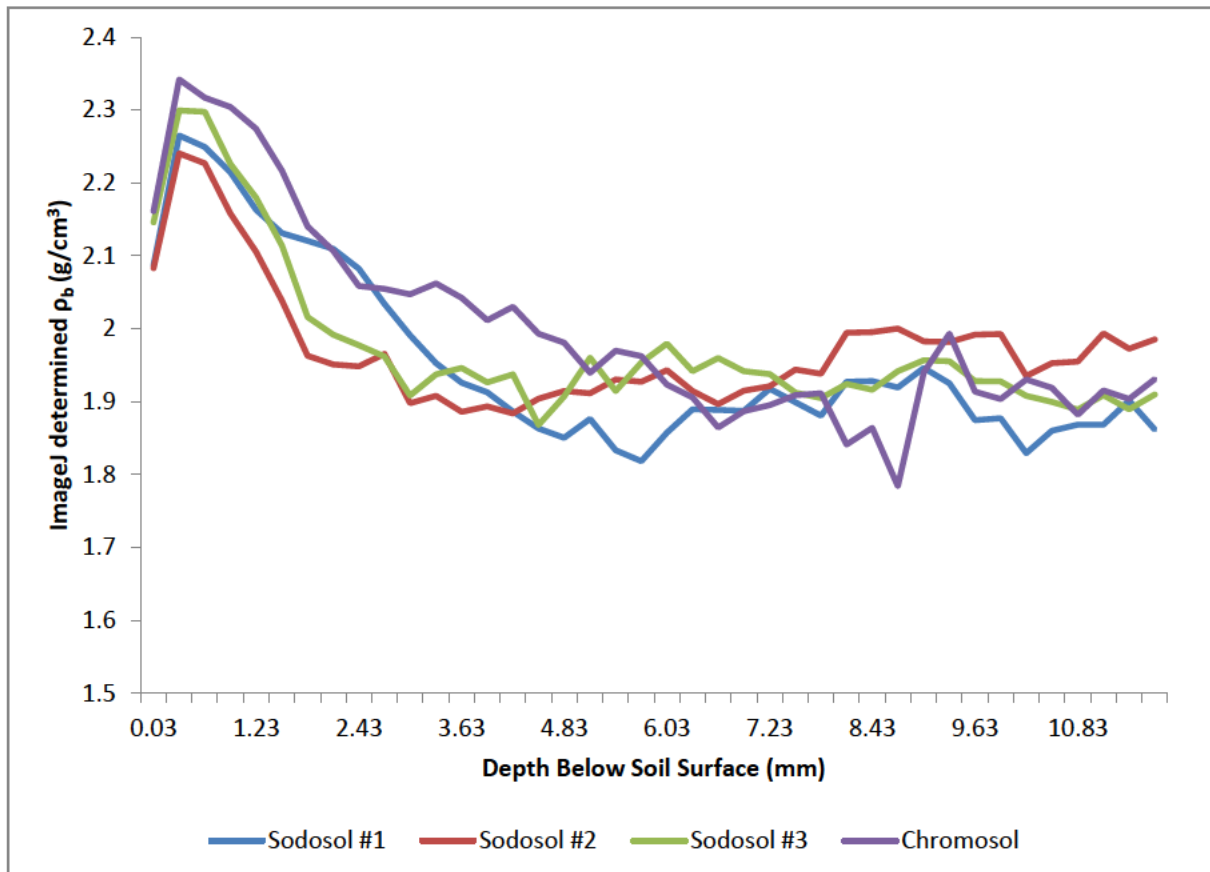


Figure 64 ImageJ derived average ρ_b (not adjusted) with depth below soil surface.

Given the variation in density throughout the depth of the image stack there was no distinct depth where the surface crust ended. To determine a crust depth value that could be incorporated into HYDRUS-1D for modelling purposes the following approach was applied:

- The average ρ_b and standard deviation of the last 25 measurements was calculated. This was assumed to be the subsoil density ρ_b .
- A five point moving average was calculated to smooth out the measured ρ_b values.
- The averages and the original data were plotted. After reviewing the plots it was decided to include the average ρ_b plus one standard deviation to account for the variability within the data. An example of the results from Sodosol #3 are detailed in Figure 65.

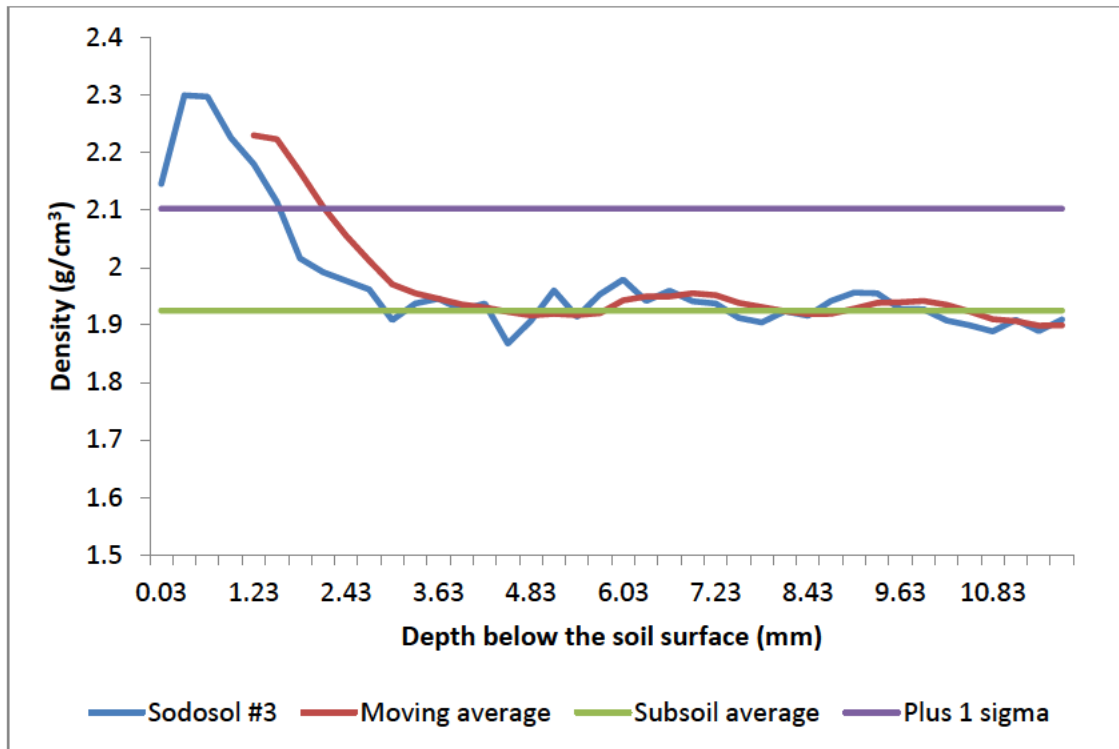


Figure 65 Determining the thickness of the surface crust (Sodosol #3)

The thickness of the crust was then calculated using two methods. The first was subtracting depth of maximum density (0.3 mm in all instances) from the depth where the moving average intercepted the subsoil average. The second approach was similar but used the depth where the moving average intercepted the subsoil average plus one standard deviation. The results are detailed in Table 40.

Table 40 Crust thickness determination

Soil	Depth subsoil average interception (mm)	Crust thickness (mm)	Depth subsoil average plus one sigma interception (mm)	Crust thickness (mm)
Sodosol #1	4.83	4.53	3.93	3.63
Sodosol #2	3.03	2.73	2.43	2.13
Sodosol #3	4.23	3.93	2.13	1.83
Chromosol	6.93	6.63	3.03	2.73

The initial HYDRUS-1D modelling proved that small variations in crust thickness made little difference in the predicted infiltration. As a result after reviewing the density with depth profile for each soil, the results in Table 41, photographic images of the crusts as well as ImageJ images, it was decided that a 2 mm crust would be used for all soils.

5.5.5. Summary of bulk density results

Bulk density results from the various methods are detailed in Table 41 and compared by method in Figure 66.

Table 41 Summary of bulk density crust results

Soil	Bulk (Core)	Soil	Crust - Water Retention	Crust - Intact clod	Crust - Adjusted X-ray CT
Sodosol #1	1.24		1.32	1.49	1.36
Sodosol #2	1.30		1.33	1.27	1.52
Sodosol #3	1.36		1.56	1.33	1.44
Chromosol	1.13		0.93	1.25	1.59

The X-ray crust CT method of determining ρ_b is the only method which results in the crust having a higher density than the underlying soil for all soils. The water retention method and intact clod method results in one and two of the four soils respectively having a crust density that is lower than the bulk soil crust. As a result of this the crust ρ_b values determined by the adjusted X-ray CT method have been used for the subsequent modelling using HYDRUS-1D.

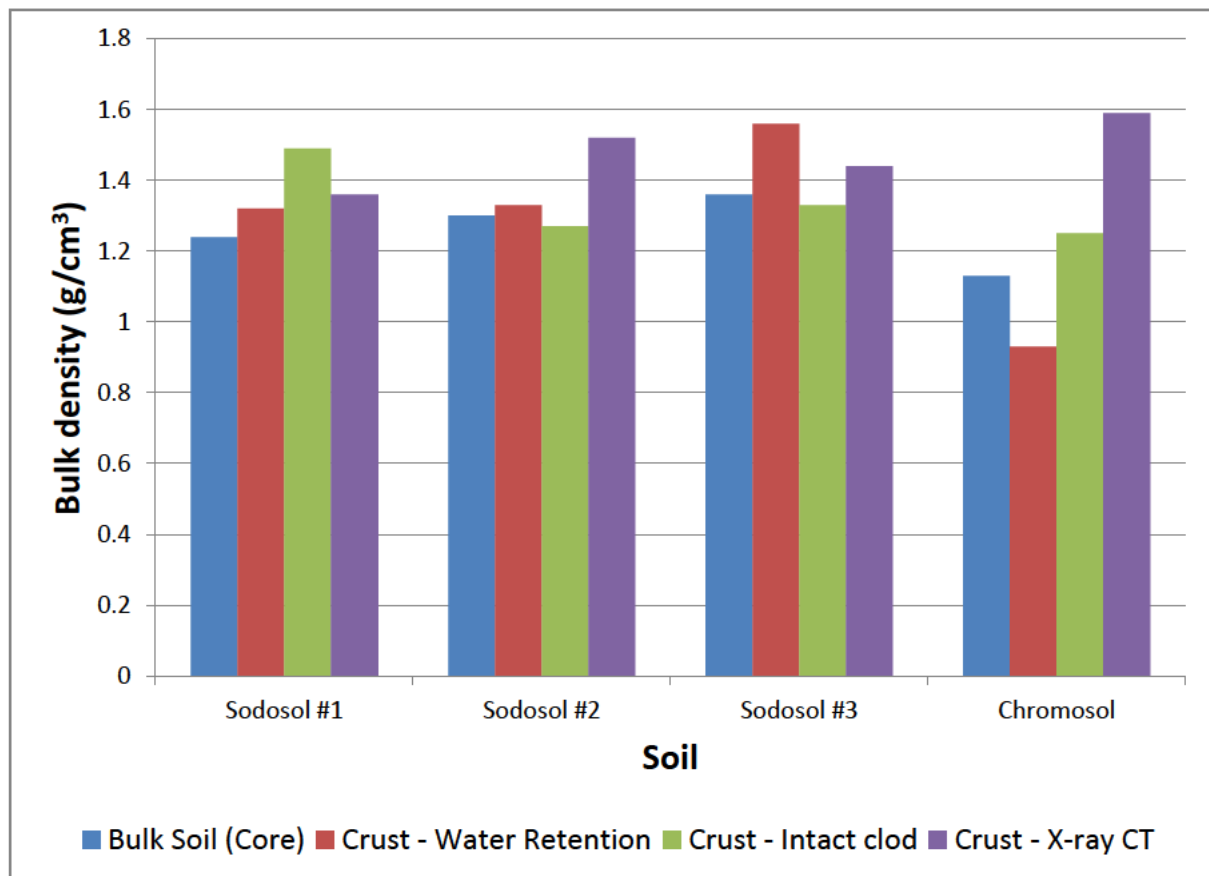


Figure 66 Comparison of bulk density results by different methods

5.6. Modelling observed infiltration using HYDRUS-1D

5.6.1. Introduction

The purpose of this project is to determine whether measuring the ρ_b of a surface crust improves the accuracy of modelled infiltration. In this section infiltration is modelled using HYDRUS-1D with the same parameters as used in the rainfall simulation experiments (e.g. simulation time, rainfall intensity) and measured soil data (e.g. soil texture, bulk density). HYDRUS-1D's inverse modelling capability has also been used to derive soil hydraulic parameters from the observed rainfall simulation

infiltration data. The results of these methods are subsequently compared to the observed infiltration rates from the rainfall simulation experiments.

5.6.2. Modelling using SSCBD inputs

Key model parameter values for the SSCBD modelling are detailed in Table 42. The soil profile was set to 100 mm and a 2 mm crust thickness incorporated to approximate the thickness of the surface crusts created during rainfall simulation. The value for ψ was set to -10,000 mm throughout the profile to replicate a partially dry soil.

Table 42 SSCBD parameter values for HYDRUS-1D modelling comparison to observed infiltration

Soil	% Sand	% Silt	% Clay	Soil mass ρ_b	Crust ρ_b
Chromosol	63	15	22	1.13	1.36
Sodosol #1	72	11	17	1.24	1.52
Sodosol #2	72	11	17	1.30	1.44
Sodosol #3	72	11	17	1.36	1.59

The second run of each soil was used to provide the observed infiltration data using the regression equations detailed in Table 28. The infiltration from the first run for each soil was ignored as this included the time where the crust was being formed. It is not possible to model infiltration during crust formation using HYDRUS-1D.

An example of the results is provided in Figure 67 for the Chromosol. The horizontal lines during the initial part of the simulation represent the infiltration before runoff commenced. The results indicate that incorporating the crust ρ_b makes relatively difference to the modelled infiltration. Similar results were obtained for the Sodosol simulations.

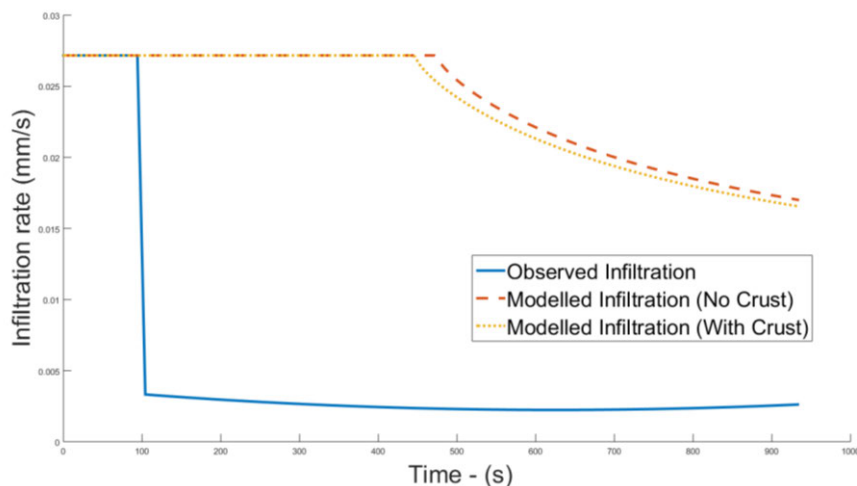


Figure 67 Comparison of approximate observed infiltration against modelled infiltration with and without a surface crust for the Chromosol

A comparison was made between modelled versus observed infiltration. The range of values for determining the criteria was constrained by only using infiltration values that occurred after the first run off measurement. This decision was made as for larger rainfall events, which are of more importance from an infiltration/runoff modelling perspective, the first few minutes is only a small proportion of the total rainfall. The values for the Nash Sutcliffe objective function for each soil are detailed in

Table 43. In all instances a large negative value results indicates very poor fits between modelled and observed results.

Table 43 Objective function values

Soil	Nash Sutcliffe Criteria
Chromosol	-4998
Sodosol #1	-1743
Sodosol #2	-31
Sodosol #3	-85

An optimisation process was completed for each soil with the aim of increasing the increasing the closeness of the modelled versus observed data. The process was to select the 'Air Entry Value of -2cm' option in the Soil Hydraulic Model dialog box within HYDRUS-1D and then increase the ρ_b value for the crust until the simulation did not converge. The final step was to reduce K_s until the simulation results did not converge. The results (Table 44) were compared to the original 2 mm crust simulation and the Nash-Sutcliffe criterion value calculated to determine how closely the modelled results approached the observed results.

Table 44 Values obtained from optimisation activity

Soil	Highest ρ_b (g/cm ³)	Lowest K_s (mm/s)	Nash-Sutcliffe Criteria
Chromosol	1.6	0.00035	-5291
Sodosol #1	1.7	0.0019	-1614
Sodosol #2	1.7	0.0017	-86
Sodosol #3	1.6	0.0031	-186

As demonstrated in Table 44 the optimisation activity did not enhance the accuracy of the modelling results.

5.6.3. Modelling using SSCBD and θ_{33} inputs

This modelling used the same input parameters as detailed in the previous section with one change. The change was the use of the H5 model within HYDRUS-1D when predicting the soil hydraulic properties which requires θ_{33} . The θ_{33} value was obtained from the HYPROP soil water retention measurements obtained from a repacked soil core of similar ρ_b to the surface crust. Three problems were encountered using this approach, being:

- The ρ_b values for the soil cores did not align to the ρ_b of the surface crust.
- There was a major difference in derived soil hydraulic properties even when the soil core ρ_b values were very similar.
- For the Sodosol HYPROP measurements, the ρ_b of the soil cores were much higher than that measured for the crust.

As a result the SSCBD and θ_{33} modelling was limited to the Chromosol with two values of θ_{33} being used (0.85 and 0.47) that were obtained from soil core ρ_b values of 1.33 and 1.41 g/cm³. These ρ_b values bounded the measured crust ρ_b of 1.36 g/cm³.

The modelling results are detailed in Figure 68 and Figure 69. In both instances the incorporation of the θ_{33} water retention point improves the modelling results compared to the observed infiltration however there is still a marked difference and the water retention values are not considered reliable.

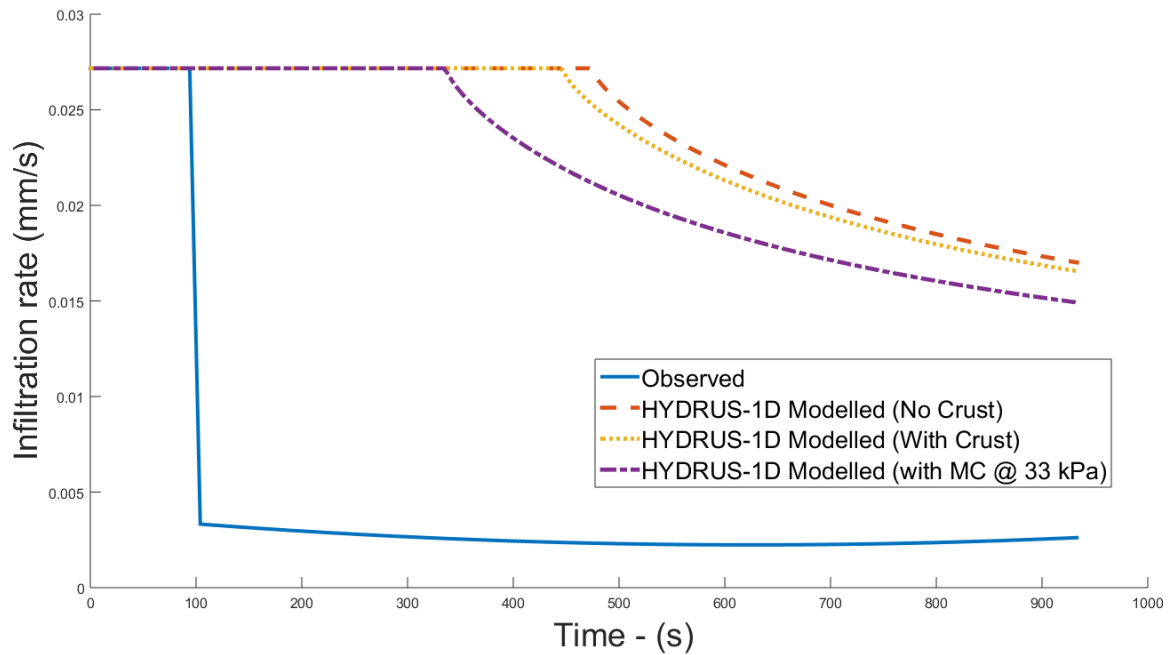


Figure 68 HYDRUS-1D modelling including incorporation of θ_{33} (value of 0.47) compared to observed infiltration

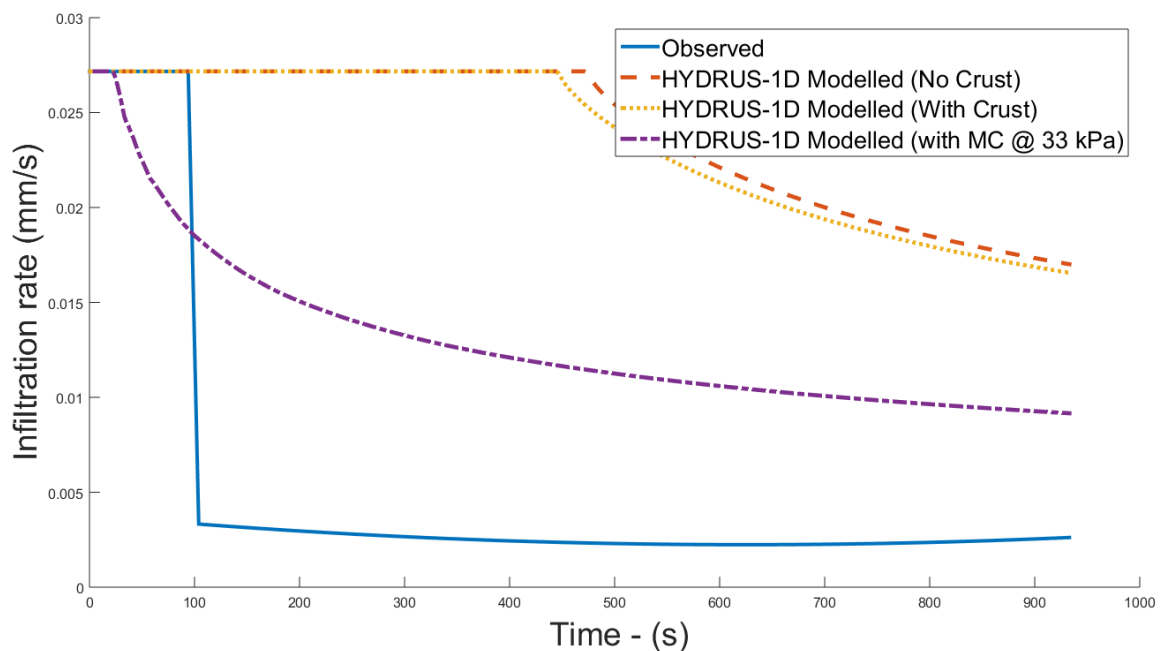


Figure 69 HYDRUS-1D modelling including incorporation of θ_{33} (value of 0.85) compared to observed infiltration

5.6.4. Inverse solution

The direct method of predicting infiltration through the use of measured soil properties provided a very poor comparison to the observed infiltration. As a result the inverse modelling capability of HYDRUS-1D was used to determine the crust soil hydraulic parameters.

HYDRUS-1D enables the user to choose which parameters are optimised when calculating the inverse solution. After trialling different input data options the rainfall simulation 'Time – Flux' option was selected as it resulted in predicted infiltration that was a close match to the observed infiltration. The α , n and K_s parameters were optimised for the surface crust horizon. When θ_s and θ_r were also optimised the modelled infiltration was a close match to the observed infiltration however this resulted in θ_r being greater than θ_s , which from a practical perspective is impossible (this is not

necessarily an issue however as θ_r can be thought of as a fitting parameter according to Radcliffe and Simunek (2010). No parameters for the underlying soil were optimised as it was found that this resulted in the solution not converging.

Figure 70 is an example of the results from the inverse solution compared to the modelled results (with no crust and with a 2mm crust) and the idealised observed infiltration. The inverse solution provides a very good match to the observed infiltration once runoff has commenced (At $t = 99$ s in this example). Similar results were achieved using the inverse solution for all soils.

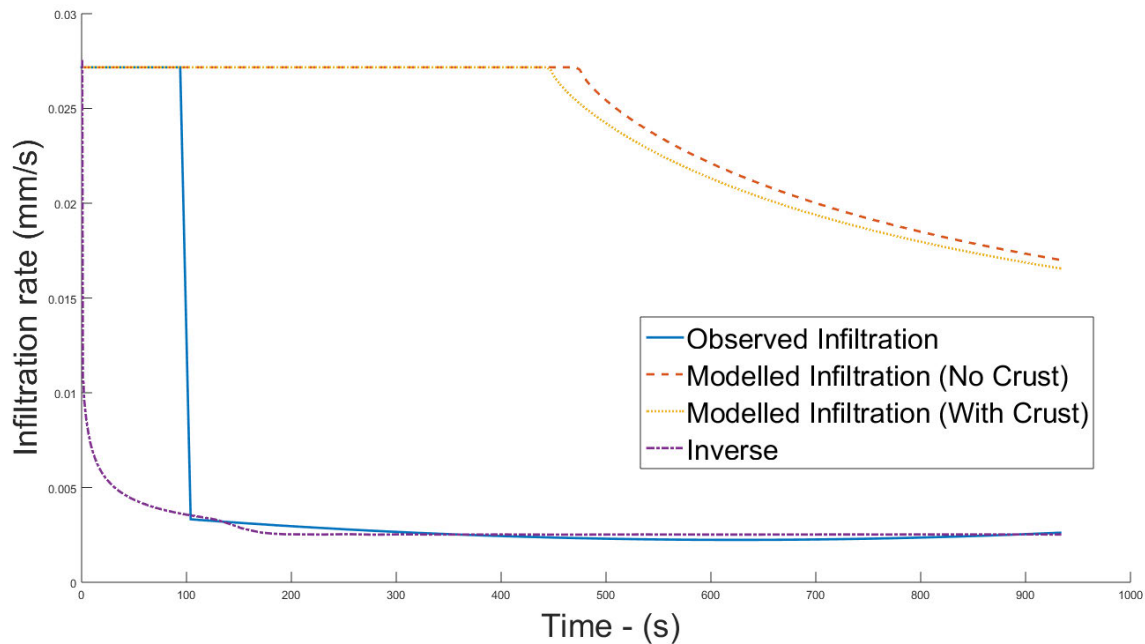


Figure 70 Comparison of observed infiltration with modelled infiltration and inverse solution – Chromosol

The Nash-Sutcliffe Criteria for the inverse solution against the observed infiltration function are detailed in Table 45 indicating that the parameters derived from the inverse solution provide a much better approximation of observed infiltration compared to the direct attempts using SSCBD data.

Table 45 Nash-Sutcliffe criterion for inverse solution modelled versus observed infiltration data

Soil	Nash-Sutcliffe Criteria
Chromosol	0.691
Sodosol #1	0.655
Sodosol #2	-0.0623
Sodosol #3	0.137

The soil hydraulic properties from the inverse solution are detailed in Table 46, including the third rainfall simulation for the Sodosol soils. The optimised parameters are α , n and K_s . These parameters were compared to the soil hydraulic properties used in the direct solution. The key difference between the direct and inverse parameters is the K_s values. The inverse solution K_s values are three to four orders of magnitude smaller than the direct solution values as shown in Figure 71.

Table 46 Inverse solution soil hydraulic parameters

Soil	θ_r mm ³ /mm ³	θ_s mm ³ /mm ³	α (1/mm)	n	K_s (mm/s)	r^2	Air Entry (Y/N)
Chromosol	0.067	0.442	0.02351	0.7125	1.756E-06	0.2882	Y
Sodosol #1 Run 2	0.058	0.395	0.02352	0.7315	2.336E-06	0.7405	Y
Sodosol #2 Run 2	0.06	0.418	0.00357	0.8082	3.242E-07	NaN	N
Sodosol #3 Run 2	0.055	0.375	0.00280	0.7092	3.470E-06	0.7272	N
Sodosol #1 Run 3	0.058	0.395	0.00866	0.7315	9.962E-07	0.2450	N
Sodosol #2 Run 3	0.06	0.418	0.00133	0.8513	1.855E-07	0.2124	Y
Sodosol #3 Run 3	0.055	0.375	0.00250	0.7092	2.415E-07	0.2094	N

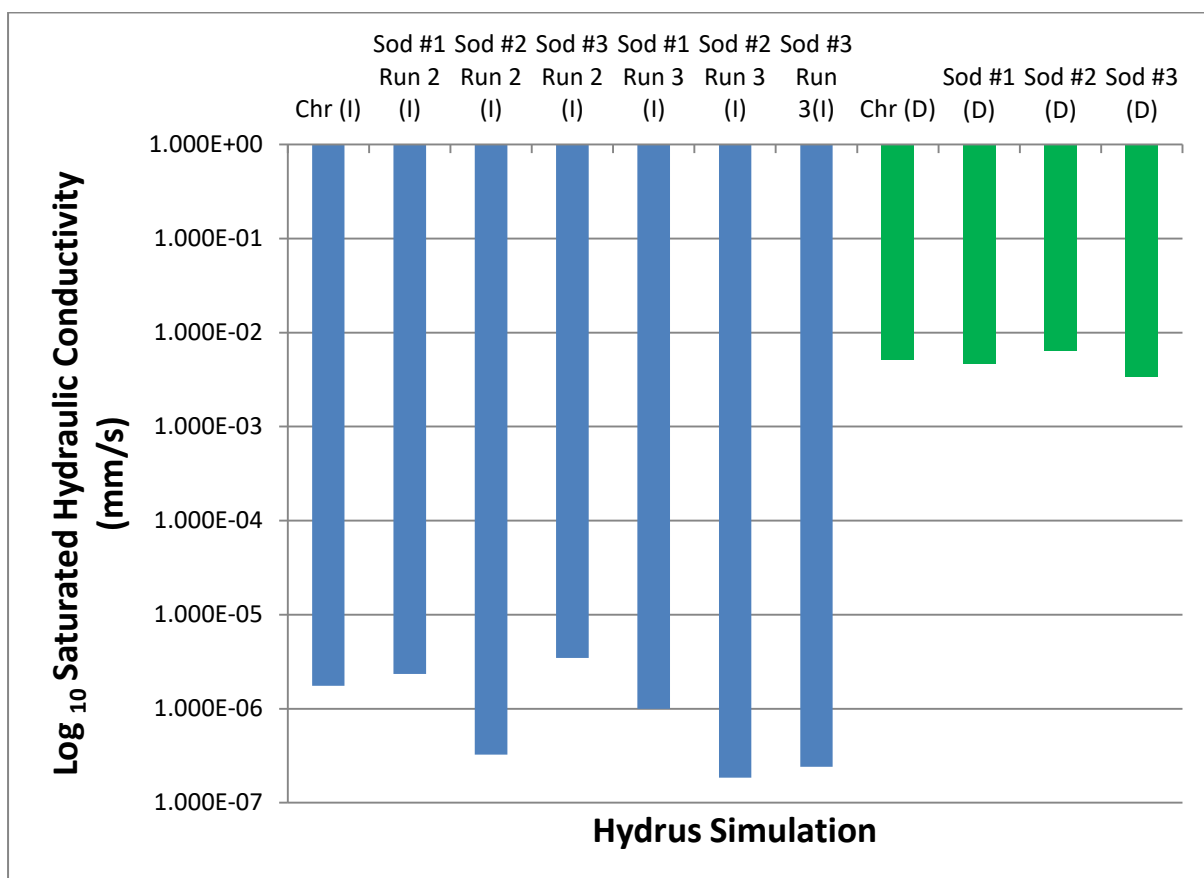


Figure 71 Comparison of K_s between inverse and direct HYDRUS-1D simulations using a log scale. Sodosol is abbreviated to 'Sod' and Chromosol to 'Chr'. (I) indicates inverse method and (D) direct method.

This enormous variation suggests that the major reason why the direct method of predicting infiltration on the crusted soils does not come close to the observed infiltration rates is because of the underestimation of K_s .

A check was made that the derived parameters from the inverse solution would produce the same results when used in the direct approach. Figure 72 is an example of this check for Sodosol #3 indicating that the derived parameters produce the same result. This occurred for all soils.

When entering the derived parameters into HYDRUS-1D a warning message ‘Retention Curve parameter is smaller than 1.001’ was triggered. This did however prevent the simulation from being completed however a boundary condition for HYDRUS-1D is that $n > 1$ (Šimůnek et al. 2009). The implications of this are discussed in Chapter Six.

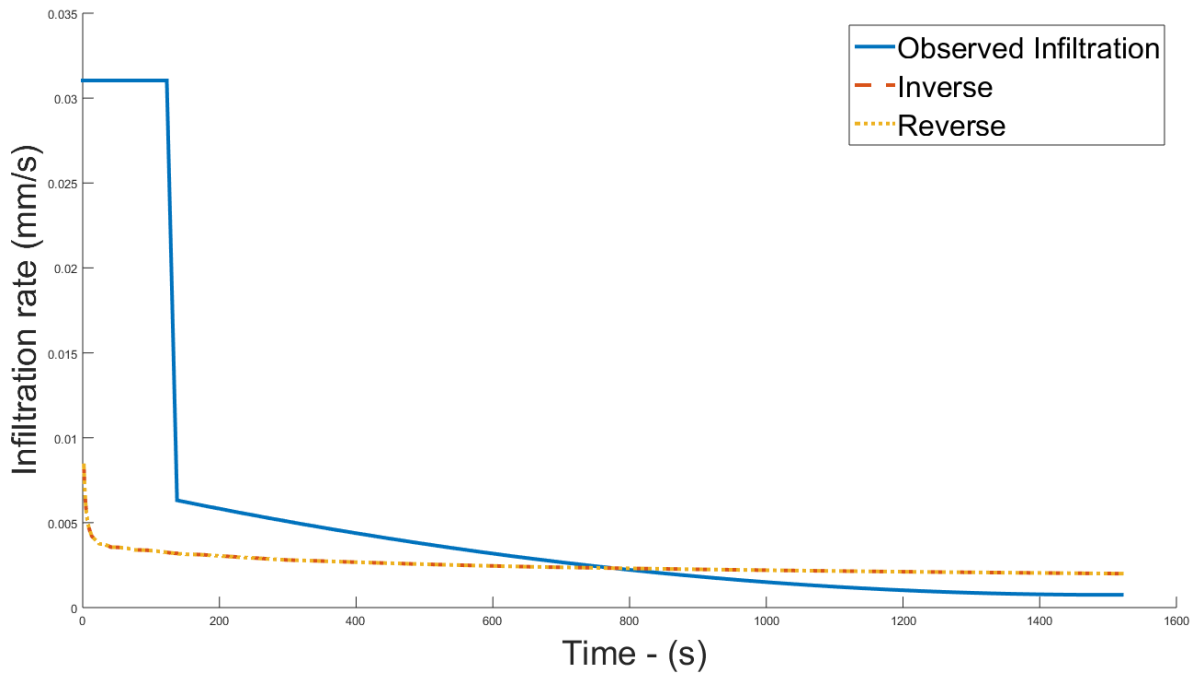


Figure 72 Check of inverse derived soil hydraulic properties – Sodosol #3

5.6.5. Modelling using average parameters

Simulations using the inverse method in HYDRUS-1D have been able to provide a close approximation to the observed infiltration rates. An initial assessment of the parameters for α , n and K_s (Table 46) indicated that they were generally similar. It was therefore investigated whether the average results (Table 47) from these parameters could be used in HYDRUS-1D simulations to provide an accurate approximation of the observed infiltration.

Table 47 Comparison of average soil hydraulic parameters obtained from inverse and direct HYDRUS-1D simulations

		α (1/mm)	n	K_s (mm/s)
Inverse	Mean	0.009412	0.75048	1.33E-06
	Std Dev	0.009911	0.0564	1.25E-06
Direct	Mean	0.002783	1.4576	0.004777
	Std Dev	0.000146	0.036898	0.001463

For each of the soils the 2 mm crusted soil simulation was copied. All parameter values were kept the same except for α , n and K_s . These values were replaced with the average values detailed in Table 47. An example simulation for Sodosol #1 using the average parameters compared to the inverse solution is provided in Figure 73. Simulations for all soils produced a similar result.

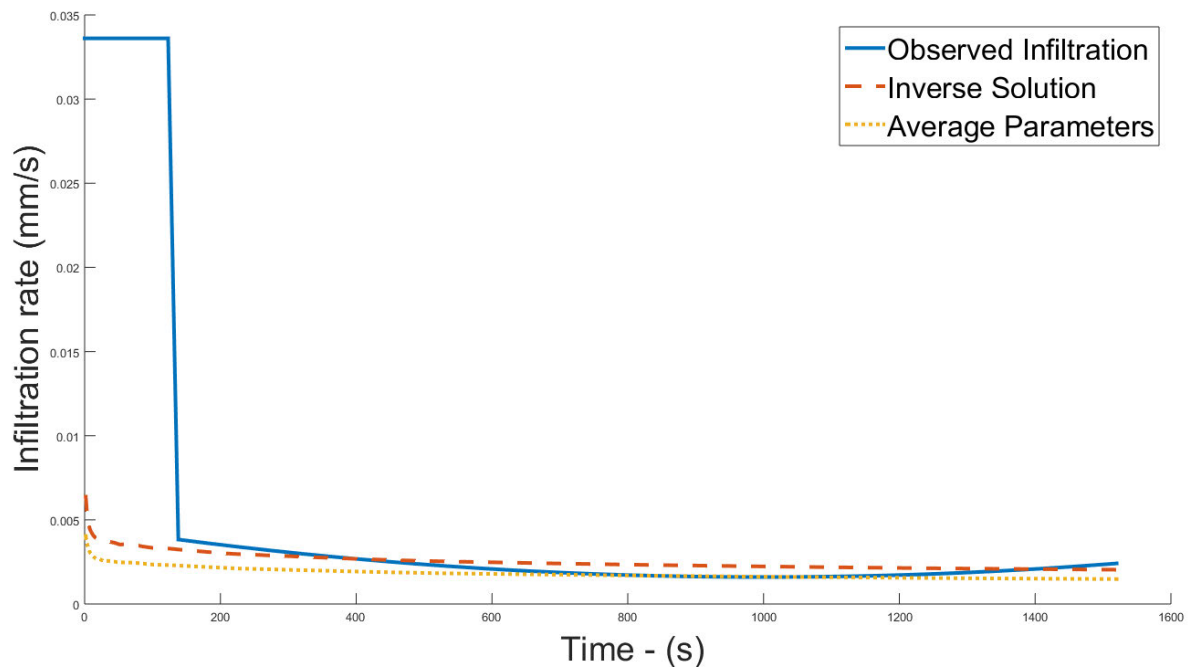


Figure 73 Comparison of inverse solution, direct solution using average parameters and the observed infiltration for Sodosol #1

The Nash-Sutcliffe Criterion was calculated for all soils. The results are detailed in Table 48. Whilst the results are negative, indicating a poor fit, they are substantially better than the results obtained from simulations using the SSCBD input data (see

Table 43). Given the ‘noise’ within the original infiltration data resulting in only moderately high r^2 values for the derived infiltration functions, the Nash Sutcliffe Criterion values are as assessed as being acceptable.

Table 48 Nash-Sutcliffe Criterion values for average parameter simulations

Soil	Nash Criterion	Sutcliffe
Chromosol	-3.74	
Sodosol #1	-0.278	
Sodosol #2	-0.11	
Sodosol #3	-0.86	

A sensitivity analysis was completed by changing the parameters around the mean plus or minus a multiple of the standard deviation. For parameters α and n this had no effect on the modelled infiltration; that is the results from each simulation were the same regardless of the parameter value used. Adjusting K_s did however have an impact upon the modelled infiltration as demonstrated in Figure 74 for Sodosol #3. All three sensitivity analysis values for K_s (represented by Min, Mean and Max in Figure 74) provided a much better approximation of the observed infiltration than the SSCBD predicted infiltration. The results were similar for the other soils.

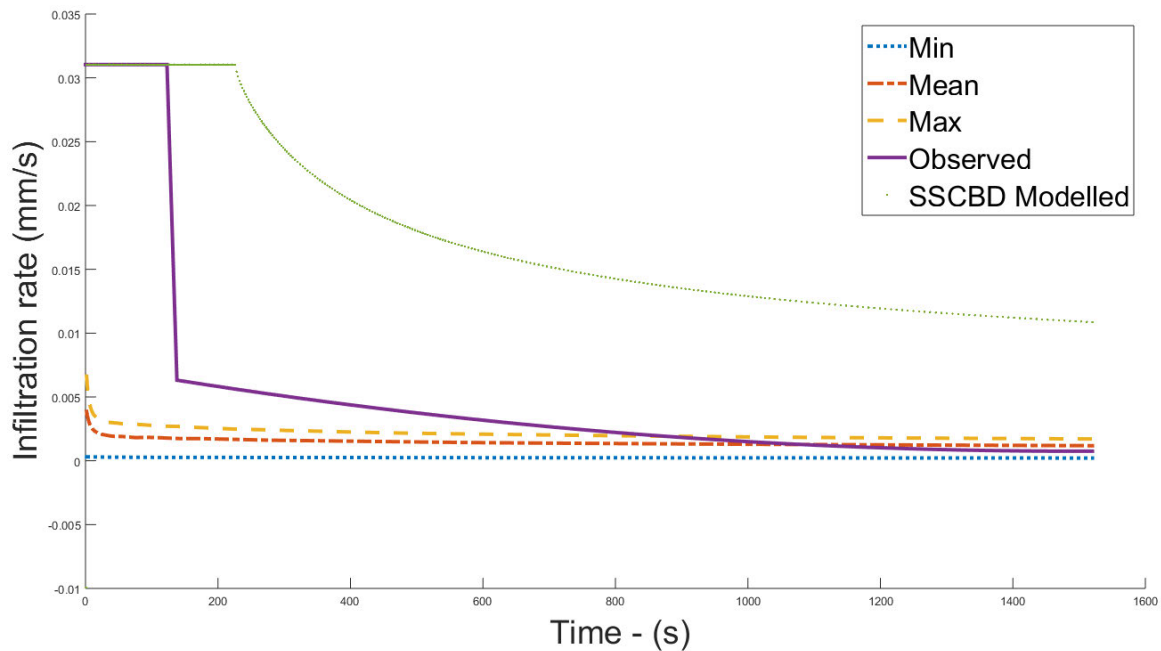


Figure 74 Results of sensitivity analysis when K_s is changed by plus or minus the standard deviation of inverse solution K_s values for Sodosol #3

That changing values for α and n made no impact on the modelled infiltration indicates that the K_s is the predominate parameter in modelling crust infiltration.

5.6.6. Comparing cumulative infiltration

Cumulative infiltration for all soils was calculated for the following simulations:

- SSCBD modelled (no crust)
- SSCBD modelled (2mm crust)
- Inverse solution modelled
- Average SHP parameter modelled
- Rainfall simulation observed.

Cumulative infiltration was approximated from the time that runoff commenced (for the previously stated reason) until the end of the simulation. This was achieved by averaging the infiltration rate between each time step, multiplying this value by the time step, repeating for all time steps and summing the results.

An example comparison is provided for Sodosol #3 in Figure 75. It clearly shows that the use of average soil hydraulic results in a close match to observed infiltration when compared to the SSCBD modelled infiltration.

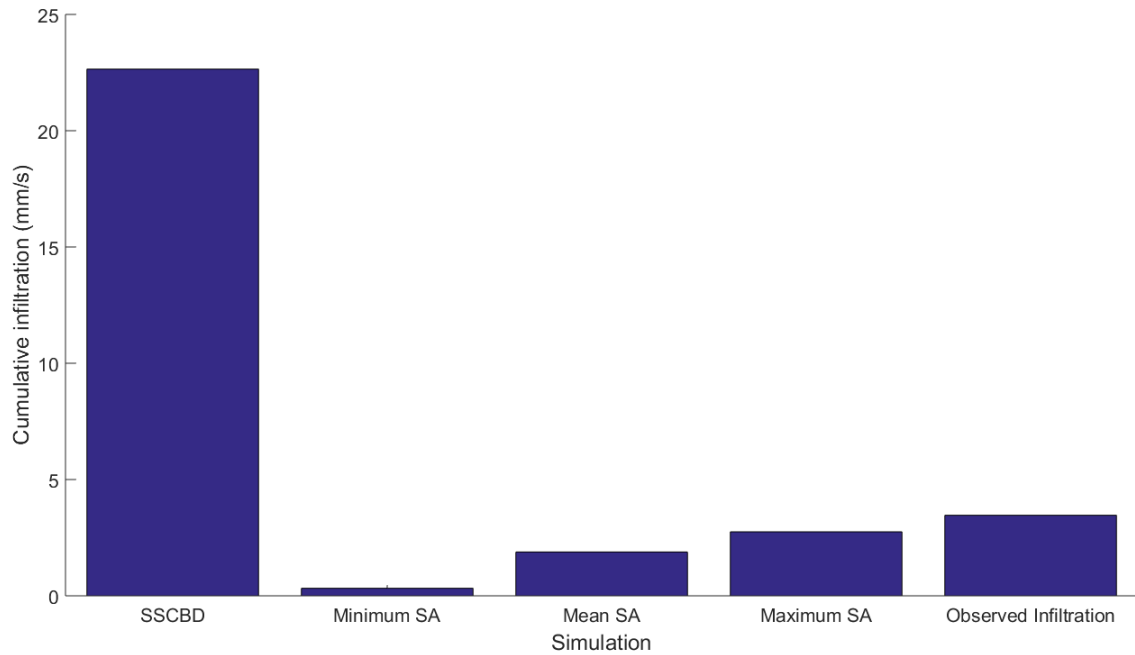


Figure 75 Cumulative infiltration comparison – Sodosol 3

A summary of cumulative infiltration for each soil type along with the percentage difference from observed infiltration are detailed in Table 49. The conclusion that can be drawn from these results is that the use of average parameters for α , n and K_s provides a reasonable approximation of observed infiltration.

Table 49 Summary of cumulative infiltration results and percentage difference from observed rainfall simulation infiltration

Soil	SSCBD modelled	% difference from observed	Inverse solution derived mean	% difference from observed	Observed
Chromosol	19.2	834%	1.54	-25%	2.05
Sodosol #1	33.9	1550%	2.37	15%	2.93
Sodosol #2	25.8	1159%	1.98	-4%	2.93
Sodosol #3	22.6	1003%	1.88	-8%	3.46

6. CHAPTER SIX – DISCUSSION

6.1. Modelling

The modelling indicated, which was confirmed by the experimental work, that HYDRUS-1D does not accurately model the large reductions in infiltration that can occur with thin crusts. Whilst this was not the initial aim of the modelling aspect of the work, this has proven vital to moving our understanding and modelling of thin crust impact forward. The initial concept for modelling was to obtain experimental data on infiltration in crusting soils and use that data to quantify errors resulting from the impact of the surface crust. Whilst there has been extensive research and experimentation completed in this work toward that approach, it proved technically difficult with complexity beyond the scope of work to obtain this data. Hence, the change in focus to investigating how HYDRUS-1D modelling responds to surface crusts using simulated data. Both the literature and X-ray CT calculated ρ_b identify that surface crusts are non-uniform layers; the modelling indicated however that there was little benefit in modelling the crust with HYDRUS-1D as a non-uniform layer. As a result a constant crust density was used in subsequent modelling.

A significant portion of the modelling investigated the potential to develop PTFs to predict the SWC and HCF of a soil as its ρ_b changed. However, further experimental work beyond the current scope is required to be conclusive in validating the outcomes of this modelling.

6.2. Infiltration into a crusting soil

The crusts formed on the Sodosol and the Chromosol samples proved to be an effective ‘throttle’ to infiltration, with over 90 % of the applied rainfall becoming runoff. This was further evidenced by the low subsoil moisture content, even after multiple rainfall simulations (an average of 13 % for the Sodosol and 12 % for the Chromosol), indicating that very little water infiltrated below the surface crust. These findings reinforce the importance of accounting for the impact of surface crusts in infiltration and surface runoff modelling.

The observed infiltration for both the Sodosol and Chromosol occurred in two distinct phases. The first phase commenced with the start of the rainfall simulation and ceased when runoff commenced. The infiltration rate during this phase was relatively high. HYDRUS-1D modelling of this phase provided a good approximation to the observed infiltration rate; however, there was a significant time lag within the model before the infiltration rate commenced declining (Figure 67). After the occurrence of runoff, the second phase commenced with a significant decline in the infiltration rate. HYDRUS-1D modelled this phase very poorly. These infiltration phases align with the general findings of Moore (1981) who used the Richard’s equation (the infiltration model used in HYDRUS-1D) to model infiltration under no seal, developing seal and constant surface seal conditions. The observed infiltration rate profile aligned with the infiltration under constant seal conditions calculated by Moore (1981), whilst the HYDRUS-1D predicted infiltration had a similar profile to the developing surface seal condition. This appears to suggest that while the seal is documented as a physical density gradient (Roth 1997), its effect on infiltration is abrupt. This is likely a function of the surface infiltration characteristic at sub-millimetre scale governing infiltration, while the gradient becomes redundant. In such a model, infiltration beyond the densest layer would render all other flow unsaturated by virtue of matric potential, effectively rendering the crust gradient redundant as flow becomes constant within the smaller pore sizes.

Based on the rainfall simulation experiments completed as part of this project it is concluded that complete infiltration modelling in HYDRUS-1D requires two simulations to cover pre and post runoff conditions. The results from the two soils used in this project indicate that the cumulative infiltration in the first phase (Table 29) only averaged around 2 mm. Given the surface runoff/infiltration measurement inaccuracies identified during the rainfall simulation experiments (assessed as +/- 5 mm/h) this small amount of rainfall is insignificant and unlikely to lead to major modelling errors. Thus, for practical purposes it is assessed that modelling of the second phase only is sufficiently accurate to represent the physical system function.

6.3. Measurement of crust bulk density

Four methods of measuring crust density were trialled during the project being: the water retention method, thin slice, modified intact clod (physical methods) and X-ray CT. The surface crusts created on the soils used in the project were thin with physical connection to the underlying soil. This made it practically impossible to separate just the soil crust to enable its measurement. The manual nature of the physical methods trialled resulted in samples incorporating the underlying soil as well as the crust resulting in inaccurate measurements of crust ρ_b . The manual nature of the physical method also resulted in inconsistent sampling and, thus, more variability in the results.

The results from the modified intact clod method could potentially have been improved if the full intact clod method was applied (Cresswell & Hamilton 2002) where the clods are coated in paraffin wax. However the underlying problem of sampling just the crust and not the underlying soil would have remained. For the type of crusts formed in this project it is assessed that the physical methods are not suitable for measuring crust ρ_b . These methods maybe suitable on soils that form thicker crusts (e.g. 5 mm or greater) but this has not been tested during this project.

X-ray CT was applied to enable measurement of the soil core porosity using image analysis techniques. The resolution provided through the use of this technique highlighted the heterogeneous nature of the soils, both between cores and within the core (i.e. when viewing vertical slices taken at different angles around the vertical axis). The advantage of using X-ray CT was it enabled repeatable measurements to be made of porosity and the averaging of results. The porosity values obtained were however lower than is generally reported in the literature. This is primarily attributed to the resolution of the imagery (30 μm) which implied that pores smaller than this resolution could not be measured. As X-ray CT images were taken of the core and not just the crust, the measured bulk soil ρ_b values were used to derive crust ρ_b . It is assessed that the errors resulting from this approach are minor given the reliability of the soil core method and the consistency of X-ray CT derived porosity values.

6.4. Applications of X-ray CT for soil porosity profiling

X-ray CT was also used to identify the depth of the surface crust. Due to time constraints associated with image processing, only two vertical slices were analysed to develop the ρ_b versus depth profile. It is expected that the profiles would have been smoother if more slices had of been analysed. The profiles highlighted that ρ_b constantly changes throughout the depth of the soil mass. The general shape of the profile was similar in all instances. The shape can be explained by a thin layer of unconsolidated material on the soil surface (lower density than the crust) immediately underneath of which is the thin surface crust (high density). The density then generally decreases with depth into the underlying soil. This profile aligns with the findings of both Armenise et al. (2018) and Roth (1997).

Despite the high resolution of changes in ρ_b that were identified by X-ray CT, defining crust thickness was still somewhat arbitrary. The purpose of measuring crust ρ_b in this project was as an input into HYDRUS-1D modelling. The modelling of variable density crusts identified that incorporating

multiple crust layers with differing ρ_b made little difference to predicted infiltration rates. As a result the crust thickness was defined as 2 mm, which aligned with the portion of the crust with the highest density. This was assessed as being sufficiently accurate for modelling purposes within HYDRUS-1D.

The reduced porosity of the surface crust relative to the underlying soil was obvious through both visual observation and image analysis of X-ray CT images. Whilst it was not fully investigated in this project, cursory visual observation revealed not only were there fewer and smaller pores in the surface crust, there appeared to be a large number of vesicular pores. This helps explain why the inverse solution K_s values of the surface crust are so small compared to the HYDRUS-1D predicted values. Further investigation using the 3D image analysis capabilities of ImageJ could define the pore networks within the surface crust. There is potential that this could subsequently be used to determine crust K_s as research by Elliot et al. (2010) has suggested.

6.5. HYDRUS-1D predicted soil hydraulic properties

HYDRUS-1D uses the ROSETTA application to predict soil hydraulic properties. ROSETTA includes PTFs that estimate water retention and hydraulic conductivity in a hierarchical manner based on the provided input data (Schaap et al. 2001). The underlying data for ROSETTA is obtained from the UNSODA database (Nemes et al. 2015) which contains basic soil properties such as ρ_b as well as measured soil hydraulic data. There is no indication that the soil data included in the UNSODA database includes measurements taken from crusting soils/surface crusts. With crust data not included in the databases used to parameterise ROSETTA, it is not reasonable to expect ROSETTA to accurately predict for crust conditions; as such observations would sit outside the boundary conditions.

Inverse solution derived surface crust K_s values were three to four orders of magnitude smaller than those predicted from ROSETTA. Similar variances in K_s values between the surface crust and underlying soil have been identified in other studies. For example, Šimůnek et al. (1998) found that the K_s of the surface crust was two orders of magnitude less than the underlying soil. Experimental results for both the Sodosol and Chromosol demonstrated a 72 % reduction in K_s between the compacted soil core and the same core after a rainfall impact surface crust had been formed. When the short duration of the applied rainfall during the crust formation process (required as the cores began to breakdown under rainfall impact), and core shrinkage resulting in potential preferential flow paths around the circumference of the core are considered, a much greater reduction in K_s is possible. These experimental results indicate that the HYDRUS-1D predicted K_s values are not appropriate for use on crusting soils. However, inclusion of crust data in a specific parameterising module within HYDRUS could be the focus of future work to reach a truly predictive approach for a given soil.

6.6. HYDRUS-1D modelling of crusted soils

Modelling of artificially developed ‘crusted soils’ using HYDRUS-1D identified that incorporating an increased ρ_b of a surface crust does result in a reduction in the infiltration rate, as compared to an uncrusted soil. Increasing crust thickness resulted in a corresponding decrease in infiltration results. This outcome is logical; however it does not represent what has been observed in some soils, including those used in this project. For the Sodosol and Chromosol soils, thin crusts result in major reductions in infiltration. The crust hydraulic properties obtained from the inverse solution varied significantly (in particular K_s) from those of the underlying soil. HYDRUS-1D does not appear to handle very well circumstances where there the hydraulic properties of a crust vary significantly from the underlying soil. This was demonstrated during optimisation modelling (Section 5.6.2) where only minor changes

could be made to soil hydraulic properties before simulations failed to converge. Admittedly this research has only focused on the commonly used VG – Mualem hydraulic model and some parameters remained unchanged (l for example). Further modelling using other hydraulic models and/or parameter values may result in improved infiltration modelling of crusted soils.

6.7. Use of average crust parameters

The average soil hydraulic properties calculated from the inverse solution data set (sample $n=7$) are detailed in Table 50. When used with the HYDRUS-1D predicted values for θ_s and θ_r and the default value of l (0.5) these parameters, as demonstrated in Section 5.6.5, provided a good approximation of observed infiltration. The results provided a marked improvement compared to the direct method of predicting infiltration using soil texture and ρ_b data to predict soil hydraulic properties. The use of these parameters has thus achieved the project aim of improving the accuracy of infiltration modelling.

Table 50 Average crust parameters

α (1/mm)	n (unitless)	K_s (mm/s)
0.009412	0.75048	1.33E-06

There is, however, an issue with the n value in these parameters. The m parameter has been constrained by the common practice of using the relationship $m=1-1/n$ (Radcliffe & Simunek 2010). For values of $n < 1.01$ this results in m becoming a negative number. The result is that these parameters cannot be used to model the SWC using the VG equation (Figure 76). The modelled SWC with an $n < 1.01$ is physically impossible which explains why n should be greater than one (Šimunek et al. 2009). As such whilst the average value of n can be used to accurately model infiltration it cannot be used for modelling the SWC (and potentially the HCF although this has not been tested). It is interesting to note the inverse solution generates a HYDRUS-1D parameter that is outside of the stated boundary conditions. This appears to be a weakness in the inverse modelling capability of HYDRUS-1D that allows parameters to be estimated that are outside of the boundary conditions for the underlying model.

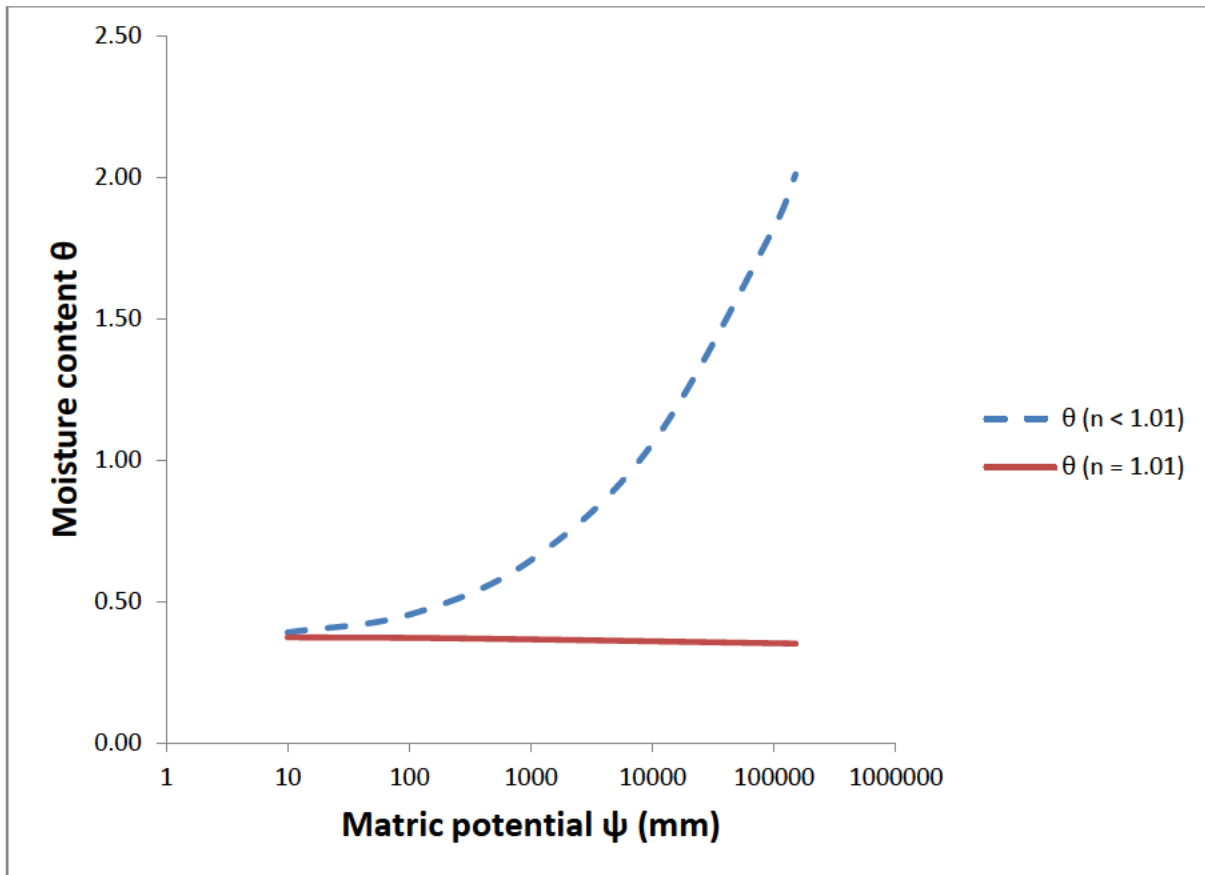


Figure 76 Soil Water Characteristic using inverse solution derived average hydraulic parameters with comparison where $n=1.01$.

Whilst the use of inverse solution derived average crust parameters has improved infiltration modelling accuracy, it is clear that the current parameters cannot be used to model all aspects of a soil crust's hydraulic behaviour. Further modelling using the inverse solution approach, where different parameter combinations are optimised, is required. The aim of this modelling would be to determine whether a set of parameters can be obtained that improve infiltration accuracy whilst also providing sensible solutions for the SWC and HCF.

Typical hydraulic parameters for use with the VG model are available across a range of soil textures (Tuller & Or 2004). The values provided by Tuller and Or (2004) have been obtained from the UNSODA database. This was developed to provide readily available and reliable soil data to avoid the time consuming and costly requirement to measure soil hydraulic properties (Nemes et al. 2001). With direct measurements of crust hydraulic properties being very difficult to obtain, inverse solutions offer an attractive alternative (Šimůnek et al. 1998). Surface crust hydraulic parameters derived from inverse solutions provided a very good approximation of observed infiltration rates and cumulative infiltration once runoff commenced during this project. Developing a database of surface crust hydraulic properties, similar in approach to UNSODA, would be useful for improving the modelling of infiltration on crusting soils.

6.8. Assessing the accuracy of laboratory based compaction

The modified Proctor test was used with the aim of creating soils cores with different ρ_b values. These cores, used as an analogue of a soil crust, were then to be used to derive soil hydraulic parameters for use as inputs into HYDRUS-1D simulations (water retention data at $\theta_{33 \text{ kPa}}$ and $\theta_{1500 \text{ kPa}}$) as well as enabling validation of the SWC and HCF modelling. Six different combinations of blows were used

on the Sodosol with resultant ρ_b values ranging over a relatively narrow range of 1.63 to 1.87 g/cm³. Despite differing force being applied to each core, four of these values, originally intended to be progressively increasing, were within +/- 0.01 g/cm³ of each other. These results indicate that this approach did not achieve the desired range of soil cores with differing ρ_b values. Soil cores were prepared by wetting to the approximate moisture capacity required for optimum compaction. It is assessed that the force applied by each blow of the 2.5 kg Proctor device was such that each soil core approached a maximum density after a small number of blows. This indicates that a Proctor like device with a smaller mass is required to provide greater control over the density of each soil core or another method, such as the Triaxial Shear Test (Das & Sobhan 2014) be adapted to provide greater control over core density. Further experimental work on this would be beneficial, potentially enabling the creation of a PTF that would enable prediction of the SWC and HCF as ρ_b changes for a given soil without the requirement for physical measurement.

6.9. Recommendations for field survey

One of the objectives of this project was to make recommendations on changes to current soil survey processes to improve infiltration and surface runoff predictions. It was originally envisaged that a method would be developed that enabled accurate surface crust ρ_b determination. This data could then be entered into HYDRUS-1D which would improve modelled infiltration accuracy. The experimental results however identified that this approach is not feasible for two reasons. The first being that physical methods (i.e. methods that could be used either in the field or with readily available laboratory equipment) of determining crust ρ_b are inaccurate/unreliable (at least for use the Chromosol and Sodosol soils used in this project); the second being HYDRUS-1D predicted soil hydraulic properties based upon crust ρ_b values provided a very small improvement in model accuracy. As a result directly measuring the crust ρ_b is not recommended as a change to current soil survey processes.

The Australian Soil and Land Survey Handbook Field Handbook (National Committee on Soil and Terrain 2009) is the primary reference that ensures consistent data on soil profiles is recorded during soil survey activities. The Handbook uses numerical and/or alphabetical codes to describe various properties of the soil profile. One of the properties is the condition of the surface soil when dry (National Committee on Soil and Terrain 2009, pp. 189-91). Surface crust is included as one of these conditions and is assigned the code 'c'. Whilst this information is of some general use, other information could be obtained that would help assist with improving infiltration modelling accuracy.

Perhaps the easiest crust parameter that could be included is crust thickness. Visual observation and measurement of the soil crusts used resulted in similar crust thicknesses being recorded as obtained from X-ray CT. Given the relatively small impact of minor differences (e.g. +/- 1 mm) in crust thickness when modelling infiltration in HYDRUS-1D, as identified during in Chapter Two, this data would be useful for infiltration modelling purposes.

The surface crusts created during this project appeared to be continuous across the extent of the soil surface. Whilst not considered in this project, cracks of various extents tend to form in surface crusts. The cracks are preferential flow paths for infiltrating water, which result in an increased infiltration rate compared to a continuous crust. The reporting of the extent of cracking would be of use in infiltration modelling. For example HYDRUS-1D includes a dual porosity model that enables the impact of macropores upon infiltration to be modelled.

The addition of crust thickness and extent of cracks in surface crusts to current soil survey practices would provide useful input data to assist in modelling infiltration without requiring major changes to the extant processes.

6.10. Further work

There are several areas where further work is required to complete/validate the findings of this project and/or expand upon the original scope.

The greatest limitation on the results of this project are the small number of experiments completed on only two soils that were susceptible to crusting. A larger dataset is required that includes a broader range of soils, crust morphologies and soil conditions, including field conditions, to provide a more robust dataset and validate the application of average crust parameter values to infiltration modelling.

The two functions that provide a complete description of a soil's hydraulic properties are the SWC, which describes the storage of water in soil and the HCF, which describes the movement of water in soil. These are incorporated into the Richard's equation. A major part of the modelling completed in Chapter Two was based upon the theoretical development of PTFs that would enable the prediction of the SWC and HCF as the ρ_b changes. An assumption was made that enabled the creation of a correction factor that could be applied to develop the SWC for a soil when its ρ_b changed. It was planned to complete experimental work to determine the nature of the correction factor which would have added further depth to the results from this project. Unfortunately due to several factors including time limitations and the identified issues with the modified Proctor test/measurement of the SWC using HYPROP, this work was not able to be completed within the limitations of the project resources. It is a further body of work that could be very useful in enabling the prediction of the SWC without requiring laborious measurements.

It is unlikely in the foreseeable future that the availability of X-ray CT will become widespread due to its cost. This is a key disadvantage of X-ray CT. Advancements in camera technology available in mobile phones, including high magnification lenses, offers a potential opportunity that could be applied to improve the paucity of available surface crust data. Microscope attachments are cheap, readily available and offer up to 1000 times magnification (Horsey 2019). These could be used to photograph surface crusts for subsequent analysis by image analysis software enabling the measurement of crust thickness, crust morphology to be described and potentially porosity calculated. Whilst the resolution would be less than that provided by X-ray CT, and only the exterior of the surface crust profile could be analysed, these disadvantages would be outweighed by the increased ability to collect and analyse surface crust data. This data could be applied to enhance relatively simple reference data, such as the 'infiltrability' values developed by Valentin and Bresson (1992), into more rigorous datasets that could be parameterised for use in infiltration modelling.

7. CHAPTER SEVEN - CONCLUSIONS

Surface crusts, a thin layer of higher density and reduced porosity on the soil surface, act as a throttle to infiltration resulting in increased surface runoff. Thin surface crusts (~2 mm in thickness) formed by rainfall simulation experiments on Sodosol and Chromosol soils resulted in greater than 90 % of applied rainfall becoming runoff, highlighting the importance of modelling crust impact upon infiltration. Outside of specific studies focusing on surface crusts, current approaches to the modelling of infiltration and surface runoff do not account for the impact of the increased density of the surface crust. This is a source of modelling error that this project aimed to address.

Specifically the project involved the conduct of rainfall simulation experiments on soils that were prone to surface crusting and subsequently using various methods to measure the ρ_b of the resulting crust. These experiments provided the input data required to model infiltration runoff using the commonly used HYDRUS-1D software application. This approach enabled a conclusion to be drawn on whether incorporating the surface crust ρ_b improved infiltration modelling accuracy.

Numerous HYDRUS-1D modelling activities were completed to identify how various parameters affected model outputs resulting in several key conclusions. The first was that HYDRUS-1D did not replicate the dramatic reduction in infiltration observed in numerous studies by thin surface crusts (e.g. crusts of 1 – 2 mm in thickness). The second conclusion is that HYDRUS-1D predicted values for saturated hydraulic conductivity, the key soil hydraulic property, varied by up to two orders of magnitude depending upon the input data provided. Finally whilst surface crusts consist of non-uniform layers, from a modelling perspective it was found that there was no advantage to separating the crust into multiple layers of differing ρ_b as it is the layer of highest ρ_b that controls infiltration. These conclusions provided an initial insight into the limitations of HYDRUS-1D in modelling infiltration on crusting soils.

Three physical methods of measuring crust ρ_b were tested and all were found incapable of providing accurate and reliable results. The key difficulty for physical methods is that it is practically impossible to separate the thin surface from the underlying soil. Thus for thin rain impact surface crusts it is recommended that physical methods of measuring crust ρ_b are not used.

X-ray CT combined with image analysis using ImageJ was the fourth method used to determine crust porosity and subsequently ρ_b . The calculated porosity values using this method for the underlying soil were found to be substantially less than expected resulting in unrealistically high values for ρ_b . This was assessed to be primarily caused by the image acquisition resolution (30 μm) which meant that smaller pores were not measured. This problem was addressed by normalising the X-ray CT ρ_b values against physically measured sub-soil densities using the traditional soil core method enabling crust ρ_b to be calculated. X-ray CT was also used to measure surface crust thickness. There was in all instances significant variation in ρ_b throughout the depth of the soil cores. Due to the relative insensitivity of HYDRUS-1D to this parameter, a crust thickness of 2 mm with uniform density was used in all simulations. X-ray CT proved to be the most accurate method of determining crust ρ_b and thickness.

The data obtained from the experiments was used to complete HYDRUS-1D modelling and enable a comparison to be made against observed infiltration. It was found in all instances that including crust ρ_b into HYDRUS-1D resulted in only marginal improvements to modelling accuracy. Inverse modelling was subsequently completed. It was found that the resultant soil hydraulic properties were substantially different to those predicted by HYDRUS-1D using the in-built ROSETTA database. In

particular predicted K_s values were three to four orders of magnitude greater than those determined by the inverse solution approach. This difference accounts for why HYDRUS-1D modelling incorporating crust ρ_b provided only a marginal improvement in modelling accuracy. The key conclusion to be drawn is that the ROSETTA database should not be used to predict soil hydraulic properties for surface crusts.

The averages of the soil hydraulic parameters obtained from the inverse solutions were used as inputs into further HYDRUS-1D modelling. The use of the average parameters in all instances proved to provide a close approximation to the observed infiltration. This indicates that when appropriate hydraulic parameters are used, HYDRUS-1D results can provide a good approximation to the observed infiltration, thus increasing modelling accuracy.

An initial set of parameter values (n , α and K_s) for use in HYDRUS-1D modelling have been identified that can be used to improve infiltration modelling accuracy on crusting soils. These values do however need to be used with caution for several reasons. These include the small dataset and the limited range of soil textural classes from which the parameters have been developed. Further experimentation on a broader range of soils under differing soil conditions is required to validate these parameter values. Ideally a database of soil hydraulic properties, similar to the existing ROSETTA database, should be created for crusting soils.

This project has identified that using HYDRUS-1D predicted soil hydraulic properties does not improve modelling accuracy. However, modelling accuracy can be greatly improved when appropriate soil crust hydraulic parameters are applied. An initial set of these parameters have been proposed which HYDRUS-1D modellers can apply for simulations of infiltration on crusting soils.

APPENDICES

- A. Project Specification
- B. Selected MATLAB code
- C. Rainfall simulation results
- D. ImageJ script

REFERENCES

- Abudi, I, Carmi, G & Berliner, P 2012, 'Rainfall simulator for field runoff studies', *Journal of Hydrology*, vol. 454, pp. 76-81.
- Arjun, N 2019, *Maximum Dry Density and Optimum Moisture Content of Soil*, The Constructor, The Constructor: Civil Engineering Home, viewed 26 May 2019, <<https://theconstructor.org/geotechnical/soil-maximum-dry-density-optimum-moisture-content/18426/>>.
- Armenise, E, Simmons, RW, Ahn, S, Garbout, A, Doerr, SH, Mooney, SJ, Sturrock, CJ & Ritz, K 2018, 'Soil seal development under simulated rainfall: Structural, physical and hydrological dynamics', *Journal of Hydrology*, vol. 556, pp. 211-9.
- Badorreck, A, Gerke, HH & Hüttl, RF 2013, 'Morphology of physical soil crusts and infiltration patterns in an artificial catchment', *Soil and Tillage Research*, vol. 129, pp. 1-8.
- Bajracharya, R & Lal, R 1999, 'Land use effects on soil crusting and hydraulic response of surface crusts on a tropical Alfisol', *Hydrological processes*, vol. 13, no. 1, pp. 59-72.
- Bertrand, A 1965, 'Rate of Water Intake in the Field', in C Black (ed.), *Methods of Soil Analysis Part 1: Physical and Mineralogical Properties, Including Statistics of Measurement and Sampling*, American Society of Agronomy, Wisconsin.
- Betson, RP 1964, 'What is watershed runoff?', *Journal of Geophysical research*, vol. 69, no. 8, pp. 1541-52.
- Blake, G 1965, 'Bulk density', in C Black (ed.), *Methods of Soil Analysis, Part 1. Physical and Mineralogical Properties, Including Statistics of Measurement and Sampling*, American Society of Agronomy, Madison, Wisconsin.
- Blöschl, G & Sivapalan, M 1995, 'Scale issues in hydrological modelling: a review', *Hydrological processes*, vol. 9, no. 3-4, pp. 251-90.
- Boughton, W 2005, 'Catchment water balance modelling in Australia 1960–2004', *Agricultural Water Management*, vol. 71, no. 2, pp. 91-116.
- Bowman, G & Hutka, J 2002, 'Particle Size Analysis', in N McKenzie, et al. (eds), *Soil Physical Method and Interpretation for Land Evaluation*, CSIRO Publishing Collingwood.
- Box, GE & Draper, NR 2007, *Response surfaces, mixtures, and ridge analyses*, vol. 649, John Wiley & Sons.
- Bresson, L, Moran, C & Assouline, S 2004, 'Use of bulk density profiles from X-radiography to examine structural crust models', *Soil Science Society of America Journal*, vol. 68, no. 4, pp. 1169-76.
- Bristow, K, Cass, A, Smetten, K & Ross, P 1995, 'Water Entry into Sealing, Crusting and Hardsetting Soils, A Review and Illustrative Simulation Study', in H So, et al. (eds), *Sealing, crusting and hardsetting soils: Productivity and conservation*, Australian Society of Soil Science Incorporated (Queensland Branch), Australia.
- Burt, R 2014, *Soil Survey Field and Laboratory Methods Manual: Soil Survey Investigations Report No. 51*, UDo Agriculture, Kellogg Soil Survey Laboratory, Lincoln Nebraska.

Connolly, R, Silburn, D, Glanville, S & Bridge, B 2002, 'Using Rainfall Simulators to Derive Soil Hydraulic Parameters', in N McKenzie, et al. (eds), *Soil Physical Measurements and Interpretation for Land Evaluation*, CSIRO Publishing, Collingwood.

Contreras, CP & Bonilla, CA 2018, 'A comprehensive evaluation of pedotransfer functions for predicting soil water content in environmental modeling and ecosystem management', *Science of the Total Environment*, vol. 644, pp. 1580-90.

Cresswell, H & Hamilton, G 2002, 'Bulk Density and Pore Space Relations', in *Soil Physical Measurements and Interpretation for Land Evaluation*, CSIRO Publishing, Collingwood, ch 3, pp. 35 - 58.

Cresswell, HP, Smiles, DE & Williams, J 1992, 'Soil structure, soil hydraulic properties and the soil water balance', *Soil Research*, vol. 30, no. 3, pp. 265-83.

Darcy, H 1856, *Les fontaines publiques de la ville de Dijon: exposition et application*, Victor Dalmont.

Das, B & Sobhan, K 2014, *Principles of Geotechnical Engineering*, 8th edn, CENGAGE Learning, Stamford, Connecticut

Di Prima, S, Concialdi, P, Lassabatere, L, Angulo-Jaramillo, R, Pirastru, M, Cerdà, A & Keesstra, S 2018, 'Laboratory testing of Beerkan infiltration experiments for assessing the role of soil sealing on water infiltration', *Catena*, vol. 167, pp. 373-84.

Eldridge, D, Semple, W & Koen, T 2000, 'Dynamics of cryptogamic soil crusts in a derived grassland in south-eastern Australia', *Austral Ecology*, vol. 25, no. 3, pp. 232-40.

Elliot, T, Reynolds, W & Heck, R 2010, 'Use of existing pore models and X-ray computed tomography to predict saturated soil hydraulic conductivity', *Geoderma*, vol. 156, no. 3-4, pp. 133-42.

Field, DJ, McKenzie, DC & Koppi, AJ 1997, 'Development of an improved Vertisol stability test for SOILpak', *Soil Research*, vol. 35, no. 4, pp. 843-52.

Flint, A & Flint, L 2002, 'Particle Density', in J Dane & G Clarke Topp (eds), *Methods of Soil Analysis: Part 4 Physical Methods*, Soil Science Society of America, Madison, Wisconsin.

Fohrer, N, Berkenhagen, J, Hecker, JM & Rudolph, A 1999, 'Changing soil and surface conditions during rainfall: Single rainstorm/subsequent rainstorms', *Catena*, vol. 37, no. 3, pp. 355-75.

Gee, G & Or, D 'Particle Size Analysis', in J Dane & G Clarke Topp (eds), *Methods of Soil Analysis: Part 4 Physical Methods*, Soil Science Society of America, Madison, Wisconsin.

Geeves, G 1997, 'Aggregate Breakdown and Soil Surface Sealing Under Rainfall', Australian National University, Canberra.

Grossman, R & Reinsch, T 2002, 'Bulk Density and Linear Extensibility', in D JH. & G Clarke Topp (eds), *Methods of Soil Analysis: Part 4 Physical Methods*, Soil Science Society of America, Madison, Wisconsin.

Hall, MJ 2001, 'How well does your model fit the data?', *Journal of Hydroinformatics: Official Journal of the IAHR-IWA Joint Committee on Hydroinformatics*.

Hardie, M & Almajmaie, A 2019, 'Measuring and estimating the hydrological properties of a soil crust', *Journal of Hydrology*.

Hazelton, P & Murphy, BW 2016, *Interpreting Soil Test Results: What do all the numbers mean?*, 3rd edn, CSIRO Publishing, Collingwood, Victoria.

Hill, PI, Mein, RG & Siriwardena, L 1998, *How Much Rainfall Becomes Runoff?: Loss Modelling for Flood Estimation*, Cooperative Research Centre for Catchment Hydrology.

Hillel, D 2003, *Introduction to Environmental Soil Physics*, Elsevier Science and Technology, Burlington.

Horse, J 2019, *Tipscope smartphone microscope*, Geeky Gadgets, viewed 26 September 2019, <<https://www.geeky-gadgets.com/smartphone-microscope-03-05-2019/>>.

Horton, RE 1933, 'The role of infiltration in the hydrologic cycle', *Eos, Transactions American Geophysical Union*, vol. 14, no. 1, pp. 446-60.

Horton, RE 1941, 'An Approach Toward a Physical Interpretation of Infiltration-Capacity 1', *Soil Science Society of America Journal*, vol. 5, no. C, pp. 399-417.

Humphry, JB, Daniel, TC, Edwards, DR & Sharpley, AN 2002, 'A portable rainfall simulator for plot-scale runoff studies', *Applied Engineering in Agriculture*, vol. 18, no. 2, p. 199.

Hyväluoma, J, Thapaliya, M, Alaraudanjoki, J, Sirén, T, Mattila, K, Timonen, J & Turtola, E 2012, 'Using microtomography, image analysis and flow simulations to characterize soil surface seals', *Computers & Geosciences*, vol. 48, pp. 93-101.

Isbell, R 2016, *The Australian Soil Classification*, 2nd edn, CSIRO Publishing, Melbourne.

Jabro, J 1992, 'Estimation of saturated hydraulic conductivity of soils from particle size distribution and bulk density data', *Transactions of the ASAE*, vol. 35, no. 2, pp. 557-60.

Jarvis, NJ, Zavattaro, L, Rajkai, K, Reynolds, WD, Olsen, PA, McGechan, M, Mecke, M, Mohanty, B, Leeds-Harrison, PB & Jacques, D 2002, 'Indirect estimation of near-saturated hydraulic conductivity from readily available soil information', *Geoderma*, vol. 108, no. 1, pp. 1-17.

Ketcham, R 2017, *What is X-ray Computed Tomography*, [16 May 2017], Science Education Resource Centre - Montana State University, viewed 1 May, <https://serc.carleton.edu/research_education/geochemsheets/techniques/CT.html>.

Lai, J & Ren, L 2007, 'Assessing the size dependency of measured hydraulic conductivity using double-ring infiltrometers and numerical simulation', *Soil Science Society of America Journal*, vol. 71, no. 6, pp. 1667-75.

Latorre, B, Moret-Fernández, D & Peña, C 2013, 'Estimate of soil hydraulic properties from disc infiltrometer three-dimensional infiltration curve: theoretical analysis and field applicability', *Procedia Environmental Sciences*, vol. 19, pp. 580-9.

Le Bissonnais, Y 2016, 'Aggregate stability and assessment of soil crustability and erodibility: I. Theory and methodology', *European Journal of Soil Science*, vol. 67, no. 1, pp. 11-21.

Linsley, R, Franzini, J, Freyberg, D & Tchobanoglous, G 1992, *Water-Resources Engineering*, 4th edn, McGraw Hill, Singapore.

Loch, RJ 1989, 'Rob's thesis, find proper title.'

Mackellar, D 2016, *My Country*, Estate of Dorothea Mackellar, Paddington NSW, viewed 12 October 2019, <<https://www.dorotheamackellar.com.au/archive/mycountry.htm>>.

McKenzie, N & Cresswell, HP 2002, 'Estimating Soil Physical Properties Using More Readily Available Data', in N McKenzie, et al. (eds), *Soil Physical Measurement and Interpretation for Land Evaluation*, CSIRO, Melbourne, ch 22.

Meter Group nd, *HYPROP Data Evaluation Software: User's Manual*, Meter Group, Pullman, USA, <http://library.metergroup.com/Manuals/UMS/HYPROP-FIT_Manual.pdf>.

Migliaccio, KW & Srivastava, P 2007, 'Hydrologic components of watershed-scale models', *Transactions of the ASABE*, vol. 50, no. 5, pp. 1695-703.

Minasny, B & McBratney, AB 2000, 'Evaluation and development of hydraulic conductivity pedotransfer functions for Australian soil', *Soil Research*, vol. 38, no. 4, pp. 905-26.

Moore, I 1981, 'Effect of surface sealing on infiltration', *Transactions of the ASAE*, vol. 24, no. 6, pp. 1546-52.

Moore, I & Eigel, J 1981, 'Infiltration into Two-Layered Soil Profiles', *Transactions of the ASAE*, vol. 24, no. 6, pp. 1496-503.

Moss, A 1991, 'Rain impact soil crust. I. Formation on a granite derived soil', *Soil Research*, vol. 29, no. 2, pp. 271-89.

Murphy, BW 2015, 'Impact of soil organic matter on soil properties--a review with emphasis on Australian soils.(Report)', *Soil Research*, vol. 53, no. 6, p. 605.

National Committee on Soil and Terrain 2009, *Australian Soil and Land Survey Field Handbook*, 3rd edn, CSIRO Publishing, Melbourne.

Nciizah, AD & Wakindiki, II 2015, 'Soil sealing and crusting effects on infiltration rate: a critical review of shortfalls in prediction models and solutions', *Archives of Agronomy and Soil Science*, vol. 61, no. 9, pp. 1211-30.

Nemes, A & Rawls, W 2004, 'Soil Texture and Particle-Size Distribution as Input to Estimate Soil Hydraulic Properties', in YA Pachepsky & WJ Rawls (eds), *Development of Pedotransfer Function in Soil Hydrology*, Elsevier, Amsterdam.

Nemes, A, Schaap, MG, Leij, FJ & Wösten, JHM 2001, 'Description of the unsaturated soil hydraulic database UNSODA version 2.0', *Journal of Hydrology*, vol. 251, no. 3-4, pp. 151-62.

Nemes, A, Schaap, MG, Leij, FJ, Wosten, J & Henk, M 2015, *UNSODA 2.0: Unsaturated Soil Hydraulic Database. Database and program for indirect methods of estimating unsaturated hydraulic properties*, US Salinity Laboratory - ARS - USDA, <<https://data.nal.usda.gov/dataset/unsoda-20-unsaturated-soil-hydraulic-database-database-and-program-indirect-methods-estimating-unsaturated-hydraulic-properties>>.

Nimmo, JR & Perkins, KS 2002, '2.6 Aggregate stability and size distribution', *Methods of soil analysis: part*, vol. 4, pp. 317-28.

Ogden, C, Van Es, H & Schindelbeck, R 1997, 'Miniature rain simulator for field measurement of soil infiltration', *Soil Science Society of America Journal*, vol. 61, no. 4, pp. 1041-3.

Patil, NG & Singh, SK 2016, 'Pedotransfer functions for estimating soil hydraulic properties: A review', *Pedosphere*, vol. 26, no. 4, pp. 417-30.

- Patrick, E 2002, 'Researching crusting soils: themes, trends, recent developments and implications for managing soil and water resources in dry areas', *Progress in Physical Geography*, vol. 26, no. 3, pp. 442-61.
- Paydar, Z & Ringrose-Voase, AJ 2003, 'Prediction of hydraulic conductivity for some Australian soils', *Australian Journal of Soil Research*, vol. 41, no. 6, p. 1077.
- Philip, J 1954, 'Some recent advances in hydrologic physics', *Journal of Institute Engineers Australia*, vol. 26, pp. 255-9.
- Radcliffe, DE & Simunek, J 2010, *Soil Physics with Hydrus: Modelling and Applications*, CRC Press, Taylor and Francis Group, Boca Raton, Florida.
- Raine, SR & Loch, RJ 2003, 'What is a sodic soil? Identification and management options for construction sites and disturbed lands', *Workshop on soils in rural Queensland*.
- Rawls, W, Brakensiek, D, Simanton, J & Kohl, K 1990, 'Development of a crust factor for a Green Ampt model', *Transactions of the ASAE*, vol. 33, no. 4, pp. 1224-8.
- Rawls, WJ, Gimenez, D & Grossman, R 1998, 'Use of Soil Texture, Bulk Density, and Slope of the Water Retention Curve to Predict Saturated Hydraulic Conductivity', *Transactions of the ASAE*, vol. 41, no. 4, p. 983.
- Rayment, G & Lyons, D 2011, *Soil Chemical Methods - Australasia*, CSIRO Publishing, Collingwood, Victoria.
- Read, C, Duncan, D, Vesk, P & Elith, J 2008, 'Biological soil crust distribution is related to patterns of fragmentation and landuse in a dryland agricultural landscape of southern Australia', *Landscape Ecology*, vol. 23, no. 9, pp. 1093-105.
- Rengasamy, P & Olsson, KA 1991, 'Sodicity and soil structure', *Soil Research*, vol. 29, no. 6, pp. 935-52.
- Roth, CH 1997, 'Bulk density of surface crusts: depth functions and relationships to texture', *Catena*, vol. 29, no. 3-4, pp. 223-37.
- Schaap, MG, Leij, FJ & Van Genuchten, MT 2001, 'Rosetta: A computer program for estimating soil hydraulic parameters with hierarchical pedotransfer functions', *Journal of Hydrology*, vol. 251, no. 3-4, pp. 163-76.
- Schneider, CA, Rasband, WS & Eliceiri, KW 2012, 'NIH Image to ImageJ: 25 years of image analysis', *Nature methods*, vol. 9, no. 7, p. 671.
- Selle, B, Wang, Q & Mehta, B 2011, 'Relationship between hydraulic and basic properties for irrigated soils in southeast Australia', *Journal of Plant Nutrition and Soil Science*, vol. 174, no. 1, pp. 81-92.
- Šimunek, J, Angulo-Jaramillo, R, Schaap, MG, Vandervaere, J-P & Van Genuchten, MT 1998, 'Using an inverse method to estimate the hydraulic properties of crusted soils from tension-disc infiltrometer data', *Geoderma*, vol. 86, no. 1-2, pp. 61-81.
- Šimunek, J, Šejna, M, Saito, H, Sakai, M & van Genuchten, MT 2009, *The HYDRUS-1D Software Package for Simulating the One-Dimensional Movement of Water, Heat, and Multiple Solutes in Variably-Saturated Media* 4.08, Department of Environmental Sciences, University of California

Riverside, Riverside, California, January 2009, <https://www.pc-progress.com/Downloads/Pgm_hydrus1D/HYDRUS1D-4.08.pdf>.

Singer, M & Munns, D 2006, *Soils: An Introduction*, Prentice Hall, New Jersey.

Sobieraj, J, Elsenbeer, H & Vertessy, R 2001, 'Pedotransfer functions for estimating saturated hydraulic conductivity: implications for modeling storm flow generation', *Journal of Hydrology*, vol. 251, no. 3-4, pp. 202-20.

Souchere, V, Cerdan, O, Le Bissonnais, Y, Couturier, A, King, D & Papy, F 2001, 'Incorporating surface crusting and its spatial organization in runoff and erosion modelling at the watershed scale', *Sustaining the Global Farm, selected papers from the 10th International Soil Conservation Organization Meeting, May 24-29, 1999, Purdue University*, pp. 888-95.

Sprague De Camp, L 1963, *The Ancient Engineers*, Rigby Limited, Adelaide.

Stirzaker, R, Passioura, J & Wilms, Y 1996, 'Soil structure and plant growth: Impact of bulk density and biopores', *Plant and Soil*, vol. 185, no. 1, pp. 151-62.

Taina, I, Heck, R & Elliot, T 2008, 'Application of X-ray computed tomography to soil science: A literature review', *Canadian Journal of Soil Science*, vol. 88, no. 1, pp. 1-19.

Tan, K 1996, *Soil Sampling: Preparation and Analysis*, Marcel Dekker Inc, New York.

Tarboton, D 2003, *Rainfall - Runoff Processes*, Utah State University, Utah, Civil and Environmental Engineering Faculty Publications. Paper 2570, <<http://www.engineering.usu.edu/dtarb/rrp.html>>.

Tietje, O & Hennings, V 1996, 'Accuracy of the saturated hydraulic conductivity prediction by pedotransfer functions compared to the variability within FAO textural classes', *Geoderma*, vol. 69, no. 1-2, pp. 71-84.

Timlin, D, Williams, R, Ahuja, L & Heathman, G 2004, 'Simple Parametric Methods to Estimate Soil Water Retention and Hydraulic Conductivity', in YA Pachepsky & WJ Rawls (eds), *Development of Pedotransfer Functions in Soil Hydrology*, Elsevier, Amsterdam, ch 5.

Tuller, M & Or, D 2004, 'Water retention and characteristic curve', in vol. 4, pp. 278-89.

Turner, A, Willatt, S, Wilson, J & Jobling, G 1984, *Infiltration of water into dry soil*, Soil water management, International Development Program of Australian Universities and Colleges Ltd, Canberra.

UMS GmbH nd, *Operation Manual: HYPROP*, UMS GmbH, Munich, Germany, <<http://labcell.com/media/127793/hyprop%20manual.pdf>>.

Valentin, C & Bresson, L-M 1992, 'Morphology, genesis and classification of surface crusts in loamy and sandy soils', *Geoderma*, vol. 55, no. 3-4, pp. 225-45.

van Genuchten, M, Leij, F & Yates, S 1991, *The RETC Code for Quantifying the Hydraulic Functions of Unsaturated Soils*, US Laboratory, US Department of Agriculture, Agricultural Research Service, California.

Verbist, K, Torfs, S, Cornelis, W, Oyarzún, R, Soto, G & Gabriels, D 2010, 'Comparison of single- and double-ring infiltrometer methods on stony soils', *Vadose Zone Journal*, vol. 9, no. 2, pp. 462-75.

Vickers, B 1987, *Laboratory Work in Soil Mechanics*, HarperCollins Publishers, London.

Yin Chan, K 2002, 'Bulk Density', in R Lal (ed.), *Encyclopedia of Soil Science*, Marcel Dekker New York.

Zhang, Y & Schaap, MG 2019, 'Estimation of Saturated Hydraulic Conductivity with Pedotransfer Functions: A Review', *Journal of Hydrology*.

Zhao, C, Shao, Ma, Jia, X, Nasir, M & Zhang, C 2016, 'Using pedotransfer functions to estimate soil hydraulic conductivity in the Loess Plateau of China', *Catena*, vol. 143, pp. 1-6.

Appendix A – Project Specification

ENG4111/4112 Research Project

Project Specification

For:	Cameron Leckie	
Title:	Improving the prediction of infiltration and surface run-off from crusted soils by measuring the density of the discrete surface seal/crust.	
Major:	Agricultural Engineering	
Supervisors:	Dr John Bennett, USQ	Dr Rob Loch, Landloch
Enrolment:	ENG4111 – EXT S1, 2019	ENG4112 – EXT S2, 2019
Project Aim:	The aim of this project is to improve the modelling capability for infiltration and surface runoff for crusting soils.	

Programme: Version 1, 13 March 2019

1. Review the literature on modelling infiltration and surface runoff on crusting soils.
2. Use previous experimental data to determine the potential contribution of surface crust density to model error.
3. Identify and/or develop a reliable method of collecting surface crust/seal samples for the purposes of accurately calculating crust bulk density and/or porosity.
4. Optimise an infiltration and/or surface runoff model that incorporates surface crust parameters such as bulk density and porosity.
5. Validate whether incorporation of soil crust parameters into the infiltration/surface runoff models improves model accuracy.
6. Make recommendations on changes to current soil survey processes to improve infiltration and surface runoff predictions.

Appendix B - Example MATLAB Scripts

Introduction

MATLAB was used extensively during modelling activities with HYDRUS-1D. MATLAB was used to automate multiple activities including changing input data, executing HYDRUS-1D and plotting the results of HYDRUS-1D simulations. The use of these scripts saved a significant amount of time compared to manual/Microsoft Excel based methods.

Code from one function and three scripts are provided below. A brief description of each is as follows:

- **Execute HYDRUS.** This function is called in other script files to execute the HYDRUS-1D application. HYDRUS-1D will execute whichever simulation that is listed in the 'Level_01.dir' file.
- **Plot_part1_modelling_hydrus.** This script plots infiltration and cumulative infiltration results for four different HYDRUS-1D simulations on the same plot.
- **Run HYDRUS with different head values.** This script is an example of a script file that changes the HYDRUS-1D simulation input values. For the selected simulation values, four different ψ values are simulated, HYDRUS is executed for each of the values and the results stored in arrays. The results from each of the simulations are then plotted.
- **Nash Sutcliffe.** This script compares simulated infiltration outputs from HYDRUS against the regression equations developed for the observed infiltration. The Nash Sutcliffe objective function is applied and the results plotted on a Predicted – Observed plot.

This code is provided 'as is.' To use the code users will need to update folder locations for their own computer system. They will also need to generate the import functions to import data from the HYDRUS-1D output files (e.g. TLevel.out).

Function: Execute HYDRUS

```
function [] = execute_hydrus()
%Execute_hydrus
% This function calls and executes Hydrus application. The simulation
% that is called is detailed in the Level_01.dir file.

hydrus_location = 'C:\Program Files (x86)\PC-Progress\Hydrus-1D 4.xx\'; %
Level_01.dir file is in this directory. This file needs to be changed to
choose a new simulation.

% hydrus_location = 'C:\Users\Cameron\Documents\Engineering Degree - use
this one\19 S1 ENG4111 Research Project\Hydrus\';
cd(hydrus_location);
hydrus_executable = 'H1D_CALC.exe';
call_hydrus = fullfile(hydrus_location, hydrus_executable);

dos(call_hydrus) % executes hydrus
end
```

Script: Plot_part1_modelling_hydrus

```
% Name: Plot_part1_modelling_hydrus.
```

```

% Purpose: To plot infiltration rate and cumulative infiltration for
% arbitrarily created soil profile. Also present cumulative infiltration at
% the end of each simulation
% % Description: User selects which soils they are interested in (four are
% plotted). The data is imported from the T.OUT file for each simulation.
% The infiltration rate and cumulative infiltration versus time are plotted
% as well as the values for cumulative infiltration.
% I/O:
% Author: Cameron Leckie
% Date: 28 June 2019
% Test Log:
% Change Log:

%%
% Initialisation

clear all
clc

code_dir = 'C:\Users\Cameron\Documents\MATLAB\ENG4111'; % All MATLAB code
relevant to the project is saved here.

hydrus_dir = 'C:\Users\Cameron\Documents\Engineering Degree - use this
one\19 S1 ENG4111 Research Project\Hydrus Data Files'; % Hydrus data
directory
cd(hydrus_dir);

%%
% Find HYDRUS folders relevant to selected soil code within the current
directory.

list = ls; % assigns contents of folder to array list
list = cellstr(list); % converts list to a cell string
list(1:2) = []; % deletes the '.' and '..' entries from the array

%%
% delete all .hld file extensions

idx_hld = strfind(list,'hld'); % row array to find which elements of list
have the extension hld in them'
find_empty_hld = cellfun('isempty',idx_hld); % returns logical array

todelete = (size(idx_hld)); % vector that keeps track of which elements to
delete
i2 = 1; % reset second index for assigning values to todelete

for i = 1:length(idx_hld)
    % loop that checks each element of idx to see if it is empty. If it
is
    % empty then the index of that value is assigned to the array todelete
    if find_empty_hld(i) == 0
        todelete(i2) = i;
        i2 = i2 + 1;
    end
end

list(todelete) = []; %delete all elements at once after the loop

```

```

%%
% Narrow down simulations you are searching for. Delete unwanted entries
% from list

disp(list);
prompt = 'Enter string to narrow down selection: ';
search_string = input(prompt, 's');

idx_search_string = strfind(list, search_string); % array to find which
elements of list include the selected soil code string. This will be used
to shorten array 'list'.
find_empty_search_string = cellfun('isempty',idx_search_string); % returns
logical array
todelete_search_string = size(idx_search_string);

i2 = 1; % second index for assigning values to todelete

for i = 1:length(idx_search_string)
    % loop that checks each element of idx_soil_code to see if it is
empty. If it is
    % empty then the index of that value is assigned to the array todelete
    if find_empty_search_string(i) == 1
        todelete_search_string(i2) = i;
        i2 = i2 + 1;
    end
end

list(todelete_search_string) = []; %delete all elements at once after the
loop

%%
% Select which simulations to import

disp('The following simulations meet your search criteria. ');
disp(' ');

list_index = 1:length(list);
simulation_selector = table(list_index', list)

simulation_selector_1(1:4) = nan;

disp('Two options for chart legend are available');
disp('Option one: no crust, 2mm crust, 6mm crust, 10 mm crust');
disp('Option two: no crust, 2mm crust, 6mm crust, variable crust');

prompt = 'Enter 1 for option one and 2 for option two: ';
option_selection = input(prompt);

for i = 1:4

    if option_selection == 1
        simulation_selector_1(i) = input('Enter index number in order:
no crust, 2mm crust, 6mm crust, 10 mm crust: ');
    else
        simulation_selector_1(i) = input('Enter index number in order: no
crust, 2mm crust, 6mm crust, variable crust: ');
    end
end

```

```

end

%%
% import selected data

cd(code_dir)
[no_crust, crust_2mm, crust_6mm, crust_10mm] =
plot_part1_function(hydrus_dir, list, simulation_selector_1); % function
which imports data

%%

%%
% Plot data in a subplot

% prompt = ('Enter soil texture type (e.g. Clay Loam) for chart title: ');
% chart_title = input(prompt, 's');
subplot1_title = 'Infiltration Rate';
subplot2_title = 'Cumulative Infiltration';

clf % close any open plots

subplot(2,1,1)

loglog(no_crust(:,1), -3600 * no_crust(:,4), crust_2mm(:,1), -3600
*crust_2mm(:,4), '--', crust_6mm(:,1), -3600 * crust_6mm(:,4), 'k:',
crust_10mm(:,1), -3600 * crust_10mm(:,4), 'g-.', 'LineWidth', 1.5)
title(subplot1_title, 'FontSize',18);

if option_selection == 1
    legend({'No Crust', '2mm Crust', '6mm Crust', '10mm Crust'},
'FontSize',14);
else
    legend({'No Crust', '2mm Crust', '6mm Crust', 'Variable Crust'},
'FontSize',14);
end

xlabel(' log(Time) - (s)', 'FontSize',18);
ylabel('log(Infiltration rate) - (mm/h)', 'FontSize',18);

subplot(2,1,2)
semilogx(no_crust(:,1), no_crust(:,18), crust_2mm(:,1), crust_2mm(:,18), '--
', crust_6mm(:,1), crust_6mm(:,18), 'k:', crust_10mm(:,1),
crust_10mm(:,18), 'g-.', 'LineWidth', 1.5)
title(subplot2_title, 'FontSize',18);

if option_selection == 1
    legend({'No Crust', '2mm Crust', '6mm Crust', '10mm Crust'},
'FontSize',14);
else
    legend({'No Crust', '2mm Crust', '6mm Crust', 'Variable Crust'},
'FontSize',14);
end

xlabel('log(Time) - (s)', 'FontSize',18);
ylabel('Cumulative infiltration - (mm)', 'FontSize',18);

```

```

set(gcf, 'Position', get(0, 'Screensize')); % maximises figure on the
screen

save_folder = 'C:\Users\Cameron\Documents\Engineering Degree - use this
one\19 S1 ENG4111 Research Project\Phase 2 - Modelling\RETC\Images';
cd(save_folder) % changes folder to allow the figure to be saved in the
correct folder

%%
% Cumulative infiltration values - identify the total cumulative
% infiltration at the end of the simulation

max_no_crust = max(no_crust(:,18));
max_crust_2mm = max(crust_2mm(:,18));
max_crust_6mm = max(crust_6mm(:,18));
max_crust_10mm = max(crust_10mm(:,18));

summary_crust_scenario = {'max_no_crust'; 'max_crust_2mm'; 'max_crust_6mm';
'max_crust_10mm'};
summary_crust_results = [max_no_crust; max_crust_2mm; max_crust_6mm;
max_crust_10mm];

disp('Cumulative infiltration results');
table(summary_crust_scenario, summary_crust_results)

```

Script: Run HYDRUS with different head values

```

% Name: Run Hydrus with different head values
% Purpose: Allow comparison of infiltration rates when different matric
% potentials are used.
% % Description: User selects a HYDRUS-1D simulation. HYDRUS is executed
using four different head values. The results are stored in arrays and
plotted.
% I/O:
% Author: Cameron Leckie
% Date: 30 June 2019
% Test Log:
% Change Log:

%%
% Initialisation

clear all
clc

code_dir = 'C:\Users\Cameron\Documents\MATLAB\ENG4111'; % All MATLAB code
relevant to the project is saved here.
hydrus_dir = 'C:\Users\Cameron\Documents\Engineering Degree - use this
one\19 S1 ENG4111 Research Project\Hydrus Data Files'; % Hydrus simulation
data directory
matlab_dir = 'C:\Users\Cameron\Documents\MATLAB'; % directory where MATLAB
application files are stored
hydrus_app_dir = 'C:\Program Files (x86)\PC-Progress\Hydrus-1D 4.xx';
cd(hydrus_dir);

%%
% Find HYDRUS folders relevant to selected soil code within the current
directory.

```

```

list = ls; % assigns contents of folder to array list
list = cellstr(list); % converts list to a cell string
list(1:2) = []; % deletes the '.' and '..' entries from the array

%%
% delete all .hld file extensions

idx_hld = strfind(list, 'hld'); % row array to find which elements of list
have the extension hld in them'
find_empty_hld = cellfun('isempty', idx_hld); % returns logical array

todelete = (size(idx_hld)); % vector that keeps track of which elements to
delete
i2 = 1; % reset second index for assigning values to todelete

for i = 1:length(idx_hld)
    % loop that checks each element of idx to see if it is empty. If it
is
    % empty then the index of that value is assigned to the array todelete
    if find_empty_hld(i) == 0
        todelete(i2) = i;
        i2 = i2 + 1;
    end
end

list(todelete) = []; %delete all elements at once after the loop

%%
% Narrow down simulations you are searching for. Delete unwanted entries
% from list

disp(list);
prompt = 'Enter string to narrow down selection: ';
search_string = input(prompt, 's');

idx_search_string = strfind(list, search_string); % array to find which
elements of list include the selected soil code string. This will be used
to shorten array 'list'.
find_empty_search_string = cellfun('isempty', idx_search_string); % returns
logical array
todelete_search_string = size(idx_search_string);

i2 = 1; % second index for assigning values to todelete

for i = 1:length(idx_search_string)
    % loop that checks each element of idx_soil_code to see if it is
empty. If it is
    % empty then the index of that value is assigned to the array todelete
    if find_empty_search_string(i) == 1
        todelete_search_string(i2) = i;
        i2 = i2 + 1;
    end
end

list(todelete_search_string) = []; %delete all elements at once after the
loop

```

```

%%
% Select the simulation which will be run through Hydrus and update
% Level_01.dir

disp('The following simulations meet your search criteria. ');
disp(' ');

list_index = 1:length(list);
simulation_selector = table(list_index', list)

prompt = 'Enter index number that aligns with selected simulation: ';

simulation_selector = input(prompt); % seeks user input on which simulation
to run
sim_directory = cell2mat(list(simulation_selector)); % the list which
includes the simulation name is in a cell structure. Changes this to a
string for selected simulation

new_level_01 = fullfile(hydrus_dir, sim_directory); % create file path to
be inserted into Level_01. dir

cd(code_dir)

level_01_format = '%s'; % format input into as a string
fid = fopen('Level_01.dir', 'w');
fprintf(fid, level_01_format, new_level_01); % print new file path to
level_01.dir
fclose(fid);

copyfile('Level_01.dir', hydrus_app_dir) % copies new Level_01.dir file
into Hydrus application folder

%%
% Set up loop to simulation using four values of h and import that data.

TLEVEL_1 = nan(100,22); % pre-allocate arrays to store T_level.out
TLEVEL_2 = nan(100,22);
TLEVEL_3 = nan(100,22);
TLEVEL_4 = nan(100,22);

% provide user with choice to change head values

% h values for use in sim in millimetres.
% -100 is the default, -1000 is FC, -10000 is an intermediate, -150000 is
% PWP
default_h_values = [-100, -1000, -10000, - 150000]; % default values

disp('Hydrus will now be called to execute four simulations using the
following values of h (mm) ');
disp(default_h_values');

prompt = 'Do you wish to use these values? ';
h_values_choice = input(prompt, 's');

if h_values_choice == 'y'
    disp('You have selected the default h values');

```

```

elseif h_values_choice == 'n'
    disp('Enter four h values from least to most negative:')

    prompt = 'Enter h value: ';

    for i = 1 : length(default_h_values)
        default_h_values(i) = input(prompt);
    end

    disp('You have entered the following h values: ');
    disp(default_h_values');
end

disp('The default value for a ponded head scenario has been set at 10 mm.')
disp(' ');

prompt = 'Does this scenario have a ponded head? (y/n)? ';
ponded_head = input(prompt, 's');

if ponded_head == 'y'
    % prompt = 'Enter ponded head (positive value in mm): ';
    % ponded_head_value = input(prompt);
    ponded_head_value = 10;

else
    ponded_head_value = 0;
end

%%
%

for i = 1:4
    change_head_values_in_hydrus_automatic(new_level_01, ponded_head_value,
    default_h_values(i))
    disp(default_h_values(i))
    execute_hydrus % executes Hydrus using the simulation detailed in
    Level_01.dir.
    cd(new_level_01) % change directory to selected simulation

    if i == 1
        TLEVEL_1 = importTlevel('T_Level.out'); % imports T_Level.out from
        selected simulation
    elseif i == 2
        TLEVEL_2 = importTlevel('T_Level.out'); % imports T_Level.out from
        selected simulation
    elseif i == 3
        TLEVEL_3 = importTlevel('T_Level.out'); % imports T_Level.out from
        selected simulation
    else
        TLEVEL_4 = importTlevel('T_Level.out'); % imports T_Level.out from
        selected simulation
    end
end

%%
% Extract initial infiltration rate and final cumulative infiltration value
and save it in a text file that is appended to each iteration.

```

```

% Extract initial infiltration rate
initial_infiltration_rate = nan(1,4);
initial_infiltration_rate(1) = TLEVEL_1(1,4) * -3600;
initial_infiltration_rate(2) = TLEVEL_2(1,4) * -3600;
initial_infiltration_rate(3) = TLEVEL_3(1,4) * -3600;
initial_infiltration_rate(4) = TLEVEL_4(1,4) * -3600;

% Extract final infiltration rate
final_infiltration_rate = nan(1,4);
final_infiltration_rate(1) = max(TLEVEL_1(:,4)) * -3600;
final_infiltration_rate(2) = max(TLEVEL_2(:,4)) * -3600;
final_infiltration_rate(3) = max(TLEVEL_3(:,4)) * -3600;
final_infiltration_rate(4) = max(TLEVEL_4(:,4)) * -3600;

% Extract_cumulative_infiltration

cumulative_infiltration = nan(1,4);

cumulative_infiltration(1) = max(TLEVEL_1(:,18));
cumulative_infiltration(2) = max(TLEVEL_2(:,18));
cumulative_infiltration(3) = max(TLEVEL_3(:,18));
cumulative_infiltration(4) = max(TLEVEL_4(:,18));

% Summarise results

summary_of_simulations = cell(4,5); % create a cell array to store summary
data in.

for i = 1:4 % populate summary array
    summary_of_simulations(i,1) = {sim_directory};
    summary_of_simulations(i,2) = {default_h_values(i)};
    summary_of_simulations(i,3) = {initial_infiltration_rate(i)};
    summary_of_simulations(i,4) = {final_infiltration_rate(i)};
    summary_of_simulations(i,5) = {cumulative_infiltration(i)};
end

% disp(summary_of_simulations)

cd(hydrus_dir)
sim_sum_format = '%s %i %f %f %f\r\n'; % format input
fid = fopen('Simulation_summary.txt', 'a');

for i = 1:4
    fprintf(fid, sim_sum_format, summary_of_simulations{i,:});
end
fclose(fid);
%%
% Plot data in a subplot showing infiltration rate and cumulative
% infiltration

% chart_title = sim_directory;
subplot1_title = strcat(' Infiltration Rate ');
subplot2_title = strcat(' Cumulative Infiltration ');

clf % close any open plots

```

```

subplot(2,1,1)

loglog(TLEVEL_1(:,1), -3600 * TLEVEL_1(:,4), TLEVEL_2(:,1), -3600 *
TLEVEL_2(:,4), '--', TLEVEL_3(:,1), -3600 * TLEVEL_3(:,4), 'k:',
TLEVEL_4(:,1), -3600 * TLEVEL_4(:,4), 'g-', 'LineWidth', 1.5)
title(subplot1_title, 'FontSize',18);

if h_values_choice == 'y'
    legend({'Default', 'FC', 'Intermediate', 'PWP'}, 'FontSize',14);
elseif h_values_choice == 'n'
    legend({'H1', 'H2', 'H3', 'H4'}, 'FontSize',14);
end
xlabel(' log(Time) - (s)', 'FontSize',18);
ylabel('log(Infiltration rate) - (mm/h)', 'FontSize',18);

subplot(2,1,2)
semilogx(TLEVEL_1(:,1), TLEVEL_1(:,18), TLEVEL_2(:,1), TLEVEL_2(:,18), '--
', TLEVEL_3(:,1), TLEVEL_3(:,18), 'k:', TLEVEL_4(:,1), TLEVEL_4(:,18), 'g-
.', 'LineWidth', 1.5)
title(subplot2_title, 'FontSize',18);

if h_values_choice == 'y'
    legend({'Default', 'FC', 'Intermediate', 'PWP'}, 'FontSize',14);
elseif h_values_choice == 'n'
    legend({'H1', 'H2', 'H3', 'H4'}, 'FontSize',14);
end

xlabel('log(Time) - (s)', 'FontSize',18);
ylabel('Cumulative infiltration - (mm)', 'FontSize',18);

set(gcf, 'Position', get(0, 'Screensize')); % maximises figure on the
screen

```

Script: Nash Sutcliffe

```

% Name: Nash_Sutcliffe
% Purpose: Compare observed versus modelled infiltration to determine the
closeness of fit
% Description:
% 1. Imports selected simulation results from HYDRUS.
% 2. Applies time values used in HYDRUS to observed infiltration function.
% 3. Plots observed versus modelled infiltration
% 4. Calculates objective function value.
% Author: Cameron Leckie
% Date: 13 August 2019
% Test Log:
% Change Log:

%%
% Initialisation

clear all
clc

output_data = 'C:\Users\Cameron\Documents\Engineering Degree - use this
one\19 S1 ENG4111 Research Project\Phase 4 - Results and
Analysis\Mod_Obs_data';
cd(output_data);

```

```

code_dir = 'C:\Users\Cameron\Documents\MATLAB\ENG4111'; % All MATLAB code
relevant to the project is saved here.
hydrus_dir = 'C:\Users\Cameron\Documents\Engineering Degree - use this
one\19 S1 ENG4111 Research Project\Hydrus Data Files'; % Hydrus simulation
data directory
matlab_dir = 'C:\Users\Cameron\Documents\MATLAB'; % directory where MATLAB
application files are stored
obs_infil_dir = 'C:\Users\Cameron\Documents\Engineering Degree - use this
one\19 S1 ENG4111 Research Project\Phase 4 - Results and
Analysis\Mod_Obs_data'

text_file_header_format = '%s %s\n';
text_file_body_format = '%5.0f %8.7f\r\n';

syms t

%%
% 1. Imports selected simulation results from HYDRUS.

[simulation_list] = Filter_hydrus_simulations(hydrus_dir)

prompt = 'Enter index number of simulation you wish to select: ';
selected_simulation_index = input(prompt);

selected_simulation = simulation_list{selected_simulation_index, 2}; %
extract folder name from table as a cell format
selected_simulation = char(selected_simulation) % convert to string
folder_name = fullfile(hydrus_dir, selected_simulation); % full file path
to simulation
cd(folder_name)

Modelled_TLevel = importTlevel('T_Level.out');
Modelled_time_values = Modelled_TLevel(1:end-1, 1);
Modelled_infiltration_values = -Modelled_TLevel(1:end-1, 4);

%%
% plot(Modelled_time_values, Modelled_infiltration_values);

%%
% Selected observed infiltration event

simulation_title_index = [1; 2; 3; 4; 5; 6; 7];
simulation_title = {'Sod 1 R2'; 'Sod 1 R3'; 'Sod 2 R2'; 'Sod 2 R3'; 'Sod 3
R2'; 'Sod 3 R3'; 'Chr 1 R2'};
simulation_selection_table = table(simulation_title_index,
simulation_title);
disp(simulation_selection_table);
prompt = 'Enter index number that aligns with selected simulation: ';
k = input(prompt);
%%
% values required to calculate infiltration function

simulation_time_to_first_measurement = [128; 99; 130; 99; 128; 99; 99]; %
need to change this to first measurement
simulation_time_to_last_measurement = [1520; 1528; 1512; 1542; 1520; 768;
933];
simulation_rainfall_intensity = [0.033610148; 0.02940118; 0.032100543;
0.029236421; 0.031037122
; 0.028115882; 0.027170804];

```

```

simulation_inputs = table(simulation_title,
simulation_time_to_first_measurement, simulation_time_to_last_measurement,
simulation_rainfall_intensity)

time_values = Modelled_time_values; % rename variable for next section

%%
% Calculate observed infiltration values using time values from HYDRUS
% simulation

    for i = 1:length(time_values) % loop to assign infiltration rate values
for each function

        if time_values(i) <= simulation_time_to_first_measurement(k)
            simulation_infiltration_rate(i) =
simulation_rainfall_intensity(k);

        else
            if k == 1
                simulation_infiltration_rate(i) = 3e-9 .* time_values(i).^2
- 6e-6 .* time_values(i) + 0.0046; % need to add if else statements here
for each regression equation

            elseif k == 2
                simulation_infiltration_rate(i) = -6e-4 .*
log(time_values(i))+ 0.0043;

            elseif k == 3
                simulation_infiltration_rate(i) = 6e-12 .*
time_values(i).^3 - 2e-8 .* time_values(i).^2 + 8e-6 .* time_values(i) +
0.0028;

            elseif k == 4
                simulation_infiltration_rate(i) = -5e-4 .*
log(time_values(i))+ 0.0036;

            elseif k == 5
                simulation_infiltration_rate(i) = 3e-9 .* time_values(i).^2
- 9e-6 .* time_values(i) + 0.0075;

            elseif k == 6
                simulation_infiltration_rate(i) = -8e-4 .*
log(time_values(i))+ 0.0051;

            else
                simulation_infiltration_rate(i) = 4e-9 .* time_values(i).^2
- 5e-6 .* time_values(i) + 0.0038;

            end

        end

    end

    % disp(simulation_infiltration_rate);

%%

```

```

% use values that occur only after runoff has occurred

time_of_first_measurement = simulation_time_to_first_measurement(k); % time
in seconds when first measurement taken
counter = 1;

while Modelled_time_values(counter) < time_of_first_measurement % while
loop to find the index (counter) when first measurement occurs
    counter = counter + 1;
    % disp(Modelled_time_values(counter));
end

% concatenate arrays
disp(Modelled_time_values(counter));
disp(counter);

a = table(simulation_infiltration_rate', Modelled_infiltration_values)

% counter
simulation_infiltration_rate(counter+1)
Modelled_infiltration_values(counter+1)

simulation_infiltration_rate = simulation_infiltration_rate(counter+1:end);
Modelled_infiltration_values = Modelled_infiltration_values(counter+1:end);

%%
% Calculate Nash Sutcliffe (measure of fit to 1:1 line)
x_bar = mean(simulation_infiltration_rate);
xi_xbar = nan(1, length(simulation_infiltration_rate));
yi_xi = nan(1, length(simulation_infiltration_rate));

for i = 1:length(simulation_infiltration_rate)

    xi_xbar(i) = (simulation_infiltration_rate(i) - x_bar).^2;
    yi_xi(i) = (Modelled_infiltration_values(i) -
simulation_infiltration_rate(i)).^2;

end

sum_xi_xbar = sum(xi_xbar);
sum_yi_xi = sum(yi_xi);
Nash_sutcliffe_E = (sum_xi_xbar - sum_yi_xi)/sum_xi_xbar;

%%
% Plot modelled versus observed

% 1 to 1 line coordinates
x_1_1 = [0, 0.007];
y_1_1 = [0, 0.007];

Modelled_infiltration_values = Modelled_infiltration_values'; % to align
indexing (rows and columns)

clf % close any open plots
hold on

% swap observed and modelled around on the axis. Observed should be on the

```

```
% x axis
plot(x_1_1, y_1_1, 'r', 'LineWidth', 2);
plot(simulation_infiltration_rate, Modelled_infiltration_values,
'LineWidth', 2);
ylabel('Modelled infiltration rate', 'FontSize', 24)
xlabel('Observed infiltration rate', 'FontSize', 24);
text(0.0005, 0.005, sprintf('Nash Sutcliffe Criteria: %f',
Nash_sutcliffe_E), 'FontSize', 24)

hold off
```

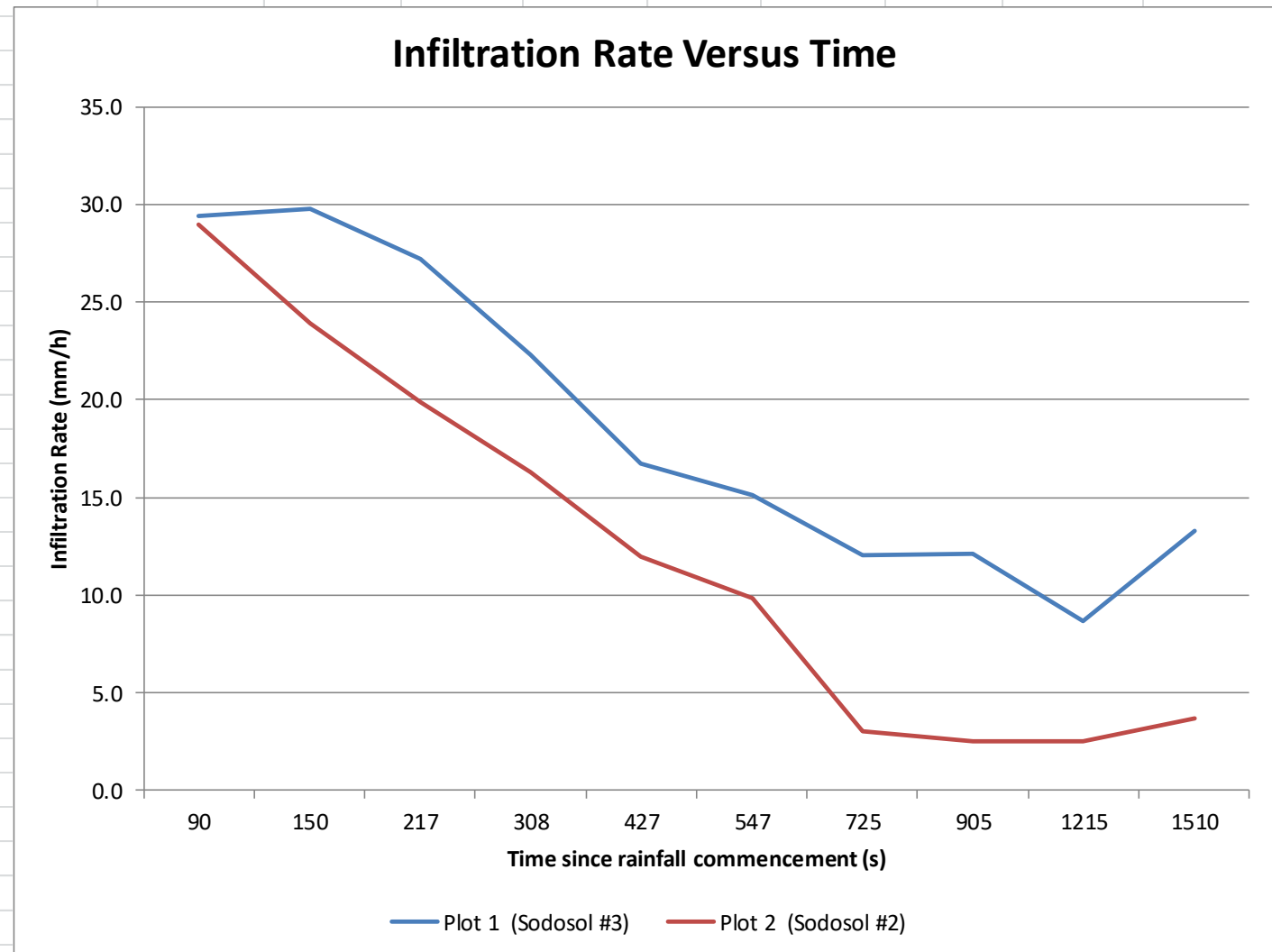
Appendix C – Rainfall simulation results

The data collected from each of the rainfall simulation experiments is detailed in this Appendix.

Date	1-Jul-19		Plot 1		(Sodosol #3)							Plot 2		(Sodosol #2)						
Plot gradient	20%																			
Runoff initiation (s)	39																			
	Bottle number	Bottle mass (g)	Wet mass (g)	OD mass (g)	Sediment mass (g)	Runoff mass (g)	Instantaneous runoff (mm/h)	Instantaneous infiltration (mm/h)	Bottle number	Bottle mass (g)	Wet mass (g)	OD mass (g)	Sediment mass (g)	Runoff mass (g)	Instantaneous runoff (mm/h)	Instantaneous infiltration (mm/h)				
Pre-rain moisture sample	771	66.864	157.2	151.1	84.236				772	66.834	143.7	139	72.166							
Time from stat (min:sec to min)	Duration (secs)																			
1 30 90	16.38	773	66.785	306.5	82.3	15.5	208.7	81.5	29.4	805	68.801	289.9	80.2	11.399	209.7	81.9	29.0			
2 30 150	16.19	774	66.768	301.1	81.3	14.5	205.3	81.1	29.8	804	68.736	300.4	80.4	11.664	220.0	87.0	23.9			
3 37 217	16.25	775	66.861	311.4	82.9	16.0	212.5	83.7	27.2	803	66.78	310.5	79.4	12.62	231.1	91.0	19.9			
5 8 308	16.59	776	66.933	331.7	84.5	17.6	229.6	88.6	22.3	802	68.781	327.1	81.9	13.119	245.2	94.6	16.3			
7 7 427	16.41	777	66.817	347.0	86.2	19.4	241.4	94.2	16.8	801	68.731	336.9	83.2	14.469	253.7	98.9	12.0			
9 7 547	15.75	778	66.453	341.5	86.1	19.6	235.8	95.8	15.1	800	66.829	330.4	81.6	14.771	248.8	101.1	9.8			
12 5 725	15.82	779	66.675	350.4	86.3	19.6	244.5	98.9	12.0	799	68.627	351.7	85.1	16.473	266.6	107.9	3.1			
15 5 905	16.13	780	66.802	355.6	86.7	19.9	249.0	98.8	12.1	798	66.851	359.2	86.1	19.249	273.1	108.4	2.5			
20 15 1215	15.72	781	66.583	356.1	85.8	19.2	251.1	102.2	8.7	797	66.739	351.5	85.2	18.461	266.3	108.4	2.5			
25 10 1510	16.09	782	66.971	344.2	82.9	15.9	245.4	97.6	13.3	796	66.862	354.0	84.5	17.638	269.5	107.2	3.7			
Post-rain moisture sample	783	66.953	175.1	156.5	89.547				795	66.903	226.3	156.5	89.597							

Rain off	Rain gauges			
25 min		48		47
58 sec	52	Plot 1	49	Plot 2
6 msec		43		42
Time (s)	1558.06			
	Plot 1 Average	48	Plot 2 Ave	45
	Rainfall intensity (mm/s)	0.031		0.029
	Rainfall intensity (mm/h)	110.9		104.0

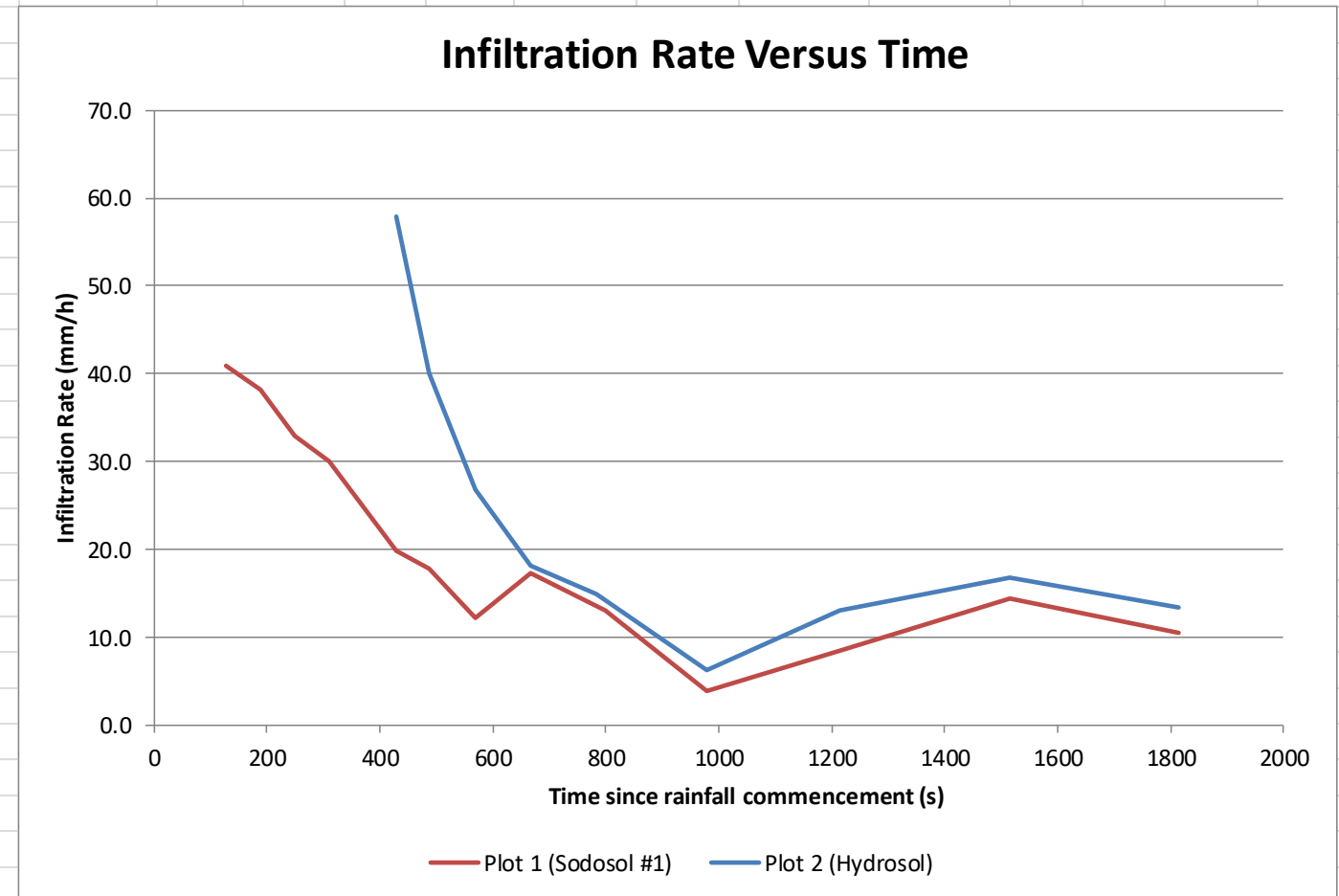
	Moisture cont	Plot 1	Plot 2
Before	Mass soil (g)	84.236	72.166
	Mass water (g)	6.1	4.7
	MC	7.2%	5.6%
After	Mass soil (g)	89.547	89.597
	Mass water (g)	18.6	69.8
	MC	20.8%	77.9%



Date		1-Jul-19		Plot 1 (Sodosol #1)								Plot 2 (Hydrosol)											
Plot gradient				20%								20%											
Runoff initiation (min)				50 sec								6 min 40 sec											
		Bottle number	Bottle mass (g)	Wet mass (g)	OD mass (g)	Sediment mass (g)	Runoff mass (g)	Instantaneous runoff (mm/h)	Instantaneous infiltration (mm/h)	Bottle number	Bottle mass (g)	Wet mass (g)	OD mass (g)	Sediment mass (g)	Runoff mass (g)	Instantaneous runoff (mm/h)	Instantaneous infiltration (mm/h)						
Pre-rain moisture sample		794	66.903	129.4	127	59.997				351	66.645	129.2	117.1	50.455									
Time from stat (min:sec to sec)		Duration (secs)																Time from stat (min:sec to min)		Duration (s)			
2	9	129	16.07	793	66.808	283.1	83.1	16.3	183.7	73.2	40.9	352	66.733	98.9	67.5	0.7	31.4	44.9	57.8	7	9	429	15.7
3	9	189	16.21	792	68.69	292.7	84.5	15.8	192.4	76.0	38.1	353	66.818	112.5	68.2	1.3	44.3	62.8	40.0	8	7	487	15.9
4	9	249	15.97	791	68.462	302.8	84.3	15.8	202.7	81.2	32.9	354	66.854	121.3	68.5	1.6	52.8	75.9	26.9	9	30	570	15.7
5	9	309	16.10	790	66.825	311.5	83.5	16.7	211.3	84.0	30.1	355	66.89	127.6	68.9	2.0	58.7	84.7	18.1	11	8	668	15.6
7	9	429	15.72	789	68.828	334.1	85.8	17.0	231.3	94.2	19.9	356	66.886	127.6	68.9	2.0	58.7	87.9	14.9	13	2	782	15.0
8	7	487	15.88	788	66.798	342.9	85.3	18.5	239.1	96.4	17.7	357	66.886	133.8	69.0	2.1	64.8	96.5	6.3	16	19	979	15.1
9	30	570	15.65	787	66.731	353.1	85.3	18.6	249.2	101.9	12.2	358	66.86	134.7	69.0	2.1	65.7	89.8	13.0	20	15	1215	16.5
11	8	668	15.60	786	66.85	338.4	84.7	17.9	235.9	96.8	17.3	359	66.88	126.1	68.7	1.8	57.4	85.9	16.8	25	15	1515	15.0
13	20	800	15.03	785	68.709	340.5	86.0	17.3	237.2	101.0	13.1	360	66.887	135.2	69.0	69.0	66.2	89.4	13.4	30	15	1815	16.7
16	19	979	15.11	784	66.706	368.3	87.4	20.7	260.2	110.2	3.9												
20	15	1215	16.47	385	66.9	378.4	86.7	19.8	271.9	105.7	8.4												
25	15	1515	15.03	384	66.886	328.4	80.6	13.7	234.1	99.7	14.4												
30	15	1815	16.66	383	66.845	365.4	81.4	14.6	269.4	103.5	10.6												
Post-rain moisture sample		382	66.405	172.5	155	88.795						361	66.877	147.1	114.1	47.223							

Rain off		Rain gauges			
30 min		60		53	
30 sec		63	Plot 1	57	Plot 2 54
39 msec		52		45	
Time (s)	1830.39				
	Plot 1 Average	58	Plot 2	52.3	
	Rainfall intensity (mm/s)	0.032		0.029	
	Rainfall intensity (mm/h)	114.1		102.8	

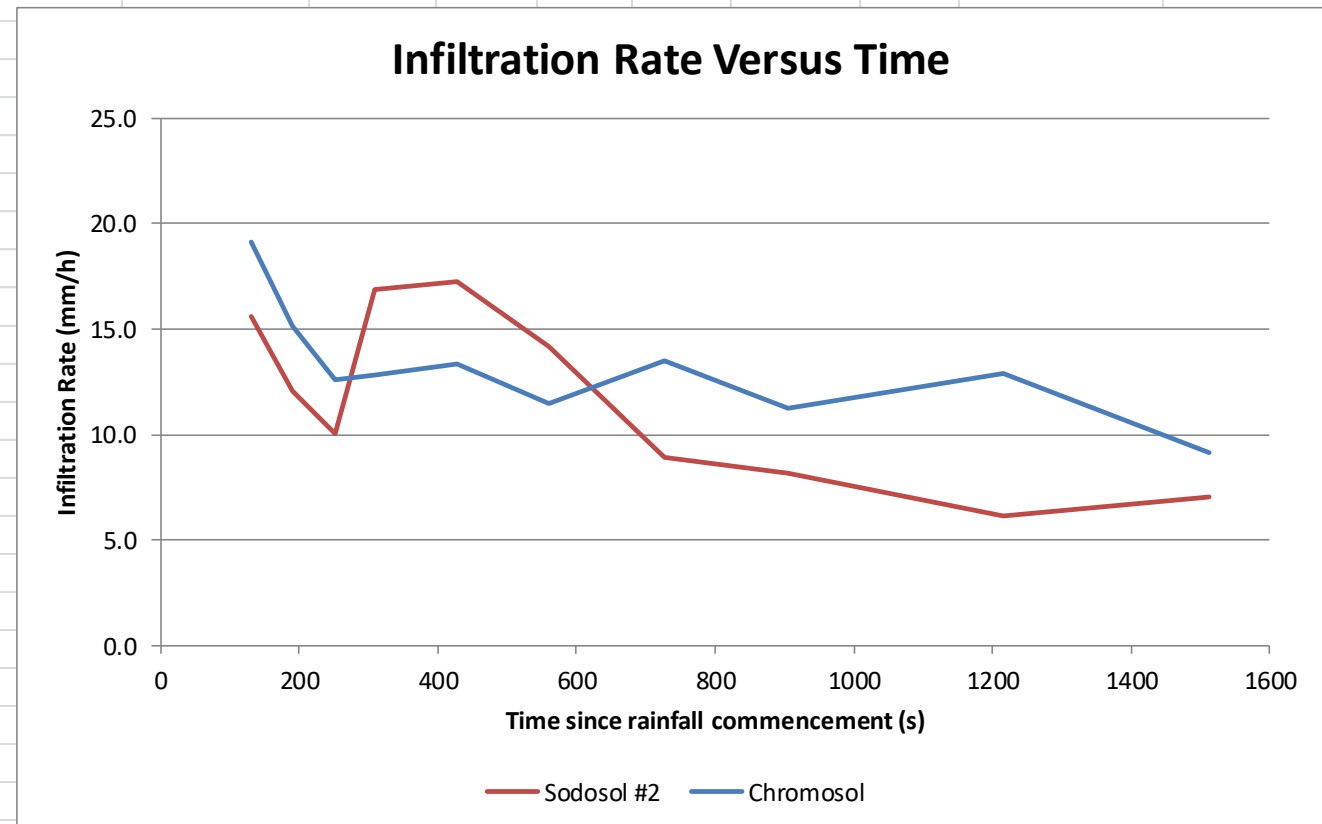
	Moisture cor	Plot 1	Plot 2
Before	Mass soil (g)	59.997	50.46
	Mass water (g)	2.5	12.1
	MC	4.2%	24.0%
After	Mass soil (g)	88.795	47.22
	Mass water (g)	17.3	33
	MC	19.5%	69.9%



Date	2-Jul-19		Plot 1	Sodosol #2						Plot 2	Chromosol								
Plot gradient			20%						20%										
Runoff initiation (s)			55						78										
	Bottle number	Bottle mass (g)	Wet mass (g)	OD mass (g)	Sediment mass (g)	Runoff mass (g)	Instantaneous runoff (mm/h)	Instantaneous infiltration (mm/h)	Bottle number	Bottle mass (g)	Wet mass (g)	OD mass (g)	Sediment mass (g)	Runoff mass (g)	Instantaneous runoff (mm/h)	Instantaneous infiltration (mm/h)			
Pre-rain moisture sample	141	67.062	117.3	111.8	44.738				175	67.089	104.4	100.6	33.511						
Time from stat (min:sec to sec)	Duratio n (secs)															Time f			
2	10	130	16.69	142	67.051	352.5	79.4	12.4	260.7	100.0	15.6	174	67.023	131.3	68.6	1.6	61.1	82.4	19.2
3	10	190	15.97	143	67.017	350.4	79.6	12.6	258.2	103.5	12.1	173	67.06	131.7	68.7	1.6	61.4	86.4	15.1
4	11	251	14.59	144	67.023	332.4	79.4	12.4	240.6	105.6	10.0	172	67.012	127.7	68.5	1.5	57.7	89.0	12.6
5	9	309	16.09	145	67.033	343.5	81.2	14.2	248.1	98.7	16.9	171	66.971	133.9	68.7	1.7	63.5	88.8	12.8
7	7	427	17.32	146	67.002	364.3	82.6	15.6	266.1	98.3	17.2	170	67.013	138.7	68.9	1.9	67.9	88.2	13.3
9	20	560	16.50	147	67.003	360.1	82.9	15.9	261.3	101.4	14.2	169	67.086	136.4	68.7	1.6	66.1	90.1	11.4
12	8	728	16.07	148	67.032	365.4	82.3	15.3	267.8	106.7	8.9	168	67.095	132.8	68.5	1.4	62.9	88.1	13.5
15	4	904	15.06	149	66.998	347.7	81.0	14.0	252.7	107.4	8.2	167	67.068	130	68.3	1.2	60.5	90.3	11.2
20	16	1216	15.62	150	67.001	362.2	81.1	14.1	267.0	109.4	6.2	166	66.959	131.2	68.3	1.3	61.6	88.7	12.9
25	12	1512	15.13	151	67.015	350	80.2	13.2	256.6	108.6	7.0	165	67.053	131.5	68.2	1.1	62.2	92.4	9.1
		0																	
		0																	
		0																	
Post-rain moisture sample	152	67.048	183.2	165.5	98.452					164	67.07	157.1	139.2	72.13					

Rain off		Rain gauges					
25 min		52		48			
42 sec		54	Plot 1	44	42	Plot 2	45
3 msec		48		39			
Time (s)	1542.03						
		Plot 1 Average	49.5	Plot 2 Average	43.5		
		Rainfall intensity (mm/s)	0.032		0.028		
		Rainfall intensity (mm/h)	115.6		101.6		

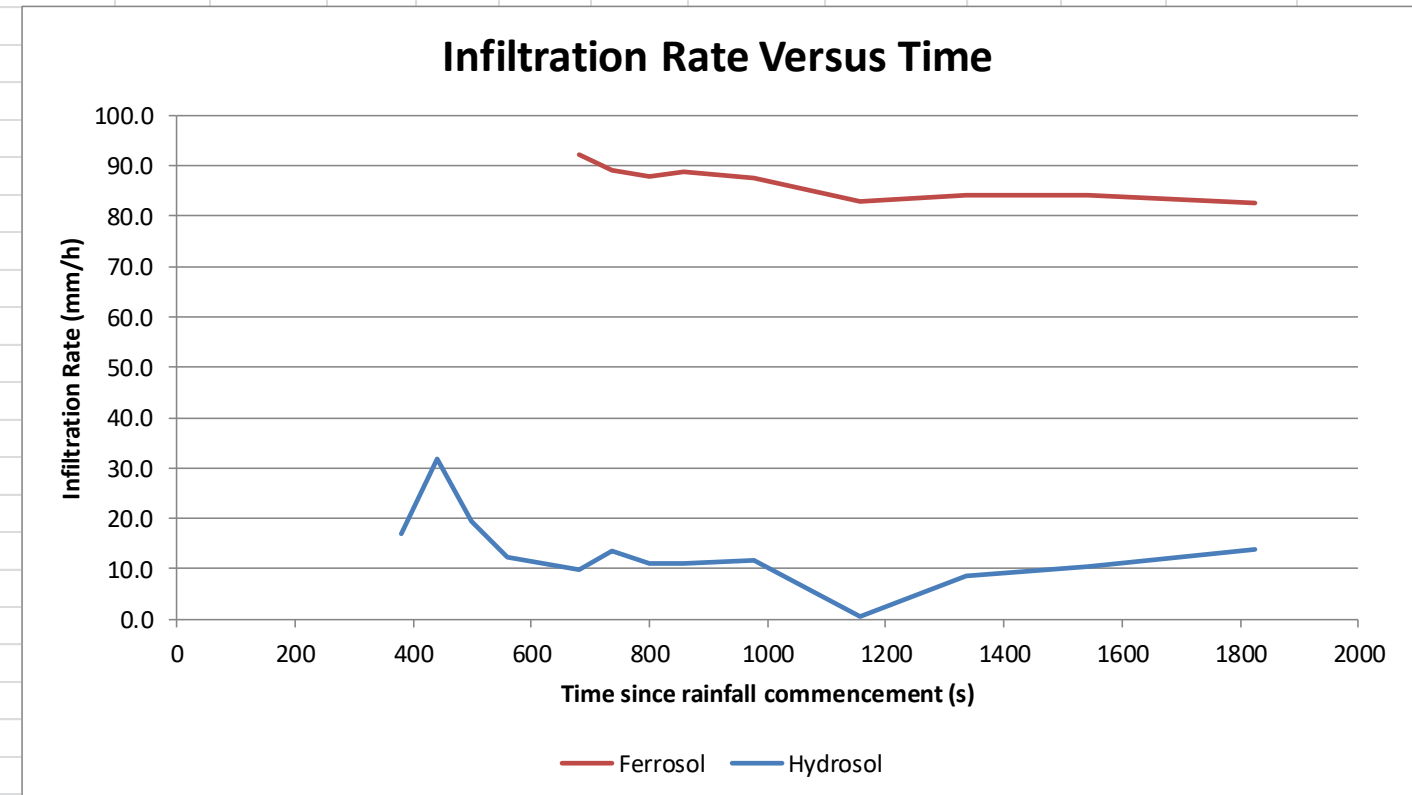
	Moisture content	Plot 1	Plot 2
Before	Mass soil (g)	44.738	33.511
	Mass water (g)	5.5	3.8
	MC	12.3%	11.3%
After	Mass soil (g)	98.452	72.13
	Mass water (g)	17.7	17.9
	MC	18.0%	24.8%



Date	2-Jul-19		Plot 1	Ferrosol									Plot 2	Hydrosol								
Plot gradient			20%									20%										
Runoff initiation (s)			669									318										
	Bottle number	Bottle mass (g)	Wet mass (g)	OD mass (g)	Sediment mass (g)	Runoff mass (g)	Instantaneous runoff (mm/h)	Instantaneous infiltration	Bottle number	Bottle mass (g)	Wet mass (g)	OD mass (g)	Sediment mass (g)	Runoff mass (g)	Instantaneous runoff (mm/h)	Instantaneous infiltration						
Pre-rain moisture sample	770	66.763	100.1	94.6	27.837				163	67.099	138.7	113	45.9									
Time from stat (min:sec to sec)	Duration (secs)															Time from stat (min:sec to min)	Duration (s)					
11 20	680	14.91	769	66.617	98.7	66.9	0.3	31.5	13.5	92.1	162	67.051	128.4	68.5	1.4	58.5	82.0	16.9	6	20	380	16.04
12 16	736	14.53	768	66.737	104.7	67.0	0.3	37.4	16.5	89.1	161	67.066	117	68.2	1.1	47.7	67.2	31.7	7	20	440	15.97
13 19	799	17.09	767	66.801	115.4	67.2	0.4	47.8	17.9	87.7	160	66.986	131.3	68.6	1.6	61.1	79.5	19.3	8	20	500	17.28
14 19	859	15.94	766	68.589	111.7	69.0	0.4	42.3	17.0	88.6	159	67.033	131.2	68.7	1.7	60.8	86.6	12.3	9	20	560	15.81
16 18	978	15.87	765	66.879	113	67.4	0.5	45.1	18.2	87.4	158	67.004	129.1	68.6	1.6	58.9	88.9	10.0	11	20	680	14.91
19 16	1156	14.69	764	66.918	120	67.3	0.4	52.3	22.8	82.8	157	66.977	125	68.4	1.4	55.2	85.4	13.4	12	16	736	14.53
22 15	1335	16.25	763	66.911	122.8	67.4	0.5	54.9	21.6	84.0	156	67.036	137.5	68.9	1.9	66.7	87.9	11.0	13	19	799	17.09
25 41	1541	16.41	762	66.884	123.5	67.4	0.5	55.6	21.7	83.9	155	67.052	132.7	68.8	1.7	62.2	87.7	11.1	14	19	859	15.94
30 25	1825	15.44	761	66.867	123.2	67.3	0.4	55.5	23.0	82.6	154	67.02	131.8	68.7	1.7	61.4	87.1	11.8	16	18	978	15.87
	0										153	67.029	134.9	68.9	1.9	64.1	98.2	0.7	19	16	1156	14.69
	0										736	68.755	137.7	70.6	1.8	65.3	90.4	8.5	22	15	1335	16.25
	0										737	66.648	134.9	68.5	1.9	64.5	88.5	10.4	25	41	1541	16.41
	0										738	66.725	128.6	68.5	1.8	58.3	85.0	13.9	30	25	1825	15.44
Post-rain moisture sample	760	66.799	123.6	105.1	38.301						739	68.773	153.1	117.3	48.53	35.8						

Rain off	Rain gauges					
31 min		59		56		
6 sec	58	Plot 1	53	52	Plot 2	51
msec		49		46		
Time (s)	1866					
	Plot 1 Average	54.75	Plot 2 Ave	51.25		
	Rainfall intensity (mm/s)	0.029		0.027		
	Rainfall intensity (mm/h)	105.6		98.9		

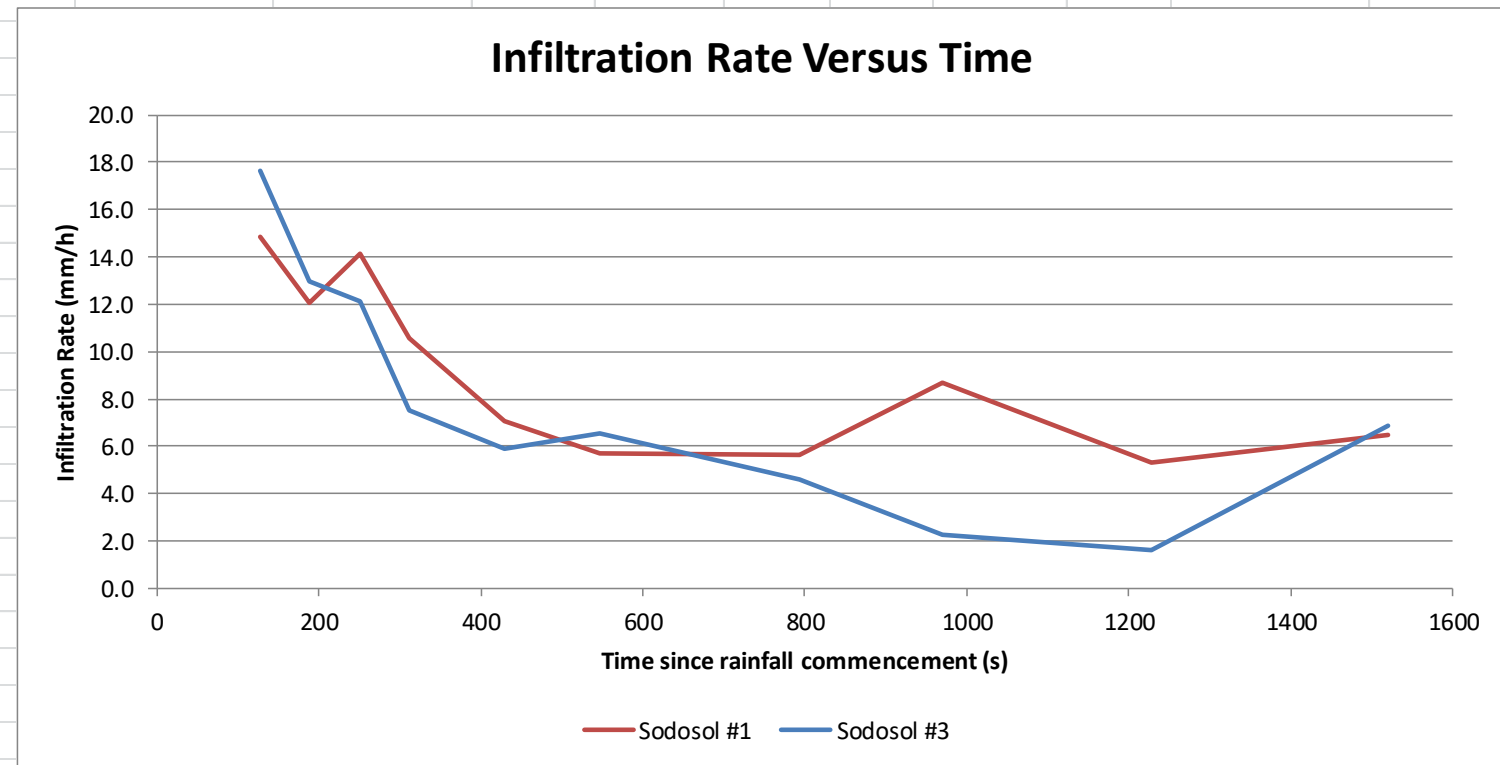
Moisture content	Plot 1	Plot 2
Before		
Mass soil (g)	27.837	45.901
Mass water (g)	5.5	25.7
MC	19.8%	56.0%
After		
Mass soil (g)	38.301	48.527
Mass water (g)	18.5	35.8
MC	48.3%	73.8%



Date	2-Jul-19	Plot 1	Sodosol #1								Plot 2	Sodosol #3							
Plot gradient	20%																		
Runoff initiation (s)	40																		
	Bottle number	Bottle mass (g)	Wet mass (g)	OD mass (g)	Sediment mass (g)	Runoff mass (g)	Instantaneous runoff (mm/h)	Instantaneous infiltration (mm/h)	Bottle number	Bottle mass (g)	Wet mass (g)	OD mass (g)	Sediment mass (g)	Runoff mass (g)	Instantaneous runoff (mm/h)	Instantaneous infiltration (mm/h)			
Pre-rain moisture sample	759	66.82	147.9	141.5	74.68				525	66.988	145	139.4	72.412						
Time from stat (min:sec to sec)	Duration (secs)																		
2 8 128	15.50	758	66.831	353.6	81.7	14.9	257.0	106.1	14.9	524	66.379	325.3	81.9	15.5	227.9	94.1	17.6		
3 9 189	16.54	757	66.856	380.3	82.8	15.9	281.6	108.9	12.1	523	66.672	355.6	83.5	16.8	255.3	98.8	13.0		
4 10 250	16.44	756	66.866	369.4	80.9	14.0	274.5	106.8	14.1	522	66.546	352.2	81.4	14.9	255.9	99.6	12.1		
5 11 311	14.81	755	66.807	348.3	79.8	13.0	255.5	110.4	10.6	521	66.617	336.8	81.1	14.5	241.2	104.2	7.5		
7 9 429	15.66	754	66.792	373.6	80.8	14.0	278.8	113.9	7.1	520	66.487	359.3	83.4	16.9	259.0	105.8	5.9		
9 6 546	16.00	753	68.749	383.3	81.9	13.2	288.2	115.3	5.7	519	66.682	363.7	83.7	17.0	263.0	105.2	6.5		
13 13 793	15.12	752	66.818	361.5	77.9	11.1	272.5	115.4	5.6	518	66.695	349.5	81.5	14.8	253.2	107.2	4.6		
16 10 970	16.19	751	66.739	375.3	79.0	12.3	284.0	112.3	8.7	517	66.803	372.5	81.2	14.4	276.9	109.5	2.3		
20 28 1228	15.50	750	66.669	373.3	79.9	13.2	280.2	115.7	5.3	516	66.837	359.7	79.9	13.1	266.7	110.1	1.6		
25 20 1520	16.25	749	66.774	383.4	79.7	12.9	290.8	114.5	6.5	515	66.837	359.6	80.1	13.3	266.2	104.9	6.9		
0																			
0																			
0																			
Post-rain moisture sample	748	68.734	153.8	139.9	71.166					514	66.875	176.8	159.6	92.725					

Rain off	Rain gauges					
25 min		52		50		
54 sec	54	Plot 1	53	53	Plot 2	45
59 msec		50		45		
Time (s)	1554.6					
	Plot 1 Average	52.25	Plot 2 Avera	48.25		
	Rainfall intensity (mm/s)	0.034		0.031		
	Rainfall intensity (mm/h)	121.0		111.7		

	Moisture content	Plot 1	Plot 2
Before	Mass soil (g)	74.68	72.412
	Mass water (g)	6.4	5.6
	MC	8.6%	7.7%
After	Mass soil (g)	71.166	92.725
	Mass water (g)	13.9	17.2
	MC	19.5%	18.5%



Date	3-Jul-19			Plot 1 Hydrosol								Plot 2 Ferrosol							
Plot gradient	20%																		
Runoff initiation (s)	344																		
	Bottle number	Bottle mass (g)	Wet mass (g)	OD mass (g)	Sediment mass (g)	Runoff mass (g)	Instantaneous runoff (mm/h)	Instantaneous infiltration	Bottle number	Bottle mass (g)	Wet mass (g)	OD mass (g)	Sediment mass (g)	Runoff mass (g)	Instantaneous runoff (mm/h)	Instantaneous infiltration (mm/h)			
Pre-rain moisture sample	491	66.78	115.3	97.1	30.32				513	66.793	139.4	120.4	53.607						
Time from stat (min:sec to sec)	Duration (secs)																Time f		
3	40	220	15.03	492	66.744	125.5	68.0	1.3	56.2	23.9	79.7	512	66.703	113.9	67.0	0.3	46.6	69.8	23.9
4	39	279	15.06	493	66.831	131.5	68.2	1.4	61.9	26.3	77.3	511	66.725	116.1	67.1	0.4	48.6	72.6	21.1
5	38	338	14.97	494	66.851	126.4	68.2	1.3	56.9	24.3	79.3	510	66.829	117.8	67.1	0.3	50.4	75.8	17.9
6	38	398	15.32	495	66.858	128.4	68.3	1.4	58.7	24.5	79.1	509	66.767	118.3	67.3	0.5	50.5	74.1	19.6
8	36	516	15.88	496	66.856	133.6	68.4	1.5	63.7	25.7	78.0	508	66.776	118.1	67.1	0.3	50.7	71.8	21.9
11	35	695	16.41	497	66.704	143.1	68.7	2.0	72.4	28.2	75.4	507	66.799	127.6	67.1	0.3	60.2	82.5	11.2
15	36	936	15.53	498	66.398	140.4	68.2	1.8	70.4	29.0	74.6	506	66.728	126.2	67.2	0.5	58.5	84.8	8.9
20	47	1247	15.81	499	66.529	140.5	68.5	2.0	70.0	28.3	75.3	505	66.485	125.2	66.8	0.3	58.1	82.7	11.0
26	45	1605	15.50	500	66.543	133.9	68.3	1.7	63.9	26.4	77.2	504	66.714	125.3	67.0	0.3	58.0	84.2	9.5
		0																	
		0																	
		0																	
		0																	
Post-rain moisture sample	501	66.632	166.1	124	57.368							503	66.716	164.5	133.6	66.884			

Rain off

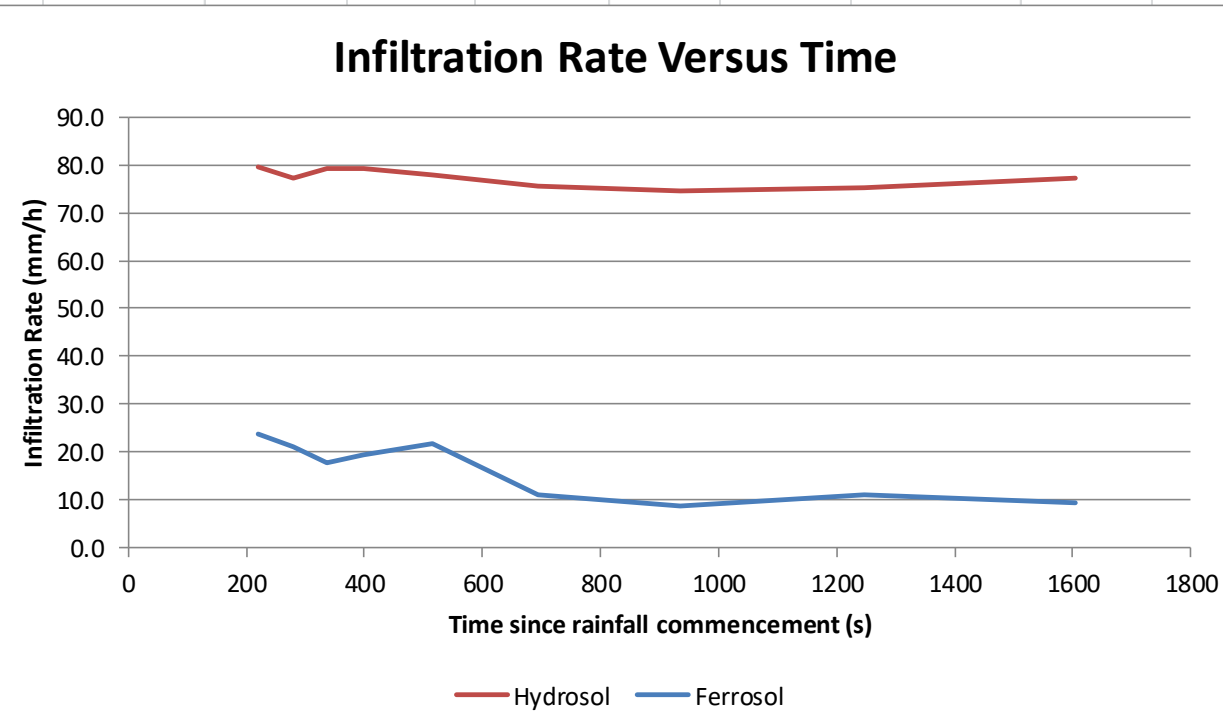
Rain gauges

27 min		51		46		
12 sec	45	Plot 1	48	44	Plot 2	42
78 msec		44		38		

Time (s) 1632.78

Plot 1 Average	47	Plot 2 Av	42.5
Rainfall intensity (mm/s)	0.029		0.026
Rainfall intensity (mm/h)	103.6		93.7

	Moisture content	Plot 1	Plot 2
Before	Mass soil (g)	30.32	53.607
	Mass water (g)	18.2	19
	MC	60.0%	35.4%
After	Mass soil (g)	57.368	66.884
	Mass water (g)	42.1	30.9
	MC	73.4%	46.2%

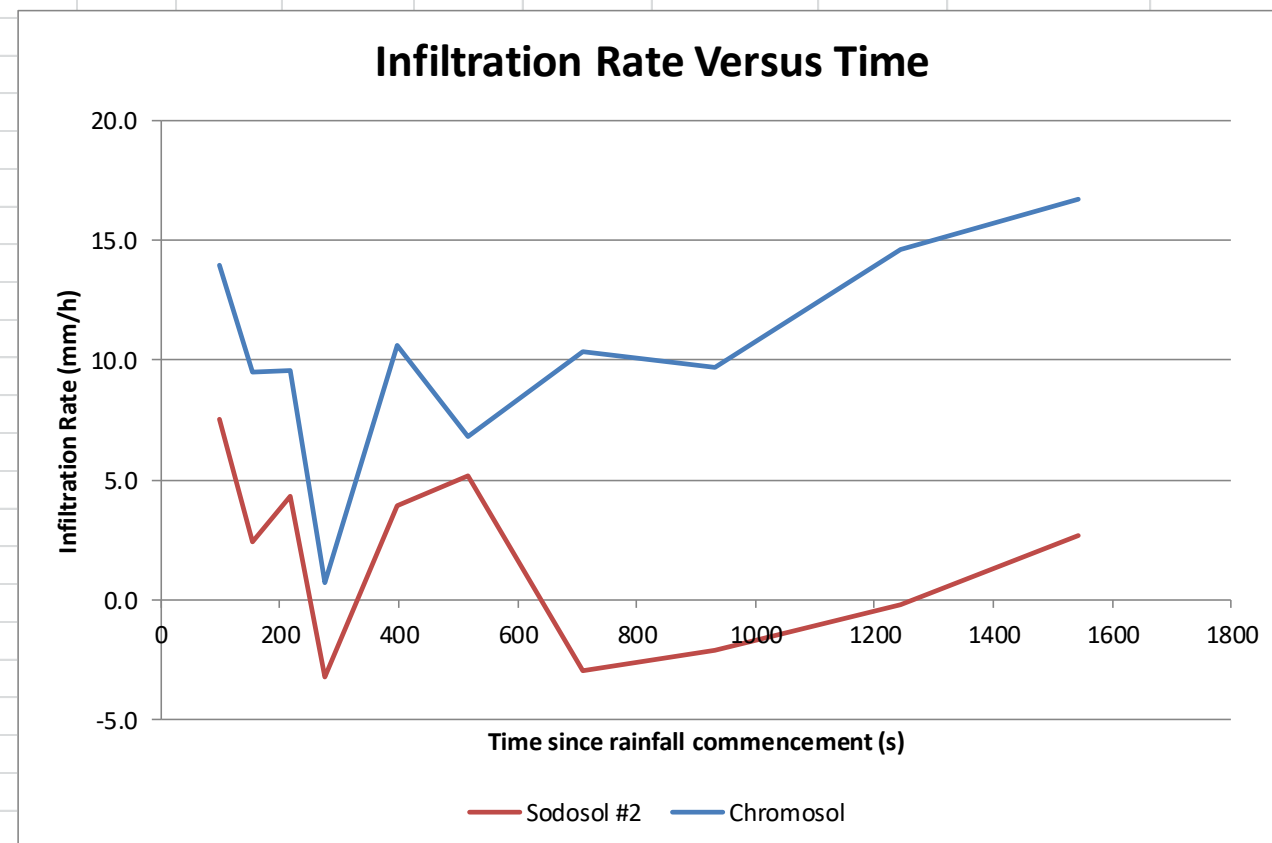


Date	3-Jul-19	Plot 1 Sodosol #2										Plot 2 Chromosol							
Plot gradient	20%										20%								
Runoff initiation (s)	40										76								
	Bottle number	Bottle mass (g)	Wet mass (g)	OD mass (g)	Sediment mass	Runoff mass (g)	Instantaneous runoff	Instantaneous infiltration	Bottle number	Bottle mass (g)	Wet mass (g)	OD mass (g)	Sediment mass (g)	Runoff mass (g)	Instantaneous runoff (mm/h)	Instantaneous infiltration (mm/h)			
Pre-rain moisture sample		350	66.884	122	117.1	50.216			316	66.858	108.7	104.2	37.342						
Time from stat (min:sec to sec)	Duration (secs)																		
1	39	99	15.94	349	66.864	331.4	77.4	10.5	243.5	97.8	7.5	317	66.808	128	67.7	0.9	59.4	83.9	14.0
2	35	155	15.21	348	66.953	332.2	77.4	10.4	244.4	102.8	2.4	318	66.89	128.8	68.0	1.1	59.7	88.3	9.5
3	38	218	15.97	347	66.912	340.3	77.7	10.8	251.8	100.9	4.3	319	66.74	131.7	67.9	1.2	62.6	88.3	9.6
4	37	277	15.28	346	66.893	349.3	78.6	11.7	259.0	108.5	-3.2	320	66.937	135.4	68.2	1.3	65.9	97.1	0.7
6	37	397	15.66	345	66.903	336.2	77.6	10.7	247.9	101.3	3.9	321	66.875	129.6	67.9	1.0	60.7	87.2	10.6
8	36	516	15.91	344	66.841	335.8	76.9	10.1	248.8	100.1	5.2	322	66.844	133.7	68.1	1.3	64.3	91.0	6.8
11	50	710	15.37	343	66.818	348.7	77.8	11.0	259.9	108.2	-3.0	323	66.874	128.9	68.0	1.1	59.8	87.5	10.3
15	33	933	15.38	342	66.837	345.9	77.4	10.6	257.9	107.3	-2.1	324	66.937	129.1	67.9	1.0	60.2	88.1	9.7
20	45	1245	15.03	341	66.856	337.6	78.4	11.5	247.7	105.5	-0.2	325	66.964	124.8	68.1	1.1	55.6	83.2	14.6
25	42	1542	15.72	340	66.905	337.8	76.4	9.5	251.9	102.6	2.7	326	66.98	125.3	67.8	0.8	56.7	81.1	16.7
		0																	
		0																	
		0																	
Post-rain moisture sample		339	66.899	172.7	155.5	88.601													

Rain off

	Rain gauges			
26 min		48		47
13 sec	47	Plot 1	45	40
38 msec		44		40
Time (s)	1573.38			
Plot 1 Average		46	Plot 2 Av	42.75
Rainfall intensity (mm/s)		0.029		0.027
Rainfall intensity (mm/h)		105.3		97.8

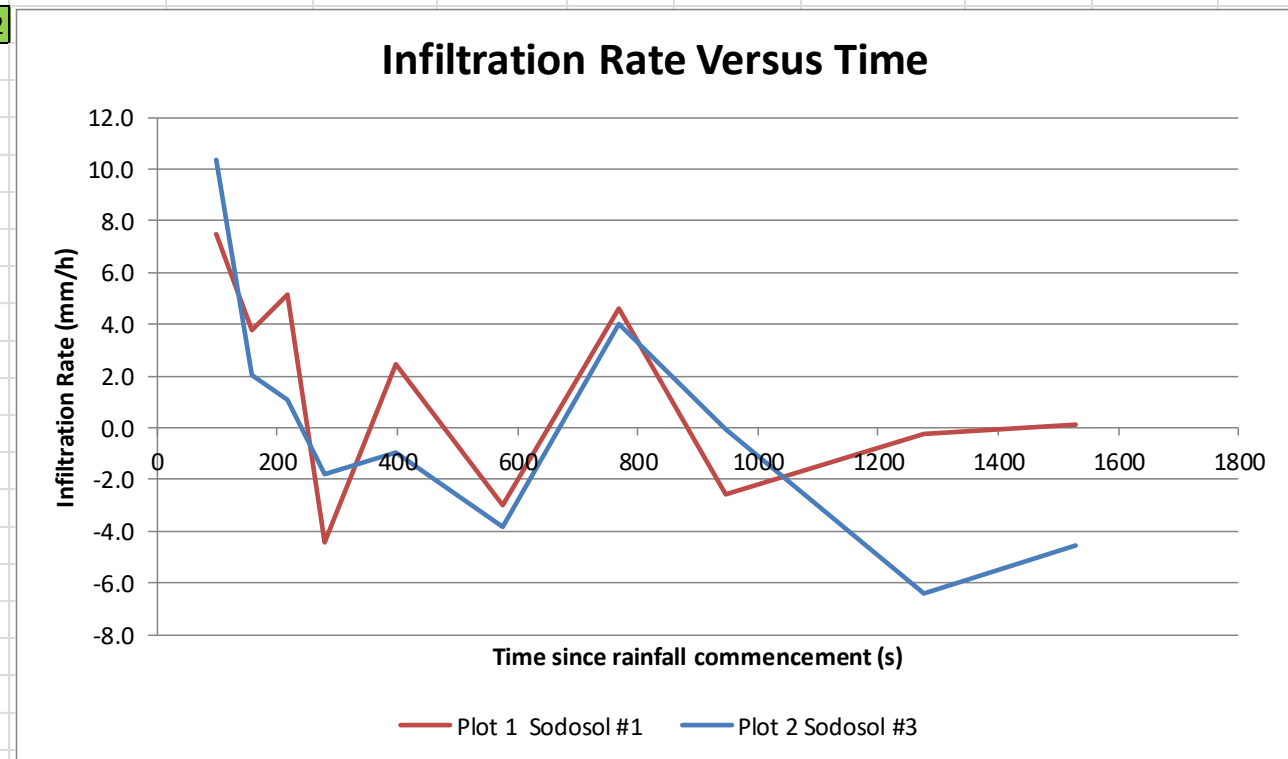
	Moisture content	Plot 1	Plot 2
Before	Mass soil (g)	50.216	37.342
	Mass water (g)	4.9	4.5
	MC	9.8%	12.1%
After	Mass soil (g)	88.601	57.072
	Mass water (g)	17.2	16.8
	MC	19.4%	29.4%



Date	3-Jul-19		Plot 1 Sodosol #1									Plot 2 Sodosol #3							
Plot gradient			20%									20%							
Runoff initiation (s)			45									45							
			Bottle number	Bottle mass (g)	Wet mass (g)	OD mass (g)	Sediment mass (g)	Runoff mass (g)	Instantaneous runoff (mm/h)	Instantaneous infiltration (mm/h)	Bottle number	Bottle mass (g)	Wet mass (g)	OD mass (g)	Sediment mass (g)	Runoff mass (g)	Instantaneous runoff (mm/h)	Instantaneous infiltration (mm/h)	
Pre-rain moisture sample			328	66.842	125	120.1	53.258				701	68.8	141.5	135.3	66.5				
Time from stat (min:sec to sec)	Duration (secs)																	Time f	
1	39	99	15.46	329	66.878	320.9	75.1	8.2	237.6	98.4	7.5	702	66.91	305.3	76.4	9.5	219.4	90.8	10.4
2	39	159	15.56	330	66.82	333.3	76.0	9.2	248.1	102.1	3.8	703	66.818	329.7	77.7	10.9	241.1	99.2	2.0
3	38	218	15.81	331	66.812	332.1	75.1	8.3	248.7	100.7	5.2	704	66.899	336.3	77.9	11.0	247.4	100.1	1.1
4	38	278	15.44	332	66.832	353	76.9	10.1	266.0	110.3	-4.4	705	66.294	338.2	78.0	11.7	248.5	103.0	-1.8
6	37	397	15.25	333	66.9	330.7	75.6	8.7	246.4	103.4	2.4	706	66.815	328.8	76.1	9.3	243.4	102.2	-0.9
9	36	576	15.00	334	66.848	340	75.9	9.1	255.0	108.8	-3.0	707	66.795	332	76.3	9.5	246.2	105.0	-3.8
12	48	768	15.25	335	66.85	324.2	74.9	8.1	241.3	101.2	4.6	708	66.826	315.4	75.3	8.5	231.6	97.2	4.0
15	46	946	15.31	336	66.797	343.7	75.6	8.8	259.3	108.4	-2.5	709	68.834	332.4	79.5	10.7	242.2	101.3	0.0
21	16	1276	15.13	337	66.843	333.7	74.9	8.1	250.7	106.1	-0.2	710	66.867	343.2	77.8	10.9	254.5	107.6	-6.4
25	28	1528	15.88	338	66.902	346.6	75.6	8.7	262.3	105.7	0.1	711	68.82	353.0	79.7	10.9	262.4	105.8	-4.5
Post-rain moisture sample			502	66.779	179.1	160.3	93.521				712	68.767	154.3	141.1	72.333				

Rain off		Rain gauges				
25 min		48		47		
56 sec		47	Plot 1	46	Plot 2	42
6 msec		42		40		
Time (s)	1556.06					
		Plot 1 Average	45.75	Plot 2 Av	43.75	
		Rainfall intensity (mm/s)	0.029		0.028	
		Rainfall intensity (mm/h)	105.8		101.2	

	Moisture content	Plot 1	Plot 2
Before	Mass soil (g)	53.258	66.5
	Mass water (g)	4.9	6.2
	MC	9.2%	9.3%
After	Mass soil (g)	93.521	72.333
	Mass water (g)	18.8	13.2
	MC	20.1%	18.2%



Appendix D - Example ImageJ Script

Introduction

ImageJ was used to complete the image analysis of cores scanned by X-ray CT. To semi-automate the image analysis processes, a number of script files were developed. The script below is an example.

This script file identifies the soil surface through the use of the Gaussian blur function and creation of an EDM mask. Once the surface has been identified a for loop is used to measure the porosity of the image 40 times at incrementally increasing depths throughout the soil. This was used to determine the changes of porosity with depth.

The language used is an ImageJ scripting language.

Script

```
//  
// Initialisation  
// run("Close All")  
print("New run");  
  
// set the options to:  
// foreground = white  
// background = black  
run("Options...", "iterations=1 count=1 black edm=16-bit do=Nothing");  
run("Colors...", "foreground=white background=black selection=yellow");  
  
// Prepare for measurements  
run("Clear Results");  
run("Set Measurements...", "area bounding area_fraction redirect=None decimal=3");  
roiManager("reset")  
  
// open("C:/Users/Cameron/Documents/Engineering Degree - use this one/19 S1 ENG4111 Research  
Project/Created Images - ImageJ/Core2/Reslice of Core2.tif");  
  
//image_directory = getInfo("image.directory");  
//print(image_directory);  
  
// number of times mask is applied at different depths below the soil surface  
n_increments = 40;  
  
orig_image = getTitle;  
run("Invert");  
run("Duplicate...", " ");  
image = getTitle;  
close(orig_image)  
  
//  
// create mask
```

```

run("Invert");
setOption("BlackBackground", true);
run("Make Binary");
binary_image = getTitle(); // this binary image will have the mask applied to it once the mask is
developed
run("Duplicate...", " ");
new_binary_image = getTitle(); // this image is used to develop the mask
print(new_binary_image);

// Gaussian blur run to set up finding the soil surface
run("Gaussian Blur...", "sigma=10");

// threshold
// aim to get as a complete hole free soil as possible
setAutoThreshold("Default dark");
setOption("BlackBackground", true);
run("Convert to Mask");

// fill any remaining gaps
run("Fill Holes");

// Clean up any larger objects at the edge of the image
// invert image to get holes at the edge as objects
run("Invert");

// size restricted analyze particles with masks as output
run("Analyze Particles...", "size=50-Infinity show=Masks"); // change to 50 from 100 default

// reset the LUT and binary to:
// foreground = white
// background = black
run("Invert LUT");
run("Invert");

mask_image = getTitle();

// create EDM
run("Distance Map");
EDM_map = getTitle();
print("EDM_map original file name: " + EDM_map);
// run("Duplicate...");
run("Duplicate...", " ");
EDM_duplicate = getTitle();
print("Duplicate of EDM_map filename: " + EDM_duplicate);

// set initial values for threshold which are changed within the for loop
first_point = 1;

```

```

second_point = 11;

lower_threshold = newArray(n_increments);
upper_threshold = newArray(n_increments);

for (i=1; i<=n_increments; i++) {
    lower_threshold[i-1] = first_point;
    first_point = first_point + 10;

    upper_threshold[i-1] = second_point;
    second_point = second_point + 10;
}

Array.print(lower_threshold);
Array.print(upper_threshold);

print("Loop begins - Loop begins - Loop begins");
//
// loop through binary image, apply threshold and record measurement
for (i=1; i<=n_increments; i++) {

    selectWindow(EDM_duplicate);
    run("Duplicate...", " ");
    // run("Duplicate..."); // this has fixed the problem but requires enter to be entered each time
    // potentially use restore and back up to do the same as duplicate without having all the extra
    mak images created

    // set a manual threshold
    // fixed lower and upper threshold value
    // i.e. size in pixels of submask

    print("loop i value: " + i);
    print("first point: " + lower_threshold[i-1]);
    print("second point: " + upper_threshold[i-1]);

    setThreshold(lower_threshold[i-1], upper_threshold[i-1]); // changing values to apply
threshold progressively deeper into the soil
    setOption("BlackBackground", true);
    run("Convert to Mask");

    active_mask = getTitle();
    print("Active mask " + active_mask);
    // selectWindow(active_mask);

    // create selection based on mask, change to binary image and measure
    run("Create Selection");
    //roiManager("add");
    selectWindow(binary_image);

```

```
run("Restore Selection");
run("Measure");

// change threshold values for next iteration
first_point = first_point + 4;
second_point = second_point + 4;

// reset EDM_duplicate to original EDM
// EDM_duplicate = EDM_map;
resetThreshold;
}

selectWindow("Results");
run("Close All");

// create a table to store the %Area data only in
// initially this is just for one column for one image. Need to be able to store results from other images
// in other columns so that the %Area results for each slice in a stack can be stored
// from this the average porosity with depth can be calculated.

// run("Close All")
```